

University of Alberta

**Synthesis and Reactivity of New Thermally Stable Chromium(II)/(III)
 η^3 -Allyl and *s-Trans* Chromium(0) Diene Complexes**

by



David W. Norman

A thesis submitted to the Faculty of Graduate Studies and Research in partial fulfillment
of the requirements for the degree of Doctor of Philosophy

Department of Chemistry

Edmonton, Alberta

Fall 2006



Library and
Archives Canada

Published Heritage
Branch

395 Wellington Street
Ottawa ON K1A 0N4
Canada

Bibliothèque et
Archives Canada

Direction du
Patrimoine de l'édition

395, rue Wellington
Ottawa ON K1A 0N4
Canada

Your file Votre référence
ISBN: 978-0-494-47640-6
Our file Notre référence
ISBN: 978-0-494-47640-6

NOTICE:

The author has granted a non-exclusive license allowing Library and Archives Canada to reproduce, publish, archive, preserve, conserve, communicate to the public by telecommunication or on the Internet, loan, distribute and sell theses worldwide, for commercial or non-commercial purposes, in microform, paper, electronic and/or any other formats.

The author retains copyright ownership and moral rights in this thesis. Neither the thesis nor substantial extracts from it may be printed or otherwise reproduced without the author's permission.

AVIS:

L'auteur a accordé une licence non exclusive permettant à la Bibliothèque et Archives Canada de reproduire, publier, archiver, sauvegarder, conserver, transmettre au public par télécommunication ou par l'Internet, prêter, distribuer et vendre des thèses partout dans le monde, à des fins commerciales ou autres, sur support microforme, papier, électronique et/ou autres formats.

L'auteur conserve la propriété du droit d'auteur et des droits moraux qui protège cette thèse. Ni la thèse ni des extraits substantiels de celle-ci ne doivent être imprimés ou autrement reproduits sans son autorisation.

In compliance with the Canadian Privacy Act some supporting forms may have been removed from this thesis.

Conformément à la loi canadienne sur la protection de la vie privée, quelques formulaires secondaires ont été enlevés de cette thèse.

While these forms may be included in the document page count, their removal does not represent any loss of content from the thesis.

Bien que ces formulaires aient inclus dans la pagination, il n'y aura aucun contenu manquant.


Canada

To my wife and parents

Abstract

This study details the synthesis and reactivity of new chromium η^3 -allyl, η^2 -alkene, η^2 -alkyne and η^4 -(*s-trans*-1,3-diene) complexes via unprecedented organochromium reaction pathways. The key step in the synthesis of the cyclopentadienyl η^3 -allyl chromium(II) dicarbonyl complexes is the oxidative addition of allyl bromide to a labile chromium(0) source at low temperature. The carbonyl ligands of these complexes proved to be substitutionally inert.

The first thermally stable chromium(III) η^3 -allyl complexes have been prepared from a simple one-electron oxidation of the neutral cyclopentadienyl chromium(II) η^3 -allyl dicarbonyl precursors by employing nitrosonium salts. The use of 1,2-dimethoxyethane as a solvent is critical to the successful formation of these complexes. Attempted decarbonylation reactions of these cationic complexes via displacement by tertiary phosphines resulted in loss of the allyl ligand and the formation of bis(phosphine) complexes.

Photochemical mono-decarbonylation of a permethylcyclopentadienyl chromium(0) dicarbonyl nitrosyl complex in the presence of alkenes and alkynes provided the corresponding η^2 -coordinated products. Similar decarbonylation in the presence of conjugated cyclic organic dienes afforded both mononuclear and dinuclear η^2 -(1,3-diene) complexes, while photolysis in the presence of acyclic conjugated dienes gave η^4 -(1,3-diene) complexes *exclusively* in the *s-trans* configuration, unique among the first-row transition metals. A mixture of η^2 -(1,3-diene) and η^4 -(*s-trans*-1,3-diene)

complexes was obtained in the cyclopentadienyl series. No *s-cis* η^4 -(1,3-diene) products were formed in any these photolysis reactions.

Attempted hydride abstraction from the η^2 -alkene complexes instead provided novel cationic oxygen donor-bound chromium(I) nitrosyl complexes, while protonation of the η^2 -(1,3-diene) complexes with ethereal tetrafluoroboric acid provided the corresponding η^3 -allyl carbonyl nitrosyl complexes, unique among chromium. Similar conversion of the *s-trans*-butadiene complex afforded the first, albeit thermally unstable, *pseudo*-tetrahedral η^3 -allyl complex of the group six metals.

The addition of strong Lewis acids to the *s-trans*-butadiene complex provided unique zwitterionic nitrosyl adducts, while treatment with tin-hydride and allyltin reagents gave the corresponding tin(IV)-chromium(II) η^3 -crotyl and η^3 -allyl complexes. A more efficient photolytic pathway was developed for the synthesis of these structurally unprecedented complexes from an analogous dicarbonyl chromium(0) source. The development of non-carbonyl chromium precursors for the preparation of η^3 -allyl complexes was unsuccessful.

Acknowledgements

I would like to thank my research advisor, mentor, and friend, Professor Jeffrey M. Stryker for all his guidance and encouragement in my pursuit of a scientific career. Jeff, your passion for science and education are remarkable traits that I hope to reflect throughout my life; thank you for everything. I would also like to thank my undergraduate supervisor, Dr. Steven Westcott; thanks for taking a chance on me Lil' Weg.

I would also like to acknowledge and thank the current and former members of the Stryker group: Dr. Masaki Morita, Dr. Meekyung Chung, Ross Witherell, Jason Norman, Nolan Erickson, James Sochan, Owen Lightbody, Bryan Chan, Kai Ylijoki, Bichu Cheng, Andrew Kirk, Rick Bauer, Paul Fancy, Jeremy Gauthier. Thank you for the many laughs, drinks, and helpful discussions. An extra thank you goes out to Owen for sticking by me even after I tried to blow him up, and to Ross for teaching me so many tricks of the trade.

The phenomenal resources and staff at the University of Alberta were crucial to understanding many of my air sensitive and paramagnetic compounds. Particularly, thanks goes to Drs. Bob McDonald and Mike Ferguson for the many X-ray crystal structures of my unusual, and typically unexpected, compounds. Their persistence and cooperation were invaluable to my project and contributed greatly to my education as an inorganic chemist.

And of course, a world of thanks must go to my parents: without their love and guidance I would never have thought that my present situation would ever have been possible. They cannot know how much they mean to me. And to my beautiful wife Fonda: her love and devotion have given me the strength to push through graduate school and tackle any challenge that arose. Our seven years together have been magical and I can't wait to see what the future has in store for us!

Table of Contents

Chapter 1. Overview and introduction

1.0	Overview	1
1.1	Introduction	2
1.1.1	Nucleophilic alkylation of η^3 -allyl complexes	2
1.1.2	Titanacyclobutane formation via organic free radical addition to titanium(III) η^3 -allyl complexes	13
1.1.3	A brief overview of organochromium applications	21
1.1.4	Known chromium η^3 -allyl complexes	27
1.2	Proposed chromium η^3 -allyl precursors for chromacyclobutane formation	32
1.3	References	36

Chapter 2. General synthesis of cyclopentadienylchromium(II) η^3 -allyl dicarbonyl complexes

2.0	Introduction	46
2.1	Synthesis of neutral $\text{Cp}'\text{Cr}(\eta^3\text{-allyl})(\text{CO})_2$ complexes	49
2.2	Reactivity of the $\text{CpCr}(\eta^3\text{-allyl})(\text{CO})_2$ complex	61
2.3	References	65

Chapter 3. Synthesis of the first thermally stable chromium(III) η^3 -allyl complexes

3.0	One-electron oxidation of the neutral $\text{CpCr}(\eta^3\text{-allyl})(\text{CO})_2$ complexes	67
3.1	Crystallographic structural comparison of the Cr(II) and Cr(III) η^3 -allyl redox isomers	70
3.2	Coordination of nitric oxide to the cationic η^3 -crotyl dicarbonyl complex	74

3.3	Reactivity of the $[\text{CpCr}(\eta^3\text{-allyl})(\text{CO})_2]\text{PF}_6$ complex	77
3.4	References	86

Chapter 4. Synthesis of unprecedented first-row *s-trans* 1,3-diene complexes

4.0	Introduction	87
4.0.1	Salient features of nitric oxide	88
4.0.2	A brief history of <i>s-trans</i> 1,3-diene complexes	90
4.0.3	Alternative strategies for the preparation of chromium η^3 -allyl carbonyl nitrosyl complexes	98
4.1	Photolysis of $\text{Cp}'\text{CrNO}(\text{CO})_2$ complexes in the presence of olefins	99
4.1.1	Formation of $\text{CpCrNO}(\text{CO})(\eta^2\text{-alkene})$ complexes	99
4.1.2	Formation of $\text{Cp}^*\text{CrNO}(\text{CO})(\eta^2\text{-alkene})$ and $(\eta^2\text{-alkyne})$ complexes	101
4.2	Photolysis of $\text{CpCrNO}(\text{CO})_2$ in the presence of conjugated dienes	109
4.2.1	Formation of $\text{CpCrNO}(\text{CO})(\eta^2\text{-1,3-diene})$ and $\text{CpCrNO}(\eta^4\text{-s-trans-1,3-diene})$ complexes	109
4.2.2	Formation of $\text{Cp}^*\text{CrNO}(\eta^4\text{-s-trans-1,3-diene})$ complexes	116
4.3	Photolysis of $\text{Cp}'\text{CrNO}(\text{CO})_2$ complexes in the presence of conjugated cyclic dienes	123
4.3.1	Formation of $\text{CpCrNO}(\text{CO})(\eta^2\text{-cyclic-1,3-diene})$ complexes	123
4.3.2	Mononuclear and dinuclear $[\text{Cp}^*\text{CrNO}(\text{CO})]_n(\eta^2\text{-cyclic-1,3-diene})$ complexes	124
4.4	Electronic justification of preferential <i>s-trans</i> diene binding observed in the $\text{Cp}'\text{CrNO}(1,3\text{-diene})$ complexes	130
4.5	References	133

Chapter 5. Reactivity of Cp'CrNO(η^4 -1,3-diene) complexes: thermally stable η^3 -allyl compounds, novel zwitterionic complexes, and an η^2 -(hydrido-tin) species

5.0	Introduction	138
5.1	Attempted Insertion reactions	142
5.2	Addition of strong Lewis acids	147
5.3	Conversion of the chromium(1,3-diene) and chromium(alkene) complexes to cationic η^3 -allyl derivatives	152
5.3.1	Protonation reactions of Cp*CrNO(<i>s-trans</i> -butadiene)	142
5.3.2	Protonation reactions of Cp'CrNO(CO)(η^2 -1,3-diene) complexes	160
5.3.3	One-electron oxidation of Cp'CrNO(CO)(η^2 -alkene) complexes	167
5.4	Addition of tin reagents to Cp*CrNO(<i>s-trans</i> -butadiene)	172
5.4.1	Formation of unique η^3 -crotyl chromium-tin complexes via tin-hydride addition	172
5.4.2	Proposed mechanism for the formation of the η^3 -allyl chromium-tin complexes	177
5.4.3	Oxidative addition of allyltriphenyltin	184
5.5	Photolytic decarbonylation of Cp*CrNO(CO) ₂ in the presence of tin reagents	189
5.5.1	Preparation of Cp*CrNO(η^3 -allyl)(SnPh ₃)	189
5.5.2	Spectroscopic identification of Cp*CrNO(CO) η^2 -(H-SnPh ₃)	191
5.6	References	194

Chapter 6. Non-carbonyl sources of chromium: alternative strategies for the preparation of *pseudo*-tetrahedral η^3 -allyl chromium complexes

6.0	Overview	199
6.1	Attempted synthesis of chromium(I) nitrosyl η^3 -allyl complexes	200

6.1.1	Introduction	200
6.1.2	Halo-bridged dimers as chromium nitrosyl sources	202
6.1.3	Reactivity of cationic bis(donor) chromium(I) nitrosyl complexes	203
6.2	Synthesis and reactivity of dihalochromium complexes bearing neutral ligands	205
6.2.1	Introduction	205
6.2.2	Addition of sterically hindered donor ligands to $[\text{Cp}^*\text{CrCl}_2]_2$	208
6.2.3	Protonation of chromium(I) η^4 -butadiene complexes	208
6.3	Monohalo chromium(II) complexes as η^3 -allyl and η^4 -(1,3-diene) precursors	209
6.3.1	Introduction	209
6.3.2	Synthesis and reactivity of a 14-electron 2,4,6-trimethylpyridine complex	211
6.3.3	Attempted coordination of conjugated dienes to $\text{Cp}^*\text{CrCl}(\text{PyMe}_3)$	213
6.3.4	Synthesis and reactivity of $\text{Cp}^*\text{Cr}(\text{IMes})\text{Cl}$ complexes	216
6.3.5	Formation of a tris(2,6-diisopropylphenyl isocyanide)chromium(I) complex	220
6.3.6	The reaction of imidazolium salts with $\text{Cp}^*\text{Cr}(\eta^3\text{-allyl})_2$	224
6.4	Phosphinimide chromium complexes as η^3 -allyl precursors	227
6.4.1	Introduction	227
6.4.2	Disproportionation of a phosphinimide ligand	230
6.5	Conclusions	232
6.6	References	237
	Experimental procedures, spectroscopic and analytical data	242
	Appendix A: References to complete reports from crystal structure determinations	324

List of Tables

Table 1.1:	Hydride-allyl carbon overlap populations.	4
Table 2.1:	^1H NMR data of complex 66 .	50
Table 3.1:	Reaction details for the synthesis of cationic chromium(III) η^3 -allyl complexes 77-79 .	68
Table 3.2:	Comparison of selected bond lengths and angles for allyl complexes 66 and 77 .	72
Table 3.3:	Selected bond distances and carbonyl infrared absorptions of $[\text{Cr}(\text{CO})_2(\pi\text{-alkyne})(\eta^6\text{-arene})]^n$ ($n = 0, 1$) complexes.	74
Table 3.4:	^1H NMR data for complex 81/81' .	76
Table 4.1:	Selected bond lengths and angles of several transition metal <i>s-trans</i> diene complexes.	95
Table 4.2:	^1H NMR data of complexes 91 and 95 .	105
Table 4.3:	Reaction details pertaining to equation 4.8 .	110
Table 4.4:	^1H NMR data of complexes 101 and 102 .	111
Table 4.5:	^1H NMR data of complexes 106 and 107 .	112
Table 4.6:	^1H NMR data of complexes 111-113 .	118
Table 5.1:	^1H NMR data of complexes 129 and 130 .	151
Table 5.2:	^1H NMR and IR data of complexes 138 and 139 .	164
Table 5.3:	^1H NMR data of complexes 146 and 147 .	175
Table 5.4:	^1H NMR data of complexes 151 and 152 .	186
Table 6.1:	^1H NMR data IMesHX ($\text{X} = \text{Cl}^-$, PF_6^- , BPh_4^-) salts.	226

List of Figures

Figure 1.1:	The antibonding acceptor molecular orbitals of complex 1 .	3
Figure 1.3:	The molecular orbitals of an η^3 -allyl ligand fragment.	10
Figure 1.4:	MO energy level diagram for d^0 group IV metallocene η^3 -allyl complexes.	11
Figure 1.5:	MO energy level diagram for d^1 group IV metallocene η^3 -allyl complexes.	14
Figure 2.1:	Solid-state molecular structure of complex 66 .	51
Figure 2.2:	Solid-state molecular structure complex 70 .	58
Figure 2.3:	Low resolution solid-state molecular structure of complex 73 .	59
Figure 2.4:	Solid-state molecular structure of complex 74 .	60
Figure 2.5:	Solid-state molecular structure of complex 76 .	63
Figure 3.1:	Solid-state molecular structure of complex 77 .	71
Figure 3.2, A:	Expansion of the methyl region from the ^1H NMR spectrum of complex 86 .	83
Figure 3.2, B:	A comparison of the effect of phosphine ligand geometry on the methyl ^1H NMR signals of bis(PMeR_2) ($\text{R} = \text{alkyl or aryl}$) complexes.	83
Figure 3.3:	Solid-state molecular structure of complex 86 .	84
Figure 3.4:	Solid-state molecular structure of complex 87 .	85
Figure 4.1:	Resonance structures of linear and bent bonding modes of nitric oxide.	90
Figure 4.2:	Possible stereoisomers of complex 92 .	101
Figure 4.3:	Two possible rotamers of one of the stereoisomers of complex 95 .	103

Figure 4.4:	Solid-state molecular structure complex 96/96' .	104
Figure 4.5:	Solid-state molecular structure of the complex 97 .	107
Figure 4.6:	Assignment of the η^4 -diene region of the ^1H NMR spectrum of complex 106 .	113
Figure 4.7:	Possible diene ligand configuration of complex 108/108' .	115
Figure 4.8:	Assignment of the η^4 -diene region of the ^1H NMR spectrum of complex 111 .	119
Figure 4.9:	Solid-state molecular structure of complex 112 .	120
Figure 4.10:	Solid-state molecular structure of complex 113 .	121
Figure 4.11:	Solid-state molecular structure of complex 119 .	127
Figure 4.12:	Qualitative molecular orbital energy diagram of the frontier molecular orbitals of <i>s-cis</i> and <i>s-trans</i> -butadiene and the $\text{CpMo}(\text{NO})$ fragment.	132
Figure 5.1:	Solid-state molecular structure of complex 128 .	145
Figure 5.2:	Solid-state molecular structure of complex 129 .	150
Figure 5.4:	Solid-state molecular structure of complex 132 .	153
Figure 5.6:	Solid-state molecular structure of complex 140 .	166
Figure 5.7:	Solid-state molecular structure of complex 143 .	170
Figure 5.8:	Solid-state molecular structure of complex 144 .	171
Figure 5.9:	Solid-state molecular structure of complex 146 .	176
Figure 5.10:	Solid-state molecular structure of complex 149 .	180
Figure 5.11:	Expansion of the hydrido region of the ^1H NMR spectrum of complex 157 .	192
Figure 6.1:	Solid-state molecular structure of complex 181 .	212
Figure 6.2:	Solid-state molecular structure of complex 185 .	216
Figure 6.3:	Solid-state molecular structure of complex 186 .	218

Figure 6.4:	Solid-state molecular structure of complex 187 .	220
Figure 6.5:	Solid-state molecular structure of complex 189 .	222
Figure 6.6:	Solid-state molecular structure of complex 195 .	231

List of Charts

Chart 1.4:	Selected examples of thermally stable chromium η^3 -allyl complexes bearing carbonyl ligands.	30
Chart 1.5:	Selected examples of known thermally stable chromium η^3 -allyl complexes bearing donor ligands.	31
Chart 2.1:	Novel $\text{Cp}'\text{Cr}(\eta^3\text{-allyl})(\text{CO})_2$ complexes 66 and 69-74 .	54
Chart 4.1:	Preparative methods for known group VI <i>s-trans</i> -diene complexes.	93
Chart 4.2:	Bonding modes of conjugated dienes.	94

List of Abbreviations

Å	angstrom
AIBN	2,2'-azobisisobutyronitrile
Atm	atmosphere
Bu	butyl
calcd	calculated
Cp	cyclopentadienyl
Cp*	pentamethylcyclopentadienyl or permethylcyclopentadienyl
Cy	cyclohexyl
COSY	correlated spectroscopy
d	doublet
DME	1,2-dimethoxyethane
EMHO	extended Hückel molecular orbital calculations
Et	ethyl
equiv	equivalent
FMO	frontier molecular orbital(s)
g	gram(s)
GC	gas chromatography
h	hour(s)
HMQC	heteronuclear multiple quantum coherence
Hz	Hertz
HOMO	highest occupied molecular orbital
IMes	1,3-bis-(2,4,6-trimethylphenyl)-imidazolin-2-ylidene
<i>i</i>	iso
IR	infrared
κ	Lewis base coordination
L	liter(s)

LUMO	lowest unoccupied molecular orbital
m	medium or multiplet
M	metal or mol/liter
Me	methyl
mL	milliliter(s)
MS	mass spectrometry
NMR	nuclear magnetic resonance
OTs	<i>p</i> -tolylsulfonate
Ph	phenyl
Pr	propyl
py	pyridine
PyMe ₃	2,4,6-trimethylpyridine
q	quartet
qu	quintet
R	alkyl group
s	singlet or strong
sept	septet
SOMO	singly occupied molecular orbital
<i>t</i>	tert
t	triplet
THF	tetrahydrofuran
TMS	trimethylsilyl
w	weak
X	halide
η	hapticity
μL	microliter(s)
↔	correlation

Chapter 1. Overview and introduction

1.1 Overview

The impetus for the research discussed in this dissertation is the formation of novel chromacyclobutane complexes via central carbon alkylation of chromium η^3 -allyl complexes. While addressing issues pertinent to the understanding of fundamental organochromium chemistry, this document unfortunately does not present any examples of chromacyclobutane formation. Instead, a thorough investigation of the synthesis and reactivity of novel chromium(II) and chromium(III) η^3 -allyl complexes is discussed.

Thermally stable chromium(0) nitrosyl complexes bearing conjugated diene ligands *exclusively* in the *s-trans* configuration have also been discovered during the course of this research. These unprecedented examples of first-row *s-trans* diene coordination, and related η^2 -diene precursors, are elaborated into unique cationic chromium(II) η^3 -allyl complexes. Even more tantalizing is the unprecedented oxidative addition of trialkyltin hydride moieties across a metal-diene bond to form highly stable bimetallic chromium-tin η^3 -crotyl complexes. Unfortunately, none of these η^3 -allyl complexes can be converted into chromacyclobutanes, but all nonetheless provide valuable insight into the relatively underdeveloped area of allylchromium chemistry.

To appreciate the potential significance of these advances in η^3 -allyl chromium chemistry toward the ultimate goal of chromacyclobutane formation, the relevance of metal-mediated reactions of the η^3 -allyl ligand in selective organic transformations will be introduced, with an emphasis on central carbon alkylations.

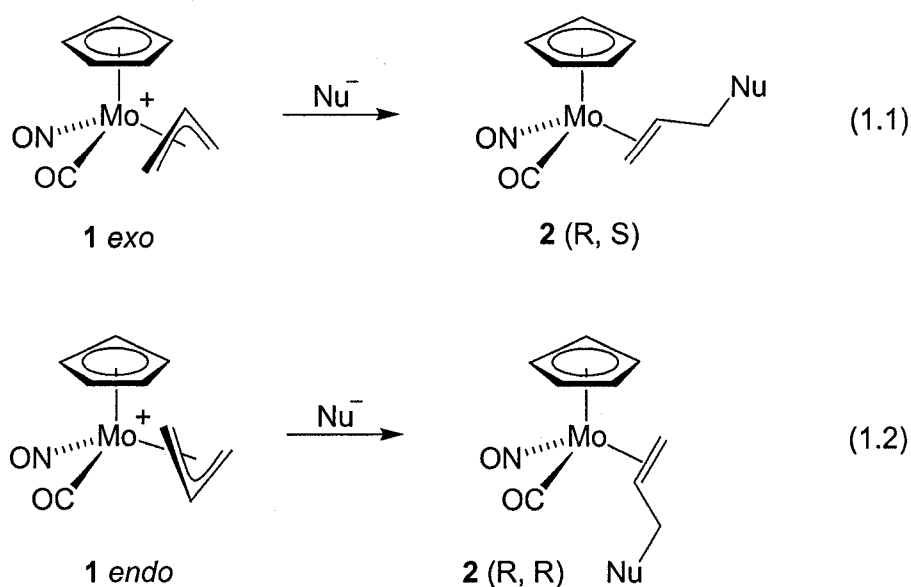
1.1 Introduction

1.1.1 Nucleophilic alkylation of η^3 -allyl complexes

Recently, the widely applied fields of transition metal-based asymmetric catalysis and olefin metathesis reactions were the subject of two Nobel prizes in chemistry.^{1, 2} These prestigious awards were testaments to the vital role played by transition metal complexes in contemporary benchtop and industrial chemistry. Of the numerous other applications of transition metal complexes in modern organic chemistry,³⁻⁶ regio- and stereoselective substitution at allylic carbon centres has been the subject of extensive investigation.

Much of this research has focused on generating allylically substituted organic compounds via nucleophilic alkylation of the terminal η^3 -allyl carbon of electrophilic η^3 -allyl complexes.⁷⁻¹⁹ Significant contributions in this area emerged from the groups of Tsuji^{20, 21} and Trost,²²⁻²⁴ where proallylic substrates were shown to react with nucleophiles in the presence of a palladium(0) catalyst, in a manner functionally analogous to the displacement of an allylic leaving group by an S_N2 or S_N2' mechanism. Nucleophilic additions to the terminal allylic carbon in several other transition metal η^3 -allyl systems including those of cobalt,²⁵⁻²⁸ iron,^{29, 30} rhodium,³¹⁻³⁶ and nickel³¹⁻³⁷ have also been reported.

More directly relevant to this investigation, remarkable stereoselectivity was observed upon nucleophilic additions to chiral cationic η^3 -allyl molybdenum complexes.³⁸⁻⁴² It was found, for example, that nucleophilic attack occurs *cis* to the nitrosyl ligand in the *exo* isomer of $\text{CpMo}(\text{CO})\text{NO}(\eta^3\text{-allyl})$, complex **1**, and *trans* in the complementary *endo* isomer (eqs. **1.1** and **1.2**, respectively).³⁸



To explain this notable selectivity, Faller and Hoffmann⁴⁰ calculated the LUMO for each isomer of complex **1** (Fig. 1.1). Since this antibonding combination has no orbital coefficient on the central carbon of the allyl ligand, it is reasonable that nucleophilic attack occurs at a terminal carbon. Since NO is a stronger π -acceptor than CO, there is an asymmetric electronic distribution on the terminal carbons of the allyl fragment. Thus, incident nucleophiles preferentially attack the most electropositive terminal carbon, giving rise to the above η^2 -olefin diastereomers **2** (R, S) and **2** (R, R), the configurations of which were determined in the solid-state.³⁹

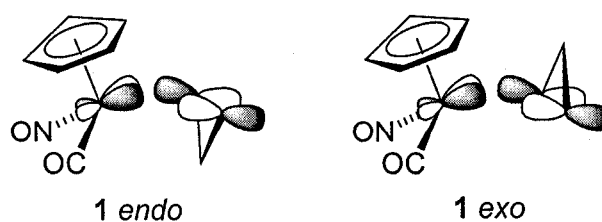


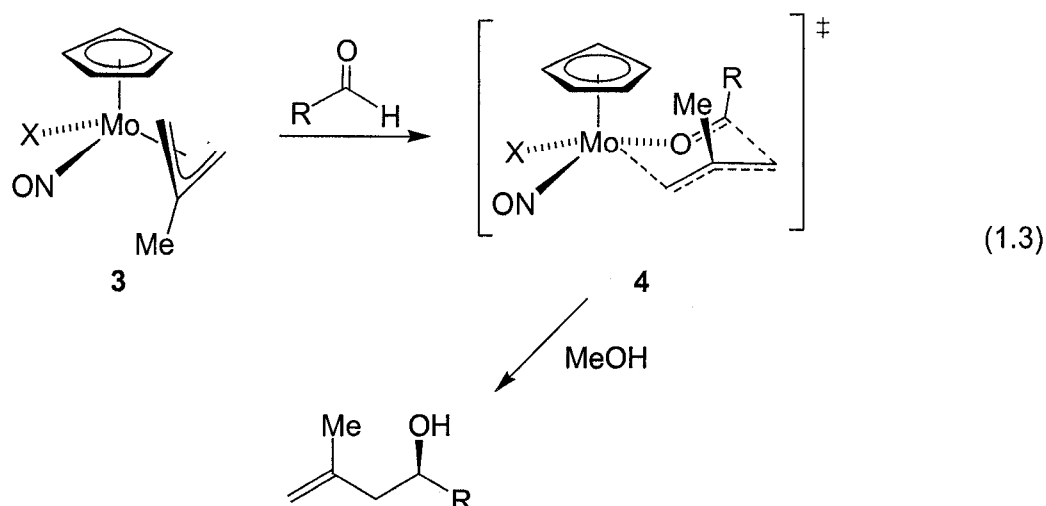
Figure 1.1: The antibonding acceptor molecular orbitals (LUMOs) of the *endo* and *exo* isomers of $\text{CpMo}(\text{CO})\text{NO}(\eta^3\text{-allyl})^+$ **1** (ref. 40).

Further analysis of the source of this selectivity involved extended Hückel calculations; the degree of hydride-allyl orbital overlap was calculated for the reaction of a hydride on each terminal carbon of the *endo* and *exo* isomers of complex **1**.^{40, 43-45} As seen in Table 1.1, the calculated results are in perfect agreement with the corresponding empirical observations.

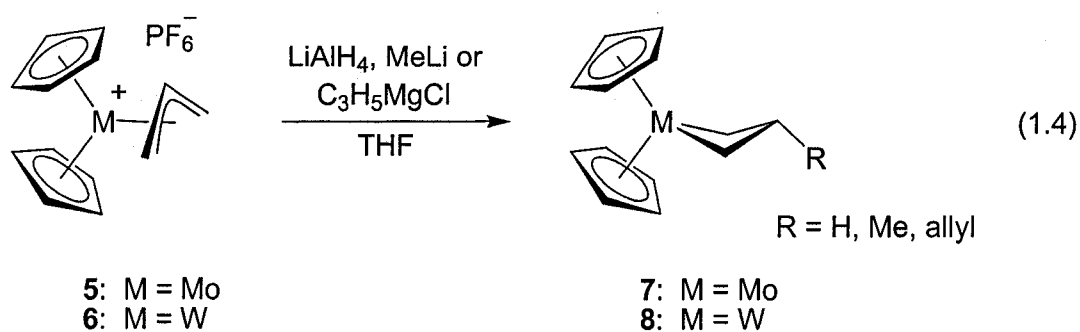
Table 1.1: Hydride-allyl carbon overlap populations, at a C-H distance of 1.75 Å; calculation for the reaction: $\text{CpMo(CO)NO}(\eta^3\text{-allyl})^+ + \text{H}^-$ (ref. 40).

Terminal Carbon	1 <i>exo</i>	1 <i>endo</i>
<i>cis</i> to NO	0.1870	0.1627
<i>trans</i> to NO	0.1034	0.1636

It is also worth noting that cationic complexes such as **1** are easily converted to neutral species of the general formula $\text{CpMo(NO)}(\eta^3\text{-allyl})\text{X}$ (X = camphorsulfonate, Cl, Br, or I) via addition of corresponding salts.^{46, 47} More interesting, however, is the nucleophilic reaction of these neutral chiral complexes, such as $\eta^3\text{-(2-methylallyl)}$ complex **3**, with aldehydes, via the putative six-membered oxometallacyclic transition state **4**, to give enantiomerically pure homoallylic alcohols (eq. 1.3). Reaction rates are highly dependant on the halide ligand; chloride complexes produce alcohols after one day at room temperature, while the iodide analogues require over one week for completion. Additionally, aliphatic aldehydes were shown to react faster at room temperature.⁴⁶



The first example of central carbon alkylation of η^3 -allyl complexes was reported by M. L. H. Green *et al.*;^{48, 49} cationic molybdocene and tungstenocene η^3 -allyl complexes **5** and **6**, when treated with nucleophiles, experienced exclusive attack at the central η^3 -allyl carbon position to give metallacyclobutane complexes **7** and **8**, respectively (eq. 1.4).



This spectacular result was rationalized using the Davies-Green-Mingos (DGM) rules,⁵⁰ which hold that nucleophilic addition is directed to the most electrophilic carbon of the allyl ligand. The effect of complexing an allyl ligand to an electron rich metal

fragment, such as the d^2 Cp_2M systems ($\text{M} = \text{Mo}, \text{W}$), is partial negative charges on the terminal carbons relative to the central carbon (Fig. 1.2).

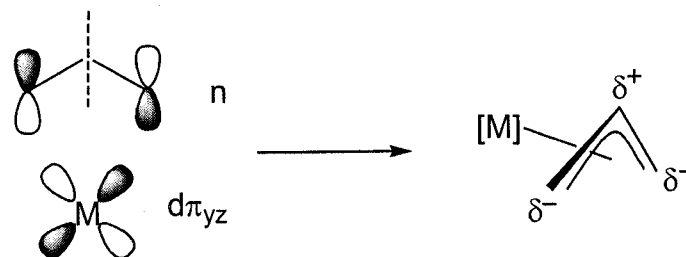
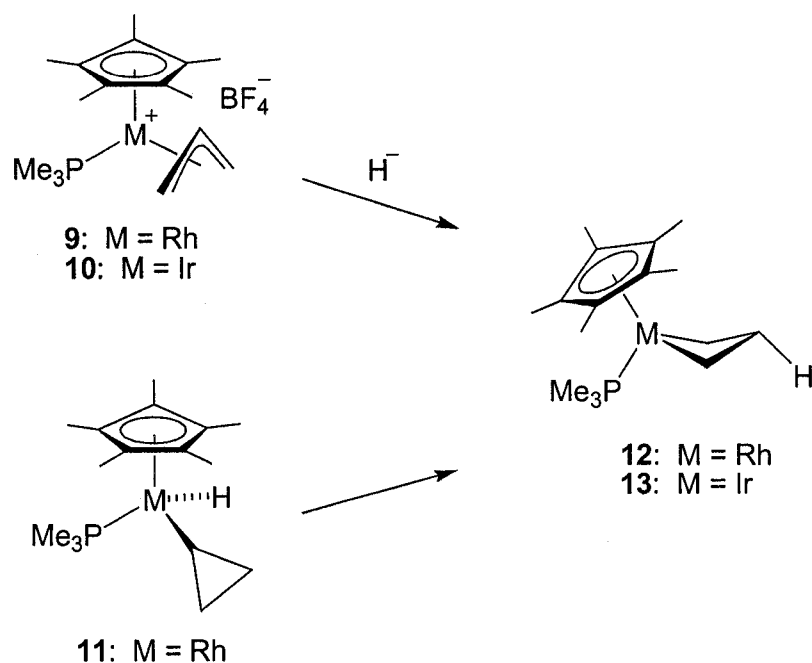


Figure 1.2: The bonding FMO interaction of the allyl and Cp_2M fragments of complexes **5** and **6** ($\text{M} = \text{Mo}, \text{W}$), and the resulting partial charges of the η^3 -allyl ligand.

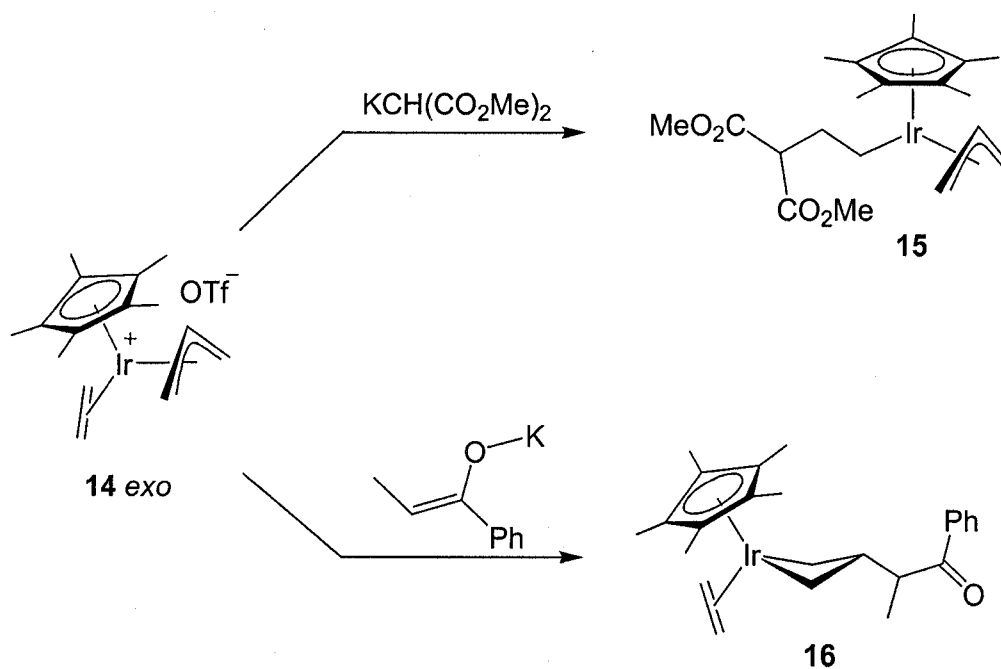
This charge control argument sufficiently explained the reactivity for many subsequently reported transition metal η^3 -allyl complexes.⁵¹⁻⁵⁸ However, a detailed investigation into half-sandwich group IX allylmetallocene complexes $[\text{Cp}^*(\text{L})\text{M}(\eta^3\text{-allyl})]\text{X}$ ($\text{M} = \text{Rh}, \text{Ir}$; $\text{X} = \text{BF}_4, \text{PF}_6, \text{OTf}$; $\text{L} = \text{PMe}_3$; $\text{Cp}^* = \text{C}_5\text{Me}_5$) provided intriguing findings, many in direct contradiction to the DGM rules. Addition of hydride reagents to $[\text{Cp}^*(\text{PMe}_3)\text{M}(\eta^3\text{-allyl})]\text{BF}_4$ ($\text{M} = \text{Rh}, \text{Ir}$) **9** and **10**, for example, provides rhodacyclobutane complex **12** and the iridium analogue **13** (Scheme 1.1). Complex **12** may also be obtained from an intramolecular thermal rearrangement of the hydrido cyclopropyl complex **11** at low temperature.

Scheme 1.1



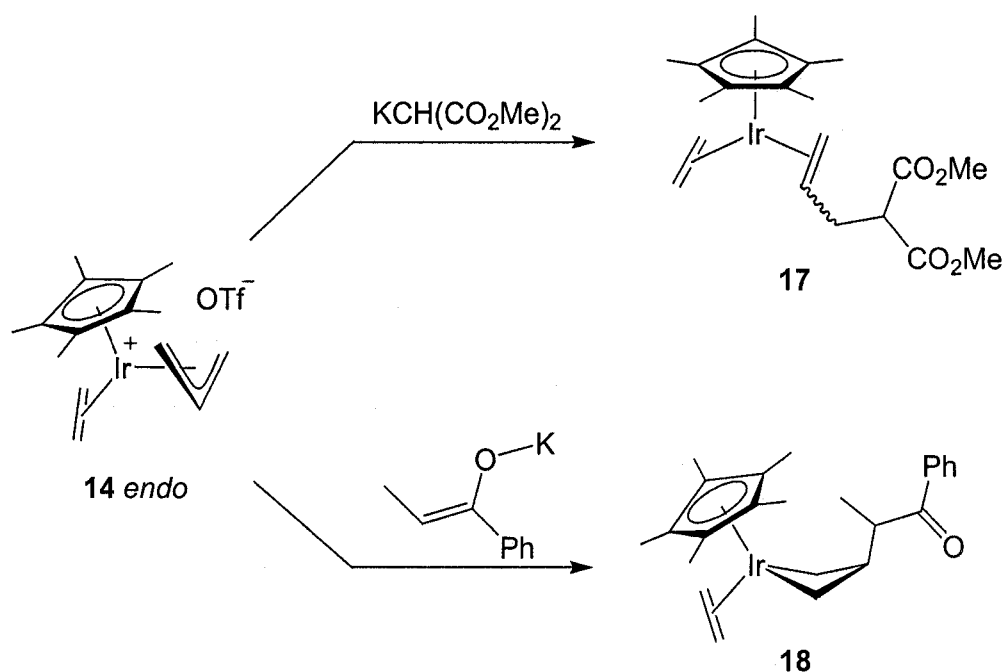
Subsequent investigations by the Stryker group⁵⁹⁻⁶⁵ revealed that nucleophilic addition to the ethylene analogue **14** of η^3 -allyl complex **9** is not only dependent on the nature of the nucleophile, but also on the configuration of the allyl ligand. When the *exo* isomer of complex **14** is treated with the potassium enolate of dimethyl malonate, the nucleophile attacks the ethylene carbon exclusively to give the allyliridium complex **15**. Here, the experimental results are in agreement with the DGM rule: nucleophilic attack preferentially occurs at an even, open polyene over addition to an odd, open polyene. Treating complex **14** *exo* with the potassium enolate of propiophenone, however, violates this DGM rule and results in exclusive formation of the iridacyclobutane complex **16**, the result of central carbon addition to the η^3 -allyl ligand (Scheme 1.2).

Scheme 1.2



In the case of the *endo* isomer of complex **14**, addition of the same enolate salts results in substitution solely at the allyl ligand; not at the ethylene group as the DGM rules predict. When using the potassium enolate of dimethylmalonate, addition is directed to the *terminal* carbon of the allyl ligand, resulting in a mixture of bis(olefin) stereoisomers of complex **17**. The potassium enolate of propiophenone, however, gives exclusively the central carbon alkylation product **18** (Scheme 1.3); diastereomeric with the *exo* η³-allyl adduct.

Scheme 1.3



In addition to the molecular orbital rationalization for terminal η^3 -allyl carbon substitution in the electron deficient molybdenum complex **1**, and the qualitative charge control argument for central carbon addition in the relatively electron rich molybdenum and tungsten complexes **5** and **6**, subsequent molecular orbital calculations^{54, 58, 66-71} have been employed to further explain the regioselectivity of nucleophilic addition to η^3 -allyl complexes, such as the late metal complexes **10**, **11**, and **14** described above.

Computations⁶⁶ have shown, for example, that the central carbon is positively charged with respect to the terminal carbons in all η^3 -allyl complexes; kinetic regioselectivity is thus likely frontier orbital controlled. The position undergoing nucleophilic attack must have a substantial coefficient in a vacant low energy orbital (LUMO) to accept electrons from the incoming nucleophile. In the case of most late metal η^3 -allyl complexes, the metal d orbitals overlap with the allyl bonding (π),

nonbonding (n), and antibonding (π^*) orbitals (Fig. 1.3). Of the resultant molecular orbitals, the combination which acts as the LUMO determines the regiochemical outcome of the nucleophilic reaction. Nucleophilic addition to a terminal allyl carbon occurs if the LUMO is a combination between a metal d orbital and the allyl nonbonding orbital. As discussed for molybdenum complex **1**, this combination of orbitals possesses coefficients only on the terminal carbons. Central carbon alkylation, on the other hand, occurs when the LUMO is a combination between a metal d orbital and the allyl π^* orbital, as the coefficient on the central carbon is calculated to be larger than those on the terminal carbon atoms (Fig. 1.3).⁶⁶

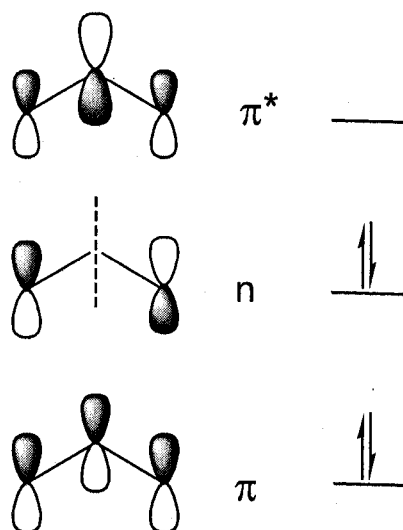


Figure 1.3: The molecular orbitals of an η^3 -allyl ligand fragment.

It was also tentatively predicted by computations that cationic group IV metallocene complexes $[\text{Cp}_2\text{M}(\eta^3\text{-allyl})]^+$ might also experience nucleophilic attack at the central carbon to give metallacyclobutane complexes.⁶⁶ As shown in Figure 1.4, the MO energy level diagram for d^0 group IV metallocene η^3 -allyl complexes indicates that the

LUMO is the bonding combination between the metal $d(3a_1)$ orbital and the allyl π^* orbital.^{66, 72, 73}

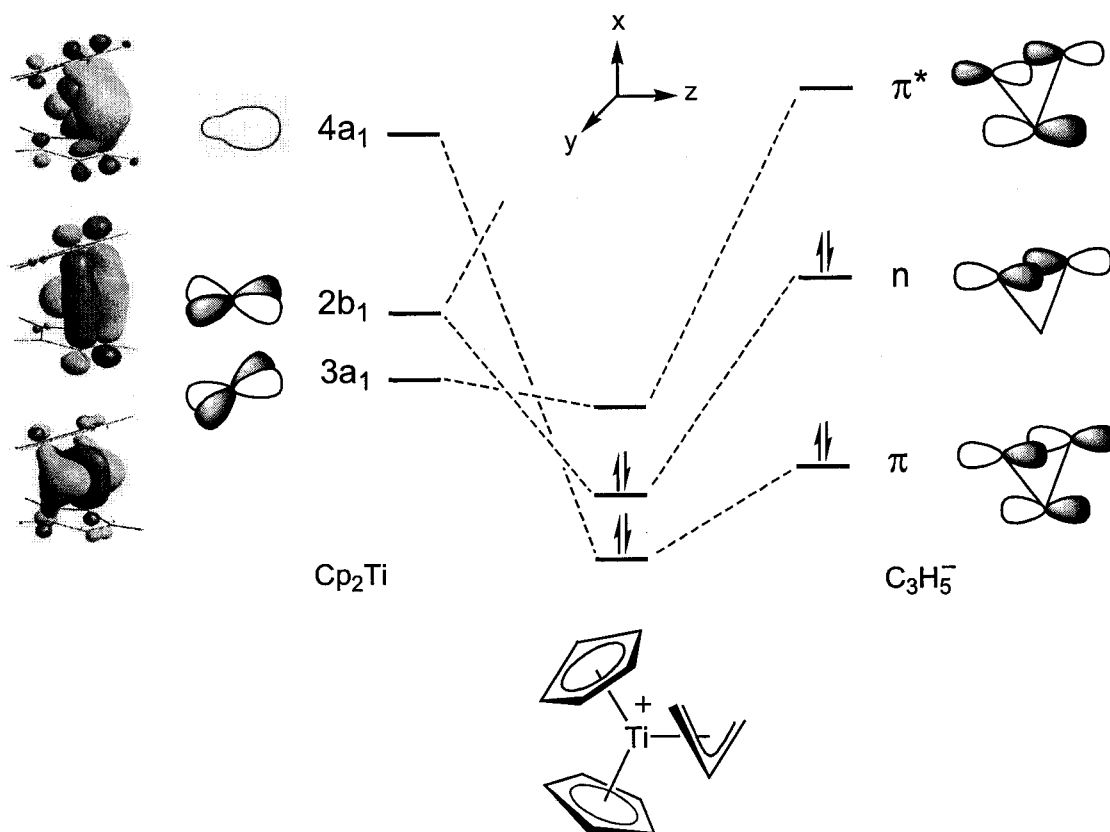
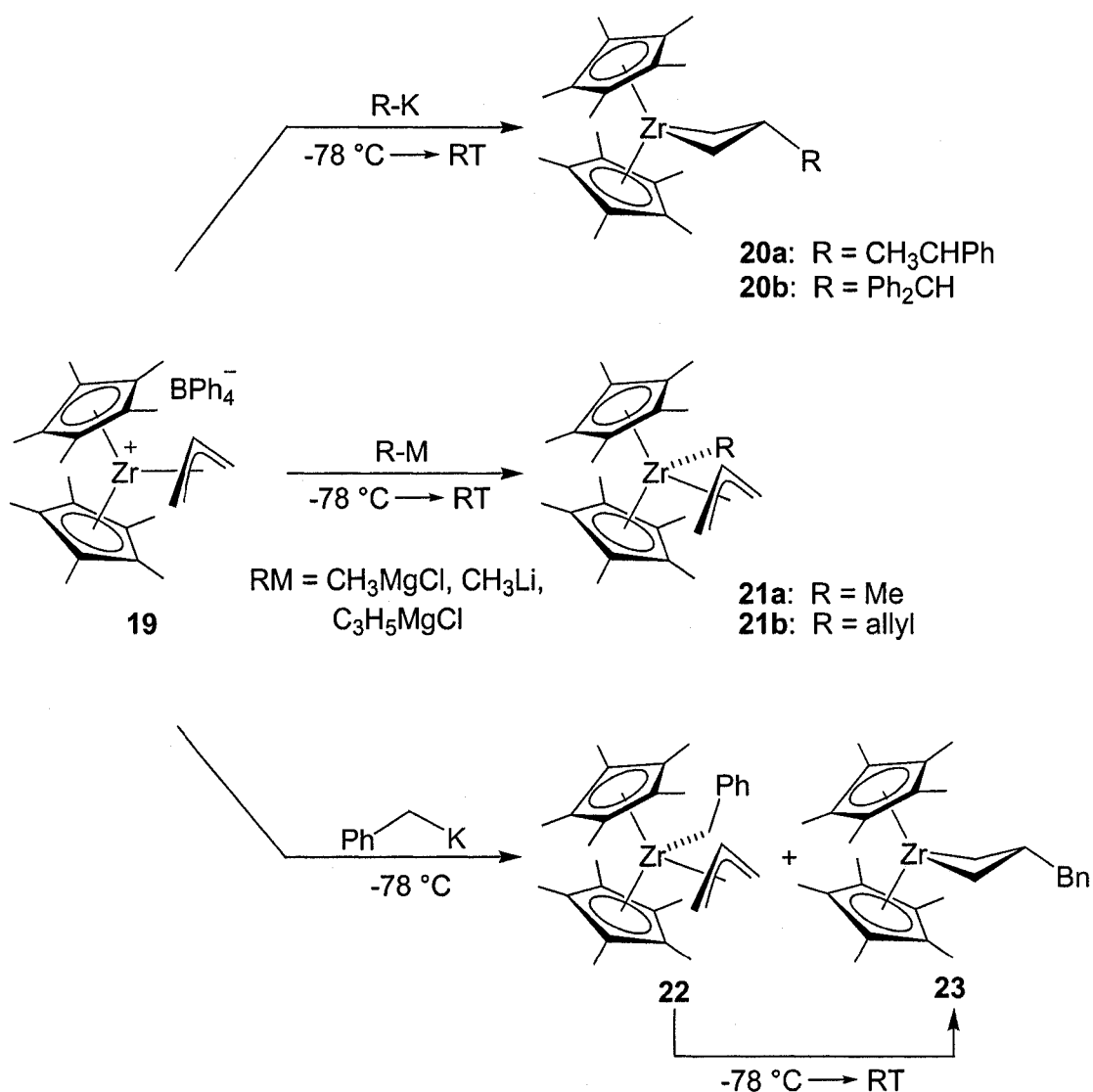


Figure 1.4: MO energy level diagram for d^0 group IV metallocene η^3 -allyl complexes.

Corroboration of this theory with experiment was established by the Stryker group^{60, 74} which showed that addition of sterically imposing nucleophiles to the zirconocene η^3 -allyl complex **19** does indeed provide the β -substituted zircona-cyclobutane complex **20**. Smaller nucleophiles, however, preferentially attack the metal centre, giving the alkyl allyl zirconocene complex **21**, while benzylpotassium, a

nucleophile with an intermediate steric profile, shows a kinetic partitioning between the metal and central carbon positions, giving rise to complexes **22** and **23**, respectively (Scheme 1.4). It was also noted that, upon warming to room temperature, complex **22** slowly rearranges to the more thermodynamically favoured zirconacyclobutane complex **23**, a reaction that most probably involves radical intermediates.

Scheme 1.4



Similar treatment of the analogous titanium(IV), d^0 complex $[\text{Cp}^*_2\text{Ti}(\eta^3\text{-allyl})]\text{BF}_4$ **24** with nucleophiles of various steric profiles *exclusively* gives central carbon alkylation products.^{60, 75, 76} One explanation for this more selective reactivity is the smaller ionic radius of titanium compared to that of zirconium restricts access to the electronically unsaturated metal centre by the approaching nucleophile.

Extending this reactivity to very small (*e.g.*, MeLi, LiAlH_4 , LiEt_3BH) or highly hindered (*e.g.*, KCHPh_2) nucleophiles met with little success. Only in the case of LiEt_3BH , under an atmosphere of ethylene did the desired titanacyclobutane complex form cleanly. The use of substituted allyl substrates in this series also generally failed to give 2,3-disubstituted titanacyclobutane complexes.⁷⁶ For example, addition of nucleophiles to the cationic 1-phenylallyl complex $[\text{Cp}^*_2\text{Ti}(\eta^3\text{-C}_3\text{H}_4\text{Ph})]\text{BPh}_4$ **25** results in formation of cinnamyl radical and reduced organotitanium products.

1.1.2 Titanacyclobutane formation via organic free radical addition to titanium(III) η^3 -allyl complexes

To overcome the apparent limitations of titanacyclobutane formation via nucleophilic addition to cationic titanium(IV) η^3 -allyl complexes, the Stryker group began investigations into organic free radical addition to neutral d^1 titanium(III) η^3 -allyl complexes. Indeed, extending the above FMO prediction^{66, 72, 73} to include such additions to metallocene radicals requires only that the $3a_1$ orbital of the organometallic fragment be occupied by one electron. The electron from an incoming organic free radical is then expected to add to the singly occupied molecular orbital (SOMO) bonding combination between the metal $3a_1$ orbital and the η^3 -allyl π^* orbital (Fig. 1.5).

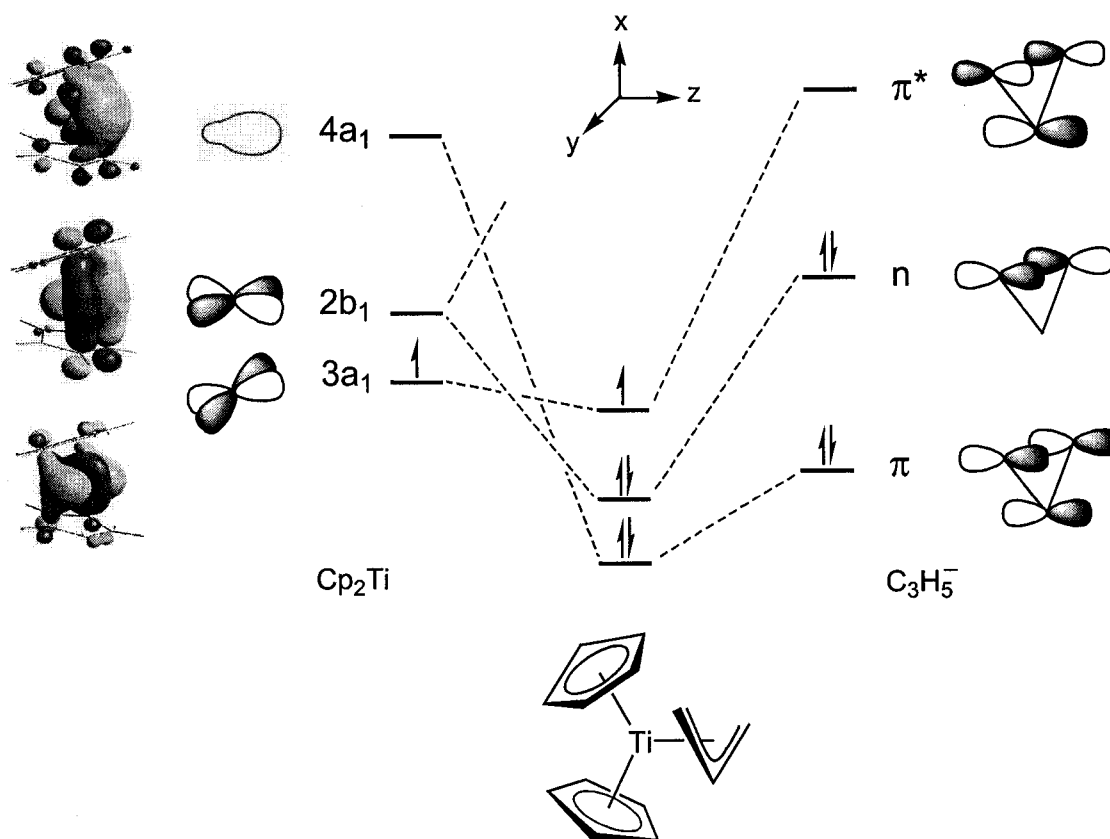
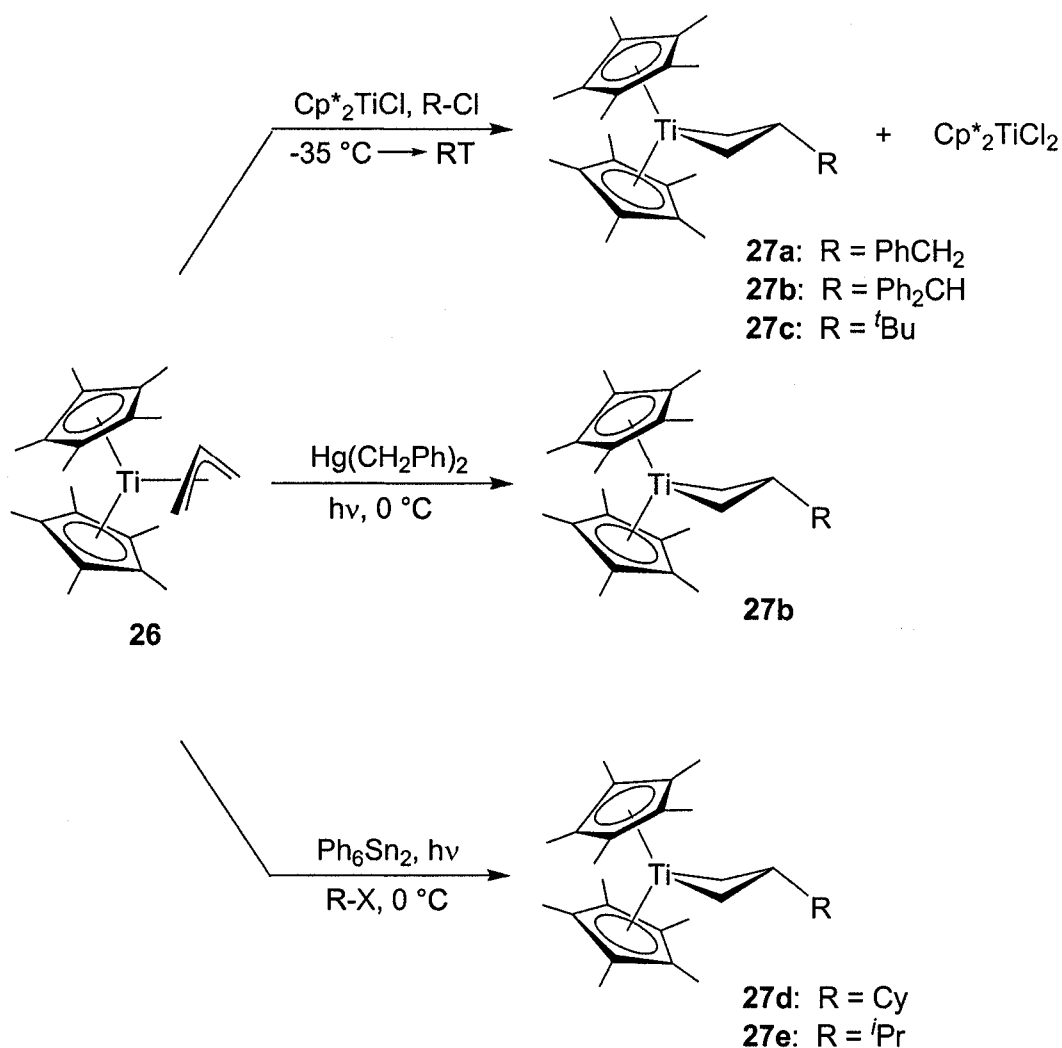


Figure 1.5: MO energy level diagram for d^1 group IV metallocene η^3 -allyl complexes.

Thus, Casty and Stryker reported the first highly regioselective free radical addition to the central allyl carbon of $\text{Cp}^*_2\text{Ti}(\eta^3\text{-allyl})$ complex **26** under a variety of radical generating reaction conditions (Scheme 1.5).^{75, 77} Use of Cp^*_2TiCl as a radical generating source was limited to halide abstraction from activated organic halides, but provides titanacyclobutane complexes **27** and $\text{Cp}^*_2\text{TiCl}_2$ in excellent yield. Generation of radicals by photolytic decomposition of benzyl mercuric salts⁷⁸ provided benzyl titanacyclobutane complex **27b**, albeit in much lower yield. Photolytic activation of hexaphenylditin⁷⁹ in the presence of secondary alkyl halides resulted in the formation of

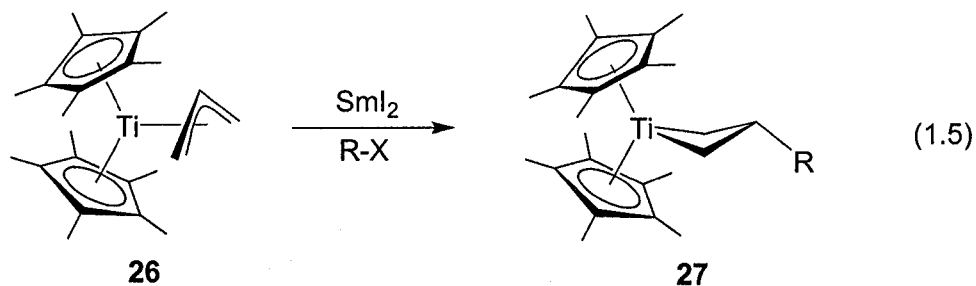
titanacyclobutane complexes **27d** and **27e**, but failed when more activated tertiary and benzylic halides were used. Although these experiments provide compelling evidence for a radical alkylation process, they lack the generality required for synthetic applications.

Scheme 1.5



Samarium diiodide,^{80, 81} however, proved to be the most general and synthetically practical reagent for the preparation of titanacyclobutane complexes (eq. 1.5). This halophilic one electron reductant easily generates stabilized and unstabilized alkyl

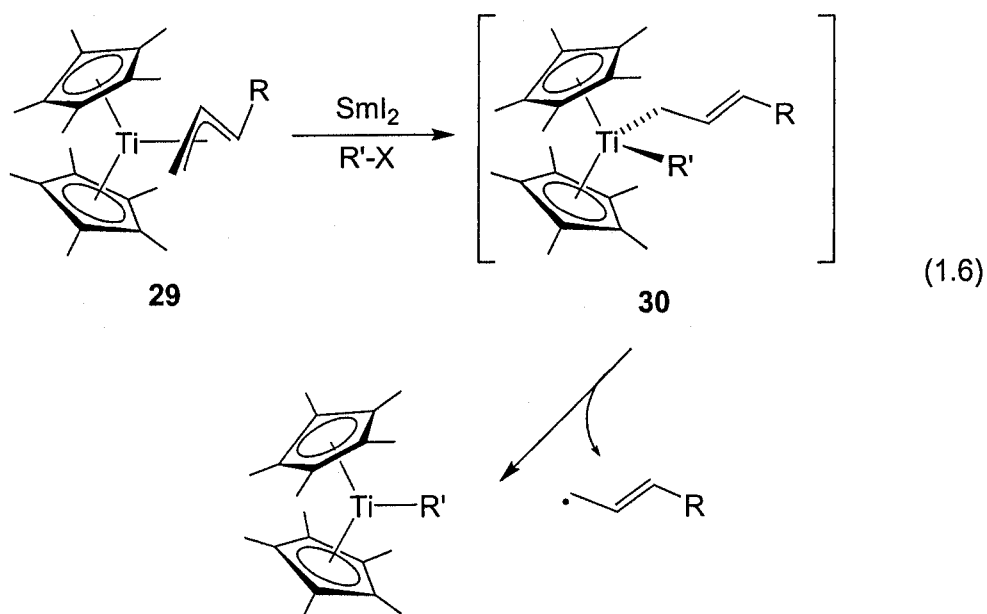
radicals from alkyl halides. Moreover, the co-generated Sm(III)trihalide compounds are easily separated from the titanacyclobutane products by trituration of the crude reaction mixture with pentane.



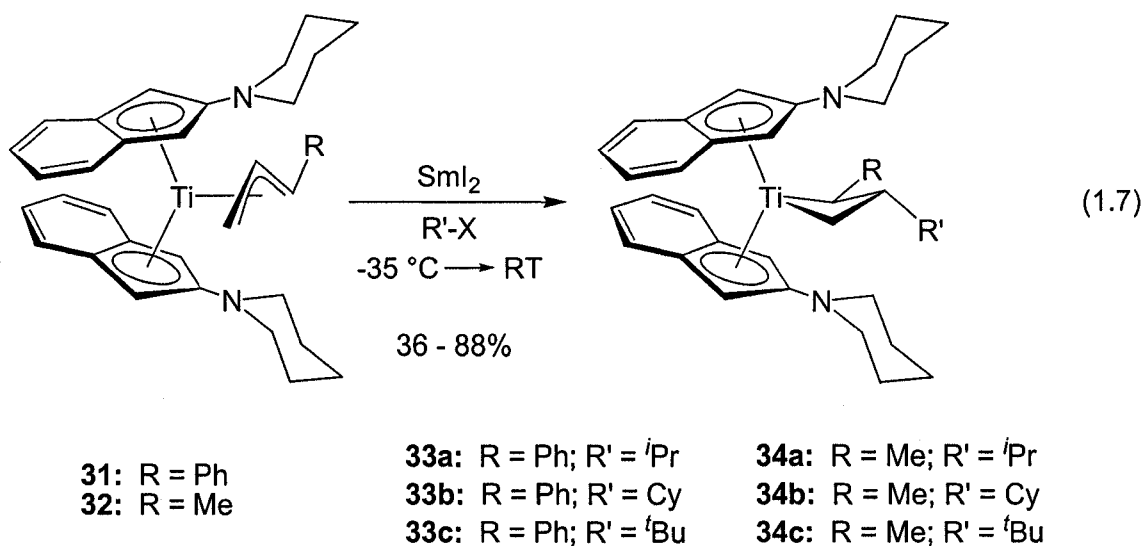
It was also found that the electron donating ability of the ancillary ligands is essential for successful titanacyclobutane formation. Only the addition of the *tert*-butyl radical gave a titanacyclobutane complex upon attempted alkylation of the more electron deficient $\text{Cp}_2\text{Ti}(\eta^3\text{-allyl})$ complex **28**.^{75, 82} This decrease in electron density at the metal is assumed to deleteriously affect the degree of $d \rightarrow \pi^*$ backbonding into the π^* orbital of the allyl ligand, reducing the delocalization of the odd-electron density on the central allyl carbon (see Fig. 1.5).⁸³

Despite the encouraging results with the $\text{Cp}^*_2\text{Ti}(\eta^3\text{-allyl})$ template, this system is incompatible with substituted allyl ligands; radical addition to such complexes was found to occur at the metal centre rather than at the central carbon of the allyl ligand.^{75, 76, 84} A hapticity change from η^3 - to η^1 -coordination of the allyl ligand (**29** to **30** in eq. 1.6) or significant distortion to η^1, η^2 - (σ, π)-bonding was cited as the most probable source of this unfortunate reactivity pathway.⁸³ This type of isomerism is common in d^0 metallocene complexes of zirconium and titanium, where no backbonding is available to localize

the η^3 -coordination mode.⁸⁵⁻⁸⁹ This bias toward η^1 -allyl coordination in substituted Cp*Ti(III) allyl complexes is thought to arise from a combination of weak one-electron backbonding, unfavourable steric interactions between the allyl and ancillary ligands, and inherently weak metal-carbon bonding anticipated for the substituted position.⁸³ Thus, more recent research in the Stryker group has been directed toward the use of less sterically imposing and strongly electron-donating templates to enhance the $d(3a_1) \rightarrow \pi^*$ one-electron backbond.

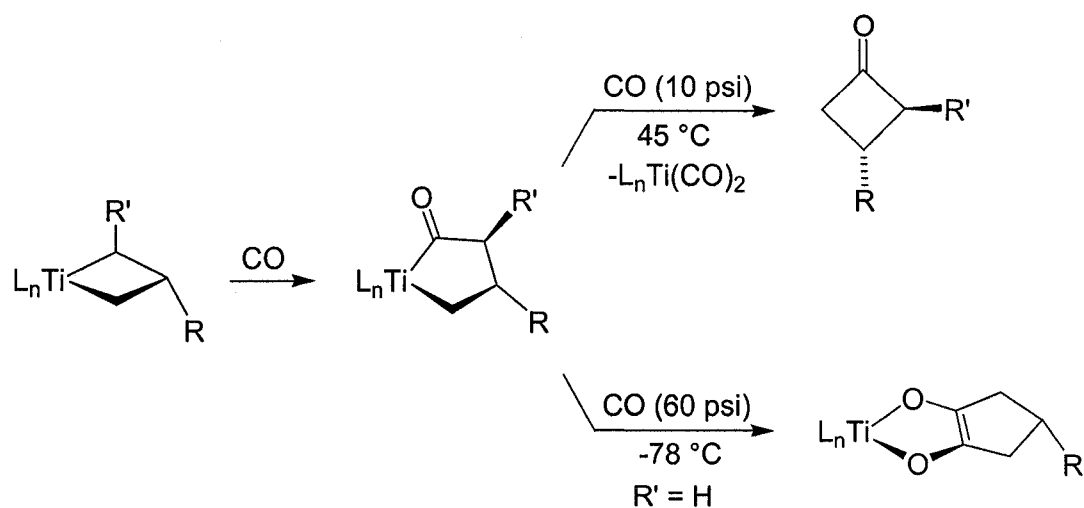


The first regio- and stereoselective synthesis of 2,3-disubstituted titanacyclobutane complexes was subsequently developed via the use of η^3 -cinnamyl and η^3 -crotyl bis(2-piperidinoindenyl)titanium(III) complexes **31** and **32** (eq. 1.7).⁹⁰ Unfortunately, the crotyl-derived titanacyclobutane complexes **34a-c** are thermally sensitive, degrading slowly at room temperature via β -hydride elimination from the α -methyl substituent.

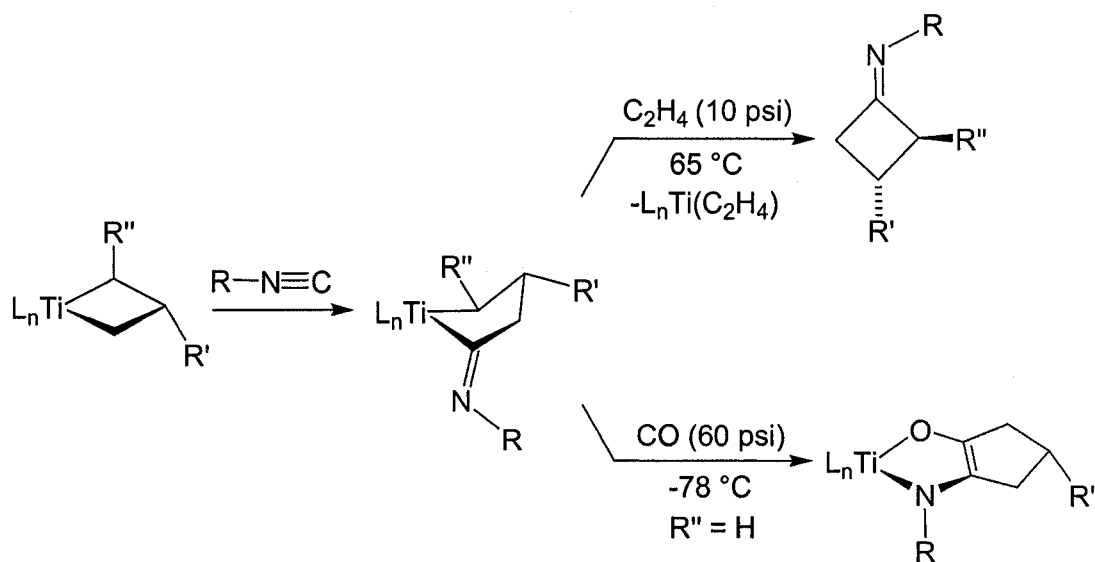


It has also been shown that these and other titanacyclobutane complexes undergo carbonylation and isonitrile insertion reactions to provide unique organotitanium species or synthetically valuable⁹⁰ carbocyclic compounds, along with readily recyclable titanium byproducts (*e.g.*, Schemes 1.6 and 1.7).^{76, 83, 91, 92} These unprecedented synthetic pathways are but a sample of the numerous reactions available for converting titanacyclobutane complexes to important organic and organometallic compounds.⁹³

Scheme 1.6



Scheme 1.7



To avoid the limitations inherent in some of the above titanacyclobutane syntheses, others in the Stryker group have endeavoured to expand the library of $Ti(III)(\eta^3\text{-allyl})$ templates by designing additional indenyl ancillary ligands of varying

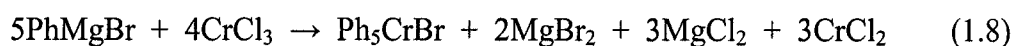
steric and electronic profiles.^{83, 94, 95} An alternative strategy, however, is the identification of another series of odd-electron first-row transition metal η^3 -allyl complexes, which may be more tolerant of a higher degree of substitution on both the η^3 -allyl and metallacyclobutane moieties.

A trend common to all of the above metallacyclobutane complexes is the qualitative geometry of the η^3 -allyl precursor. Whether the mechanism of metallacyclobutane formation involves nucleophiles or radicals, these group IX, VI, and IV η^3 -allyl complexes adopt a *pseudo*-tetrahedral geometry. As a result, η^3 -allyl complexes suggested for further investigation of novel metallacyclobutane formation are assumed to require this reaction-specific geometry; this coordination requirement presumably reflects maintaining the desirable FMO situation to promote central carbon alkylation. These complexes must also be comprised of a metal centre with readily accessible adjacent oxidation states, a necessary condition for free radical central carbon addition.

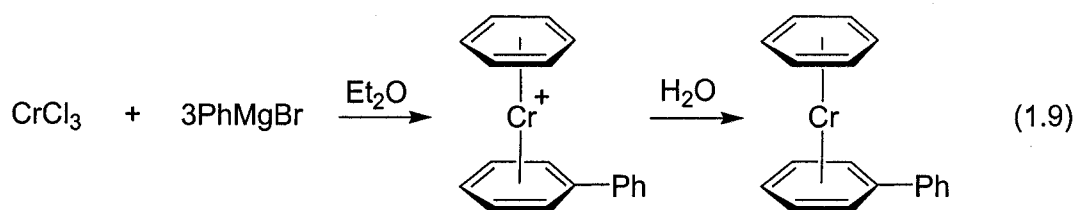
Since energetically reasonable organometallic complexes of chromium adopt adjacent oxidation states from +1 to +4 (+2 and +3 being the most common),⁹⁶ we began our study by targeting the synthesis of η^3 -allyl chromium complexes potentially amenable to central carbon addition. In addition to preparing fundamentally interesting chromacyclobutanes, developing such chemistry is itself a significant contribution to applied organochromium chemistry in general.

1.1.3 A brief overview of organochromium applications

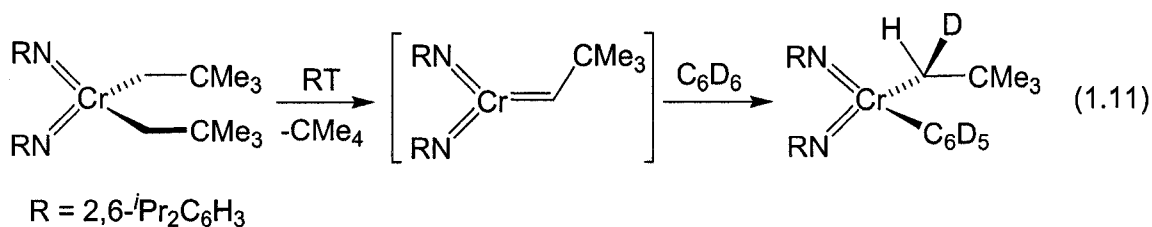
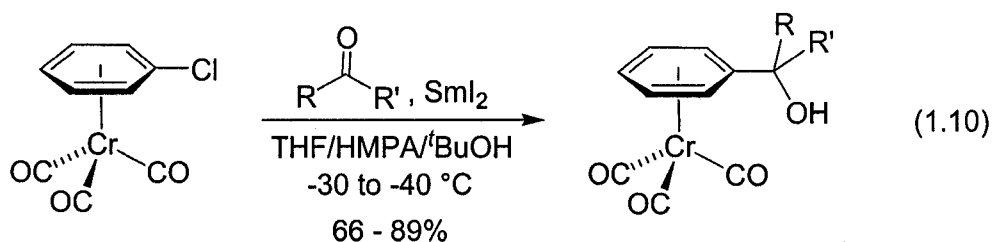
The first investigations in organochromium chemistry began in 1919 when Franz Hein studied the reaction between PhMgBr and CrCl_3 . Following hydrolytic workup, a crude orange powder was isolated and tentatively identified as Ph_5CrBr . Formation of this unexpected product was rationalized by a valence disproportionation reaction (eq. 1.8).⁹⁷

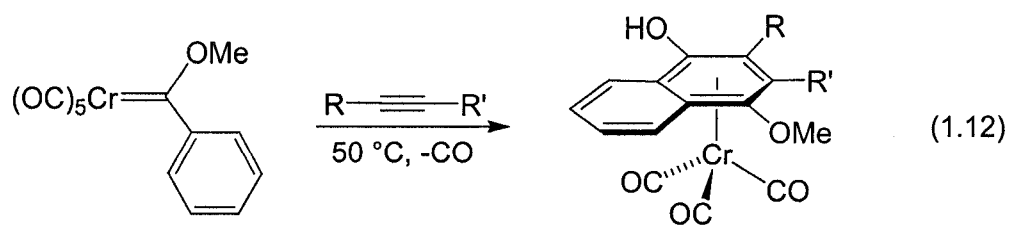


Due in part to Hein's 1919 statement, "...I therefore direct to all my esteemed colleagues in this area the request to leave to me the organochromium compounds for my further study",⁹⁷⁻¹⁰⁰ it was more than thirty years before the true identity and significance of this compound became known. Following the landmark discovery of ferrocene¹⁰¹⁻¹⁰³ and subsequent synthesis of chromocene,¹⁰⁴⁻¹⁰⁶ Zeiss and Tsutsui¹⁰⁷ proposed that Hein's crude product was actually a bis(arene) species (eq. 1.9), the first η^6 -arene transition metal complex (*i.e.*, a π -bonded, rather than a σ -bonded, complex).¹⁰⁸ This assertion was later confirmed by Fischer,¹⁰⁹ the co-discoverer of bis(benzene)chromium.¹¹⁰⁻¹¹² After the identification and improved understanding of these complexes, the number of applications of organochromium compounds in synthetic organic chemistry, particularly those involving organochromium π -complexes, increased tremendously, the details of which have been extensively reviewed.^{98-100, 113-119}

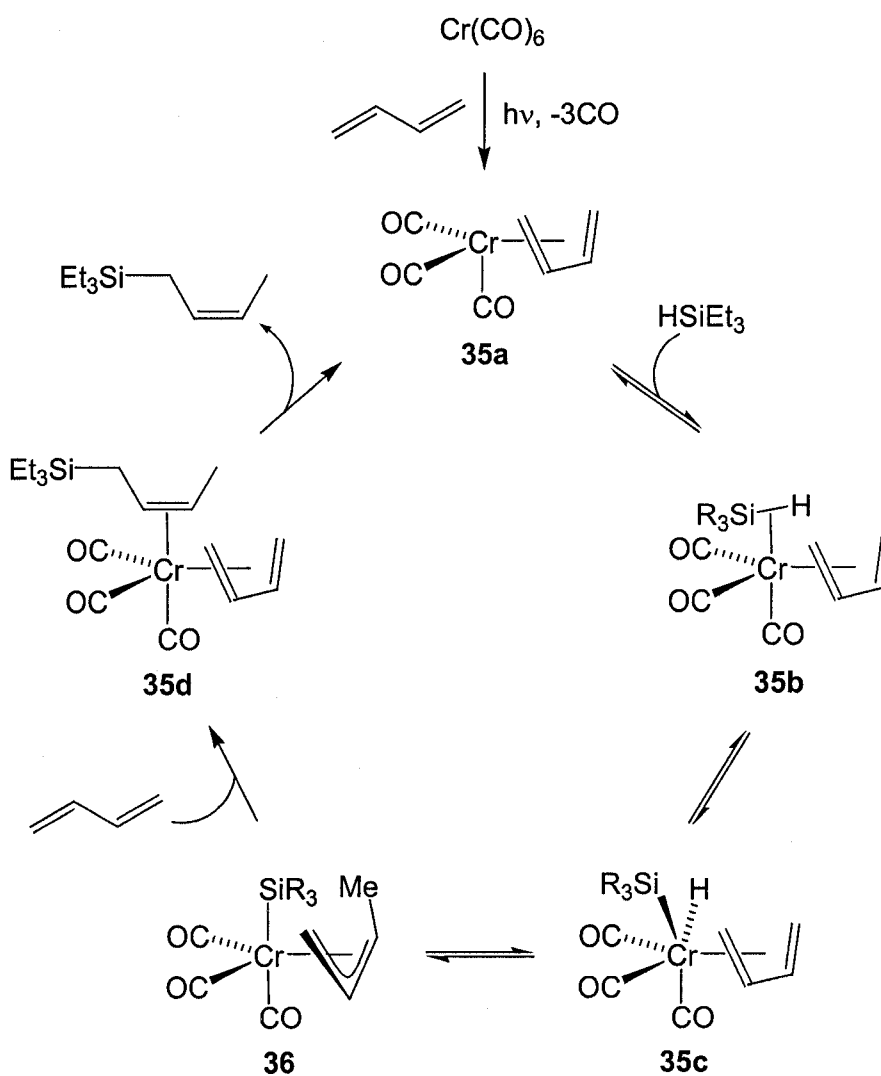


Notable among these interesting developments in organochromium chemistry are carbon-carbon bond formations starting with arene-chromium templates (*e.g.*, eq. 1.10),¹²⁰ C-H activation reactions (eq. 1.11),¹²¹ Fischer-carbene alkyne cyclizations (*i.e.*, the Dötz reaction, eq. 1.12),^{119, 122} and catalytic hydrosilylation reactions (Scheme 1.8).¹²³

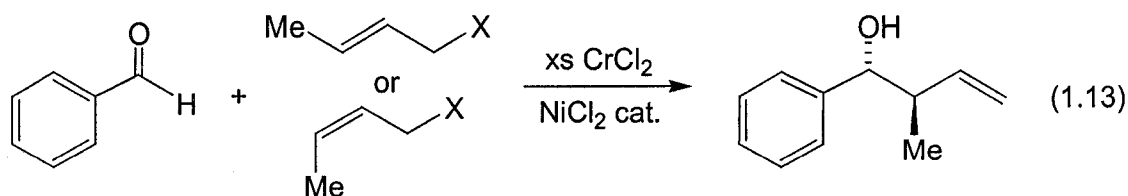




Scheme 1.8

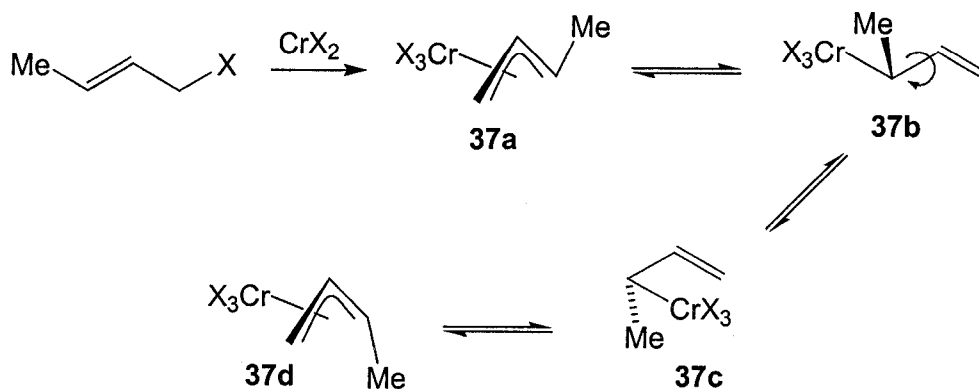


Perhaps the most common use of chromium reagents in synthetic organic chemistry is the Nozaki-Hiyama-Kishi (NHK) reaction, a highly stereo- and chemoselective organochromium-mediated nucleophilic addition of vinyl or allyl moieties to aldehydes that provides allylic or homoallylic alcohols.^{118, 124} An attractive feature of this reaction is the product selectivity observed when isomeric mixtures of allyl compounds are used. The reduction of benzaldehyde, for example, in the presence of both (*E*) and (*Z*) isomers of 3-methylallyl leads exclusively to the *anti* product (eq. 1.13).¹²⁵

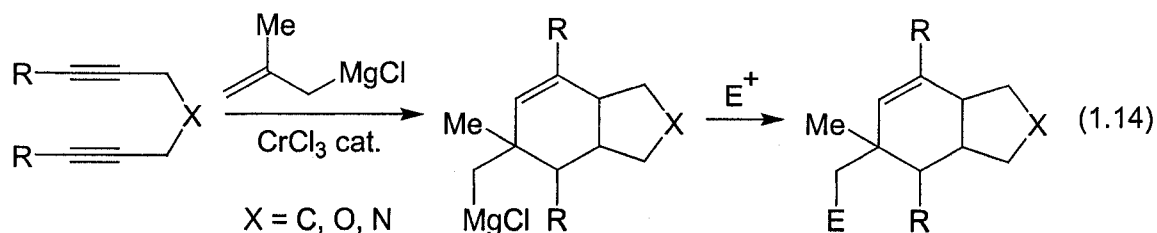


The origin of this stereoconvergence is attributed to the equilibration of the chromium(III) *syn*- η^3 -crotyl species **37a**, which isomerizes to the *anti*-species **37d** via formation of the η^1 -crotyl complex **37b**. Subsequent bond rotation and re-formation of the η^3 -crotyl moiety generates **37d** (Scheme 1.9).¹²⁵ This and other synthetically valuable NHK reactions¹¹⁸ were made even more appealing with the advent of Fürstner's chromium-*catalyzed* NHK methodology,¹²⁶ which in subsequent investigations has been extended to include enantioselective reactions via the incorporation of chiral ancillary ligands.^{127, 128}

Scheme 1.9



Oshima has recently modified the NHK reaction by the *in situ* preparation of allylchromate reagents [*i.e.*, (allyl)₄Cr anions]. These uncharacterized compounds effectively catalyze [2 + 2 + 2] cyclization reactions of diynes and enynes in the presence of excess allyl Grignard reagents. The resulting bicyclic organomagnesium compounds undergo further functionalization with electrophiles (eq. 1.14).^{129, 130}



Mononuclear organochromium complexes are also effective homogeneous catalysts for olefin polymerization and oligomerization reactions. For example, the research groups of Theopold,^{131, 132} Jolly,^{133, 134} and Enders¹³⁵ have independently developed constrained geometry pre-catalysts bearing *ansa*-bridged cyclopentadienyl

ligands (complexes **38-40**), while Bercaw^{136, 137} has recently developed hemilabile nitrogen-bridged diphosphine complexes **41** for the trimerization of ethylene (Chart 1.1).

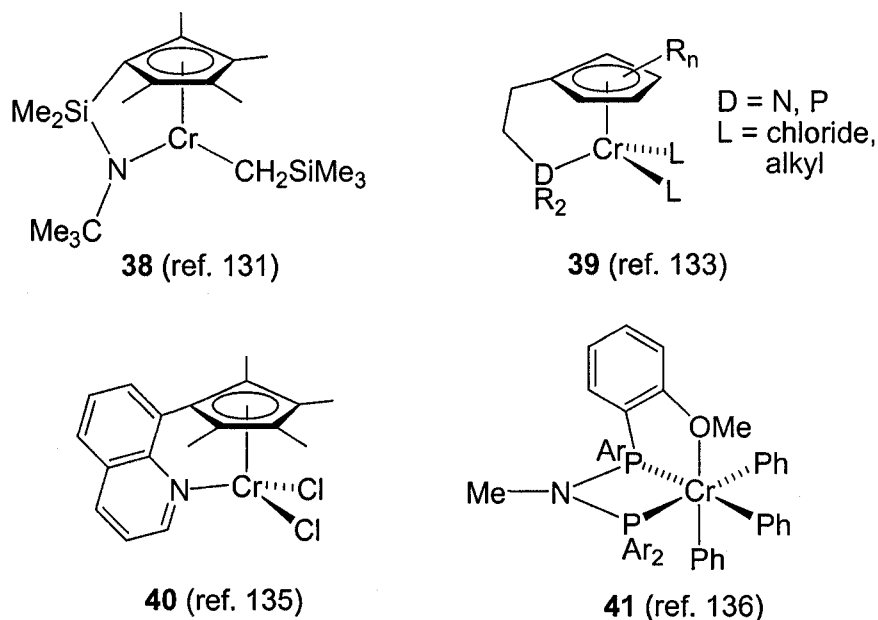
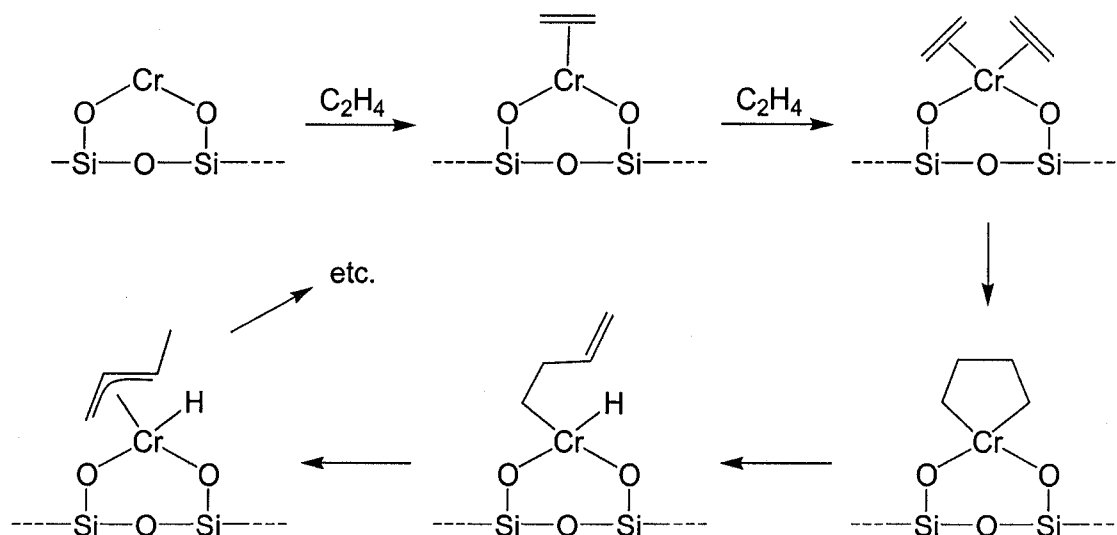


Chart 1.1: Constrained geometry chromium(III) pre-catalysts employed in olefin polymerization (complexes **38-40**) and trimerization reactions (complex **41**).

One of the main functions of these single-site catalysts is to improve understanding of commercial multi-site heterogeneous chromium polymerization catalysts; the chemical nature of the active sites of such catalysts remains the subject of wide-ranging speculation.^{131, 138} One such heterogeneous chromium catalyst, originally developed at Union Carbide, is prepared by impregnating silica with chromocene, while a second (the Phillips catalyst) is prepared by reduction of chromate (CrO_4^{2-}) deposited on silica.^{131, 138} In both systems the chemical structure, valence state, and mechanism of formation of the active site remains unknown. However, it is known that to initiate

polymer chain growth a chromium alkyl complex is necessary, the identity of which may involve any or all of the complexes shown in Scheme 1.10.¹³¹

Scheme 1.10



1.1.4 Known chromium η^3 -allyl complexes

It is therefore apparent that chromium η^3 -allyl complexes may play an important role in the polymerization of ethylene and other olefins. Indeed, tris(η^3 -allyl)chromium **45**,^{139, 140} one of several thermally unstable η^3 -allyl chromium complexes (Chart 1.2),^{133, 141-144} and derivatives thereof have been shown to react on the surface of calcined silica to form active catalysts for ethylene polymerization.¹⁴⁵⁻¹⁴⁷

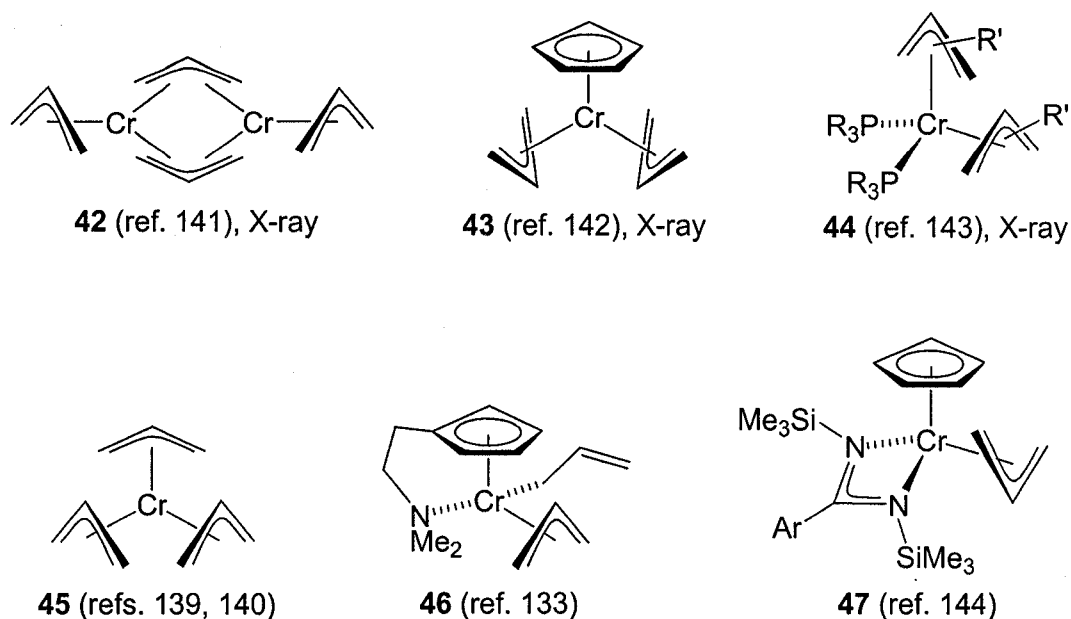
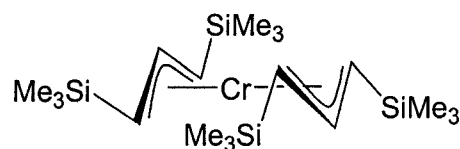
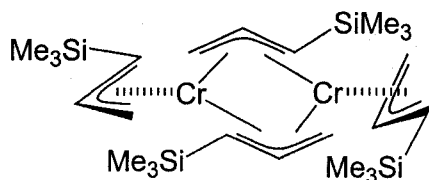


Chart 1.2: Selected examples of known thermally unstable chromium η^3 -allyl complexes. Those structurally characterized by X-ray crystallography are labeled accordingly.

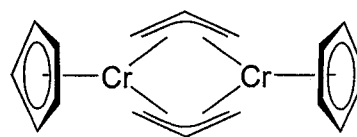
Homoleptic chromium η^3 -allyl complexes also polymerize olefins by acting as homogeneous catalysts. For example, the thermally stable bis(η^3 -allyl) complex **48** was recently reported to co-polymerize norbornene and ethylene.¹⁴⁸ The kinetic stability of this and the related bridging complex **49** arises from the sterically imposing trimethylsilyl substituents of the allyl ligands.^{149, 150} The structurally related and thermally stable bridging η^3 -allyl complex **50** (Chart 1.3), however, does not possess such bulky stabilizing groups and has not been investigated as an olefin polymerization catalyst.¹⁵¹



48 (ref. 149), X-ray



49 (ref. 150), X-ray



50 (ref. 151), X-ray

Chart 1.3: Selected examples of known thermally stable chromium η^3 -allyl complexes bearing hindered and/or bridging η^3 -allyl ligands. Those structurally characterized by X-ray crystallography are labeled accordingly.

Nearly all other thermally stable chromium η^3 -allyl complexes possess π -accepting carbonyl ligands (Chart 1.4), which impose a low-spin electronic configuration on the chromium centres and allows for effective π -backdonation from the metal into η^3 -allyl antibonding orbitals.¹⁵²⁻¹⁶⁰ This results in diamagnetic complexes that generally disfavour σ -allyl coordination. With the exception of the anionic chromium(0) η^3 -crotyl complex **52**, all of these stable chromium complexes maintain the metal formally in the +2 oxidation state. Curiously, prior to the work reported herein, no isolable chromium(III) η^3 -allyl complexes have ever been reported.

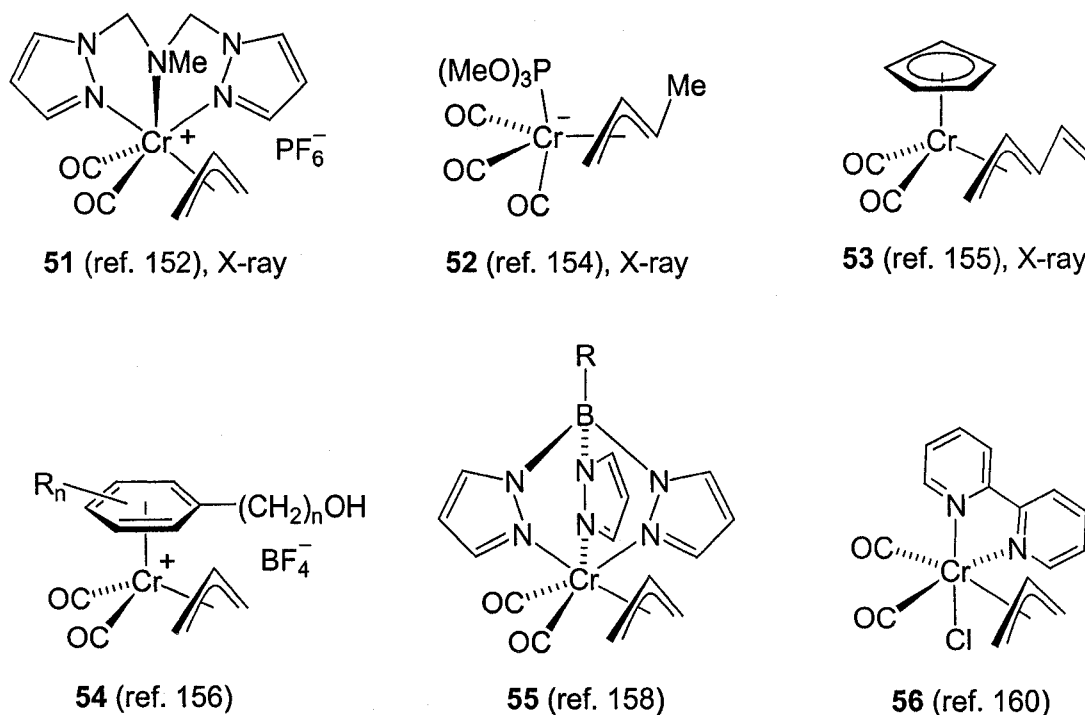


Chart 1.4: Selected examples of thermally stable chromium η^3 -allyl complexes bearing carbonyl ligands. Those structurally characterized by X-ray crystallography are labeled accordingly.

The few remaining thermally stable chromium η^3 -allyl complexes are low-valent and possess one or more electron rich tertiary phosphine ligands (Chart 1.5).^{161, 162} Donor ligands, however, generally destabilize chromium η^3 -allyl complexes (e.g., complexes **46** and **47**, Chart 1.2) by favouring σ -allyl coordination.^{133, 143, 144} Indeed, recent DFT calculations by Smith, *et al.*,¹⁴⁴ suggest that the optimized structure of the amidinato allylchromium complex **47** is actually a σ -allyl species. Thus, the origin of thermal stability of phosphine-bound complexes **57-59** remains unclear, and remains a matter for future study.

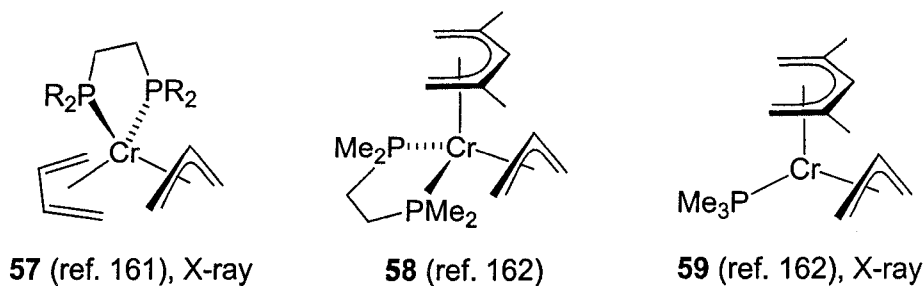
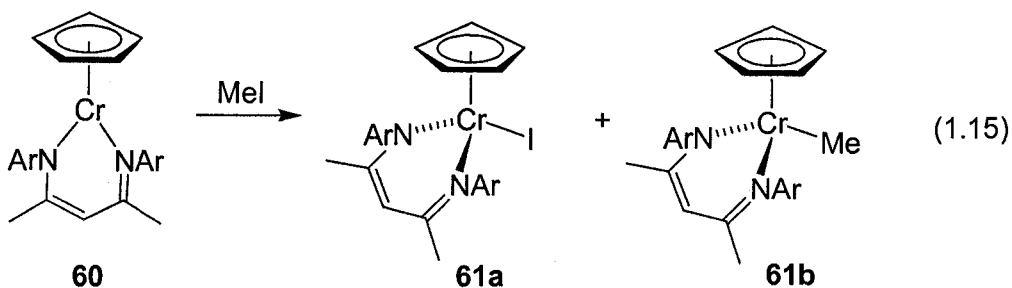


Chart 1.5: Selected examples of known thermally stable chromium η^3 -allyl complexes bearing donor ligands. Those structurally characterized by X-ray crystallography are labeled accordingly.

Due to the weak crystal-field effect of donor ligands on chromium, such complexes are generally paramagnetic and, as a result, display markedly different chemistry from diamagnetic congeners.^{144, 163, 164} The paramagnetic chromium(II) β -diketiminato complex **60**, for example, undergoes one-electron chemistry, activating iodomethane to form the chromium(III) iodide and chromium(III) methyl complexes **61a** and **61b** (eq. 1.15).¹⁶³



1.2 Proposed chromium η^3 -allyl precursors for chromacyclobutane formation

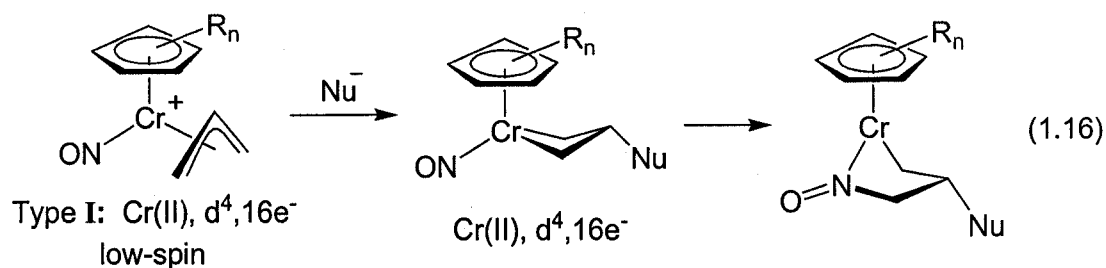
It is thus clear that η^3 -allyl chromium complexes are presumed to play key roles in catalytic hydrosilylation, olefin polymerization, and NHK reactions, and possibly in Oshima-type chemistry. Improved understanding of these allylchromium applications requires the synthesis of isolable chromium η^3 -allyl complexes that model proposed intermediates of these reactions. Indeed, such relevant systems may be an additional benefit of the pursuit of chromium η^3 -allyl precursors for chromacyclobutane formation.

Although fundamentally interesting, known chromium η^3 -allyl complexes were not adopted for our investigation of chromacyclobutane formation. Preparation of the thermally stable η^3 -allyl chromium complexes outlined in Charts 1.3 and 1.4 is decidedly not trivial, while handling thermally sensitive complexes (*e.g.*, Chart 1.2) is not attractive from a synthetic organic chemistry perspective. Moreover, only the mono-phosphine complex **59** (Chart 1.5) has the geometry necessary for allyl central carbon addition. We therefore proposed to prepare novel chromium η^3 -allyl complexes possessing *pseudo*-tetrahedral geometry or immediate precursors thereof.

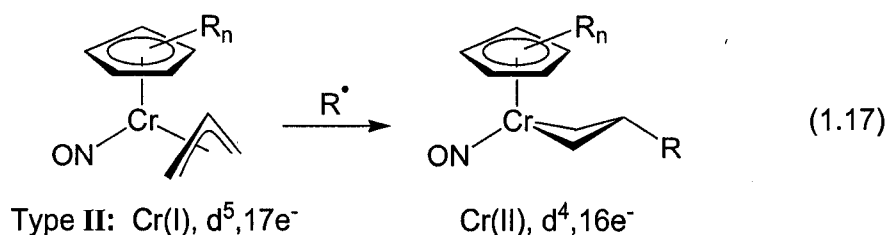
An obvious series of target complexes is the chromocene analogue of M. L. H. Green's cationic molybdenum(IV) and tungsten(IV) η^3 -allyl complexes **5** and **6** (p. 5). Unfortunately, however, chromium(IV) sandwich complexes are extremely rare and none possessing an η^3 -allyl ligand have been reported. Indeed, the parent chromocene (Cp_2Cr) complex does not tolerate additional ligands; $\text{Cp}_2\text{Cr}(\text{CO})$, for example is stable only under a CO atmosphere.¹⁶⁵ The only examples of stable $[\text{Cp}_2\text{Cr}(\text{n})\text{L}]$ ($\text{n} = \text{II}, \text{III}$) complexes incorporate *ansa*-bridged cyclopentadienyl ligands.^{165, 166} The cationic

chromium(IV) complex, $[\textit{ansa}\text{-Cp}_2\text{Cr(H)CO}]^+$, has been tentatively identified as a transient intermediate.¹⁶⁶

We thus chose to focus on the synthesis of allylchromium complexes with a nitrosyl group substituting for a cyclopentadienyl ligand in the $\text{Cp}_2\text{M}(\eta^3\text{-allyl})$ *pseudo*-tetrahedral geometry, targeting the cationic $\text{CpCr(NO)}(\eta^3\text{-allyl})^+$ complexes (labelled here as Type I targets). These unsaturated electrophilic complexes may afford chromacyclobutanes via nucleophilic attack at the allyl central carbon. Moreover, formation of nitrochromacyclopentane species may be possible via migratory insertion of the nitrosyl ligand into a Cr–C bond of the chromacyclobutane complexes (eq. 1.16).

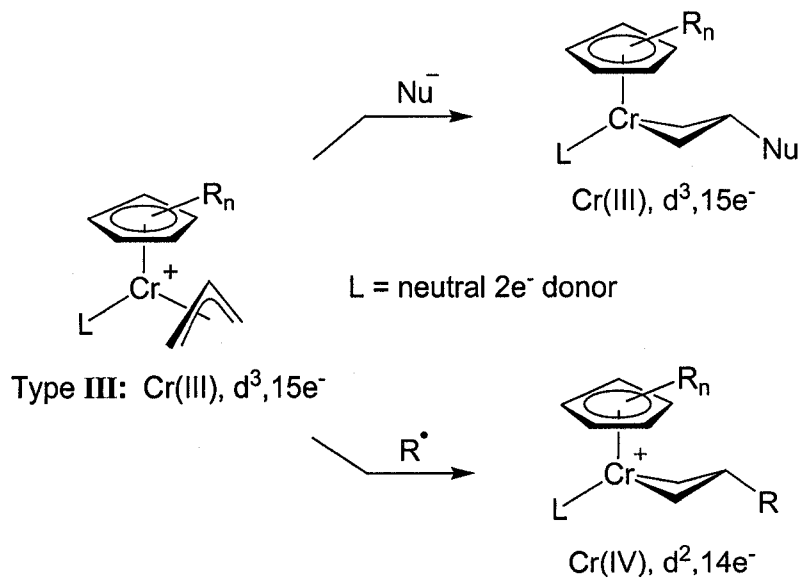


A second class of nitrosyl allylchromium complexes (designated as Type II, eq. 1.17), the neutral analogues of the Type I targets, may also be amenable to chromacyclobutane formation. The odd electron count on the chromium centres predisposes these complexes for alkylation using organic free radicals, the addition of which should occur at the allyl central carbon.



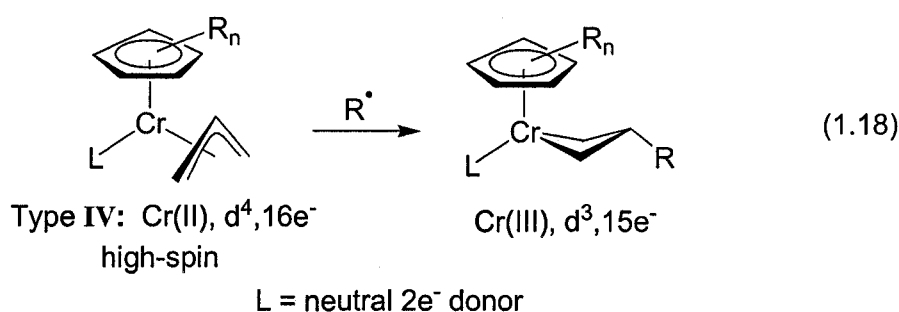
Replacing the nitrosyl ligand of target types **I** with a neutral two-electron donating group (L) will also provide unique η^3 -allyl chromium complexes. Due to the odd electron count and positive charge on this third class of proposed complexes (Type **III**), central carbon substitution via either nucleophilic or radical pathways may both be possible (Scheme 1.11). The potential downside of thermal instability, however, is obvious in this more electron-rich series.

Scheme 1.11

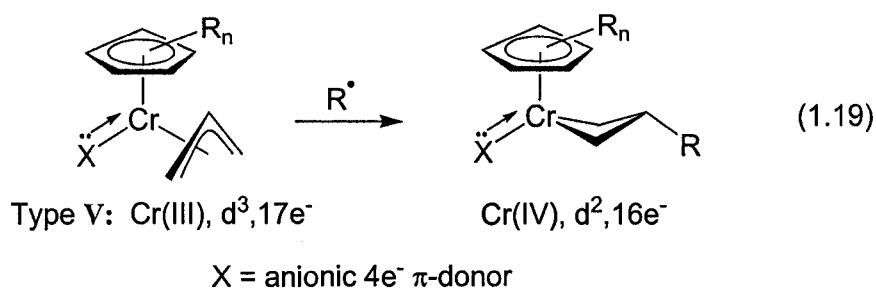


A fourth category of proposed chromium η^3 -allyl complexes consists of chromium(II) structural analogues of the Type **II** target complexes (Type **IV**, eq. 1.18).

Despite the even-electron count of these complexes, replacement of the reducing and strongly π -acidic nitrosyl ligand with a neutral donor group is expected to provide paramagnetic η^3 -allyl complexes. Similar to the paramagnetic chromium(II) complex **60**, these high-spin Type IV complexes may also be susceptible to radical-like behaviour.¹⁶⁴ If this odd electron character is delocalized onto the η^3 -allyl ligand, central carbon addition of an organic free radical may be possible (eq. 1.18).



The final class of target complexes (Type V, eq. 1.19) consists of chromium(III) η^3 -allyl compounds bearing anionic π -donor ligands (*e.g.*, R_2N^- or RO^- groups). These ligands will stabilize the electronically unsaturated allylchromium complexes by formally donating four electrons to the metal centre. Indeed, Legzdins has shown that otherwise unstable chromium alkyl complexes can be isolated by incorporating π -donating amido ligands.^{167, 168}



In lieu of π -acidic ligands, we propose to impart thermal stability on the Type **III-V** chromium η^3 -allyl targets by incorporating sterically imposing substituents on both L- and X-type ancillary ligands, and possibly on the cyclopentadienyl ligand as well. The added steric bulk of these ancillary ligands may also protect the unsaturated metal centre in most of these systems from unwanted alkylation reactions. Although thermal stability of the proposed η^3 -allyl systems is an ideal trait, it is not required for metallacyclobutane formation. As observed for the titanacyclobutane syntheses discussed above, η^3 -allyl precursors can easily be prepared *in situ* at low temperature and trapped with nucleophiles or organic free radicals.⁹²

Preparation of the Type **I-V** chromium η^3 -allyl targets may be accomplished by adapting established related molybdenum chemistry or by nucleophilic or radical allylation of relevant chromium precursors. Further discussion of these relevant synthetic strategies will appear in following chapters.

Our investigation of the Type **I** target complexes has fortunately led to a wealth of novel organochromium chemistry. As a consequence, detailed discussion of these results occupy chapters two through five. Attempts to synthesize the Type **II-V** target complexes, however, were substantially less fruitful, and an account of these investigations appears in chapter six.

1.3 References

1. Seyferth, D.; Marks, T. J.; Liebeskind, L. S.; Sweigart, D. A.; Whitmitre, K. H. *Organometallics* **2005**, 25, Editor's Page.
2. Genet, J.-P. *Acc. Chem. Res.* **2003**, 36, 908.

3. Collman, J. P.; Hegedus, L. S.; Norton, J.; Finke, R. G. *Principles and Applications of Organotransition Metal Chemistry*. University Science Books: Mill Valley, CA, 1987.
4. Crabtree, R. H. *The Organometallic Chemistry of the Transition Metals*, 2nd ed. John Wiley & Sons: New York, NY, 1994.
5. Davies, S. G. *Organotransition Metal Chemistry: Applications to Organic Synthesis*. Pergamon: Oxford, England, 1982.
6. Harrington, R. J. *Transition Metals in Total Synthesis*. John Wiley & Sons: New York, NY, 1990.
7. Feldman, J.; Schrock, R. R. *Prog. Inorg. Chem.* **1991**, *39*, 1.
8. Grubbs, R. H.; Tumas, W. *Science* **1989**, *243*, 907.
9. Lindner, E. *Adv. Heterocyclic Chem.* **1986**, *39*, 237.
10. Dragutan, V.; Balaban, A. T.; Dimonie, M. *Olefin Metathesis and Ring Opening Polymerization of Cycloolefins*. Wiley: New York, 1986.
11. Krauss, H. L.; Hagen, K.; Hums, K. *J. Mol. Catal.* **1985**, *28*, 233.
12. Ivin, K. J. *Olefin Metathesis*. Academic: London, 1983.
13. Chappell, S. D.; Dole-Hamilton, D. J. *Polyhedron* **1982**, *1*, 739.
14. Grubbs, R. H. In *Comprehensive Organometallic Chemistry*, Wilkinson, G.; Stone, F. G. A.; Abel, E. W., Pergamon: Oxford, U. K., 1982; Ch. 54.
15. Puddephatt, R. J. *Coord. Chem. Rev.* **1980**, *33*, 149.
16. Grubbs, R. H. *Prog. Inorg. Chem.* **1978**, *24*, 1.
17. Katz, T. J. *Adv. Organomet. Chem.* **1977**, *16*, 283.
18. Graziani, M.; Lenarda, M.; Ros, R.; Belluco, U. *Coord. Chem. Rev.* **1975**, *16*, 35.
19. Herisson, J.-L.; Chauvin, Y. *Macromol. Chem.* **1970**, *141*, 161.
20. Tsuji, J. In *The Chemistry of the Carbon-Carbon Bond, Vol 3. Carbon-Carbon Bond Formation Using Organometallic Compounds*, Hartley, F. R.; Patai, S., Wiley: New York, 1985; Ch. 3, Part 2.

21. Tsuji, J. *Acc. Chem. Res.* **1969**, *2*, 144.
22. Trost, B. M.; Verhoeven, T. R. *J. Am. Chem. Soc.* **1980**, *102*, 4730.
23. Trost, B. M. *Acc. Chem. Res.* **1980**, *13*, 385.
24. See also: Heck, R. F. *Acc. Chem. Res.* **1979**, *12*, 146.
25. Heck, R. F. In *Organic Synthesis via Metal Carbonyls*, Wender, I.; Pino, P., Wiley: New York, 1968; p. 379.
26. Heck, R. F.; Breslow, D. S. *J. Am. Chem. Soc.* **1963**, *85*, 2779.
27. Hegedus, L. S.; Inoue, Y. *J. Am. Chem. Soc.* **1982**, *104*, 4917.
28. Hegedus, L. S.; Perry, J. P. *J. Org. Chem.* **1984**, *49*, 2570.
29. Whitesides, T. H.; Arhart, R. W.; Slaven, R. W. *J. Am. Chem. Soc.* **1973**, *95*, 5792.
30. Pearson, A. J. *Aust. J. Chem.* **1976**, *29*, 1841.
31. Tsuji, J.; Minami, I.; Shimizu, I. *Chem. Lett.* **1984**, 1721.
32. Baker, R. *Chem. Rev.* **1973**, *73*, 487.
33. Semmelhack, M. F. *Org. React.* **1972**, *19*, 115.
34. Hegedus, L. S. *J. Organomet. Chem. Lib.* **1976**, *1*, 329.
35. Billington, D. C. *Chem. Soc. Rev.* **1985**, *14*, 93.
36. Ikeda, S.; Maruyama, Y.; Ozawa, F. *Organometallics* **1998**, *17*, 3770.
37. Benfield, F. H.; Francis, B. R.; Green, M. L. H.; Luong-Thi, N.-T.; Moser, G.; Poland, J. S.; Roe, D. M. *J. Less Common Metals* **1974**, *36*, 187.
38. Faller, J. W.; Rosan, A. M. *J. Am. Chem. Soc.* **1976**, *98*, 3388.
39. Adams, R. D.; Chadosh, D. F.; Faller, J. W. *J. Am. Chem. Soc.* **1979**, *101*, 2570.
40. Schilling, E. R.; Hoffmann, R.; Faller, J. W. *J. Am. Chem. Soc.* **1979**, *101*, 592.
41. Faller, J. W.; Chao, K. H. *J. Am. Chem. Soc.* **1984**, *106*, 887.
42. Faller, J. W.; Chao, K. H.; Murray, H. H. *Organometallics* **1984**, *3*, 1231.

43. Hoffmann, R. *J. Chem. Phys.* **1963**, 39, 1397.
44. Hoffmann, R.; Lipscomb, W. N. *J. Chem. Phys.* **1962**, 37, 2872.
45. Hoffmann, R.; Lipscomb, W. N. *J. Chem. Phys.* **1962**, 36, 3179.
46. Faller, J. W.; Linebarrier, D. L. *J. Am. Chem. Soc.* **1989**, 111, 1937.
47. Faller, J. W.; Nguyen, J. T.; Mazzieri, M. R. *Organometallics* **1993**, 12, 1434.
48. Ephritikhine, M.; Francis, B. R.; Green, M. L. H.; MacKenzie, R. E.; Smith, M. J. *J. Chem. Soc., Dalton Trans.* **1977**, 1131.
49. Ephritikhine, M.; Green, M. L. H.; MacKenzie, R. E. *J. Chem. Soc., Chem. Commun.* **1976**, 619.
50. Davies, S. G.; Green, M. L. H.; Mingos, D. M. P. *Tetrahedron* **1978**, 34, 3047.
51. Hegedus, L. S.; Darlington, W. H.; Russell, C. E. *J. Org. Chem.* **1980**, 45, 5193.
52. Carfagna, C.; Galarini, R.; Musco, A.; Santi, R. *Organometallics* **1991**, 10, 3956.
53. Carfagna, C.; Mariani, L.; Musco, A.; Sallese, G.; Santi, R. *J. Org. Chem.* **1991**, 56, 3924.
54. Hoffman, H. M. R.; Otte, A. R.; Wilde, A. *Angew. Chem. Int. Ed. Engl.* **1992**, 31, 234.
55. Benyunes, S. A.; Brandt, L.; Green, M.; Parkins, A. W. *Organometallics* **1991**, 10, 57.
56. Suzuki, T.; Fujimoto, H. *Inorg. Chem.* **1999**, 38, 370.
57. Kadota, J.; Korori, S.; Fukumoto, Y.; Murai, S. *Organometallics* **1999**, 18, 7523.
58. Aranyos, A.; Szabo, K. J.; Castano, A. M.; Backvall, J. E. *Organometallics* **1997**, 16, 1058.
59. Schwiebert, K. E.; Stryker, J. M. *Organometallics* **1993**, 12, 600.
60. Tjaden, E. B.; Casty, G. L.; Stryker, J. M. *J. Am. Chem. Soc.* **1993**, 115, 9814.
61. Tjaden, E. B.; Schwiebert, K. E.; Stryker, J. M. *J. Am. Chem. Soc.* **1992**, 114, 1100.

62. Tjaden, E. B.; Stryker, J. M. *Organometallics* **1992**, *11*, 16.
63. Wakefield, J. B.; Stryker, J. M. *J. Am. Chem. Soc.* **1991**, *113*, 7057.
64. Wakefield, J. B.; Stryker, J. M. *J. Am. Chem. Soc.* **1990**, *112*, 6420.
65. Tjaden, E. B.; Stryker, J. M. *J. Am. Chem. Soc.* **1990**, *112*, 6420.
66. Curtis, M. D.; Eisenstein, O. *Organometallics* **1984**, *3*, 887.
67. Suzuki, T.; Okada, G.; Hioki, Y.; Fujimoto, H. *Organometallics* **2003**, *22*, 3649.
68. Carfagna, C.; Galarini, R.; Linn, K.; Lopez, J. A.; Melli, C.; Musco, A. *Organometallics* **1993**, *12*, 3019.
69. Hoffman, H. M. R.; Otte, A. R.; Wilde, A.; Menzer, S.; Williams, D. *Angew. Chem. Int. Ed. Engl.* **1995**, *34*, 100.
70. Wilde, A.; Otte, A. R.; Hoffman, H. M. R. *J. Chem. Soc., Chem. Commun.* **1993**, 615.
71. Otte, A. R.; Wilde, A.; Hoffman, H. M. R. *Angew. Chem. Int. Ed. Engl.* **1994**, *33*, 1280.
72. Lauher, J. W.; Hoffmann, R. *J. Am. Chem. Soc.* **1976**, *98*, 1729.
73. Green, J. *Chem. Soc. Rev.* **1998**, *27*, 263.
74. Tjaden, E. B. *Ph. D. Thesis, Indiana University* **1993**.
75. Casty, G. L. *Ph. D. Thesis, Indiana University* **1994**.
76. Carter, C. A. G. *Ph. D. Thesis, University of Alberta* **1994**.
77. Casty, G. L.; Stryker, J. M. *J. Am. Chem. Soc.* **1995**, *117*, 7814.
78. Wardell, J. L. In *Comprehensive Organometallic Chemistry Vol. 2*, Wilkinson, G., Pergamon: New York, 1982; p. 910, and references therein.
79. Giese, B. *Radicals in Organic Synthesis: Formation of Carbon-Carbon Bonds*. Pergamon: Oxford, 1986.
80. Girard, P.; Namy, J. L.; Kagan, H. B. *J. Am. Chem. Soc.* **1980**, *102*, 2693.
81. Review: Imamoto, T. *Lanthanides in Organic Synthesis*. Academic Press: San Diego, 1994.

82. Sato, F.; Iida, K.; Moriya, H.; Sato, M. *J. Chem. Soc., Chem. Commun.* **1981**, 1140.
83. Greidanus, G. *Ph. D. Thesis, University of Alberta* **2001**.
84. Costa, E. M.; Stryker, J. M. *Unpublished results*.
85. Martin, H. A.; Lemaire, P. J.; Jellineck, F. J. *Organomet. Chem.* **1968**, *14*, 149.
86. Mashima, K.; Yasuda, H.; Asami, K.; Nakamura, A. *Chem. Lett.* **1983**, 219.
87. McDade, C.; Bercaw, J. E. *J. Organomet. Chem.* **1985**, *281*, 279.
88. Vance, P. J.; Prins, T. J.; Hauger, B. E.; Silver, M. E.; Wemple, M. E.; Pederson, L. M.; Kort, D. A.; Kannisto, M. R.; Geerligs, S. J.; Kelly, R. S.; McCandless, J. J.; Huffmann, J. D.; Peters, D. G. *Organometallics* **1991**, *10*, 917.
89. Tjaden, E. B.; Stryker, J. M. *J. Am. Chem. Soc.* **1993**, *115*, 2083.
90. Carter, C. A. G.; McDonald, R.; Stryker, J. M. *Organometallics* **1999**, *18*, 820, and references therein.
91. Greidanus-Strom, G.; Carter, C. A. G.; Stryker, J. M. *Organometallics* **2002**, *21*, 1011.
92. Carter, C. A. G.; Greidanus, G.; Chen, J.-X.; Stryker, J. M. *J. Am. Chem. Soc.* **2001**, *123*, 8872.
93. Lappert, M. F. In *Comprehensive Organometallic Chemistry*, Wilkinson, G.; Stone, F. G. A.; Abel, E. W., Pergamon: 1995; Vol. 4.
94. Greidanus, G.; McDonald, R.; Stryker, J. M. *Organometallics* **2001**, *20*, 2492.
95. Norman, J. A.; Stryker, J. M. *Unpublished results*.
96. Greenwood, N. N.; Earnshaw, A. *Chemistry of the Elements, 2nd Edition*. Butterworth-Heinemann: Oxford, 1997.
97. Hein, F. *Ber. Dtsch. Chem. Ges.* **1919**, *52*, 195.
98. Seyferth, D. *Organometallics* **2002**, *21*, 1520.
99. Seyferth, D. *Organometallics* **2002**, *21*, 2800.
100. Jolly, P. W. *Acc. Chem. Res.* **1996**, *29*, 544.

101. Kealy, T. J.; Pauson, P. J. *Nature (London)* **1951**, *168*, 1039.
102. Miller, S. A.; Tebboth, J. A.; Tremaine, J. F. *J. Chem. Soc.* **1952**, 632.
103. Wilkinson, G.; Rosenblum, M.; Whiting, M. C.; Woodward, R. B. *J. Am. Chem. Soc.* **1952**, *74*, 2125.
104. Fischer, E. O.; Hafner, W. *Z. Naturforsch.* **1953**, *8b*, 444.
105. Fischer, E. O.; Hafner, W. *Z. Naturforsch.* **1954**, *9b*, 503.
106. Cotton, F. A.; Wilkinson, G. *Z. Naturforsch.* **1954**, *9b*, 417.
107. Zeiss, H. H.; Tsutsui, M. *J. Am. Chem. Soc.* **1957**, *79*, 3062.
108. Zeiss, H. In *Organometallic Chemistry*, Zeiss, H., Reinhold: New York, 1960; p. 380.
109. Fischer, E. O.; Seus, D. *Chem. Ber.* **1956**, *89*, 1809.
110. Fischer, E. O.; Hafner, W. *Z. Naturforsch.* **1955**, *10b*, 140.
111. Fischer, E. O.; Hafner, W. *Z. Anorg. Allg. Chem.* **1956**, *286*, 146.
112. Fischer, E. O.; Hafner, W.; Stahl, H. O. *Z. Anorg. Allg. Chem.* **1955**, *282*, 47.
113. Theopold, K. H. *Eur. J. Inorg. Chem.* **1998**, 15.
114. Yamamoto, H.; Asao, N. *Chem. Rev.* **1993**, *93*, 2207.
115. Denmark, S. E.; Fu, J. *Chem. Rev.* **2003**, *103*, 2763.
116. Wessjohann, L. A.; Scheid, G. *Synthesis* **1999**, 1.
117. Poli, R.; Smith, K. M. Product Class 6: Organometallic Complexes of Chromium, Molybdenum, and Tungsten Without Carbonyl Ligands. In *Science of Synthesis*, Thieme Stuttgart: New York, 2003.
118. Furstner, A. *Chem. Rev.* **1999**, *99*, 991.
119. Harvey, D. F.; Sigano, D. M. *Chem. Rev.* **1996**, *96*, 271.
120. Lin, H.; Yang, L.; Li, C. *Organometallics* **2002**, *21*, 3848.

121. Coles, M. P.; Gibson, V. C.; Clegg, W.; Elsegood, M. R. J.; Porrelli, P. A. *Chem. Commun.* **1996**, 1963.
122. Dotz, K. H. *Angew. Chem. Int. Ed. Engl.* **1975**, *14*, 644.
123. Abdelqader, W.; Chmielewski, D.; Grevels, F.-W.; Ozkar, S.; Peynircioglu, N. B. *Organometallics* **1996**, *15*, 604.
124. Okude, Y.; Hirano, S.; Hiyama, T.; Nozaki, H. *J. Am. Chem. Soc.* **1977**, *99*, 3179.
125. Buse, C.; Heathcock, C. *Tetrahedron Lett.* **1978**, *19*, 1685.
126. Furstner, A.; Shi, N. *J. Am. Chem. Soc.* **1996**, *118*, 12349.
127. Inoue, M.; Suzuki, T.; Nakada, M. *J. Am. Chem. Soc.* **2003**, *125*, 1140.
128. Xia, G.; Yamamoto, H. *J. Am. Chem. Soc.* **2006**, *128*, 2554.
129. Nishikawa, T.; Kakiya, H.; Shinokubo, H.; Oshima, K. *J. Am. Chem. Soc.* **2001**, *123*, 4629.
130. Nishikawa, T.; Shinokubo, H.; Oshima, K. *Org. Lett.* **2002**, *4*, 2795.
131. Theopold, K. H. *Eur. J. Inorg. Chem.* **1998**, 15.
132. Liang, Y.; Yap, G. P. A.; Rheingold, A. L.; Theopold, K. H. *Organometallics* **1996**, *15*, 5284.
133. Döhring, A.; Gohre, J.; Jolly, P. W.; Kryger, B.; Rust, J.; Verhovnik, G. P. J. *Organometallics* **2000**, *19*, 388.
134. Döhring, A.; Jensen, V. R.; Jolly, P. W.; Thiel, W.; Weber, J. C. *Organometallics* **2001**, *20*, 2234.
135. Enders, M.; Fernandez, P.; Ludwig, G.; Pritzkow, H. *Organometallics* **2001**, *20*, 5005.
136. Agapie, T.; Day, M. W.; Henling, L. M.; Labinger, J. A.; Bercaw, J. E. *Organometallics* **2006**, *25*, 2733.
137. Schofer, S. J.; Day, M. W.; Henling, L. M.; Labinger, J. A.; Bercaw, J. E. *Organometallics* **2006**, *25*, 2743.
138. Bhandari, G.; Rheingold, A. L.; Theopold, K. H. *Chem. Eur. J.* **1995**, *1*, 199.

139. Wilke, G.; Bogdanovic, B.; Hardt, P.; Heimbach, P.; Kein, W.; Kroner, M.; Oberkirch, W.; Tanaka, K.; Steinrucke, E.; Walter, D.; Zimmermann, H. *Angew. Chem. Int. Ed. Engl.* **1966**, *5*, 151.
140. O'Brien, S.; Fishwick, M.; McDermott, B.; Wallbridge, M. G. H.; Wright, G. A. *Inorg. Synth.* **1972**, *13*, 73.
141. Aoki, T.; Furusaki, A.; Tomiie, Y.; Ono, K.; Tanaka, K. *Bull. Chem. Soc. Jpn.* **1969**, *42*, 545.
142. Angermund, K.; Döhring, A.; Jolly, P. W.; Krüger, C.; Romão, C. C. *Organometallics* **1986**, *5*, 1268.
143. Betz, P.; Jolly, P. W.; Krüger, C.; Zakrzewski, U. *Organometallics* **1991**, *10*, 3520.
144. Gallant, A. J.; Smith, K. M.; Patrick, B. O. *Chem. Commun.* **2002**, 2914.
145. Ballard, D. G. H. *Adv. Catal.* **1973**, *23*, 563.
146. Union Carbide Corp., U. S. Patent 4,054,538.
147. Bade, O. M.; Blom, R.; Ystenes, M. *Organometallics* **1998**, *17*, 2524.
148. Woodman, T. J.; Sarazin, Y.; Garratt, S.; Fink, G.; Bochmann, M. *J. Mol. Cat. A* **2005**, *235*, 88.
149. Smith, J. D.; Hanusa, T. P.; Young, V. G. *J. Am. Chem. Soc.* **2001**, *123*, 6455.
150. Carlson, C. N.; Smith, J. D.; Hanusa, T. P.; Brennessel, W. W.; Young, V. G. *J. Organomet. Chem.* **2003**, *683*, 191.
151. Betz, P.; Döhring, A.; Emrich, R.; Goddard, R.; Jolly, P. W.; Krüger, C.; Romão, C.; Schönfelder, K. U.; Tsay, Y.-H. *Polyhedron* **1993**, *12*, 2651.
152. Shiu, K. B.; Liou, K.-S.; Cheng, C. P.; Fang, B.-R.; Wang, Y.; Lee, G.-H.; Vong, W.-J. *Organometallics* **1989**, *8*, 1219.
153. Shiu, K.-B.; Chang, C.-J.; Wang, Y.; Cheng, M.-C. *J. Organomet. Chem.* **1991**, *406*, 363.
154. Wink, D. J.; Wang, N.-F.; Springer, J. P. *Organometallics* **1989**, *8*, 259.
155. Freeman, J. W.; Hallinan, N. C.; Arif, A. M.; Gedridge, R. W.; Ernst, R. D.; Basolo, F. *J. Am. Chem. Soc.* **1991**, *113*, 6509.

156. Krivykh, V. V.; Gusev, O. V.; Rybinskaya, M. I. *J. Organomet. Chem.* **1989**, *362*, 351.
157. Trofimenko, S. *J. Am. Chem. Soc.* **1967**, *89*, 3904.
158. Trofimenko, S. *J. Am. Chem. Soc.* **1969**, *91*, 588.
159. Trofimenko, S. *J. Am. Chem. Soc.* **1969**, *91*, 3183.
160. Brisdon, B. J.; Griffin, G. F. *J. Organomet. Chem.* **1974**, *76*, C47.
161. Iczek, F.; Jolly, P. W.; Krüger, C. *J. Organomet. Chem.* **1990**, *382*, C11.
162. Jolly, P. W.; Krüger, C.; Zakrzewski, U. *J. Organomet. Chem.* **1991**, *412*, 371.
163. Doherty, J. C.; Ballem, K. H. D.; Patrick, B. O.; Smith, K. M. *Organometallics* **2004**, *23*, 1487.
164. Smith, K. M. *Organometallics* **2005**, *24*, 778.
165. Schaper, F.; Wrobel, O.; Schworer, R.; Brintzinger, H.-H. *Organometallics* **2004**, *23*, 3552.
166. Foo, D. M. J.; Sinnema, P.-J.; Twamley, B.; Shapiro, P. J. *Organometallics* **2001**, *21*, 1005.
167. Kuzelka, J.; Legzdins, P.; Rettig, S. J.; Smith, K. M. *Organometallics* **1997**, *16*, 3569.
168. Smith, K. M.; McNeil, W. S.; Legzdins, P. *Chem. Eur. J.* **2000**, *6*, 1525.

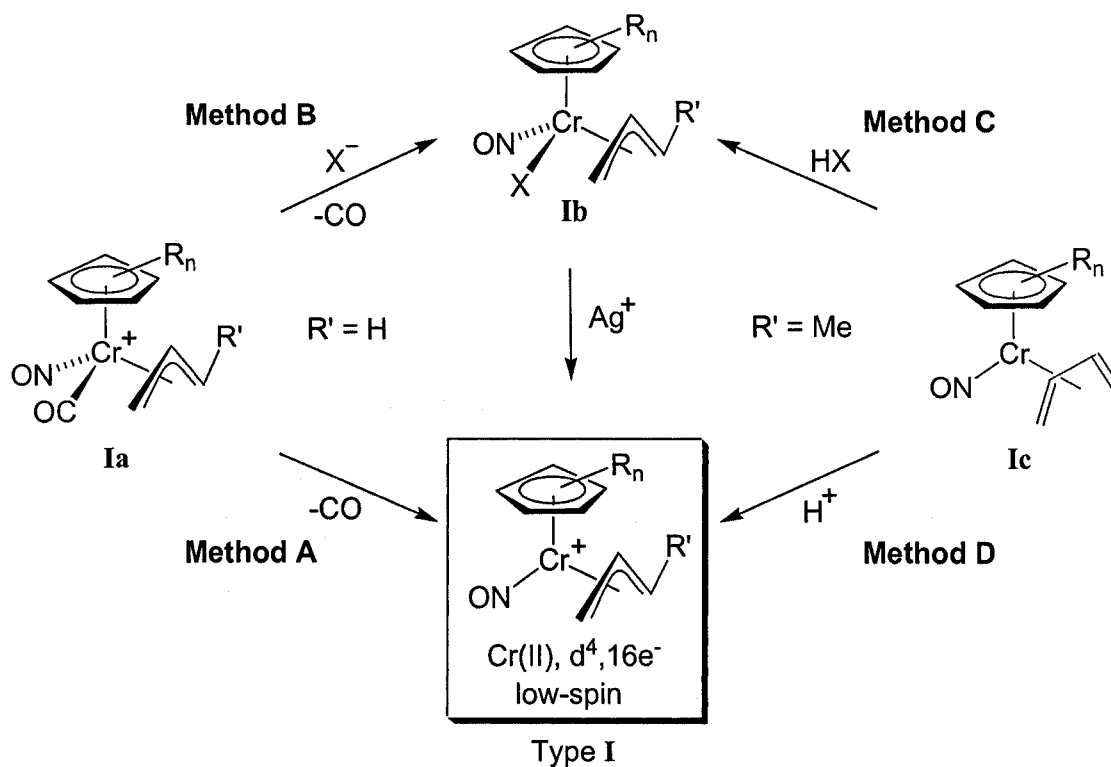
Chapter 2.

General synthesis of cyclopentadienylchromium(II) η^3 -allyl dicarbonyl complexes

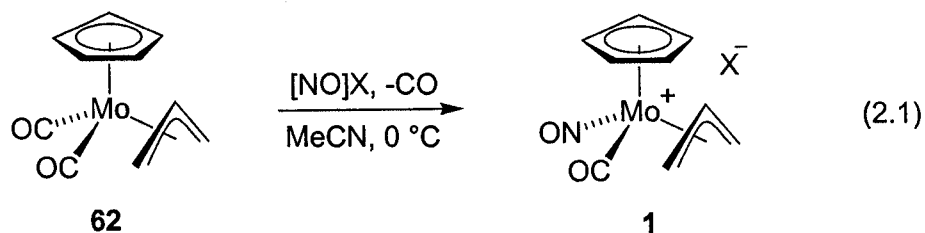
2.0 Introduction

Since organochromium complexes resembling the Type I η^3 -allyl targets, outlined in the previous chapter, are unknown, we initially envisioned several synthetic strategies to obtain these elusive unsaturated compounds (Scheme 2.1). Method A entails the decarbonylation of a cationic η^3 -allyl carbonyl nitrosyl species **Ia**, while Method B involves substitution of the CO ligand via addition of an anionic (X^-) group to form the neutral $Cp'Cr(NO)(\eta^3\text{-allyl})X$ species **Ib**. Removal of this X-type ligand with silver salts then generates the desired Type I target complex. Alternatively, species **Ib** may be obtained by protonation of a precursor η^4 -(1,3-diene) complex **Ic** by using an acid containing a coordinating counterion (Method C). Addition of an acid with a non-coordinating counterion (*e.g.*, HBF_4), however, may afford the Type I target complex directly (Method D).

Scheme 2.1

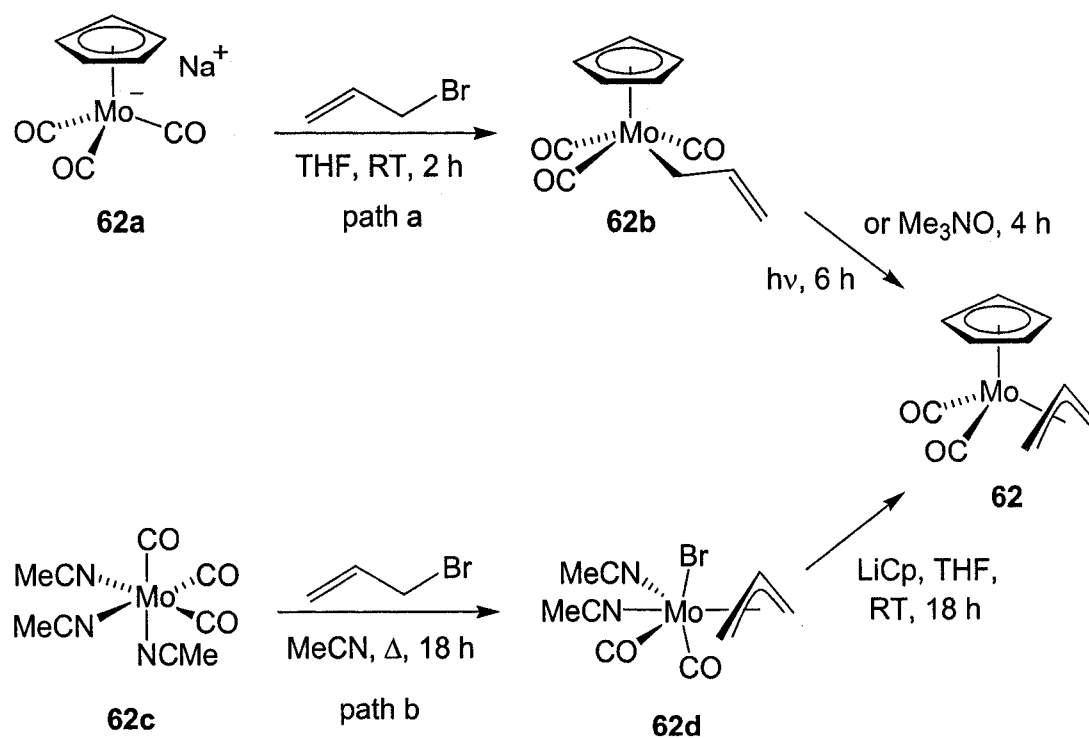


Despite these seemingly straightforward methods, chromium η^3 -allyl complexes of the type illustrated by **Ia-Ic** have not been reported. Structurally related molybdenum congeners, however, are well established. Carbonyl nitrosyl molybdenum complex **1** (e.g. 1.1, p. 3), for example, is analogous to the desired cationic η^3 -allyl chromium complex **Ia** and can be prepared via addition of a nitrosyl salt to the neutral dicarbonyl precursors (e.g., complex **62**, eq. 2.1).¹⁻⁵



These molybdenum η^3 -allyl dicarbonyl complexes are obtained via the alkylation of the cyclopentadienyltricarbonyl molybdate salt **62a** with allyl bromide, followed by decarbonylation of the consequent σ -allyl complex **62b** induced by photolysis⁶ or trimethylamine *N*-oxide⁷ (Scheme 2.2, path a). Alternatively, the addition of allyl bromide to tris-(acetonitrile)molybdenum tricarbonyl complex **62c** affords the thermally stable seven-coordinate η^3 -allyl species **62d**, which upon addition of cyclopentadienyl anion also provides dicarbonyl complex **62** (Scheme 2.2, path b).⁸

Scheme 2.2



Curiously, prior to our work, there has been no report of the use of $\text{Na}[\text{CpCr}(\text{CO})_3]$ ⁹ to prepare the chromium analogues of the η^3 -allyl complex **62**. Extension of the oxidative addition pathway (path b) to $(\text{MeCN})_3\text{Cr}(\text{CO})_3$,¹⁰ has been explored; however, under these reaction conditions only chromous halides are obtained, with no evidence of even transient η^3 -allyl formation.⁸ In addition to complex **53** (Chart 1.4, p. 30), which is prepared via a single carbonylation of the half-open chromocene precursor,¹¹ only two other members of this compound class have been previously reported: $\text{CpCr}(\eta^3\text{-cyclopentenyl})(\text{CO})_2$, prepared in <5% yield by treatment of chromocene with CO and H_2 at high pressure¹² and $\text{CpCr}(\eta^3\text{-crotyl})(\text{CO})_2$, isolated in 12% yield by photolysis of $[\text{CpCr}(\text{CO})_3]_2$ in the presence of 1,3-butadiene; this complex was only tentatively characterized.^{13, 14}

Thus, we began pursuing the synthesis and reactions of $\text{CpCr}(\eta^3\text{-allyl})(\text{CO})_2$ complexes by modifying the synthetic procedures used to prepare molybdenum complex **62**. The results of this investigation constitute the subject of Chapters 2 and 3. The synthesis and reactions of nitrosyl diene complexes **Ic** by Methods **C** and **D** will be discussed in Chapter 4.

2.1 Synthesis of neutral $\text{Cp}'\text{Cr}(\eta^3\text{-allyl})(\text{CO})_2$ complexes

Initially, adaptation of the anionic alkylation procedure (Scheme 2.2, path a) to the chromium series was investigated. Unfortunately, the addition of allyl halides to $\text{Na}[\text{CpCr}(\text{CO})_3]$ **64** at room temperature led only to decomposition. To preclude possible radical reaction pathways initiated by electron transfer from complex **64**, allyl tosylate was substituted for the allyl halides, again conducting the reaction at room temperature.

Subsequent addition of excess trimethylamine *N*-oxide to induce decarbonylation thus provided an orange-green suspension. Removal of the solvent and trituration of the residue with pentane afforded an orange compound **66** that, as determined by ^1H NMR spectroscopy (Table 2.1), does indeed possess an η^3 -allyl ligand (eq. 2.2).

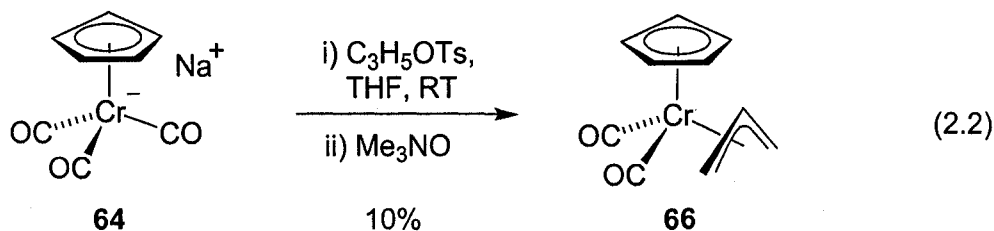


Table 2.1: ^1H NMR data (ppm) for the dicarbonyl η^3 -allyl complex **66**.^a

Cp	$\text{H}_{\text{central}}$	H_{anti}	H_{syn}
3.97	3.73 (tt, $J = 11.1, 7.0$ Hz)	0.48 (dt, $J = 10.9, 1.1$ Hz)	2.67 (dt, $J = 7.0, 1.1$ Hz)

^aThe *anti* and *syn* allyl protons are assigned on the basis of the relative magnitude of the respective coupling constants with the central allyl proton and comparison to typical values obtained from a range of known η^3 -allyl compounds.¹⁵⁻¹⁹

Infrared analysis of this product clearly reveals the presence of two carbonyl ligands, with stretching frequencies at 1939 and 1869 cm^{-1} , suggesting the formation of cyclopentadienylchromium η^3 -allyl dicarbonyl complex **66**. Combustion and mass spectral analysis were also in agreement with the assignment of this complex, which is unfortunately obtained in less than 10% yield. Nonetheless, crystals of this material were

grown by cooling a solution in pentane to $-35\text{ }^{\circ}\text{C}$ and the solid-state molecular structure solved by X-ray crystallography (Fig. 2.1).

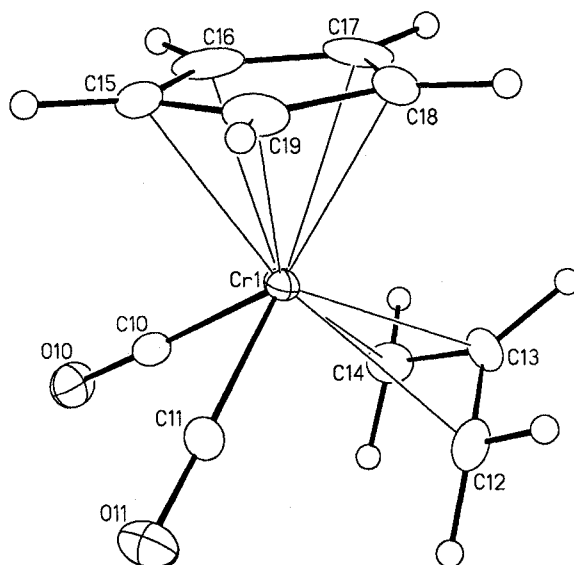
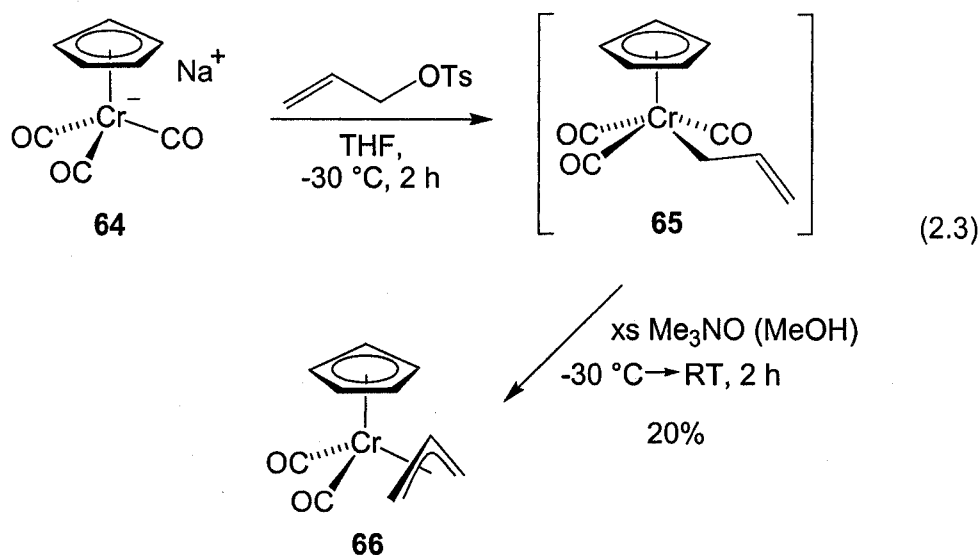


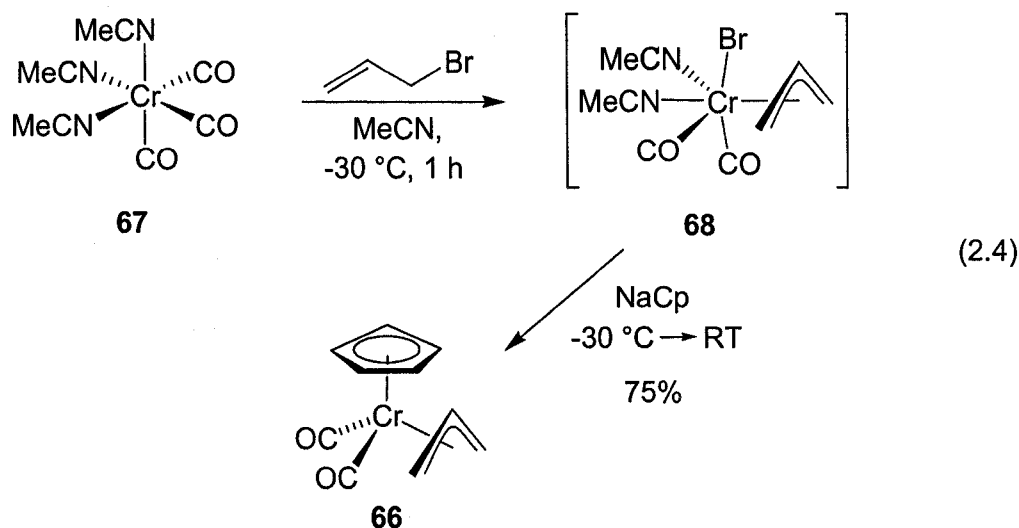
Figure 2.1: Solid-state molecular structure of η^3 -allyl dicarbonyl complex **66**. Non-hydrogen atoms are represented by Gaussian ellipsoids at the 20% probability level. Hydrogen atoms are shown with arbitrarily small thermal parameters. Selected bond lengths (\AA) and angles (deg): Cr-C(10) = 1.814(6), Cr-C(11) = 1.817(5), Cr-C(12) = 2.231(5), Cr-C(13) = 2.108(4), Cr-C(14) = 2.239(5), O(10)-C(10) = 1.168(6), O(11)-C(11) = 1.155(6), C(12)-C(13) = 1.393(8), C(13)-C(14) = 1.397(8); C(10)-Cr-C(15) = 95.3(2), C(10)-Cr-C(11) = 83.4(2), C(10)-Cr-C(13) = 107.4(2), C(12)-Cr-C(14) = 65.0(2), C(11)-Cr-C(13) = 107.9(2), C(13)-Cr-C(18) = 88.8(2), C(12)-C(13)-C(14) = 118.8(5).

The yield of complex **66** can be increased to 20% by cooling the reaction mixture to $-30\text{ }^{\circ}\text{C}$, with subsequent addition of Me_3NO as a solution in methanol rather than as a suspension in THF (eq. 2.3). The modest success of this reaction is presumably dependent on stabilizing the proposed seven-coordinate σ -allyl intermediate **65**

sufficiently to avoid complete decomposition by chromium-carbon bond homolysis; the Cr-allyl bond strength of this species is clearly weaker than that of the analogous Mo-allyl bond in the isolable σ -allyl complex **62b** (Scheme 2.2, p. 48).²⁰



Modification of the molybdenum oxidative addition procedure fortunately provides chromium η^3 -allyl dicarbonyl complex **66** in much higher yield (eq 2.4 and Table 2.2, entry 1). Treatment of $(\text{MeCN})_3\text{Cr}(\text{CO})_3$ **67**¹⁰ with allyl bromide in acetonitrile at $-30\text{ }^\circ\text{C}$, for example, results in a rapid colour change from yellow to red, logically attributed to the formation of thermally unstable η^3 -allyl intermediate **68**. Subsequent addition of NaCp in acetonitrile at low temperature yields η^3 -allyl complex **66** in 75% yield after isolation by trituration into pentane and chromatography on neutral alumina(I). Warming the reaction mixture prior to the addition of NaCp results instead in the formation of an uncharacterizable paramagnetic green material. Substituting allyl chloride for allyl bromide in this procedure results in little or no reaction with $(\text{MeCN})_3\text{Cr}(\text{CO})_3$.



The thermal stability of the putative seven-coordinate chromium η^3 -allyl intermediate **68** is markedly lower than that of the molybdenum analogue **62d** (Scheme 2.2, p. 48), presumably due to the inherently lower Cr-allyl bond strength. The structurally related seven-coordinate chromium η^3 -allyl complexes **51**, **55**, and **56** (Chart 1.4, p. 30) are, however, reported to be thermally stable. In the case of bipyridyl complex **56**, the added chelation may introduce kinetic stability, a trend also apparent for the ammine-bound complexes **51** and **55**. The hemilability of the respective bis(pyrazole)amino and tris(pyrazolyl)borate ancillary ligands of complexes **51** and **55** may also serve to relieve steric congestion by bonding in a κ^2 -fashion, allowing for increased thermal stability. Cationic complex **51** is further stabilized by the absence of a coordinating counterion; the neutral bromide analogue of complex **51**, for example, is reported to be thermally unstable.^{21, 22}

Thus, the addition of excess KPF_6 to a solution of the putative seven-coordinate complex **68** results in an extended lifetime (up to 1 h at RT) of this red intermediate. This increase in stability, however, does not significantly affect the isolated yield of

η^3 -allyl dicarbonyl complex **66**. Synthesis of additional $\text{Cp}'\text{Cr}(\eta^3\text{-allyl})(\text{CO})_2$ complexes (Chart 2.1) was thus accomplished using the general procedure shown in equation 2.4; detailed reaction conditions are summarized in Table 2.2.²³

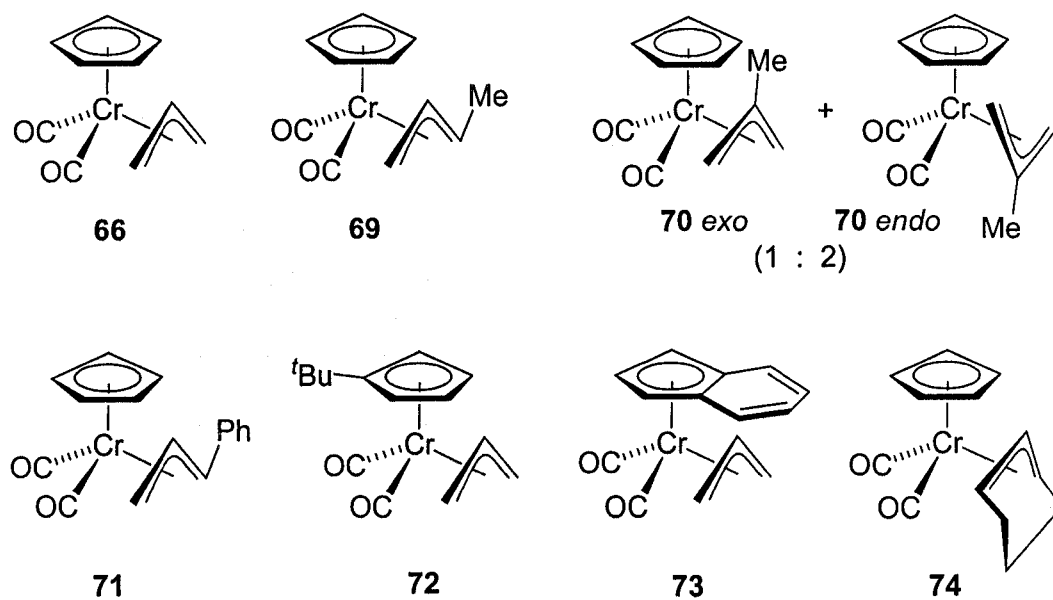
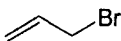
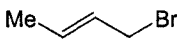
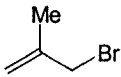
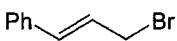
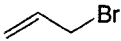
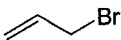
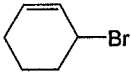


Chart 2.1: Novel $\text{Cp}'\text{Cr}(\eta^3\text{-allyl})(\text{CO})_2$ complexes **66** and **69-74**, prepared via the modified oxidative addition method (eq. 2.3).

Table 2.2: Reaction details for the synthesis of η^3 -allyl complexes **66** and **69-74** from $(\text{MeCN})_3\text{Cr}(\text{CO})_3$ **67** (eq. 2.3).

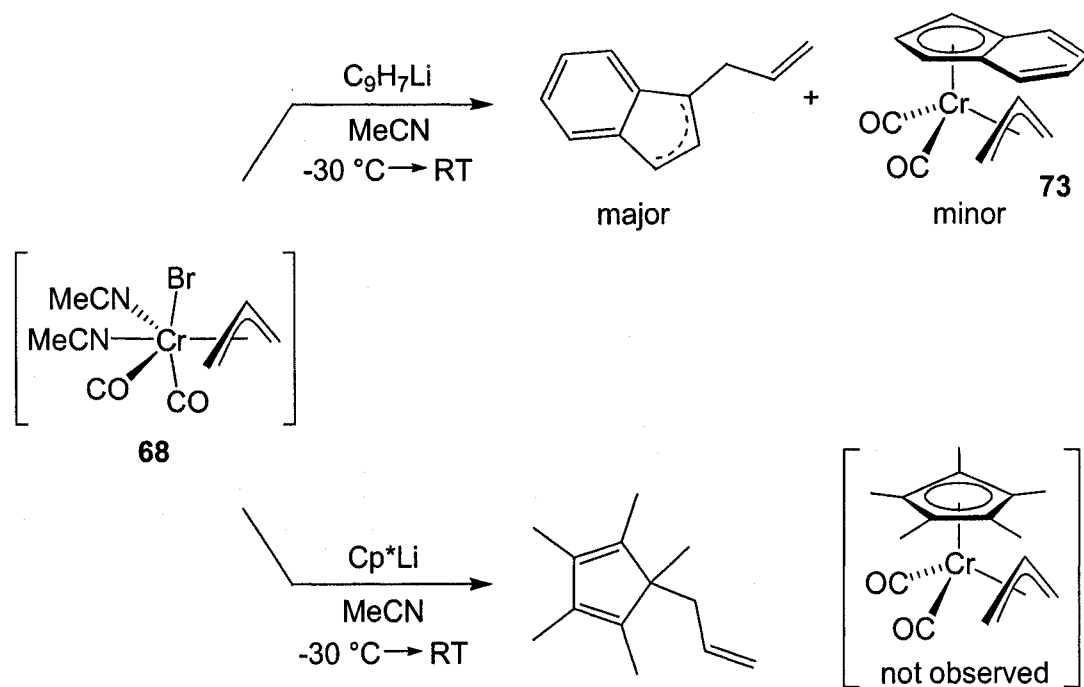
Entry	Substrate	Reaction Time (h) ^a	MCp'	Product	ν_{CO} ^b	% Yield
1		1	$\text{C}_5\text{H}_4\text{Na}$	66	1939, 1869	75
2		1	$\text{C}_5\text{H}_4\text{Na}$	69	1932, 1863	73
3		6	$\text{C}_5\text{H}_4\text{Na}$	70 <i>exo</i> ; 70 <i>endo</i>	1943, 1938, 1880, 1870	71
4		2	$\text{C}_5\text{H}_4\text{Na}$	71	1936, 1869	61
5		1	$t\text{-BuC}_5\text{H}_4\text{Li}$	72	1931, 1863	69
6		1	$\text{C}_9\text{H}_7\text{Li}$	73	1938, 1871	25
7		12	$\text{C}_5\text{H}_4\text{Na}$	74	1923, 1860	12

^aTime refers to the period allowed for the oxidative addition of allyl substrate to $(\text{MeCN})_3\text{Cr}(\text{CO})_3$. ^bInfrared spectra recorded in THF solution, cm^{-1} .

The preparation of the 3- and 2-methylallyl complexes **69** and **70**, along with the η^3 -cinnamyl and *tert*-butylcyclopentadienyl complexes **71** and **72** (Entries 2-5, respectively) proved to be straightforward. The introduction of other cyclopentadienyl-type ligands, however, provided unexpected challenges. The use of indenyl lithium provides only a low yield of the sterically more crowded η^5 -indenyl allyl complex **73** (entry 6). This we attribute to the competitive addition of the indenyl anion to the allyl ligand rather than the metal centre, producing a mixture of allylindene isomers as the major reaction product (Scheme 2.3), as identified by spectroscopic comparison to

authentic material.²⁴ The organic byproducts are obtained as initial fractions upon chromatography of the reaction mixture over neutral alumina(I), using pentane as the eluent. Consistent with this observation, the addition of permethylcyclopentadienyl lithium unsurprisingly results in exclusive formation of allylpermethylcyclopentadiene, again determined by spectroscopic comparison to authentic material²⁵ (Scheme 2.3); the identity of the organochromium byproduct(s) is unknown. Larger anions are clearly too sterically encumbered to access the metal centre, instead preferentially alkylating at the allyl ligand.

Scheme 2.3



Another limiting factor in this methodology is the persistent formation of $(\text{CO})_5\text{Cr}(\text{MeCN})$ ²⁶ as a minor side product. The formation of this complex is minimized by using a vigorous nitrogen purge throughout the reaction; fortunately, this relatively

polar impurity is readily removed by chromatography on neutral alumina(I). A second limitation arises from the decreasing rate of oxidative addition as a function of the steric size and substitution of the allyl substrate. In the reaction of 3-bromocyclohexene with $(\text{MeCN})_3\text{Cr}(\text{CO})_3$, for example, only a very slow (~ 12 h) colour change to red is observed. Subsequent addition of NaCp provides the expected cyclohexenyl complex **72**, but in only 12% isolated yield (entry 7). During the time required for oxidative addition of this substrate gradual thermal decomposition of the sterically encumbered seven-coordinate intermediate presumably dominates.

The ^1H NMR and infrared spectra of η^3 -allyl complex **66** indicate that only a single configurational isomer of the molecule is present in solution, identified in the solid-state as *exo* by X-ray crystallography (Fig. 2.1). Interestingly, this contrasts with that of the molybdenum analogue **62**, which exists in solution as an approximate 1 : 1 mixture of *endo* and *exo* isomers.^{27, 28} Given that the δ and J values for the η^3 -crotyl, η^3 -cinnamyl, and *tert*-butylcyclopentadienyl complexes **69-72** (entries 2-5, respectively) are very similar to those observed for η^3 -allyl complex **66** (see the Experimental section for details), the configuration of these complexes is also assigned as *exo*. The ^1H NMR spectrum of the 2-methylallyl complex **70** (entry 3), however, reveals that the product is formed as an approximately 2 : 1 mixture of isomers favouring the tentatively assigned *endo* configuration. The minor *exo* isomer is less soluble and selectively crystallizes from pentane, as established by X-ray crystallography (Fig. 2.2). ^1H NMR analysis of the crystals establishes that the *exo* isomer of complex **70** does not equilibrate with its *endo* congener at room temperature.

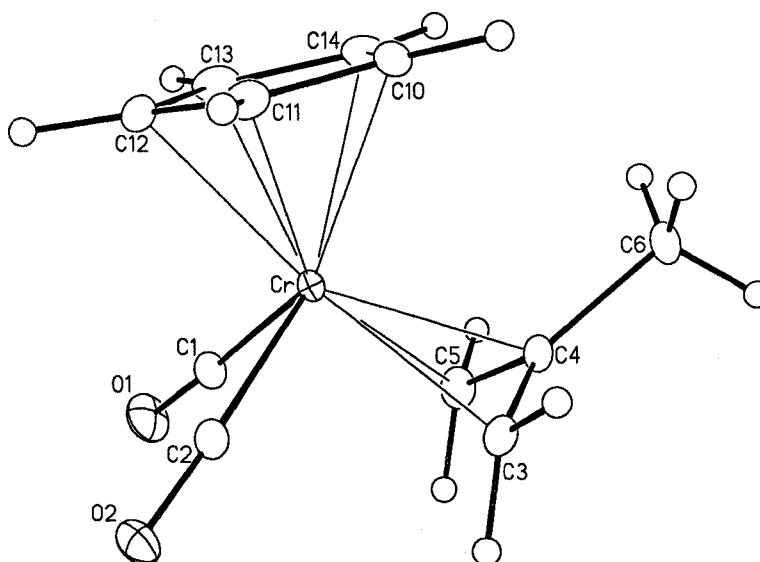


Figure 2.2: Solid-state molecular structure of the *exo* isomer of η^3 -(2-methylallyl) complex **70**. Non-hydrogen atoms are represented by Gaussian ellipsoids at the 20% probability level. Hydrogen atoms are shown with arbitrarily small thermal parameters. Selected bond lengths (Å) and angles (deg): Cr-C(1) = 1.813(18), Cr-C(2) = 1.821(19), Cr-C(3) = 2.234(17), Cr-C(4) = 2.149(16), Cr-C(5) = 2.233(18), O(1)-C(1) = 1.163(2), O(2)-C(2) = 1.153(2), C(3)-C(4) = 1.403(3), C(4)-C(5) = 1.405(3), C(4)-C(6) = 1.514(2); C(1)-Cr-C(12) = 95.5(8), C(1)-Cr-C(2) = 82.1(8), C(1)-Cr-C(4) = 107.0(8), C(3)-Cr-C(5) = 64.8(7), C(2)-Cr-C(4) = 107.6(7), C(4)-Cr-C(10) = 89.7(7), C(3)-C(4)-C(5) = 116.9(16).

Inspection of the ^1H NMR spectrum of indenyl complex **73** suggests the presence of two stereoisomers in solution, one formed in only trace amounts. In the major isomer, the signal for the central allyl proton appears at -0.11 ppm, strongly suggesting the allyl ligand is in the *exo* configuration, positioned directly beneath, and thus shielded, by the indenyl aromatic ring, as drawn in Scheme 2.3. This configuration has been confirmed in the solid-state by a crude structure determination on a poorly diffracting crystal, which

provided both atom connectivity and ligand orientation, but not high resolution structural data (Fig. 2.3). The allyl ligand configuration of the minor isomer of indenyl complex **73** is speculated to be *endo*, with the now shielded *anti* methylene protons apparent at -0.63 ppm.

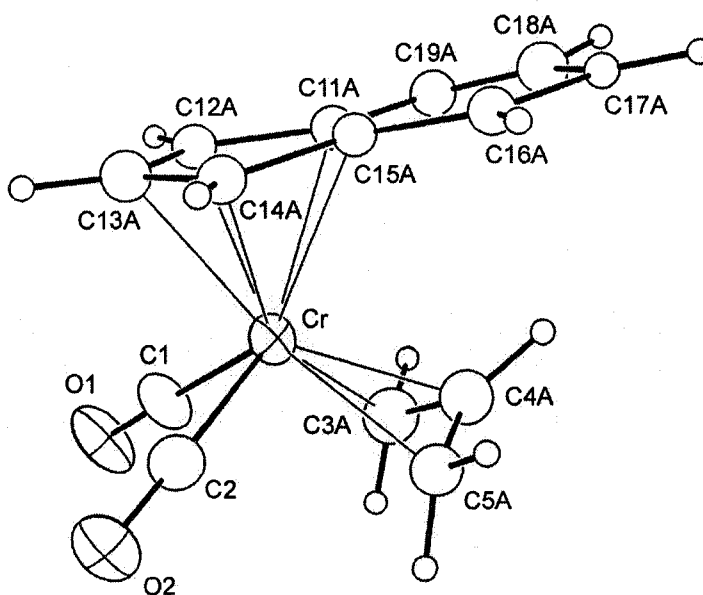


Figure 2.3: The solid-state molecular structure of the *exo* isomer of indenyl η^3 -allyl complex **73**. Due to the poorly diffracting crystal, accurate structural data could not be obtained.

Despite the low yield, η^3 -cyclohexenyl complex **74** revealed several intriguing spectroscopic and structural features. While ^1H NMR spectroscopy shows typical signals for the terminal allyl, central allyl, and adjacent methylene protons at δ 4.02 (t, 1H), 3.47 (m, 2H), and δ 1.79 (m, 4H), respectively, the two remaining aliphatic proton resonances appear at unique and unexpected positions. Thus, two upfield multiplets are observed, at δ 0.77 (m, 1H) and 0.38 (dt, 1H), corresponding to the equatorial and axial protons,

respectively, of the distal methylene group. The unusual shielding of this group is ascribed to a chair-like conformation of the cyclohexenyl ring, which places these protons underneath the metal, physically near the π -system of the carbonyl ligands. This conformation is indeed observed in the solid-state structure (Fig. 2.4), suggesting a similar structure in solution.

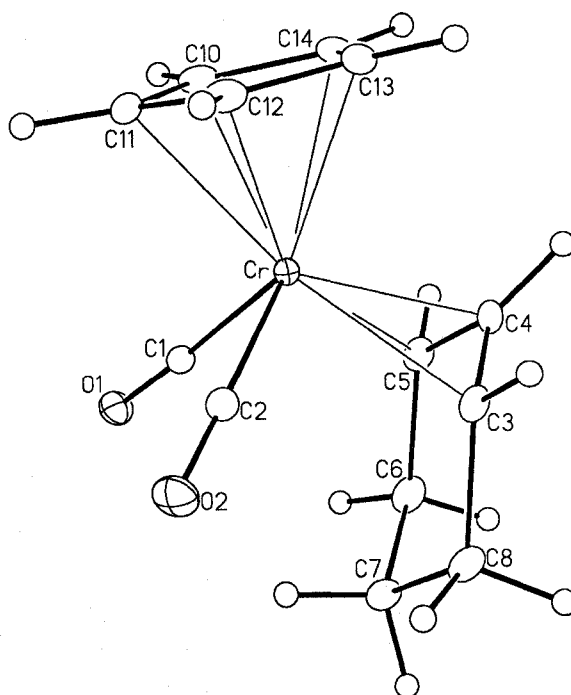
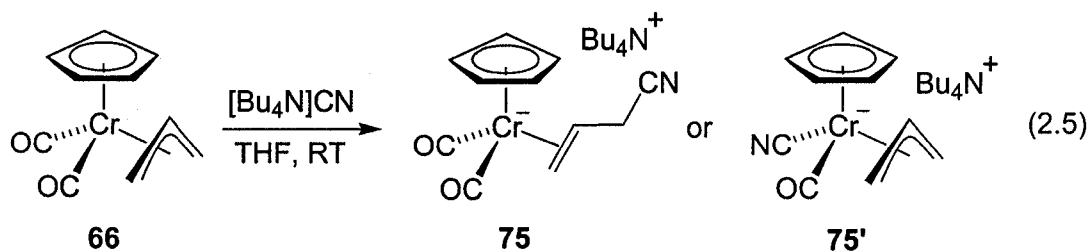


Figure 2.4: Solid-state molecular structure of η^3 -cyclohexenyl complex **74**. Non-hydrogen atoms are represented by Gaussian ellipsoids at the 20% probability level. Hydrogen atoms are shown with arbitrarily small thermal parameters. Selected bond lengths (Å) and angles (deg): Cr-C(1) = 1.825(15), Cr-C(2) = 1.821(15), Cr-C(3) = 2.275(15), Cr-C(4) = 2.091(14), Cr-C(5) = 2.276(15), O(1)-C(1) = 1.155(18), O(2)-C(2) = 1.158(19), C(3)-C(4) = 1.407(2), C(4)-C(5) = 1.411(8), C(5)-C(6) = 1.512(2), C(6)-C(7) = 1.531(2), C(7)-C(8) = 1.523(2); C(1)-Cr-C(11) = 93.3(6), C(1)-Cr-C(2) = 85.0(7), C(1)-Cr-C(4) = 109.3(6), C(3)-Cr-C(5) = 63.4(5), C(2)-Cr-C(4) = 107.4(6), C(4)-Cr-C(13) = 88.6(6), C(3)-C(4)-C(5) = 116.2(14), C(5)-C(6)-C(7) = 113.3(13), C(6)-C(7)-C(8) = 113.3(14), C(3)-C(8)-C(7) = 113.4(13).

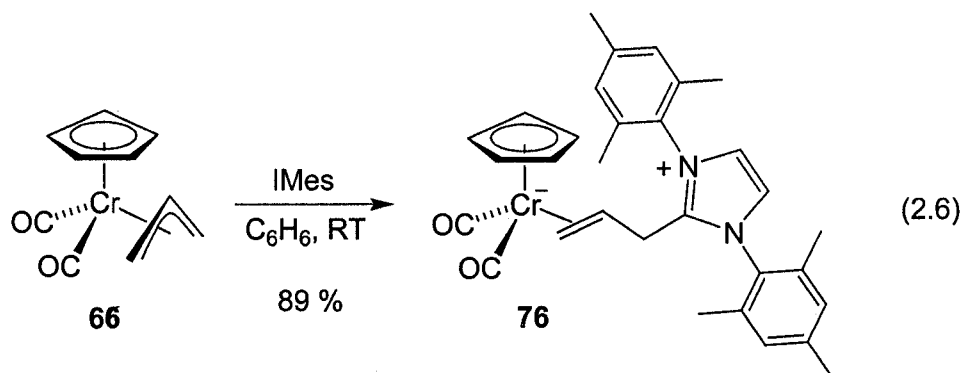
2.2 Reactivity of the $\text{CpCr}(\eta^3\text{-allyl})(\text{CO})_2$ complex

In addition to studying nitrosyl addition to η^3 -allyl dicarbonyl complex **66** (see Chapter 3), we investigated the efficacy of other potential carbonyl substitution methods. For example, addition of 0.48 equivalents of iodine to complex **66** does indeed lead to CO effervescence, but unfortunately, as ascertained by combustion analysis, the otherwise uncharacterized paramagnetic product consists only of the CpCrI fragment. Photolysis of complex **66** in the presence of tertiary phosphines or amines leads only to intractable products, with complete decomposition of the starting material. Trimethylamine *N*-oxide also failed to induce the substitution of these ligands, even in refluxing acetone or toluene. Given that the carbonyl infrared stretching frequencies of complex **66** are lower than 2000 cm^{-1} ,²⁹ it is no surprise that this reagent is unreactive toward the electron-rich metal centre.

Interestingly, the addition of tetrabutylammonium cyanide to complex **66** provides a tractable product, the structure of which is tentatively assigned as either that of the anionic η^2 -(3-cyanopropene) complex **75** or the η^3 -allyl chromate complex **75'** (eq. 2.5). Assignment of the ^1H NMR data of this product unfortunately remains ambiguous and acquiring reliable infrared data was impeded by the low product purity. However, since no effervescence was observed upon addition of $[\text{Bu}_4\text{N}]\text{CN}$, the more probable assignment for the structure of this product is that of complex **75**.



Attempted displacement of one or more carbonyl ligands of η^3 -allyl complex **66** by the strongly donating N-heterocyclic carbene, 1,3-bis-(2,4,6-trimethylphenyl)-imidazolin-2-ylidene (IMes),³⁰ also failed to afford the desired product(s), instead providing the diamagnetic zwitterionic alkylation product **76** cleanly and in excellent yield (eq. 2.6). The structure of this complex was determined by spectroscopic analysis and confirmed in the solid-state by X-ray crystallography (Fig. 2.5). Although anionic 18-electron $\text{Cr}(0)$ complexes of the form $\eta^5\text{-CpCrL}_2(\text{olefin})$ (L = neutral donor) appear to be unprecedented, corresponding neutral ($\eta^6\text{-arene})\text{CrL}_2(\text{olefin})$ analogues have been reported.³¹



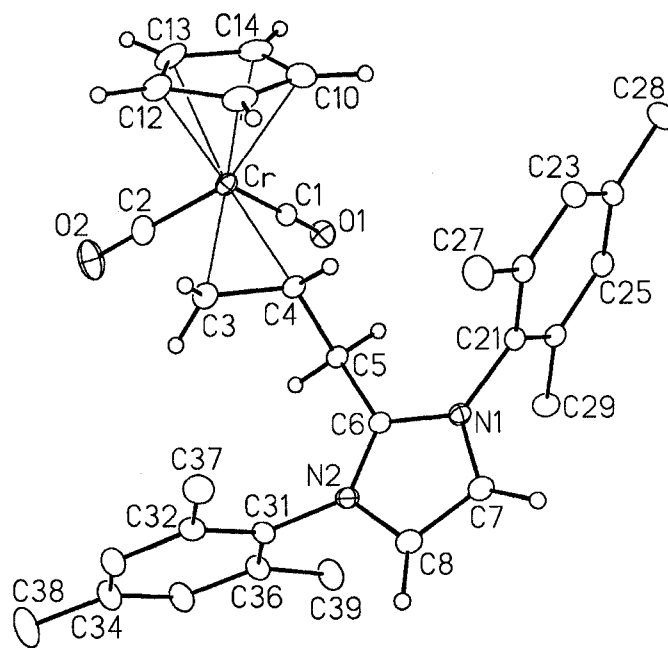


Figure 2.5: The solid-state molecular structure of zwitterionic complex **76**; 0.5 equivalents of interstitial THF are omitted. Non-hydrogen atoms are represented by Gaussian ellipsoids at the 20% probability level. Hydrogen atoms are shown with arbitrarily small thermal parameters. Selected bond lengths (Å) and angles (deg): Cr-C(1) = 1.789(2), Cr-C(2) = 1.798(3), Cr-C(3) = 2.150(2), Cr-C(4) = 2.140(2), O(1)-C(1) = 1.182(3), O(2)-C(2) = 1.180(3), C(3)-C(4) = 1.414(3), C(4)-C(5) = 1.523(3), C(5)-C(6) = 1.490(3), C(7)-C(8) = 1.340(3), N(1)-C(6) = 1.343(3), N(2)-C(6) = 1.341(3); C(1)-Cr-C(10) = 102.89(10), C(1)-Cr-C(2) = 85.89(10), C(1)-Cr-C(3) = 109.99(9), C(1)-Cr-C(4) = 84.07(9), C(3)-Cr-C(4) = 38.48(8), C(3)-C(4)-C(5) = 119.10(19), C(4)-C(5)-C(6) = 110.27(17), N(1)-C(6)-N(2) = 106.85(17).

As a result of the anionic charge on the chromium centre in zwitterionic complex **76**, there is increased π -backbonding to the carbonyl ligands, resulting in substantially lower energy C–O infrared absorptions (1845 and 1757 cm^{-1}); the average C–O bond distance is approximately 1.6% longer than the corresponding distance of the neutral η^3 -allyl precursor **66** (recall Fig. 2.1, p. 51). Accordingly, the average Cr–CO bond

length of zwitterionic complex **76** is shorter than that of η^3 -allyl complex **66**, also by a difference of 1.6%.

Although this reaction does not lead to decarbonylation, the product reveals what is unprecedented ligand-centred reactivity for the stabilized carbene, which more typically functions as an ancillary ligand in organometallic systems.^{32, 33} The high nucleophilicity of this N-heterocyclic carbene toward the neutral allyl complex **66** is also surprising given that no reaction is observed between complex **66** and excess PMe_3 , even at 65 °C.

Following these unsuccessful direct carbonyl displacement attempts, we attempted to oxidize the low valent metal to chromium(III), weakening the Cr–CO bond and facilitating displacement of the consequently more labile CO. Thus, treatment of complex **66** with ferricinium or silver salts indeed provides spectroscopic evidence of at least partial oxidation. As monitored by solution infrared spectroscopy, the carbonyl absorptions for neutral complex **66** in THF (1939 and 1869 cm^{-1}) shift to markedly higher frequency in the oxidized product (2070 and 2032 cm^{-1}), clearly indicative of stronger C–O bonds and weaker chromium-CO $\text{d} \rightarrow \pi^*$ backbonding interactions. Unfortunately, the oxidized product does not persist in THF, acetonitrile, or acetone solutions: the higher energy carbonyl vibrations disappear completely after three hours at room temperature. It has been determined, however, that the oxidized product is only sparingly soluble in 1,2-dimeth-oxyethane (DME), but due to similar solubility of the unreacted chemical oxidants, the chromium(III) species could only be isolated in very low purity. The use of a more convenient oxidant for preparing these cationic complexes is discussed in Chapter 3.

2.3 References

1. Faller, J. W.; Rosan, A. M. *J. Am. Chem. Soc.* **1976**, *98*, 3388.
2. Adams, R. D.; Chadosh, D. F.; Faller, J. W. *J. Am. Chem. Soc.* **1979**, *101*, 2570.
3. Schilling, E. R.; Hoffmann, R.; Faller, J. W. *J. Am. Chem. Soc.* **1979**, *101*, 592.
4. Faller, J. W.; Chao, K. H. *J. Am. Chem. Soc.* **1984**, *106*, 887.
5. Faller, J. W.; Chao, K. H.; Murray, H. H. *Organometallics* **1984**, *3*, 1231.
6. Cousins, M.; Green, M. L. H. *J. Chem. Soc.* **1963**, 889.
7. Luh, T. Y.; Wong, C. S. *J. Organomet. Chem.* **1985**, *287*, 231.
8. Hayter, R. G. *J. Organomet. Chem.* **1968**, *13*, P1.
9. Hoyano, J. K.; Legzdins, P.; Malito, J. T. *Inorg. Synth.* **1978**, *18*, 126.
10. Tate, D. P.; Knipple, W. R.; Augl, J. M. *Inorg. Chem.* **1962**, *1*, 433.
11. Freeman, J. W.; Hallinan, N. C.; Arif, A. M.; Gedridge, R. W.; Ernst, R. D.; Basolo, F. *J. Am. Chem. Soc.* **1991**, *113*, 6509.
12. Fischer, E. O.; Ulm, K. *Chem. Ber.* **1961**, *94*, 2413.
13. Fischer, E. O.; Kogler, H. P.; Kuzel, P. *Chem. Ber.* **1960**, *93*, 3006.
14. Fritz, H. P.; Keller, H.; Fischer, E. O. *Naturwissenschaften* **1961**, *48*, 518.
15. Ariafield, A.; Bi, S.; Lin, Z. *Organometallics* **2005**, *24*, 2241.
16. Bi, S.; Ariafield, A.; Jia, G.; Lin, Z. *Organometallics* **2005**, *24*, 680.
17. van Staveren, D. R.; Bill, E.; Bothe, E.; Buhl, M.; Weyhermuller, T.; Metzler-Nolte, N. *Chem. Eur. J.* **2002**, *8*, 1649.
18. van Staveren, D. R.; Weyhermuller, T.; Metzler-Nolte, N. *Organometallics* **2000**, *19*, 3730.
19. Older, C. M.; Stryker, J. M. *Organometallics* **2000**, *19*, 2661.
20. MacConnachie, C. A.; Nelson, J. M.; Baird, M. C. *Organometallics* **1992**, *11*, 2521.

21. Shiu, K. B.; Liou, K.-S.; Cheng, C. P.; Fang, B.-R.; Wang, Y.; Lee, G.-H.; Vong, W.-J. *Organometallics* **1989**, *8*, 1219.
22. Shiu, K.-B.; Chang, C.-J.; Wang, Y.; Cheng, M.-C. *J. Organomet. Chem.* **1991**, *406*, 363.
23. Norman, D. W.; Ferguson, M. J.; Stryker, J. M. *Organometallics* **2004**, *23*, 2015.
24. Padwa, A.; Goldstein, S.; Pulwer, M. *J. Org. Chem.* **1982**, *47*, 3893.
25. Jutzi, P.; Heidemann, T.; Neumann, B.; Stammeler, H. G. *J. Organomet. Chem.* **1994**, *472*, 27.
26. Bachman, R. E.; Whitmire, K. H. *Inorg. Chem.* **1995**, *34*, 1542.
27. King, R. B. *Inorg. Chem.* **1966**, *5*, 2242.
28. Faller, J. W.; Incorvia, M. J. *Inorg. Chem.* **1968**, *7*, 840.
29. Albers, M. O.; Coville, N. J. *Coord. Chem. Rev.* **1984**, *53*, 227.
30. Arduengo, A. J., III; Krafczyk, R.; Schmutzler, R. *Tetrahedron* **1999**, *55*, 14523.
31. Angelici, R. J.; Busetto, L. *Inorg. Chem.* **1968**, *7*, 1935, and references therein.
32. Herrmann, W. A. *Angew. Chem. Int. Ed. Engl.* **2002**, *41*, 1290.
33. Herrmann, W. A. *Adv. Organomet. Chem.* **2002**, *48*, 1.

Chapter 3.

Synthesis of the first thermally stable chromium(III) η^3 -allyl complexes

3.0 One-electron oxidation of the neutral $\text{CpCr}(\eta^3\text{-allyl})(\text{CO})_2$ complexes

Despite the discouraging results from the early attempts at decarbonylation of chromium η^3 -allyl dicarbonyl complex **66**, we were confident that cationic $\text{CpCrNO}(\text{CO})(\eta^3\text{-allyl})^+$ complexes (*i.e.*, **Ia**, p. 48) could be prepared analogously to the corresponding molybdenum complexes (see eq. 2.1, p. 47). Surprisingly, treatment of chromium(II) η^3 -allyl complex **66** with nitrosonium salts in either acetone or acetonitrile provides crude reaction mixtures that show spectroscopic evidence for simple oxidation of the metal from chromium(II) to chromium(III) without coordination of the nitroso ligand. Indeed, carbonyl infrared absorptions identical to those from the above ferricinium and silver oxidation reactions were present.

Given the insolubility of the chromium(III) product in DME and the unusual ability of this solvent to stabilize nitrosonium oxidants,¹ we next investigated the effect of this relatively benign solvent on the oxidation reaction. Thus, treatment of the chromium(II) η^3 -allyl complex **66** with nitrosonium hexafluorophosphate in DME at 0 °C, in a system open to an N_2 atmosphere, leads to nitric oxide effervescence and precipitation of an analytically pure paramagnetic green solid, subsequently identified as cationic chromium(III) η^3 -allyl complex **77** (eq. 3.1, and Table 3.1, entry 1).²

Infrared spectroscopy of this solid as a NUJOL mull shows carbonyl stretching frequencies at 2070 and 2032 cm^{-1} , with no evidence of nitric oxide coordination or the neutral η^3 -allyl dicarbonyl complex. The lack of formation of a carbonyl nitrosyl analogue of η^3 -allyl molybdenum complex **1** is surprising; the smaller ionic radius of

chromium apparently permits one electron oxidation by nitrosonium ion, but not the subsequent coordination of the co-generated nitric oxide. Similar reactivity has been observed for other chromium(II) complexes upon nitrosonium ion oxidation to the chromium(III) analogues.^{3, 4}

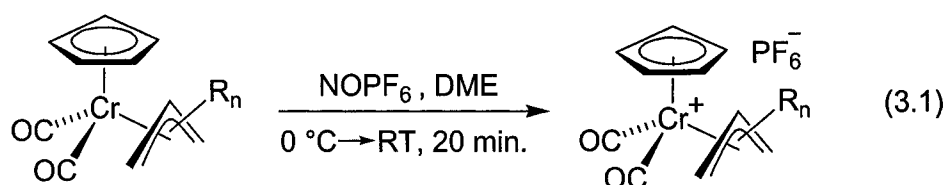


Table 3.1: Reaction details for the synthesis of cationic chromium(III) η^3 -allyl complexes **77-79** from the neutral chromium(II) precursors (eq. 3.1).

Entry	Substrate	Product(s)	ν_{CO}^a	% Yield
1	66	 77	2070, 2032	82
2	69	 78 <i>exo</i> (+ <i>endo</i>)	2065, 2040, 2031, 2022	70
3	74	 79	2039, 2002	96

^aInfrared spectra recorded as a NUJOL mull, cm^{-1} .

This methodology is readily extended to the oxidation of substituted chromium(II) η^3 -allyl complexes. Thus, treatment of neutral η^3 -crotyl and η^3 -cyclohexenyl complexes

69 and **74** with NOPF_6 in DME leads to the oxidized congeners **78** and **79**, respectively (Table 3.1, entries 2 and 3). Oxidation of the more soluble indenyl η^3 -allyl complex, however, does not provide a precipitate and no tractable reaction product can be isolated from solution. The infrared spectra of complexes **77** and **79** each show two carbonyl stretching frequencies, suggesting the presence of a single stereoisomer, whereas the spectrum of η^3 -crotyl complex **78** displays four high energy absorptions, implying the presence of at least two stereoisomers, tentatively assigned as *endo* and *exo*. Elemental analysis of this complex confirms the compositional homogeneity, supporting this tentative assignment of a mixture of allyl stereoisomers.

Both chromium(III) η^3 -allyl complexes **77** and **78** are green to yellow-green in colour; the η^3 -cyclohexenyl complex **79**, however, is an orange-red powder. This contrast in colour suggests the possibility of unique bonding interactions for the cyclohexenyl ligand, including the possibility of an agostic interaction between one methylene C-H bond of the η^3 -cyclohexenyl ligand and the now unsaturated 17-electron metal centre. Indeed, the X-ray crystal structure (Fig. 2.3) of the *neutral* η^3 -cyclohexenyl precursor **74** reveals the distance between the metal and one distal (non-allylic) methylene hydrogen to be just 3.22 Å; upon one-electron oxidation, this distance may contract sufficiently to create an agostic bonding interaction. Alternatively, the difference in colour may simply result from the unique 1,3-bis(anti) substitution pattern imposed by the endocyclic disposition of the η^3 -allyl moiety.

3.1 Crystallographic structural comparison of the Cr(II) and Cr(III) η^3 -allyl redox isomers

Single crystals of the unsubstituted cationic allyl complex **77** were deposited directly from the oxidation reaction conducted at higher dilution and the structure was confirmed by X-ray crystallography (Fig. 3.1). While the solid-state structure of this complex is in itself unremarkable, more notable is the opportunity to compare this cationic chromium(III) complex with the solid-state structure of the neutral but otherwise identical chromium(II) complex **66** (Table 3.2). The structures, while superficially similar, differ in a number of significant parameters. The chromium responds to the oxidation by marginally decreasing the metal-carbon bond distances for the two terminal allyl positions to 2.220(3) Å from 2.231(5) and 2.239(5) Å in complex **66**, but the distance between the allyl central carbon and the chromium centre increases to 2.151(4) Å from 2.108(4) Å. These differences in bond distances alter the dihedral angle between the planes containing the allyl ligand and the cyclopentadienyl, respectively, which increases by more than 5° in the oxidized complex.

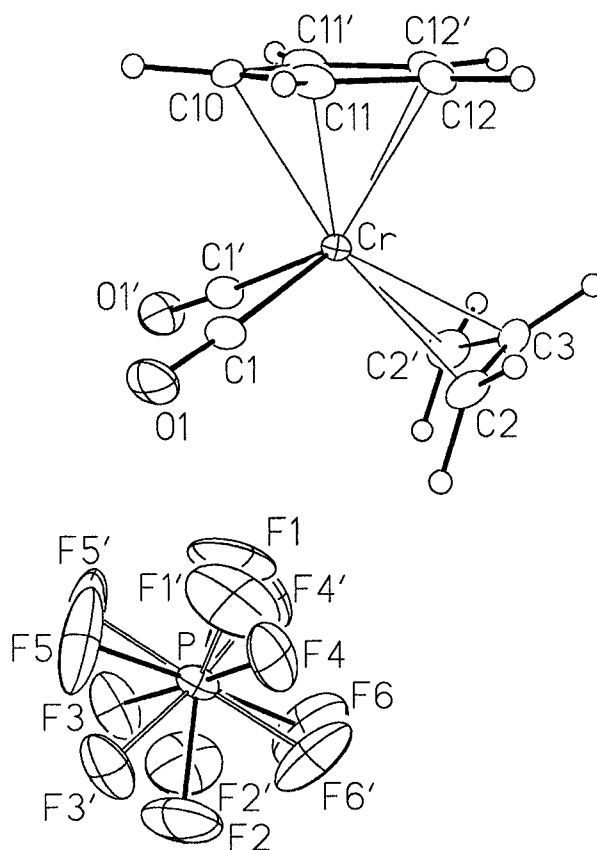
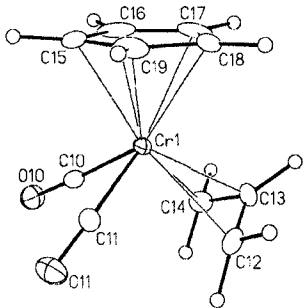
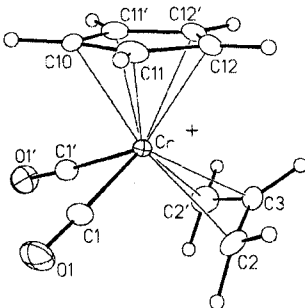


Figure 3.1: The solid-state molecular structure of cationic η^3 -allyl complex **77** showing the disordered PF₆ counterion; 0.5 equivalents of non-coordinated interstitial DME are omitted. Non-hydrogen atoms are represented by Gaussian ellipsoids at the 20% probability level. Hydrogen atoms are shown with arbitrarily small thermal parameters. Primed atoms are related to unprimed ones via the crystallographic mirror plane (0, y, z) passing through Cr, C3, C10, and the midpoint of the C12–C12' bond. See Table 3.2 for selected bond lengths and angles of the cation.

Table 3.2: Selected bond lengths (Å), angles (deg), and dihedral angles between planes (deg) for allyl complexes **66** (neutral) and **77** (cation).^a

			
Neutral Cr(II) η^3 -allyl complex 66		Cationic Cr(III) η^3 -allyl complex 77 ^b	
Bond lengths (Å)		Bond lengths (Å)	
Cr(1)-C(10)	1.814(6)	Cr-C(1)	1.901(3)
Cr(1)-C(11)	1.817(5)		
Cr(1)-C(12)	2.231(5)	Cr-C(2)	2.220(3)
Cr(1)-C(13)	2.108(4)	Cr-C(3)	2.151(4)
Cr(1)-C(14)	2.239(5)		
Cr(1)-C(15)	2.164(5)	Cr-C(10)	2.164(4)
Cr(1)-C(16)	2.178(6)	Cr-C(11)	2.184(3)
Cr(1)-C(17)	2.315(5)	Cr-C(12)	2.215(3)
Cr(1)-C(18)	2.215(5)		
Cr(1)-C(19)	2.190(5)		
O(10)-C(10)	1.168(6)	O(1)-C(1)	1.125(4)
O(11)-C(11)	1.155(6)		
Bond angles (deg)		Bond angles (deg)	
C(11)-Cr-C(10)	83.4(2)	C(1)-Cr-C(1')	87.72(19)
C(11)-Cr-C(12)	72.6(2)	C(1)-Cr-C(2)	77.51(14)
C(11)-Cr-C(13)	107.9(2)	C(1)-Cr-C(3)	113.38(12)
C(11)-Cr-C(14)	113.4(2)	C(1)-Cr-C(2')	122.30(14)
C(11)-Cr-C(19)	89.0(2)	C(1)-Cr-C(11)	81.69(12)
C(12)-Cr-C(18)	93.7(2)	C(2)-Cr-C(12)	92.90(13)
C(13)-Cr-C(18)	88.8(2)	C(3)-Cr-C(12)	88.09(14)
C(12)-C(13)-C(14)	118.8(5)	C(2)-C(3)-C(2')	120.0(5)
Dihedral angle planes (deg)		Dihedral angle planes (deg)	
Cr(CO) ₂ / allyl	2.8(8)	Cr(CO) ₂ / allyl	1.8(8)
Cr(CO) ₂ / Cp	38.24(18)	Cr(CO) ₂ / Cp	28.27(17)
allyl / Cp	35.5(6)	allyl / Cp	30.1(6)

^aComplete listings of bond lengths and angles are provided in the Appendices. ^bCounterion omitted for clarity.

The most striking difference between the two η^3 -allyl complexes, however, is manifest in the dihedral angle between the plane containing the $\text{Cr}(\text{CO})_2$ fragment and that of the cyclopentadienyl ring: in cationic complex **77**, the $\text{Cr}(\text{CO})_2$ plane is tilted fully 10° closer to the plane of the ring than the neutral complex **66**. This substantial relaxation of the roughly square pyramidal coordination sphere may be attributed to the reduction in $d \rightarrow \pi^*$ back-donation from the oxidized metal centre to the ancillary carbonyl and allyl ligand. The location of the counterion in or just under the cleft formed between the allyl and carbonyl ligands (Fig. 3.1), however, suggests that the ancillary ligands undergo a shift toward the cyclopentadienyl ring in order to accommodate a closer association of counter anion and the cationic chromium centre.

With the reduction in $d \rightarrow \pi^*$ back-donation, the chromium-CO bond distances in complex **77** increase to $1.901(3) \text{ \AA}$, notably longer than in the lower valent complex **66** ($1.814(6)$ and $1.817(5) \text{ \AA}$). Accordingly, the C-O bond lengths of the cationic complex are approximately 3% shorter than those in complex **66**, resulting in an almost 150 cm^{-1} increase in the average carbonyl stretching frequency in the infrared spectrum of the cationic complex. Such changes in bond distances and infrared absorptions have been previously reported for redox pairs of chromium dicarbonyl complexes, albeit with entirely different ligand sets (Table 3.3).^{4,5}

Table 3.2: Selected bond distances (Å) and carbonyl infrared absorptions (cm⁻¹) for redox isomers of [Cr(CO)₂(π -alkyne)(η^6 -arene)]ⁿ (n = 0, 1)^a complexes (ref. 4, 5).

Complex	Cr–CO	C–O	ν_{CO} ^b
Cr(CO) ₂ (PhC≡CPh)(η^6 -C ₆ Me ₆)	1.823(3), 1.816(4)	1.166(3), 1.166(3)	1900, 1823
[Cr(CO) ₂ (PhC≡CPh)(η^6 -C ₆ Me ₆)] ⁺	1.880(6), 1.869(8)	1.140(8), 1.131(9)	2024, 1974
Cr(CO) ₂ (<i>p</i> -MeOC ₆ H ₄ C≡CC ₆ H ₄ OMe- <i>p</i>)(η^6 -C ₆ Me ₆)	N/A ^c	N/A ^c	1889, 1811
[Cr(CO) ₂ (<i>p</i> -MeOC ₆ H ₄ C≡CC ₆ H ₄ OMe- <i>p</i>)(η^6 -C ₆ Me ₆)] ⁺	1.895(5), 1.865(5)	1.142(5), 1.146(6)	2011, 1965

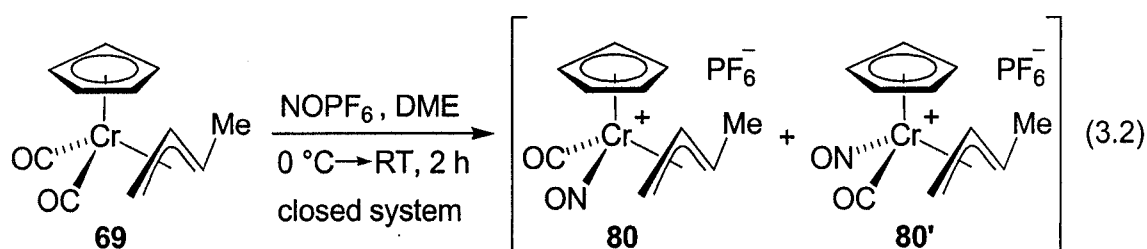
^aThe cationic complexes were prepared via the addition of [Cp₂Fe]PF₆ to the neutral precursors. ^bInfrared spectra recorded as solutions in dichloromethane. ^cThis data was not published.

3.2 Coordination of nitric oxide to the cationic η^3 -crotyl dicarbonyl complex

The addition of nitrosonium hexafluorophosphate to the neutral η^3 -allyl dicarbonyl complexes **66**, **69**, and **72** in an open system thus leads exclusively to the first examples of thermally stable chromium(III) η^3 -allyl complexes.² We speculated, however, that the originally targeted Type **Ia** [CpCrNO(CO)(η^3 -allyl)]⁺ complexes could instead be obtained by performing the addition reaction in a *closed* system, allowing the co-generated nitric oxide to eventually coordinate to the chromium centre with displacement of a CO ligand.

Thus, a solution of NOPF₆ in DME was added from the sidearm of a solvent bomb to a solution of η^3 -crotyl dicarbonyl complex **69** in DME at 0 °C; the Teflon stopcock was sealed immediately after addition. After filtering the heterogeneous

reaction mixture through Celite, the solvent was removed *in vacuo* and the dark orange residue dissolved in 0.8 mL of acetone- d_6 . Among the numerous resonances in the ^1H NMR spectrum of this impure product mixture, two methyl doublets are apparent (in trace amounts) at δ 2.58 ($J = 6.8$ Hz) and 2.32 ($J = 6.4$ Hz) in a 3.5 : 1.0 ratio, along with the corresponding η^5 -cyclopentadienyl ligand resonances at δ 5.96 and 6.05. Although the yield of these products remains undetermined and the low product purity obscured the infrared data, we tentatively attribute these proton resonances as arising from a mixture of structurally unassigned diastereomeric isomers of $[\text{CpCrNO}(\text{CO})(\eta^3\text{-crotyl})]\text{PF}_6$ complex **80** (eq. 3.2).



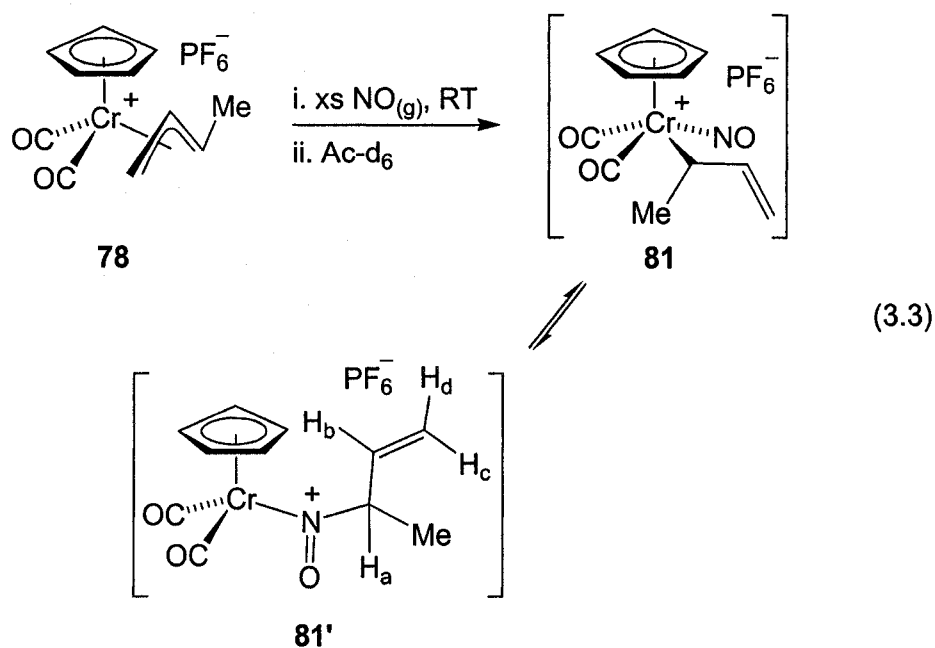
Interestingly, addition of gaseous nitric oxide to pure cationic η^3 -crotyl dicarbonyl complex **78** does not provide the same product mixture. For instance, when a Schlenk flask containing complex **78** (without solvent) was purged with nitric oxide and the resulting mixture subsequently dissolved in acetone- d_6 , a *homogeneous* dark orange solution was obtained. NMR analysis of this sample after two hours at room temperature shows *four* distinct crotyl methyl doublets (different from those observed for cationic complex **80** and neutral complex **69**) at δ 1.61 ($J = 6.8$ Hz), 1.45 ($J = 6.4$ Hz), 1.41 ($J = 6.4$ Hz), and 1.16 ($J = 6.4$ Hz) in a 3.4 : 6.8 : 1.0 : 8.7 ratio. After twenty-four hours in solution at room temperature, however, this product mixture equilibrates to just one

compound, the ^1H NMR spectrum revealing a single methyl doublet at 1.16 ppm ($J = 6.4$ Hz). One- and two-dimensional NMR analysis of this compound reveals additional proton resonances that are easily assigned to a crotyl-type ligand (Table 3.4).

Table 3.4: ^1H NMR data (ppm) for the $[\text{CpCr}(\text{CO})_2(\text{NO})(\text{crotyl})]\text{PF}_6$ complex **81/81'**. See equation 3.3 for the labeling scheme.

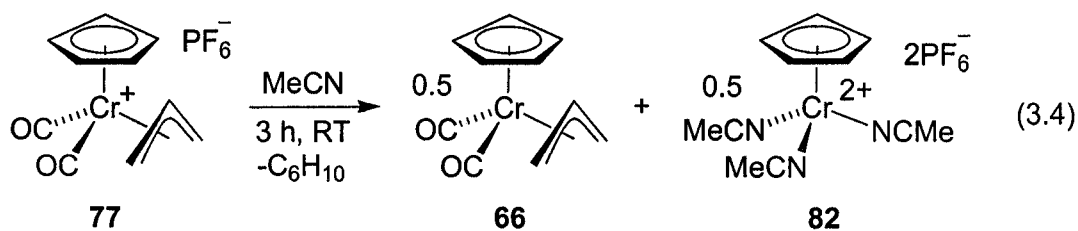
Cp	H _a	H _b	H _c	H _d	Me
6.24	4.20 (dq, $J = 6.5$, 5.5 Hz)	5.88 (ddd, $J = 17.0$, 10.5, 5.5 Hz)	5.15 (d, $J = 10.5$ Hz)	5.15 (d, $J = 17.0$ Hz)	1.16 (d, $J = 6.5$ Hz)

Since the relative downfield chemical shift of three of these protons is indicative of a terminal olefinic group, this crotyl moiety is tentatively assigned as the σ -crotyl ligand of cationic complex **81** (eq. 3.3). The chemical shift of the methyl group, however, is considerably upfield at 1.16 ppm and therefore likely arises from a methyl substituent on a non-metal-bound sp^3 carbon. The nitrosyl insertion complex **81'** (eq. 3.3) is therefore one possible alternative for the structural assignment of this product, perhaps rendered more reasonable by the fact that chromium σ -allyl ligands are generally thermally unstable at room temperature. Unfortunately, this compound could not be isolated from solution and we have been unable to obtain an infrared spectrum.



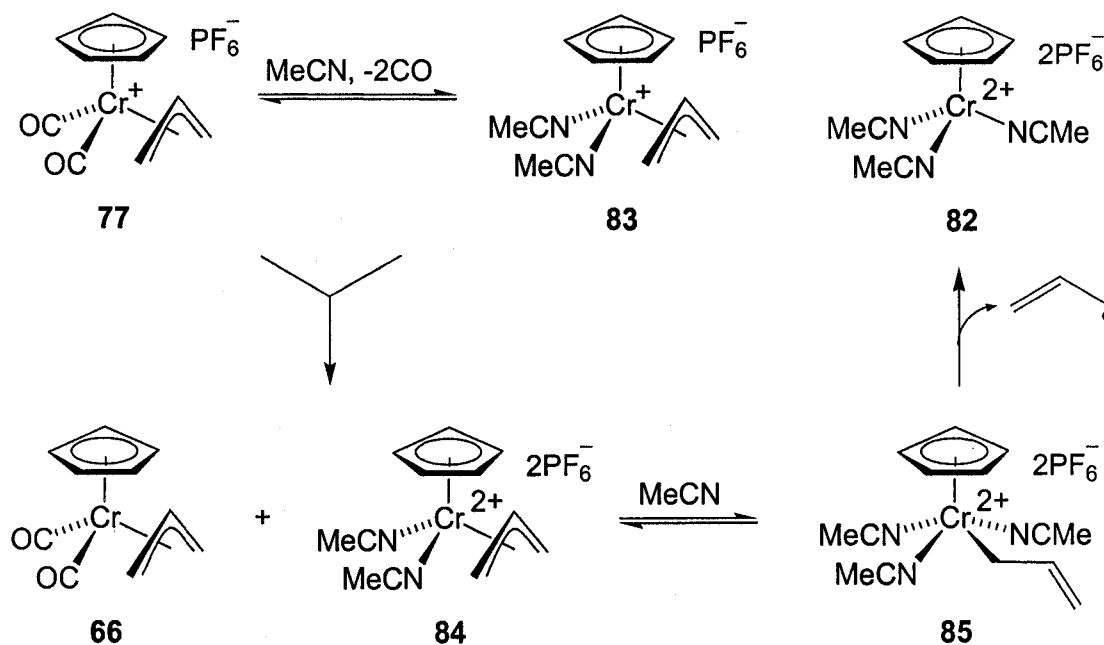
3.3 Reactivity of the $[\text{CpCr}(\eta^3\text{-allyl})(\text{CO})_2]\text{PF}_6$ complex

Cationic η^3 -allyl complexes **77-79** are indefinitely stable as solids at room temperature, unique among all previously reported chromium(III) η^3 -allyl compounds (recall Chart 1.2, p. 28). In donor solvents, however, the complexes are susceptible to rapid disproportionation. In acetonitrile, for example, complex **77** is completely consumed after three hours to give a 1 : 1 mixture of the neutral η^3 -allyl complex **66** and the novel dicationic cyclopentadienylchromium(III) tris(acetonitrile) complex **82** in high yield (eq. 3.4). 1,5-Hexadiene (unquantified), presumably arising from homolytic cleavage of the allyl ligand, was identified in the crude reaction mixture by gas chromatography (see the Experimental section for details).



The mechanism of this reaction is presumed to involve equilibrium dissociation of the carbonyl ligands to give some of the cationic bis(acetonitrile) complex **83** (Scheme 3.1). This relatively electron rich intermediate can then reduce the remaining dicarbonyl cation **77**, ultimately producing a 1 : 1 mixture of the neutral η^3 -allyl complex **66** and the thermally unstable dicationic chromium(IV) allyl intermediate **84**. Subsequent association of acetonitrile followed by homolysis of the consequent σ -allyl ligand of intermediate complex **85** leads to the formation of 1,5-hexadiene and the observed dicationic tris(acetonitrile) complex **82**. Consistent with this mechanism, the rate of the disproportionation is reduced at higher dilution. The structural assignment is supported by independent synthesis: treatment of the known dichloro dimer $[(\eta^5\text{-C}_5\text{H}_5)\text{CrCl}_2]_2$ ⁶ with four equivalents of silver hexafluorophosphate in acetonitrile affords the interesting tris(acetonitrile) complex **82** in high yield.

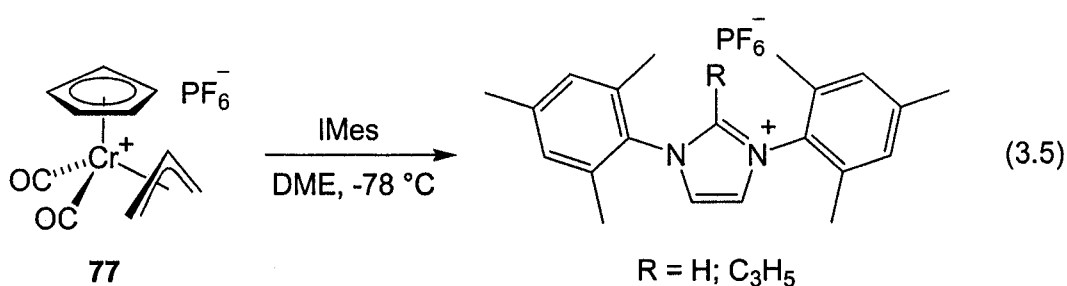
Scheme 3.1



Other attempts to induce substitution of the carbonyl ligands in cationic complex **77** without concomitant redox disproportionation have met no notable success. Although trimethylamine *N*-oxide is generally used to remove metal carbonyl ligands,⁷ it can also form metal oxides upon reaction with organochromium complexes.⁸ Thus, addition of this reagent to a suspension of complex **77** in DME at low temperature leads only to the formation of an intractable product mixture. Heating a suspension of complex **77** in toluene gave a variable amount of the neutral η^3 -allyl dicarbonyl complex **66** and an uncharacterizable blue material.

Displacement of the carbonyl ligands with strong neutral donors also failed to yield products retaining the allyl ligand. For example, the reaction of complex **77** with IMes gave only unidentified metal-containing product(s). A diamagnetic organic fraction was also isolated, which by ^1H NMR spectroscopy proved to be primarily the protonated

carbene, $\text{IMesH}^+\text{PF}_6^-$, a known compound,⁹ along with a trace of the tentatively identified allylated analogue, 1,3-bis(2,4,6-trimethylphenyl)-2-(1-propenyl)imidazolium hexafluorophosphate (eq. 3.5), this product was assigned on the basis of broad ^1H NMR signals between 5.0 and 6.5 ppm, indicative of a terminal olefin. The major reaction pathway thus appears to be the deprotonation of the starting complex (presumably at the allyl ligand), accompanied by a trace of the less favourable nucleophilic addition to the η^3 -allyl terminal position. It is not obvious why the more electrophilic chromium(III) complex **77** favours deprotonation over nucleophilic addition, despite the obviously low activation barrier for the nucleophilic pathway in the neutral congener **66** (recall eq. 2.5, p. 52).

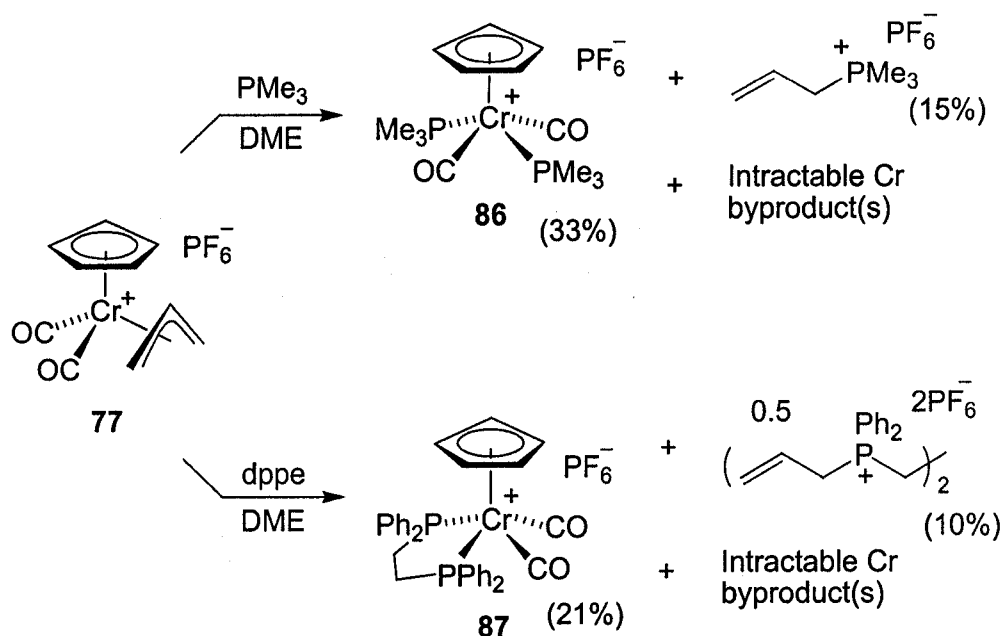


The investigation of phosphine substitution was equally disappointing. In contrast to the chemistry of the neutral chromium(II) η^3 -allyl complex, the reaction of chromium(III) complex **77** with monodentate or bidentate tertiary phosphine proceeds at or below room temperature, but leads only to the isolation of de-allylated diamagnetic cationic cyclopentadienylchromium(II) bis(phosphine) complexes in low yield (Scheme 3.2).

Thus, treatment of a suspension of complex **77** in DME with two equivalents of trimethylphosphine leads to the formation of a yellow-green solid, identified

spectroscopically as the *trans*-bis(trimethylphosphine)cyclopentadienylchromium(II) dicarbonyl cation **86**. A second product, isolated from the supernatant, was determined to be the known allyltrimethylphosphonium hexafluorophosphate by spectroscopic comparison to authentic material prepared independently.¹⁰ Similar reaction conditions provided the *cis*-[1,2-bis(diphenylphosphino)ethane]cyclopentadienyl chromium(II) dicarbonyl cation **87** from treatment with one equivalent of bis(diphenylphosphino)ethane, along with the tentatively assigned doubly allylated phosphonium salt, also obtained in very low yield (Scheme 3.2)

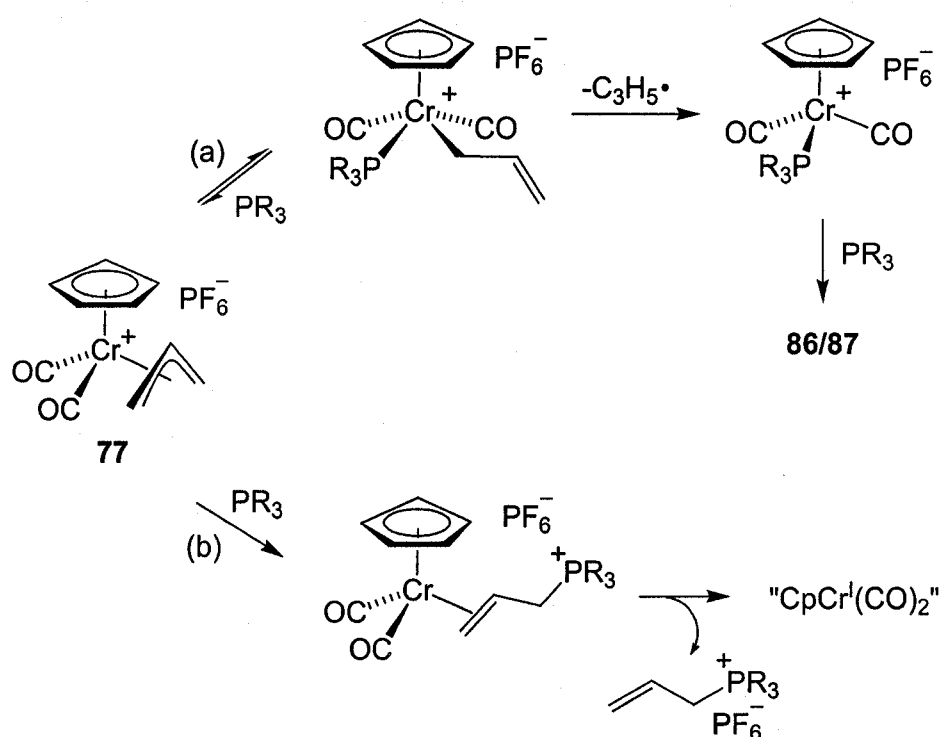
Scheme 3.2



Complexes **86** and **87** presumably arise from the association of one phosphine to the metal with concomitant isomerization of the allyl ligand from η^3 - to η^1 -hapticity (Scheme 3.3, path a). Subsequent homolytic loss of allyl radical and association of a

second phosphine provides the observed product. The allylphosphonium salts must then result from *an independent pathway* triggered by nucleophilic addition of phosphine to the allyl ligand (Scheme 3.3, path b), followed by dissociation of the alkene from the now lower valent Cr(I) centre. Unfortunately, no other tractable metal-containing products could be isolated from these reactions, leaving the fate of the reduced chromium species as yet undetermined.

Scheme 3.3



The presence of the PMe_3 and dppe ligands is quite evident in the ^1H NMR spectra of complexes 86 and 87. The proton resonances for the cyclopentadienyl ligands of both complexes, for example, are present as triplets ($J = 2.0$ and 1.5 Hz, respectively), resulting from three-bond ^1H - ^{31}P coupling. More interesting, however, is the proton

resonance of the methyl groups of bis(PMe₃) complex **86** (Fig. 3.2, A). Rather than a simple doublet resulting from two-bond ¹H-³¹P coupling, this signal is present as a second order multiplet. Such methyl signal patterns are common among bis(PMeR₂) (R = alkyl or aryl) complexes and are known to arise as a result of virtual coupling.¹¹ Thus, the bis(phosphine) geometry/NMR comparison reported by Crabtree¹¹ (reproduced in Fig. 3.2, B) suggests that the relative angle between the PMe₃ ligands of bis(PMe₃) complex **86** may be in the range of 125° and 130°.

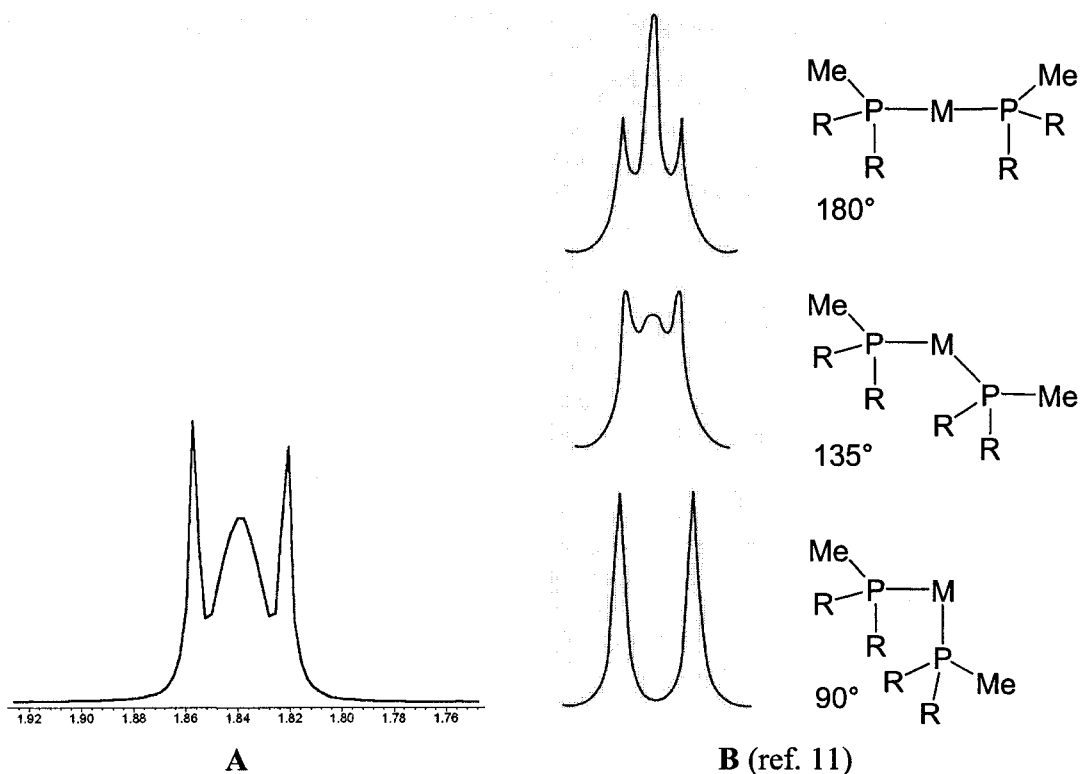


Figure 3.2, A: Expansion of the methyl region from the ¹H NMR spectrum of cationic bis(PMe₃) complex **86**, and **B:** a comparison of the effect of phosphine ligand geometry on the methyl ¹H NMR signals of bis(PMeR₂) (R = alkyl or aryl) complexes.

In addition to this NMR spectroscopic analysis, the structural determination of both complexes **86** and **87** was complemented by X-ray crystallography (Figs. 3.3 and 3.4). In accordance with the above proposed phosphine geometry, the crystal structure of bis(PMe₃) complex **86** clearly reveals a P(1)-Cr-P(1') angle of 129.66(4)°. The dppe complex **87**, on the other hand, clearly possesses *cis* geometry: P(1)-Cr-P(2) = 77.84(5)°. Both of these complexes are structurally very similar to previously reported *cis*- and *trans*-bis(phosphine) complexes.^{3, 4, 12-15}

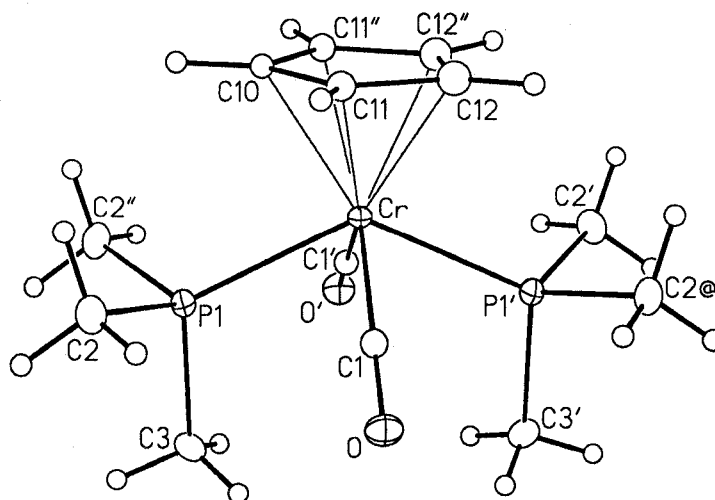


Figure 3.3: Solid-state molecular structure of complex **86**, showing only the cationic fragment. Non-hydrogen atoms are represented by Gaussian ellipsoids at the 20% probability level. Hydrogen atoms are shown with arbitrarily small thermal parameters. Primed atoms are related to unprimed ones via the crystallographic twofold rotational axis ($1/4, 1/4, z$) passing through the Cr atom. Double-primed atoms are related to unprimed ones via the crystallographic mirror plane ($1/4, y, z$) containing Cr, P1, and P1'. The carbon atom labelled C2@ is related to C2 via the mirror plane ($x, 1/4, z$) containing Cr and the carbonyl groups. Selected bond lengths (Å) and angles (deg): Cr-C(1) = 1.843(3), Cr-P(1) = 2.3509(8), Cr-C(10) = 2.193(5), Cr-C(11) = 2.199(4), Cr-C(12) = 2.1997(5), O-C(1) = 1.150(4); C(1)-Cr-C(10) = 118.70(8), C(1)-Cr-C(1') = 111.26(17), P(1)-Cr-P(1') = 129.66(4), P(1)-Cr-C(1) = 76.11(4), P(1)-Cr-C(10) = 83.45(13).

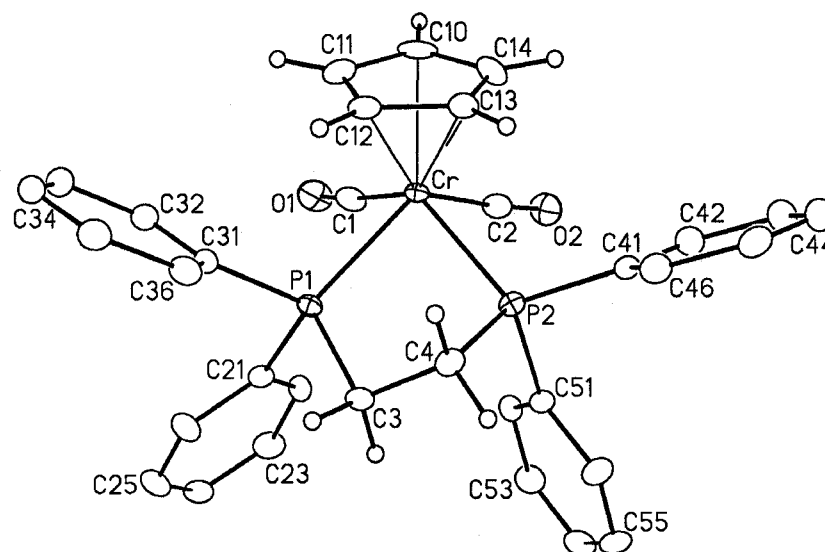


Figure 3.4: Solid-state molecular structure of complex **87** showing only the cationic fragment; 1.5 equivalents of interstitial acetone are omitted. Non-hydrogen atoms are represented by Gaussian ellipsoids at the 20% probability level. Hydrogen atoms are shown with arbitrarily small thermal parameters. Selected bond lengths (Å) and angles (deg): Cr-C(1) = 1.854(6), Cr-C(2) = 1.834(5), Cr-P(1) = 2.3994(13), Cr-P(2) = 2.3889(13), Cr-C(10) = 2.171(5), Cr-C(11) = 2.186(5), Cr-C(12) = 2.234(5), Cr-C(13) = 2.242(5), Cr-C(14) = 2.187(5), O(1)-C(1) = 1.146(7), O(2)-C(2) = 1.162(7), P(1)-C(13) = 1.866(4), C(3)-C(4) = 1.511(7), P(2)-C(4) = 1.820(5); C(1)-Cr-C(10) = 88.1(2), C(1)-Cr-C(2) = 78.6(2), P(1)-Cr-C(12) = 87.29(14), P(2)-Cr-C(13) = 82.43(14), P(1)-Cr-P(2) = 77.84(5), P(1)-C(3)-C(4) = 110.9(3), P(2)-C(4)-C(3) = 105.7(3).

3.4 References

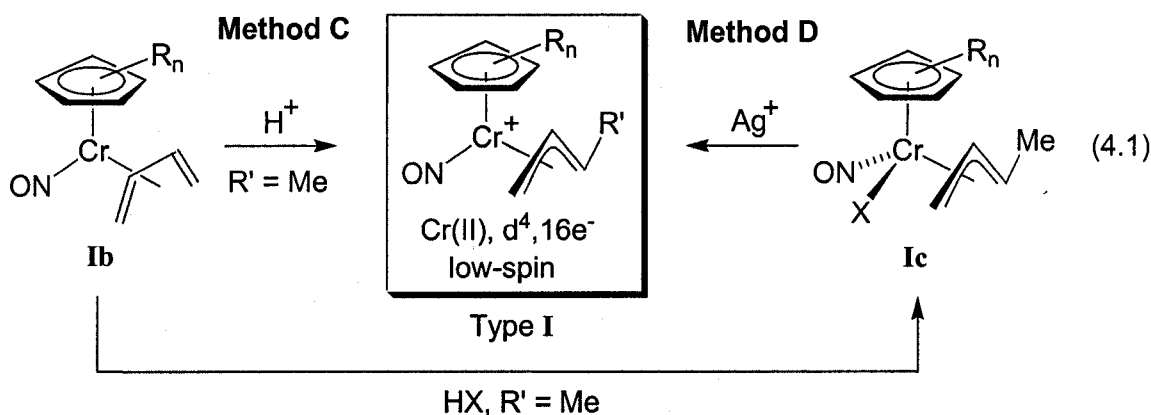
1. Liebeskind, L. S.; Cosford, N. D. P. *Organometallics* **1994**, *13*, 1498.
2. Norman, D. W.; McDonald, R.; Stryker, J. M. *Organometallics* **2005**, *24*, 4461.
3. Shen, J. K.; Freeman, J. W.; Hallinan, N. C.; Rheingold, A. L.; Arif, A. M.; Ernst, R. D.; Basolo, F. *Organometallics* **1992**, *98*, 1498.
4. Connelly, N. G.; Johnson, G. A. *J. Organomet. Chem.* **1974**, *77*, 341.
5. Adams, C. J.; Bartlett, I. M.; Connelly, N. G.; Harding, D. J.; Hayward, O. D.; Martin, A. J.; Orpen, A. G.; Quayle, M. J.; Rieger, P. H. *J. Chem. Soc., Dalton Trans.* **2002**, 4281.
6. Betz, P.; Döhring, A.; Emrich, R.; Goddard, R.; Jolly, P. W.; Krüger, C.; Romão, C. C.; Schönfelder, K. U.; Tsay, Y. H. *Polyhedron* **1993**, *12*, 2651.
7. Luh, T. Y.; Wong, C. S. *J. Organomet. Chem.* **1985**, *287*, 231.
8. Bottomley, F.; Paez, D. E.; Sutin, L.; White, P. S.; Köhler, F. H.; Thompson, R. C.; Westwood, N. P. C. *Organometallics* **1990**, *9*, 2443.
9. Arduengo, A. J., III; Gamper, S. F.; Tamm, M.; Calabrese, J. C.; Davidson, F.; Craig, H. A. *J. Am. Chem. Soc.* **1995**, *117*, 572.
10. Cardaci, G. *J. Chem. Soc., Dalton Trans.* **1984**, 815.
11. Crabtree, R. H. *The Organometallic Chemistry of the Transition Metals*, 2nd ed. John Wiley & Sons: New York, NY, 1994.
12. Schubert, U.; Ackermann, K.; Janta, R.; Voran, S.; Malisch, W. *Chem. Ber.* **1982**, *115*, 2003.
13. Cooley, N. A.; MacConnachie, P. T. F.; Baird, M. C. *Polyhedron* **1988**, *7*, 1965.
14. Watkins, W. C.; Hensel, K.; Fortier, S.; Macartney, D. H.; Baird, M. C.; McLain, S. J. *Organometallics* **1992**, *11*, 2418.
15. Salsini, L.; Pasquali, M.; Zandomenghi, M.; Festa, C.; Leoni, P.; Braga, D.; Sabatino, P. *J. Chem. Soc., Dalton Trans.* **1990**, 2007.

Chapter 4.

Synthesis of unprecedented first-row *s-trans* 1,3-diene complexes

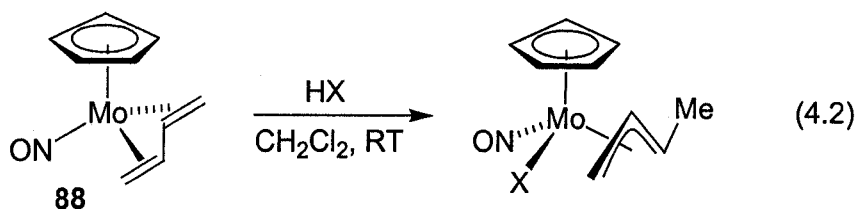
4.0 Introduction

Although addition of the nitrosonium ion to our novel chromium η^3 -allyl dicarbonyl complexes does not lead to the desired cationic carbonyl nitrosyl species **Ib**, we remained hopeful that the Type I cationic chromium(II) η^3 -allyl target complexes could be obtained by an alternative method involving protonation of chromium(0) nitrosyl complexes bearing η^4 -conjugated diene ligands (eq. 4.1, Methods C and D). Prior to this work, however, such reactions had not been demonstrated for chromium diene complexes.



Fortunately, the conversion of molybdenum nitrosyl η^4 -(1,3-diene) complexes to four-legged piano stool η^3 -allyl complexes, analogous to the proposed chromium chemistry, is well established. For example, the addition of aqueous hydroiodic acid to a solution of $\text{CpMo(NO)}(\eta^4\text{-s-}trans\text{-butadiene})$ **88** in dichloromethane affords the

corresponding η^3 -crotyl complex in excellent yield (eq. 4.2).¹ The addition of tetrafluoroboric acid to η^4 -diene complex **88**, however, leads only to intractable products,¹ suggesting that this second-row metal will not support the desired unsaturated coordination sphere.



Our attempts to prepare chromium analogues of complex **88**, either *s-cis* or *s-trans*, are documented below. Since these results include unprecedented examples of exclusively *s-trans* 1,3-diene coordination at chromium, a succinct introduction to the history of this peculiar coordination mode is warranted. Moreover, given the presence of the nitrosyl ligand throughout these complexes, a brief foreword is also required to introduce this uniquely reducing, yet π -acidic, ligand.

4.0.1 Salient features of nitric oxide

As a neutral molecule, nitric oxide is a stable radical, containing an unpaired electron in a partially filled π^* molecular orbital.²⁻⁵ Surprisingly, in addition to being ubiquitous throughout organometallic chemistry, trace amounts of this seemingly toxic molecule were discovered to play a critical role in physiological regulation.^{5,6} Consequently, there is now considerable interest in developing organometallic nitrosyl

complexes capable of delivering trace amounts of nitric oxide to specific biological targets.⁷⁻¹²

As a transition metal ligand, nitric oxide easily reduces coordinated metal centres by donating its odd electron, formally generating the coordinated nitrosonium ion NO^+ , an isoelectronic analogue of CO. Given the greater electronegativity of nitrogen over that of carbon, NO^+ is typically a stronger π -accepting ligand than CO and therefore generally less labile. Similar to CO, the nitrosyl ligand is also known to bridge bimetallic systems^{2,3} and insert into metal-carbon bonds.¹³⁻¹⁸

Unlike carbon monoxide, however, this ligand can adopt more than one bonding mode. Depending on the electronic and/or steric requirements of the metal, nitric oxide exists as either a linear or bent ligand (*i.e.*, the M–N–O angle approaches 180° or 120° , respectively). In electron counting terms, a linear nitrosyl ligand can either be considered as the 2-electron donating NO^+ moiety or as the 3-electron donating $\bullet\text{NO}$ radical (Fig. 4.1, structures **i** and **ii**, respectively). In the bent NO geometry the ligand formally exists as the nitroside group NO^- , and therefore behaves either as an anionic 2-electron donor or as a neutral 1-electron donor (Fig. 4.1, structures **iii** and **iv**, respectively).

The infrared absorption for non-coordinated nitric oxide is 1870 cm^{-1} , a value that may increase or decrease upon binding to a metal.²⁻⁵ In general, however, NO stretching frequencies of linear nitrosyl ligands range from $1950\text{--}1450\text{ cm}^{-1}$, while those for complexes containing bent nitrosyl ligands are in the range of $1720\text{--}1400\text{ cm}^{-1}$. Bridging nitrosyl ligands may have NO stretching frequencies anywhere between 1650 and 1300 cm^{-1} .²⁻⁵ Unfortunately, given the significant overlap of these ranges, there is no reliable

correlation between the value of ν_{NO} and the M–N–O bond angle. Definitive assignment of this latter parameter is therefore only possible via X-ray crystallography.

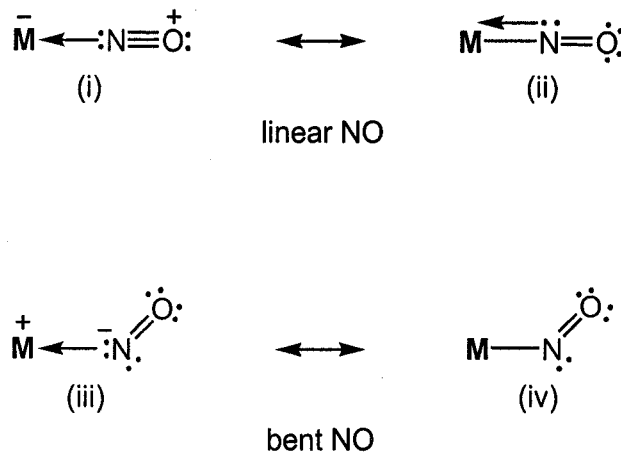


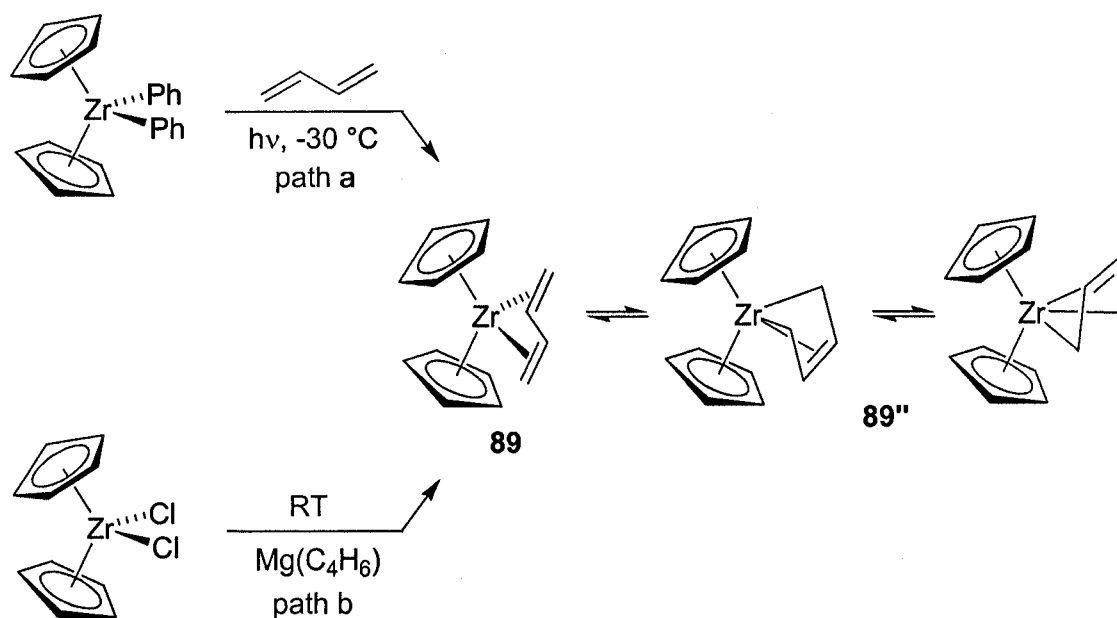
Figure 4.1: Resonance structures of linear and bent bonding modes of nitric oxide.

4.0.2 A brief history of *s-trans* 1,3-diene complexes

Butadiene, the simplest of the conjugated olefins, can attain two planar orientations. The *s-trans* conformation, in which both double bonds are positioned on opposite sides of the single bond, is more stable than the complementary *s-cis* isomer by ca. 3–4 Kcal/mol, with the isomeric interconversion being kinetically rapid ($\Delta G^\ddagger \approx 7$ Kcal/mol). However, due to more favourable metal-diene orbital overlap,¹⁹ most transition metal butadiene complexes adopt η^4 -coordination in the thermodynamically less favourable *s-cis* conformation. The first of this ubiquitous class of complexes, $\text{Fe}(\text{CO})_3(\text{s-cis-butadiene})$, was reported over seventy-five years ago;²⁰ however, the first *s-trans* 1,3-diene complex, zirconocene(butadiene) **89**, was reported a full half century later by Erker^{21, 22} and Nakamura²³ (Scheme 4.1, paths a and b, respectively). Both

investigators provided evidence that the *s-trans* product forms kinetically via an η^2 -intermediate **89'** (not shown), which subsequently gives rise to the *s-cis* η^4 -butadiene isomer **89''** under equilibrium conditions. Under thermodynamic control, an approximately 1 : 1 mixture of *s-trans* and *s-cis* butadiene complexes eventually forms. The *s-cis* isomer exhibits a typical σ^2, π -metallacyclic structural framework that undergoes a rapid “ring-flip” isomerization process, as illustrated.

Scheme 4.1



The degree and position of substitution of the coordinated diene in these complexes was found to be important for the bonding preference. Dienes substituted at the terminal positions by alkyl groups, for example, prefer the *s-trans* coordination mode, while internal alkyl substitution strongly favours *s-cis* coordination.²⁴

Following the discovery of the zirconocene(1,3-diene) complexes, the *s-trans* bonding mode has been expressed among many of the transition metals. For instance, mononuclear *s-trans* diene complexes have been prepared from early metals such as hafnium, niobium, tantalum, molybdenum, and tungsten, and relatively late metals such as rhenium and ruthenium.²⁴⁻²⁶ The reactivity, structural, and electronic trends associated with these complexes, along with those of the zirconium series, have been extensively reviewed.²⁴⁻²⁶ Characteristic among these *s-trans* complexes is a diene torsional angle [*i.e.*, C(1)-C(2)-C(3)-C(4)] ranging from 114° to 141°, in contrast to that of *s-cis* 1,3-diene complexes which approaches 0°. Table 4.1 (p. 95) lists comparative bond distances and angles for numerous examples of previously reported *s-trans* diene complexes as well as those of the novel chromium η^4 -(1,3-diene) complexes discussed in this chapter.^{1, 27-36}

Of the various methods used to synthesize molybdenum(*s-trans*-1,3-diene) complexes (Chart 4.1, routes a-c),^{1, 29, 30, 37-42} the addition of 1,3-dienes to $[\text{Cp}'\text{Mo}(\text{NO})\text{I}_2]_2$ under reducing conditions is the most widely used. The few examples of tungsten(*s-trans*-diene) complexes are obtained from the hydrogenation of $\text{Cp}'\text{W}(\text{NO})(\text{CH}_2\text{SiMe}_3)_2$ in the presence of conjugated dienes (Chart 4.1, route d).^{43, 44} Unfortunately, chromium compounds of the formula $\text{CpCr}(\text{NO})\text{X}_2$, where X is a halogen or alkyl, are not stable⁴⁵ and therefore cannot be used for the formation of the corresponding chromium(η^4 -1,3-diene) complexes.

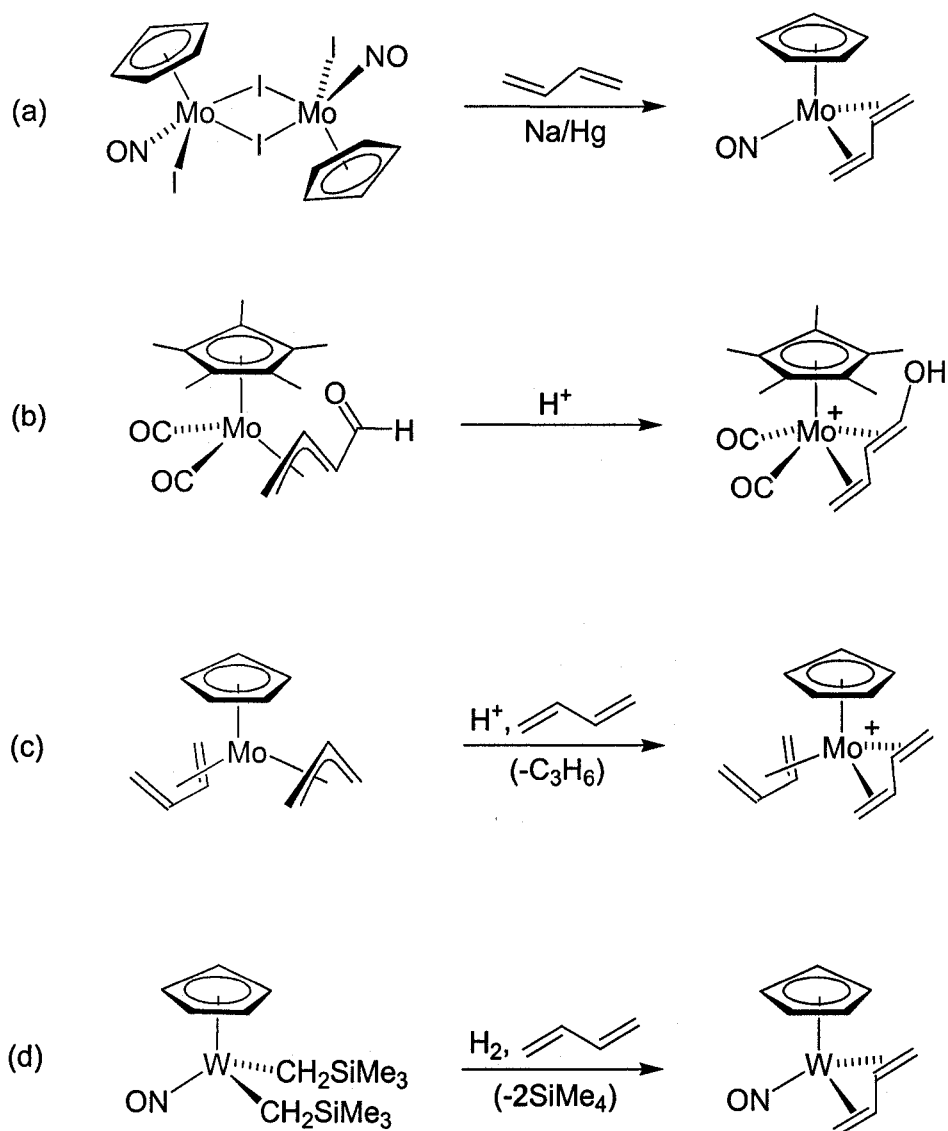


Chart 4.1: Preparative methods for known group VI *s-trans*-diene complexes: (a) ref. 1, 29, 37; (b) ref. 38-40; (c) ref. 30, 41, 42; (d) ref. 43, 44.

Several dinuclear and multinuclear complexes have also been reported to exhibit both *s-trans* and *s-cis* diene coordination across the metal-metal bond.²⁴ As such, several modes of mono- and dinuclear conjugated diene bonding have been identified (Chart 4.2).²⁴

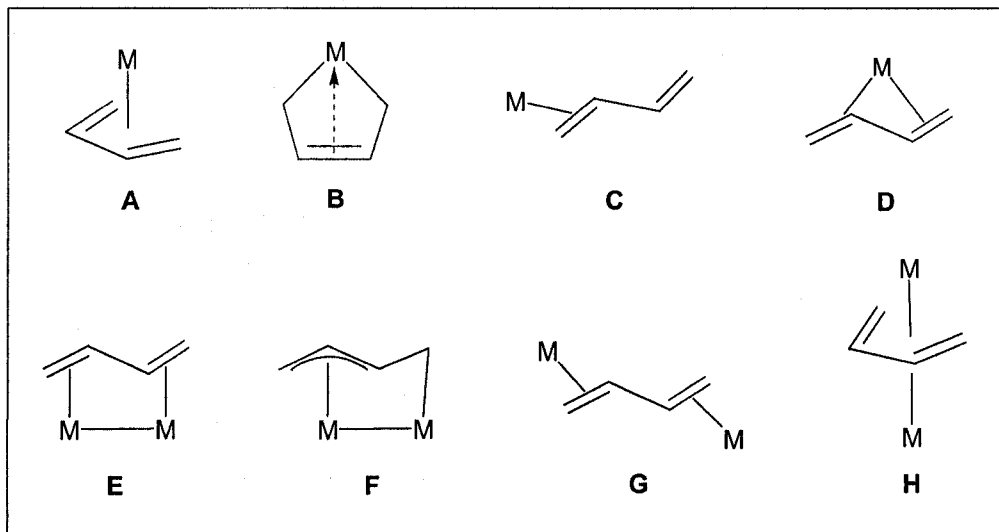


Chart 4.2: Bonding modes of conjugated dienes: **A** = *s-cis*- η^4 (π^2); **B** = *s-cis*-(σ^2, π); **C** = η^2 ; **D** = *s-trans*- η^4 ; **E** = *s-trans*-(*syn*- $\eta^2:\eta^2$); **F** = *syn*-($\eta^3:\sigma$); **G** = *s-trans*-(*anti*- $\eta^2:\eta^2$); **H** = bilateral coordination (common to alkali metals).

Table 4.1: Selected bond lengths (Å) and angles (deg) of several transition metal *s-trans* diene complexes.

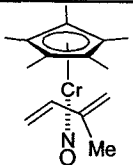
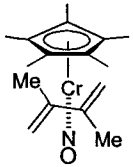
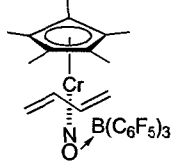
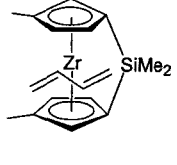
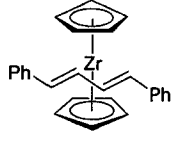
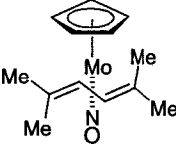
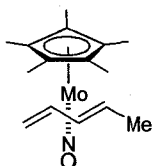
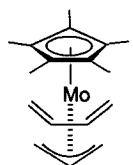
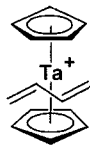
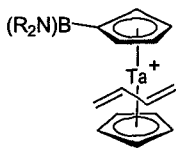
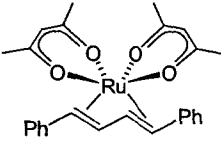
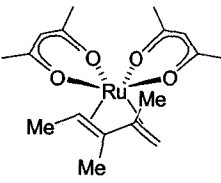
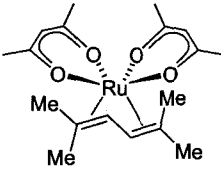
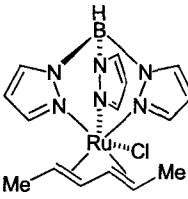
Entry	Complex	C(1)-C(2)	C(2)-C(3)	C(3)-C(4)	M-C(1), M-C(4)	M-C(2), M-C(3)	C(1)-C(2)-C(3), C(2)-C(3)-C(4)	C(1)-C(2)-C(3)-C(4)	Ref.
1		1.417(14)	1.356(11)	1.317(15)	2.188(4), 2.245(12)	2.146(6), 2.080(6)	112.7(8), 121.7(8)	125.2	Ch. 4
2		1.386(4)	1.448(4)	1.401(5)	2.222(3), 2.235(3)	2.163(3), 2.135(3)	116.7(3), 118.4(3)	119.3	Ch. 4
3		1.382(3)	1.418(3)	1.390(3)	2.2806(19), 2.2531(18)	2.1294(19), 2.1375(19)	120.3(2), 118.5(2)	123.5(2)	Ch. 5
4		1.402(5)	1.393(5)	1.364(6)	2.453(3), 2.455(3)	2.352(3), 2.338(3)	122.3(4), 123.4(4)	124.3(4)	27
5		1.41(2)	1.44(2)	1.39(2)	2.50(1), 2.54(1)	2.37(1), 2.39(1)	120.01	126.8, 129.4	28

Table 4.1 (continued): Selected bond lengths (Å) and angles (deg) of transition metal *s-trans* diene complexes.

Entry	Complex	C(1)-C(2)	C(2)-C(3)	C(3)-C(4)	M-C(1), M-C(4)	M-C(2), M-C(3)	C(1)-C(2)-C(3), C(2)-C(3)-C(4)	C(1)-C(2)-C(3)-C(4)	Ref.
6		1.418(4)	1.408(4)	1.401(4)	2.390(3), 2.365(3)	2.209(3), 2.234(3)	122.3(3), 122.1(3)	124.77	29
7		1.386(8)	1.422(8)	1.405(8)	2.331(5), 2.306(5)	2.206(5), 2.236(5)	120.0(5), 119.5(5)	121.54	1
8 ^a		1.39(2)	1.40(2)	1.29(3)	2.264(7), 2.29(4)	2.20(3), 2.30(4)	125(2), 120(2)	0.23	30
9		1.32(3)	1.53(4)	1.33(3)	2.418(17), 2.297(19)	2.306(15), 2.313(12)	102(2), 102(2)	140(2)	31
10		1.44(2)	1.45(1)	1.42(2)	2.45(1), 2.39(1)	2.29(1), 2.34(1)	123(1), 120(1)	121.57	32

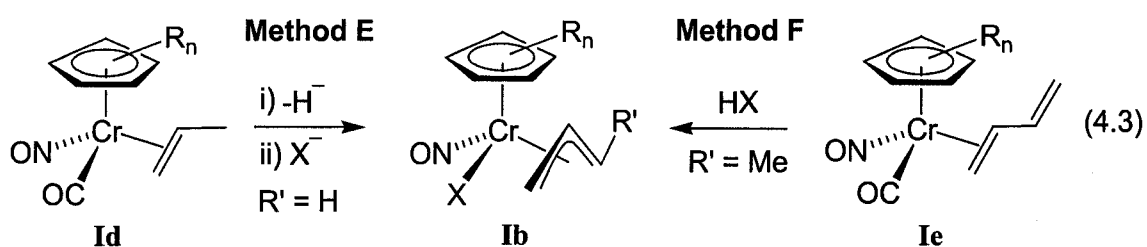
^aThis *s-cis* butadiene complex is included only to illustrate structural differences with the *s-trans* coordination mode.

Table 4.1 (continued): Selected bond lengths (Å) and angles (deg) of transition metal *s-trans* diene complexes.

Entry	Complex	C(1)-C(2)	C(2)-C(3)	C(3)-C(4)	M-C(1), M-C(4)	M-C(2), M-C(3)	C(1)-C(2)-C(3), C(2)-C(3)-C(4)	C(1)-C(2)-C(3)-C(4)	Ref.
11		1.380(4)	1.447(4)	1.391(4)	2.259(3), 2.285(3)	2.114(3), 2.110(3)	119.4(3), 116.7(3)	126.9(3)	33
12		1.392(4)	1.457(4)	1.402(4)	2.196(3), 2.291(3)	2.146(3), 2.107(3)	123.1(3), 112.1(3)	122.6	34
13		1.391(7)	1.421(6)	1.399(7)	2.255(4), 2.278(5)	2.091(4), 2.089(4)	118.0(4), 118.3(4)	123	35
14		1.372(5)	1.447(7)	1.372(5)	2.306(3), 2.306(3)	2.153(3), 2.153(3)	120.7(6), 119.8(6)	125.4(7)	36

4.0.3 Alternative strategies for the preparation of chromium η^3 -allyl carbonyl nitrosyl complexes

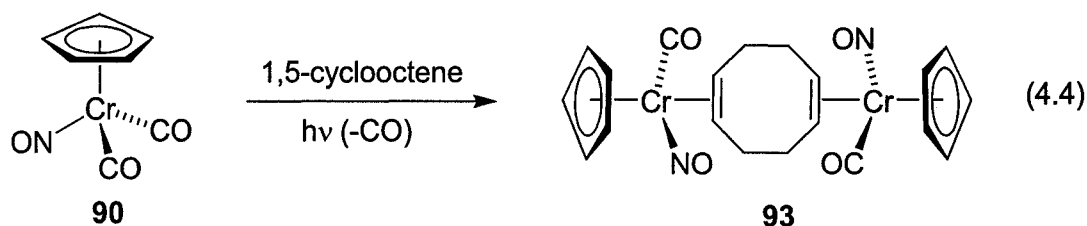
Given the apparent difficulties associated with the preparation of chromium η^4 -(1,3-diene) nitrosyl complexes via reductive methods,⁴⁵ direct preparation of the 16-electron Type **I** η^3 -allyl complexes via protonation of chromium dienes seemed unlikely. We therefore postulated an alternative strategy for obtaining the Type **Ib** $\text{Cp}'\text{Cr}(\text{NO})\text{X}(\eta^3\text{-allyl})$ complexes, which might then be converted to Type **I** (see p. 87). Thus, a single decarbonylation of a carbonyl-containing chromium precursor in the presence of a mono-olefin such as propene or a conjugated diene such as butadiene may afford the η^2 -alkene or η^2 -diene products **Id** and **Ie** (eq. 4.3). Hydride abstraction from the former complex followed by addition of a halide (X^-) is then expected to provide the parent η^3 -allyl complex of the **Ib** series, while protonation of the latter with haloacids should lead to the analogous η^3 -crotyl species (eq. 4.3, Methods **E** and **F**, respectively).



Herberhold⁴⁶⁻⁴⁸ has auspiciously demonstrated that $\text{CpCrNO}(\text{CO})_2$ **90**⁴⁹ does indeed lose CO under photolytic conditions and, in the presence of olefins or alkynes, forms compounds similar to the target **Id** complexes. Unfortunately, due to competitive photolytic decomposition, these products are generally obtained in low to medium yields

(10-50%). Given the lack of X-ray crystallographic data and the use of low resolution (60 MHz) ^1H NMR spectroscopy, structural determination of many of these complexes remains circumstantial.⁴⁶

Curiously, the only diene substrates reported by Herberhold were norbornadiene and 1,5-cyclooctadiene, both of which are non-conjugated. Photolysis with the former diene provides the expected η^2 -norbornadiene product while photolysis with the latter affords dinuclear complex **93**, very tentatively assigned to have two $\text{CpCrNO}(\text{CO})$ fragments bridged by the 1,5-diene (eq. 4.4). Characterization of this unique but thermally sensitive product was limited only to mass spectrometric analysis. Thus, prior to our work, there has been no investigation of photochemical substitution using *conjugated* dienes. Exploration of this understudied area, however, clearly would require significant optimization of Herberhold's photochemical method.



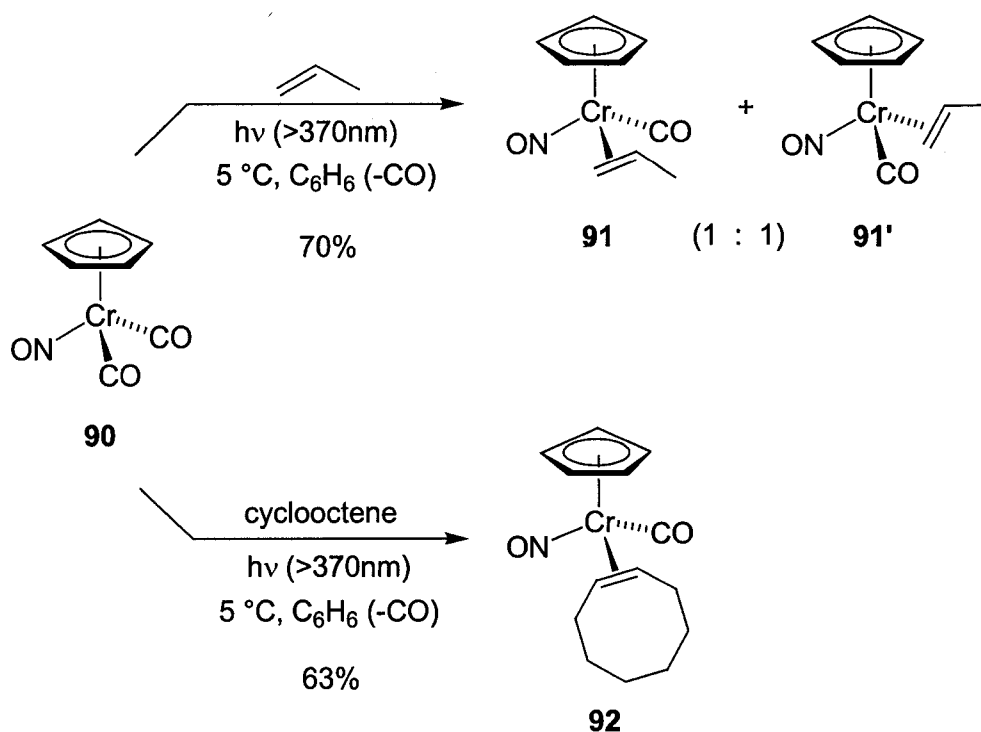
4.1 Photolysis of $\text{Cp}'\text{CrNO}(\text{CO})_2$ complexes in the presence of olefins

4.1.1 Formation of $\text{CpCrNO}(\text{CO})(\eta^2\text{-alkene})$ complexes

The photolytic decomposition observed by Herberhold is completely suppressed when the photolysis is conducted under ultraviolet irradiation through a 370 nm cutoff filter. In this way, photolysis of $\text{CpCrNO}(\text{CO})_2$ **90** in benzene in the presence of excess propene affords the $\text{CpCrNO}(\text{CO})(\eta^2\text{-propene})$ complex **91** in 70% yield, a substantial

improvement over Herberhold's yield of 10% (Scheme 4.2). Performing the reaction in neat liquid propene also affords complex **91** in comparable yield. Analysis of this complex by ^1H NMR spectroscopy (Table 4.2, entries 1 and 2, p. 105) revealed an approximate 1 : 1.5 stereochemical mixture of η^2 -propene isomers. Without further structural data, however, assignment of the configuration of the stereogenic metal centre as well as the orientation of the η^2 -propene ligand (*i.e.*, *endo* vs. *exo*) is not possible (Fig. 4.2). Two-dimensional NOE experiments (TROESY) failed to resolve this uncertainty.

Scheme 4.2



The same photochemical methodology also provides the η^2 -cyclooctene complex **92**, formed as a single isomer, in a yield higher than previously reported (63% vs. 50%) (Scheme 4.2). Since cyclooctene is a high boiling liquid, the progress of this reaction can

be monitored via carbon monoxide evolution from the reaction vessel into an inverted graduated water column. Thus, after 9 h of photolysis using the 370 nm cutoff filter, a 2.07 mmol scale reaction evolved ~22 mL of CO_(g) (88% of the calculated maximum). Removal of the volatiles leaves a brown residue which, upon recrystallization from pentane, affords the η^2 -cyclooctene complex **92**. Previous characterization of complexes **91** and **92** is of poor quality.⁴⁶ Thus, refer to the Experimental section for the improved characterization details of these complexes.

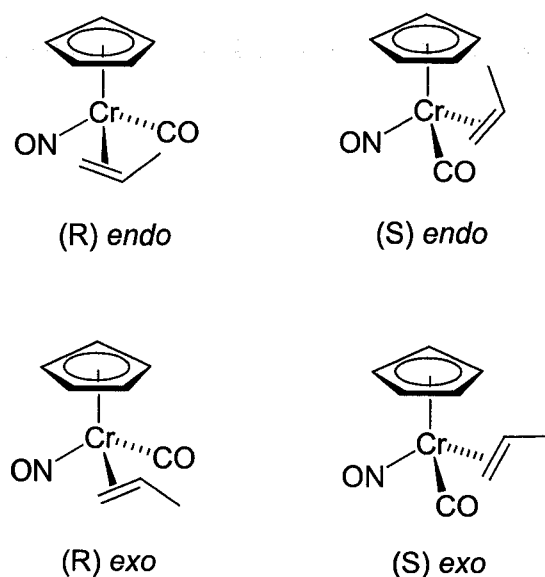
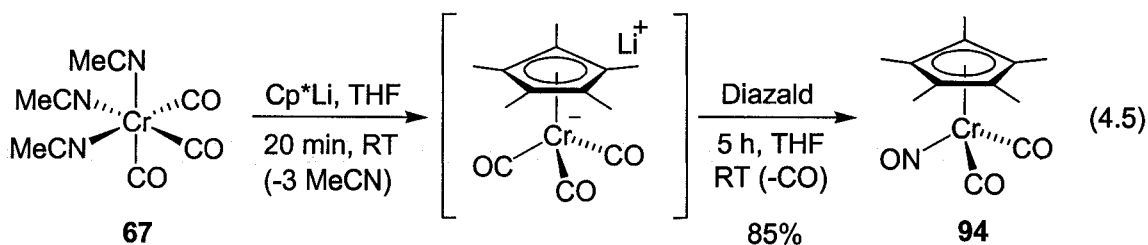


Figure 4.2: Possible stereoisomers of the CpCrNO(CO)(η^2 -propene) complex **92**.

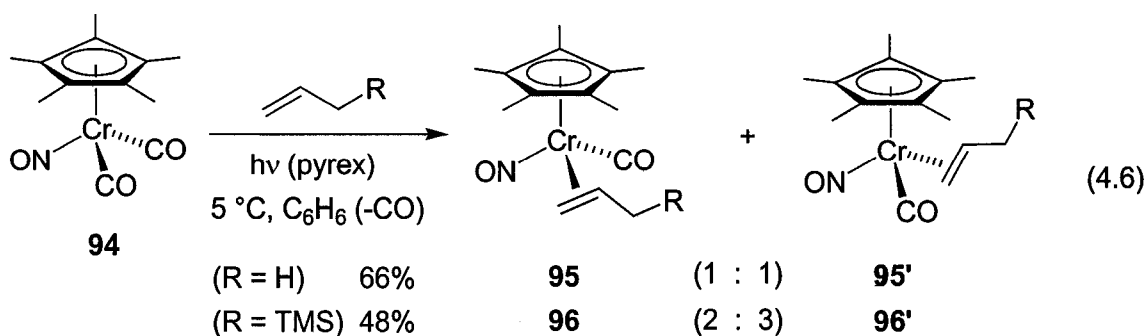
4.1.2 Formation of Cp*CrNO(CO)(η^2 -alkene) and (η^2 -alkyne) complexes

With the improvement of this photochemical methodology, we hoped to extend the synthesis of the CpCrNO(CO)(η^2 -olefin) complexes to the permethylcyclopentadienyl analogues. Unfortunately, according to the literature,⁵⁰ the required starting material, Cp*CrNO(CO)₂ **94**, is prepared in only 48% yield from an inefficient week-long heating

to reflux of $\text{Cr}(\text{CO})_6$ and NaCp in THF, followed by the addition of Diazald. We have found, however, that the yield of this reaction is increased to 85% under much milder reaction conditions and in far shorter time by the addition of Cp^*Li to the more labile chromium(0) complex $(\text{MeCN})_3\text{Cr}(\text{CO})_3$ **67**, with subsequent nitrosylation as previously described (eq. 4.5). This method can also be modified to yield $\text{CpCrNO}(\text{CO})_2$ **90** in 90%.



In the substitution reaction, treatment of dicarbonyl complex **94** with excess propene under photolytic conditions provides an otherwise unassigned mixture of the novel η^2 -propene diastereomers **95** and **95'** in good yield. The related η^2 -allyltrimethylsilane isomers **96** and **96'** are also prepared in the same manner, but in somewhat lower yield (eq. 4.6). The 370 nm UV cutoff filter is superfluous in this series: no decomposition is observed even after prolonged photolysis (>36 h) through Pyrex glassware.



Spectroscopic analysis clearly reveals that the ^1H and ^{13}C NMR signals of one isomer of complex **95** are broad at room temperature. At $-80\text{ }^{\circ}\text{C}$, however, the resonances of both diastereomers are sharp and clearly resolved (Table 4.2, entries 3 and 4). The broadness observed at room temperature may be ascribed to a rapid equilibration of one of the diastereoisomers of complex **95** with one or more chemically inequivalent rotamers (Fig. 4.3). Upon cooling to $-80\text{ }^{\circ}\text{C}$, the improved resolution presumably results from thermodynamic equilibration to just one rotamer. A similar equilibrium is believed to be responsible for the broad room temperature NMR signals of one of the isomers of allylsilane complex **96**. It is not entirely clear why the second stereoisomer of the propene and allylsilane complexes is apparently static at room temperature.

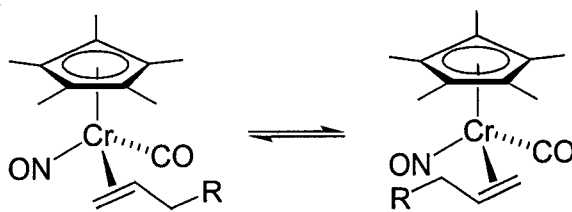


Figure 4.3: Two possible rotamers of one of the stereoisomers of complex **95**.

As observed for the $\text{CpCrNO(CO)(}\eta^2\text{-alkene)}$ complexes **91** and **92**, both Cp^* η^2 -alkene complexes **95** and **96** suffer from slow dissociation of the alkene in solution at room temperature. Donor solvents such as acetonitrile also promote rapid loss of the alkene ligand. Nonetheless, crystallization proceeds at low temperature without notable decomposition and, for allylsilane complex **96**, delivers single crystals comprising a single diastereomer (Fig. 4.4). Unfortunately, due to subsequent decomposition, the NMR spectra of these crystals could not be obtained, leaving the spectroscopic assignment of stereochemistry unresolved.

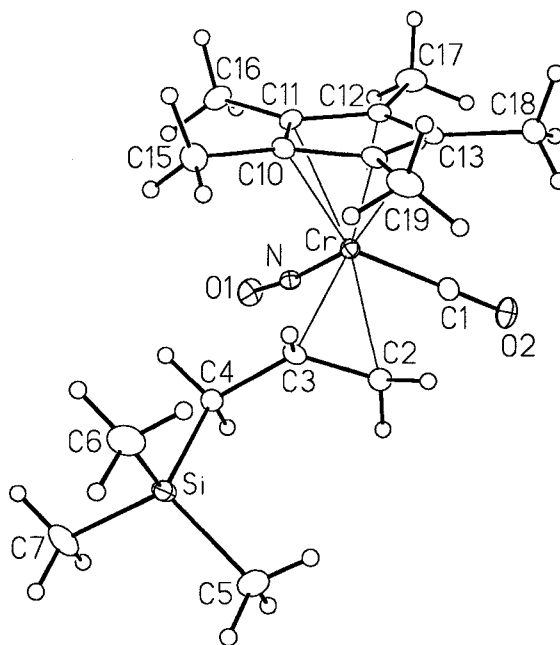
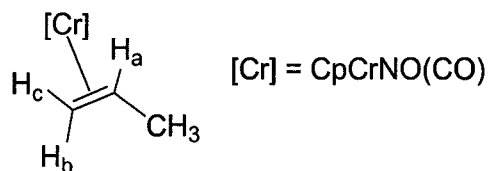


Figure 4.4: Solid-state molecular structure of the η^2 -allyltrimethylsilane complex **96/96'**. Non-hydrogen atoms are represented by Gaussian ellipsoids at the 20% probability level. Hydrogen atoms are shown with arbitrarily small thermal parameters. Selected bond lengths (Å) and angles (deg): Cr-N = 1.676(2), O(1)-N = 1.198(3), Cr-C(1) = 1.856(3), O(2)-C(1) = 1.149(3), Cr-C(2) = 2.214(3), Cr-C(3) = 2.206(3), C(2)-C(3) = 1.380(4), C(3)-C(4) = 1.508(4); Cr-N-O(1) = 173.0(2), Cr-C(1)-O(2) = 178.2(3), N-Cr-C(1) = 92.77(12), N-Cr-C(2) = 102.09(12), N-Cr-C(3) = 93.77(11), C(2)-C(3)-C(4) = 122.9(3).

Table 4.2: ^1H NMR data (ppm) for the $\text{CpCrNO}(\text{CO})(\eta^2\text{-propene})$ complex **91**^a and the Cp^* analogue **95**.^b

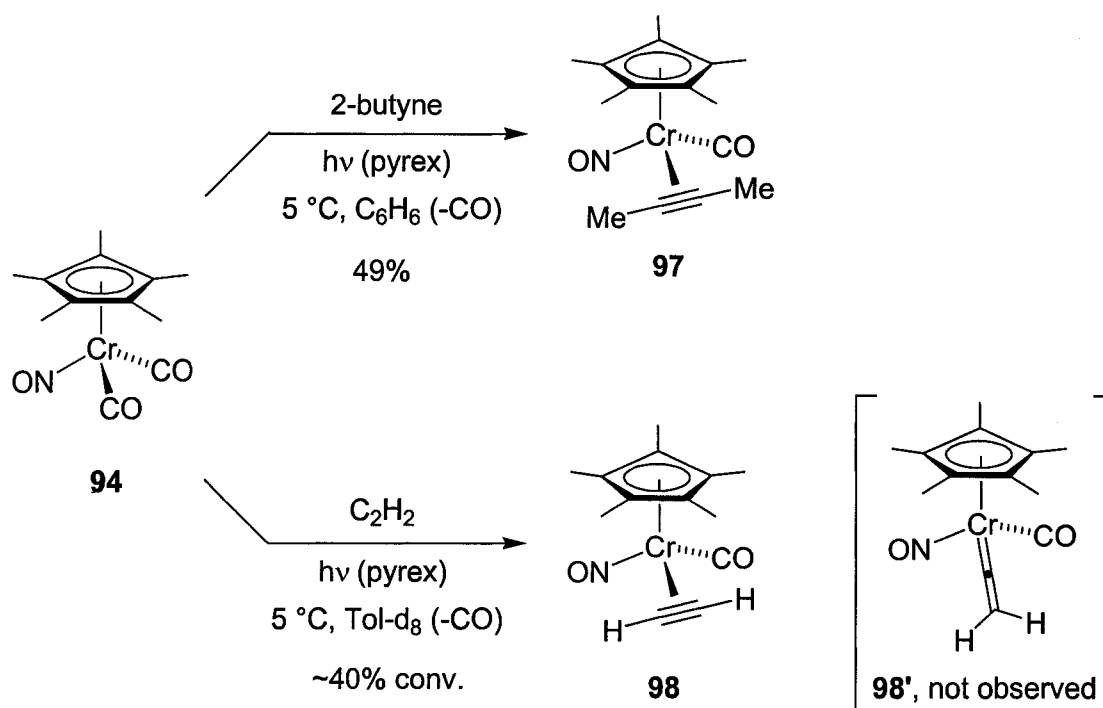


Entry	Complex	Cp'	H _a	H _b	H _c	CH ₃
1	91 major	3.14	3.14 (ddd, $J = 12.8, 9.2, 6.0$ Hz)	2.11 (d, $J = 12.8$ Hz)	2.02 (d, $J = 9.2$ Hz)	1.44 (d, $J = 6.0$ Hz)
2	91 minor	4.31	2.67 (ddd, $J = 13.2, 9.2, 6.0$ Hz)	2.2 (d, $J = 13.2$ Hz)	2.04 (d, $J = 9.2$ Hz)	1.68 (d, $J = 6.0$ Hz)
3	95 static	1.45	2.19 (ov m)	2.29 (d, $J = 13.2$ Hz)	1.3 (d, $J = 8.8$ Hz)	1.79 (d, $J = 6.0$ Hz)
4	95 fluxional ^c	1.41	2.17 (br m)	2.51 (d, $J = 12.0$ Hz)	1.07 (d, $J = 8.4$ Hz)	1.88 (ov d, $J \approx 5.0$ Hz)

^aRecorded in C_6D_6 . ^bRecorded in Toluene- d_8 . ^cData for the fluxional isomer of complex **95** was obtained at -80°C .

It is surprising that the $\text{Cp}'\text{CrNO}(\text{CO})$ fragment in both the Cp and Cp^* η^2 -alkene complexes does not undergo a second photolytic carbonyl loss to form bis(η^2 -olefin) complexes, even upon prolonged irradiation in the presence of a large excess of olefin. Similarly, photolysis of complex **94** in the presence of excess 2-butyne or under an atmosphere of acetylene provides only the monosubstituted η^2 -alkyne complexes **97** and **98**, each as a single isomer in solution (Scheme 4.3).

Scheme 4.3



Regrettably, only the η^2 -(2-butyne) complex **97** can be isolated as a solid.

Moreover, conversion of complex **94** to products **97** or **98** cannot be driven to more than 50%, even upon prolonged UV exposure. This may be attributable to the deep red colour of these products, which upon reaching a particular intensity, undergoes competitive absorption of UV radiation. In contrast, the η^2 -propene complexes **91** and **95**, obtained in significantly higher yield, are much less intensely yellow in solution.

Photolysis in the presence of other terminal alkynes such as phenylacetylene or 1,7-octadiyne leads only to unidentified paramagnetic product mixtures. Reaction with allene, crotonaldehyde, or 1,4-pentadiene-3-ol also leads to paramagnetic mixtures, while photolysis in the presence of ethylene fails to afford any observable product.

The η^2 -coordination mode of the 2-butyne ligand in complex **97** was confirmed by X-ray crystallography (Fig. 4.5), while the bonding mode of η^2 -acetylene complex **98** was determined in solution. The relatively upfield alkyne resonances (101.5 and 85.4 ppm) in the ^{13}C NMR spectrum of this latter complex are consistent with the presence of a simple two-electron, π -coordinated alkyne (similar to that of 2-butyne complex **97**), rather than the alternative vinylidene⁵¹ structural isomer **98'** (Scheme 4.3).

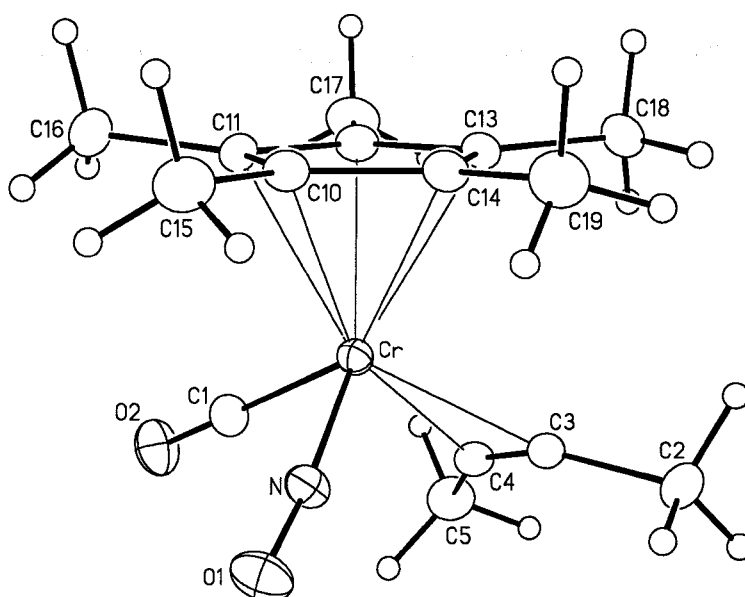
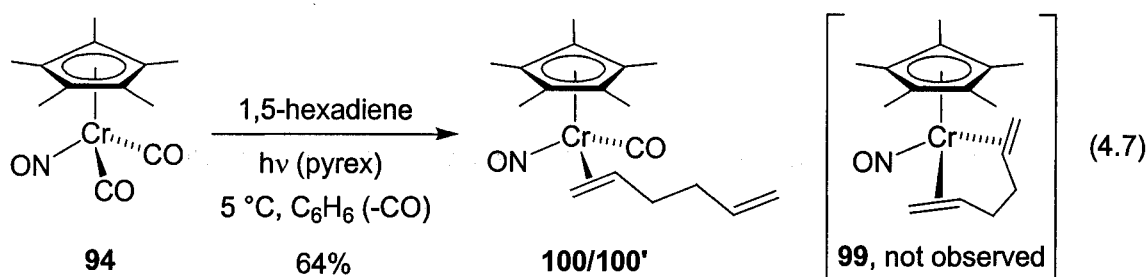


Figure 4.5: Solid-state molecular structure of the $(\eta^5\text{-C}_5\text{Me}_5)(\eta^2\text{-2-butyne})\text{carbonylnitrosylchromium}$ complex **97**. Non-hydrogen atoms are represented by Gaussian ellipsoids at the 20% probability level. Hydrogen atoms are shown with arbitrarily small thermal parameters. Selected bond lengths (Å) and angles (deg): Cr-N = 1.681(2), Cr-C(1) = 1.850(3), Cr-C(3) = 2.096(3), Cr-C(4) = 2.179(3), O(1)-N = 1.197(3), O(2)-C(1) = 1.144(3), C(2)-C(3) = 1.473(4), C(3)-C(4) = 1.241(4), C(4)-C(5) = 1.469(4); Cr-N-O(1) = 172.5(2), Cr-C(1)-O(2) = 179.2(3), Cr-C(3)-C(2) = 132.0(2), Cr-C(4)-C(5) = 137.1(2), C(2)-C(3)-C(4) = 150.8(3), C(3)-C(4)-C(5) = 153.4(3).

Remarkably, even after extensive reaction times (~30 h), the photolysis of $\text{Cp}^*\text{CrNO}(\text{CO})_2$ **94** in the presence of 1,5-hexadiene provides no evidence for the expected η^2 -, η^2 -(1,5-hexadiene) complex **99**. The only product identified spectroscopically in solution is the η^2 -(1,5-hexadiene) complex **100/100'**, present as an approximately 1 : 1 mixture of unassigned isomers (eq. 4.7).



Dissociation of the 1,5-hexadiene ligand in solution unfortunately occurs much more rapidly than that of the related η^2 -propene and η^2 -allyltrimethylsilane complexes **95** and **96**. This propensity for thermal decomposition is manifest even in the solid-state. Freshly isolated powder samples of 1,5-hexadiene complex **100**, for example, decompose into a viscous oil over a twelve hour period under an inert atmosphere at room temperature. Complete characterization of this unstable mixture of isomeric complex was therefore not possible. Nonetheless, the presence of fully consistent metal-bound and -unbound olefinic proton resonances (between δ 3.5 and 2.0 and δ 6.0 and 4.5, respectively) in the ^1H NMR spectrum of complex **100**, as well as correlated aliphatic proton signals, conclusively establishes the η^2 -bonding mode of the non-conjugated diene.

4.3 Photolysis of $\text{CpCrNO}(\text{CO})_2$ in the presence of conjugated dienes

4.3.1 Formation of $\text{CpCrNO}(\text{CO})(\eta^2\text{-1,3-diene})$ and $\text{CpCrNO}(\eta^4\text{-s-}trans\text{-1,3-diene})$ complexes

Extension of the photochemical substitution to conjugated dienes afforded rather surprising results. Photolysis (UV, >370 nm) of $\text{CpCrNO}(\text{CO})_2$ **90** in the presence of butadiene, for example, leads to a mixture of three products, identified *in situ* but not isolated. The distinct ^1H NMR resonances of the Cp ligand for each product, as well as that of the starting material, rendered determination of product ratios and conversion quite trivial. Analysis of this crude reaction mixture thus reveals a 1 : 1 : 12 mixture of three principal products, with a total conversion of 90% (eq. 4.8, and Table 4.3, entry 1)

The minor products could be assigned to η^2 -alkene complexes, which resemble the proposed target complexes **Ie** (p. 98), is based on the relative integration of the independent Cp resonances at 4.40 and 4.38 ppm with that of the unbound terminal olefin proton signals between 4.7 and 5.8 ppm (Table 4.4). Two-dimensional ^1H - ^1H correlations in the COSY NMR spectrum clearly connect these downfield signals to resonances between 2.1 and 3.6 ppm. Since these signals must arise from the second olefin of butadiene and are found relatively upfield, the diene ligand can be confidently assigned as η^2 -coordinate. Thus, the two minor products are assigned to be $\text{CpCrNO}(\text{CO})(\eta^2\text{-butadiene})$ complexes **101** and **101'**, each a diastereomer of the other.

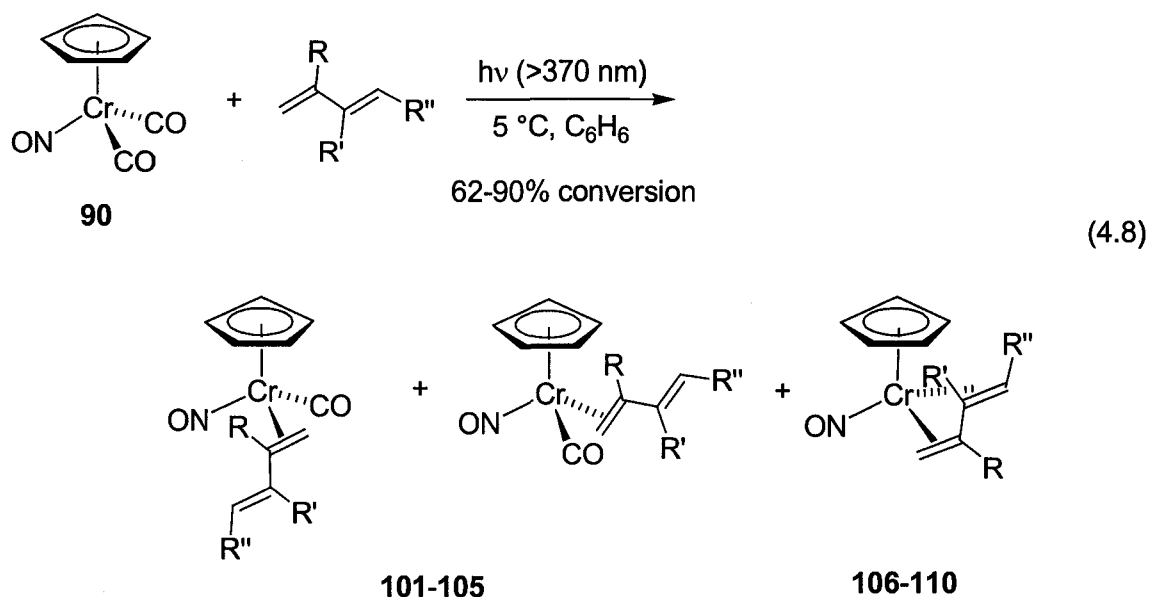
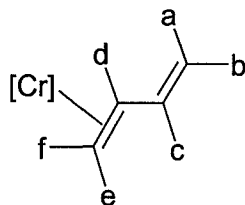


Table 4.3: Reaction details pertaining to equation 4.8.

Entry	Substrate	η^2 -products	η^4 -products	Respective product ratio ^a	Total Conversion ^a
1	R, R', R'' = H	101, 101'	106	1 : 1 : 12	90%
2	R, R'' = H; R' = Me	102, 102'	107	1 : 1 : 6	90%
3	R, R' = H; R'' = Me	103, 103'	108, 108'	2.4 : 1 : 1.6 : 4.2	76%
4	R, R' = Me; R'' = H	104, 104'	109	1.6 : 1 : 1.3	62%
5	R, R'' = Me; R' = H	105, 105'	110	1 : 1.4 : 3.3	76%

^aBased on relative integration of Cp signals in the ^1H NMR spectra after 17 h of photolysis.

Table 4.4: Summarized ^1H NMR data (δ) of both isomers of η^2 -butadiene and η^2 -isoprene complexes **101** and **102**. Coupling constants (J) are in Hertz (Hz).



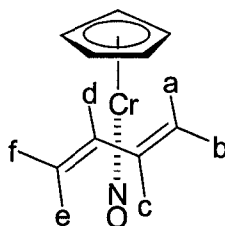
Complex	Cp	a	b	c	d	e	f
101/101'	4.33	5.17 (br m)	4.72 (dd, J = 6.0, 0.4)	5.22 (dd, J = 16.8, 1.2)	3.6 (2 nd order m)	2.18 (dd, J = 12.4, 1.2)	2.11 (br d, J = 8.4)
101/101'	4.37	5.37 (2 nd order m)	4.89 (dd, J = 10.4, 1.2)	5.74 (ddd, J = 18.0, 8.0, 6.8)	3.21 (2 nd order m)	2.29 (d, J = 13.2)	2.15 (d, J = 8.4)
102/102'	4.34	5.0 (br m)	4.77 (br m)	1.49 (ov s)	3.88 (dd, J = 13.2, 9.3)	2.41 (dd, J = 13.2, 2.1)	1.83 (br dd, J = 9.3, 1.5)
102/102'	4.30	5.14 (br m)	4.78 (br m)	1.49 (ov s)	3.19 (dd, J = 14.1, 9.3)	2.3 (dd, J = 14.1, 0.7)	2.24 (br d, J = 9.3)

^aSee the Experimental section for the NMR data of the tentatively assigned η^2 -(1,3-diene) complexes **103-105**. ^b[Cr] = CpCrNO(CO).

^1H NMR analysis (Table 4.5) of the major butadiene product **106** clearly establishes that the diene ligand is bound in an η^4 -butadiene fashion: the proton resonances all occur upfield between 2.0 and 3.5 ppm, consistent with being bound to the metal centre. Intriguingly, distinct resonances for six diene protons are clearly apparent, strongly suggestive of the elusive *s-trans* diene bonding mode! The *s-trans* coordination of the ligand renders all six butadiene protons chemically inequivalent (Fig. 4.6, and Table 4.4), in contrast to the more symmetric structure expected for an *s-cis* butadiene ligand.³⁷ For instance, both methine hydrogens (H_d and H_c) of the diene ligand appear at

3.18 and 2.32 ppm, respectively, as strongly coupled multiplets and are mutually coupled by 10.7 Hz. These methine hydrogens also share large coupling constants with the respective *anti* protons, which appear as doublets at 2.32 ($J = 14.0$ Hz, H_c) and 2.08 ppm ($J = 13.6$ Hz, H_e). The two *syn* protons (H_f and H_b) appear as the expected relatively narrow doublets at 3.44 and 3.0 ppm and share a 6.8 Hz coupling constant with the internal methine protons.

Table 4.5: Summarized ^1H NMR data (δ) of η^4 -butadiene and η^4 -isoprene complexes **106** and **107**.^a Coupling constants (J) are in Hertz (Hz).^b



Complex	Cp	a	b	c	d	e	f
106	4.54	2.74 (br d, $J = 14.0$)	3.0 (dd, $J = 6.8, 0.8$)	2.32 (dddd, $J = 14.0, 10.7, 6.8, 0.4$)	3.18 (ddd, $J = 13.6, 10.7, 6.8$)	2.08 (dt, $J = 13.6, 1.2$)	3.44 (dd, $J = 6.8, 1.2$)
107	4.51	1.88 (t, $J = 1.1$)	3.3 (d, $J = 1.2$)	1.45 (br s)	2.16 (dd, $J = 14.1, 7.2$)	3.0 (dd, $J = 14.1, 1.5$)	3.09 (dd, $J = 7.2, 1.2$)

^aSee the Experimental section for the NMR data of the tentatively assigned η^4 -(1,3-diene) complexes **108-110**. ^bThe relative connectivity of the diene protons of the *s-trans*-(1,3-diene) complexes could be clearly determined by multidimensional NMR spectroscopy; however, the assignment of which protons are nearer to the cyclopentadienyl ligand is purely arbitrary.

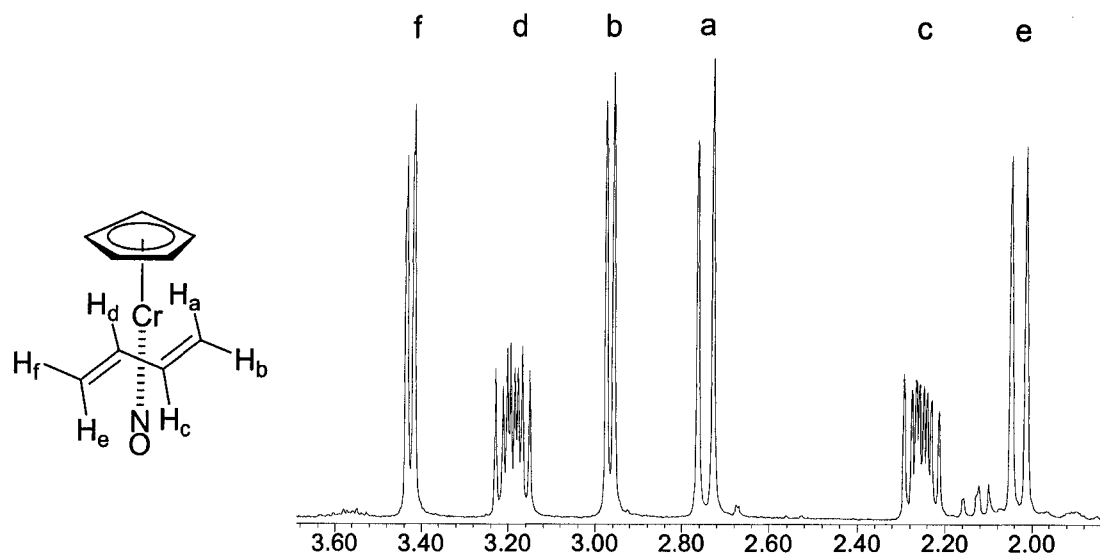


Figure 4.6: Assignment of the η^4 -diene region of the ^1H NMR spectrum of *s-trans*-butadiene complex **106**. The minor resonances are attributed to the presence of trace amounts of the η^2 -butadiene complexes **101/101'**.

As required for the synthesis of the $\text{CpCrNO}(\text{CO})(\eta^2\text{-mono-olefin})$ complexes **91** and **92**, the 370 nm cutoff filter is necessary for preparing butadiene complexes **101** and **106**. The filter evidently prevents photolytic decomposition of the reaction products, which otherwise deposit insoluble paramagnetic material on the surface of the reaction vessel. Without the UV filter, irreversible loss of the η^2 -butadiene complex **101** occurs faster than decomposition of the η^4 -butadiene complex **106**. In this manner, however, prolonged photolysis delivers the η^4 -butadiene complex in very pure form, albeit in very low yield (<5%). Infrared analysis of this complex in THF reveals only a single nitrosyl stretch at 1670 cm^{-1} , with no observable carbonyl stretch, furthering the assignment of an η^4 -coordinated diene complex. Likewise, infrared analysis of the crude mixture of η^2 - and η^4 -butadiene complexes **101** and **106** reveals two additional bands at 1973 and 1639

cm^{-1} , which correspond, respectively, to the carbonyl and nitrosyl ligands of the η^2 -butadiene complex **101**.

Similar results are obtained from photolysis of $\text{CpCrNO}(\text{CO})_2$ **90** in the presence of isoprene, 1,3-pentadiene, 2,3-dimethylbutadiene, or 2,4-dimethylbutadiene, giving mixtures of the η^2 -(1,3-diene) complexes **102-105** and the *s-trans* coordinated η^4 -(1,3-diene) complexes **107-110**, respectively (eq. 4.8, Table 4.3, entries 2-5).

Both the *s-trans* η^4 -butadiene and η^4 -isoprene complexes **106** and **107** have been fully characterized spectroscopically (Table 4.5), while the 1,3-pentadiene, 2,3-dimethylbutadiene, and 2,4-dimethylbutadiene products were obtained as mixtures on a very small scale and analyzed via ^1H and homonuclear COSY NMR spectroscopy only. Since many of the NMR signals of these complexes overlap with starting material resonances, structural assignments remain tentative for these latter complexes.

The Cp signals for the η^2 -diene products **101-105** all appear around 4.4 ppm, while those of the η^4 -diene products **106-111** consistently appear downfield at approximately 4.5 ppm. This trend is helpful in assigning resonances to η^2 - and/or η^4 -diene complexes for several reactions that produce ambiguous ^1H NMR spectra. For instance, the majority of the 1,3-diene complexes shown in equation 4.8 elicit distinct individual Cp resonances for the two η^2 -diene diastereomers, along with a third Cp signal for the η^4 -diene product. In the case of the 1,3-pentadiene reaction, however, a fourth Cp signal is evident around 4.5 ppm. Although a definitive assignment of the products obtained from this reaction mixture remains inconclusive, this fourth product can be tentatively assigned as a second *s-trans*-(1,3-pentadiene) diastereomer **108'** (Fig. 4.7). A similar isomeric relationship has been noted for the molybdenum η^4 -(1,3-pentadiene)

analogue.¹ No such isomers are observed for the other chromium η^4 -(substituted butadiene) complexes, possibly because of unfavourable steric interactions with the Cp ligand.

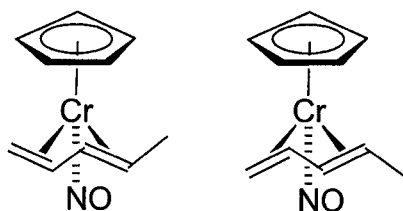
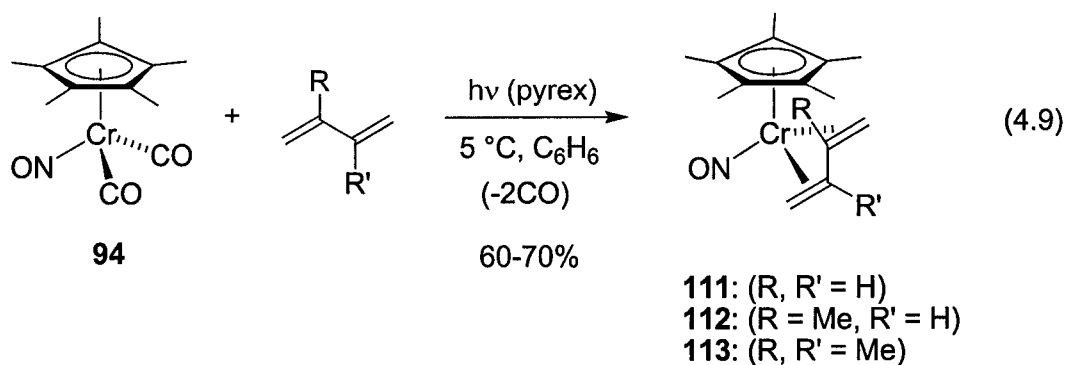


Figure 4.7: Possible diene ligand configuration of the η^4 -(1,3-pentadiene) complex **108/108'**.

Although this photolytic method easily generates η^4 -(1,3-diene) complexes with up to 90% conversion, it is unfortunately limited in that the reactions cannot be driven exclusively to the η^4 -diene products. In addition, neither the η^2 - nor the η^4 -diene products can be isolated as a stable solid and neither persists under prolonged exposure to high vacuum. Attempts to separate the product mixtures via column chromatography (silica, alumina, or florisil) under inert atmosphere result in only decomposition. Nonetheless, this chemistry provides the first examples of a first-row transition metal conjugated η^4 -diene complex in the *s-trans* configuration, and therefore merits further investigation.

2. Formation of Cp*CrNO(η^4 -*s-trans*-1,3-diene) complexes

Intriguingly, investigations into the photolytic decarbonylation of Cp*CrNO(CO)₂ **94** in the presence of 1,3-dienes returned extremely satisfying results. An NMR scale photolysis reaction of this dicarbonyl complex in the presence of excess butadiene (in benzene-d₆), for example, provides a *single* product **111** in approximately 90% conversion after twelve hours of photolysis, isolated in 70% yield after silica-gel chromatography and crystallization from pentane (eq. **4.9**). The 370 nm cutoff filter is again unnecessary: no decomposition is observed even after prolonged (>36 h) photolysis.



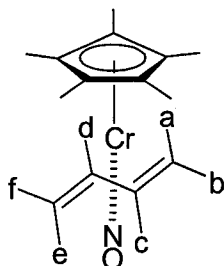
Analysis of the ¹H NMR spectrum (Fig. **4.8**, and Table **4.6**) of the butadiene reaction product **111** clearly reveals the formation of an *s-trans* butadiene ligand. As observed for the related CpCrNO(*s-trans*-butadiene) complex **106**, all six diene protons are chemically inequivalent. It is interesting, however, that the relative chemical shifts of the two complexes are not identical (recall Fig. **4.6**, p. 107). The coupling constants for both complexes differ very little (see the Experimental Section for details), thus the η^4 -diene ligands must be bound in a similar fashion (*i.e.*, having comparable dihedral, or

torsional, angles). The relative chemical shifts of the diene protons could therefore be a result of the different magnetic anisotropy and/or increased electron donation of the more electron rich Cp* ligand. Consistent with this theory, an increase in metal to ligand π -backbonding is evident in this complex: the IR absorption (1641 cm^{-1}) of the nitrosyl ligand is lower in energy relative to that of Cp complex **106** (1670 cm^{-1}).

^1H NMR analysis of aliquots taken throughout the reaction of dicarbonyl complex **94** with butadiene reveals the formation of a trace amount of a 1 : 1 diastereomeric mixture of intermediate η^2 -butadiene complex **111a**, with spectroscopic signatures similar to the analogous cyclopentadienyl η^2 -butadiene complex **101**. The unbound olefin proton resonances of one isomer, for example, are evident between 4.9 and 5.6 ppm and are correlated to the bound olefin proton resonances between 1.3 and 2.8 ppm. The ^1H NMR signals of the second diastereomer appear relatively in the same regions as the first but are considerably broadened and difficult to discern clearly. Unfortunately, as observed for the $\text{CpCr}(\text{NO})(\text{CO})(\eta^2\text{-butadiene})$ complex **101**, the η^2 -butadiene ligand of complex **111a** irreversibly dissociates from the metal centre in solution at room temperature.

The η^4 -isoprene and η^4 -(2,3-dimethylbutadiene) complexes **112** and **113** are also prepared in good yield using this method (eq. 4.9). Passing the crude reaction mixture through silica-gel and eluting with benzene under inert atmosphere readily purifies these complexes. Importantly, as the scale of the reaction is increased, so is the photolysis time required to effect high conversion (*e.g.*, 36 h is required for a 820 mg scale reaction to reach 70% conversion).

Table 4.6: Summarized ^1H NMR data (δ) for *s-trans*-(1,3-diene) complexes **111**-**113**.^a Coupling constants (J) are in Hertz (Hz).^b



Complex	C_5Me_5	a	b	c	d	e	f
111	1.48	2.93 (dd, J = 13.6, 0.8)	2.54 (dd, J = 6.8, 0.8)	1.65 (m)	3.45 (m)	1.55 (dt, J = 13.2, 1.0)	3.37 (d, J = 6.8)
112	1.49	3.25 (br s)	1.35 (dd, J = 1.2, 0.8)	1.54 (br s)	1.50 1.50 (ov m)	3.19 (dd, J = 14.4, 1.6)	2.61 (ddd, J = 7.2, 2.0, 0.8)
113	1.57	3.15 (br s)	1.87 (br d, J = 1.6)	1.63 (br s)	1.12 (br s)	3.17 (br d, J = 1.2)	2.53 (br s)

^aDue to the lack of coupling information, assignment of the signals for 2,3-dimethylbutadiene complex **113** is partially based on the similarity of chemical shifts compared to the related butadiene and isoprene complexes. ^bThe relative connectivity of the diene protons of the *s-trans*-(1,3-diene) complexes could be clearly determined by multidimensional NMR spectroscopy; however, the assignment of which protons are nearer to the cyclopentadienyl ligand is purely arbitrary.

The ^1H NMR spectra of complexes **111** and **112** reveal a single product in solution, whereas that of 2,3-dimethylbutadiene complex **113** shows a 9 : 1 mixture of two products. Based on very similar ^1H chemical shifts observed for the molybdenum *s-cis*-diene analogue,³⁷ this minor compound is *tentatively* assigned as the corresponding *s-cis* diene complex **113'**. Alternatively, however, this complex may be a symmetrical

bridging species, possessing a bound diene fragment more akin to diene bonding mode **G** in Chart 4.2 (p. 94). Confirmation of the coordination mode of this complex is unfortunately not possible given that this minor species forms in such low concentration and cannot be separated by chromatography or crystallization from the major *s-trans* complex **113**. Nitrosyl infrared absorptions for the η^4 -isoprene and η^4 -(2,3-dimethylbutadiene) complexes **112** and **113** appear at 1641 and 1636 cm^{-1} , respectively.

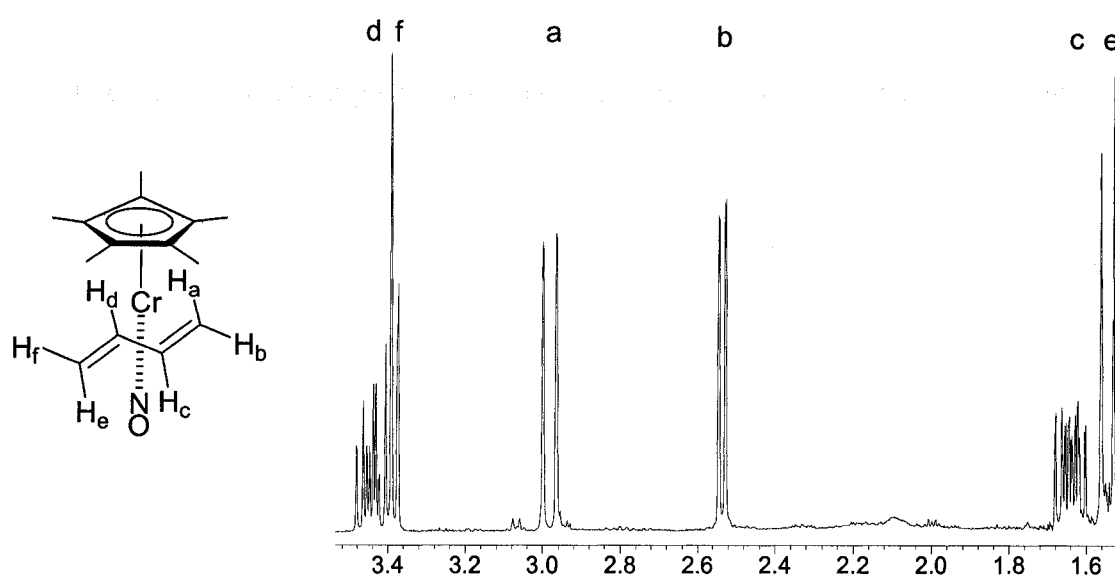


Figure 4.8: Assignment of the η^4 -diene region of the ^1H NMR spectrum of *s-trans*-butadiene complex **111**. Minor impurities are assigned to the η^2 -butadiene complex **111a**.

While the precise configuration of the η^4 -isoprene complex **112** cannot be determined by NMR spectroscopy, crystals of this complex were grown from pentane at $-35\text{ }^\circ\text{C}$ and the solid-state molecular structure obtained by X-ray crystallography (Fig. 4.9). The orientation of the isoprene ligand around the metal centre is twisted and clearly

s-trans. Similar structural characteristics are seen in the solid-state structure of the 2,3-dimethylbutadiene complex **113** (Fig. 4.10). Crystals of η^4 -butadiene complex **111** were also grown, however, X-ray analysis was complicated by a high degree of disorder within the single crystals.

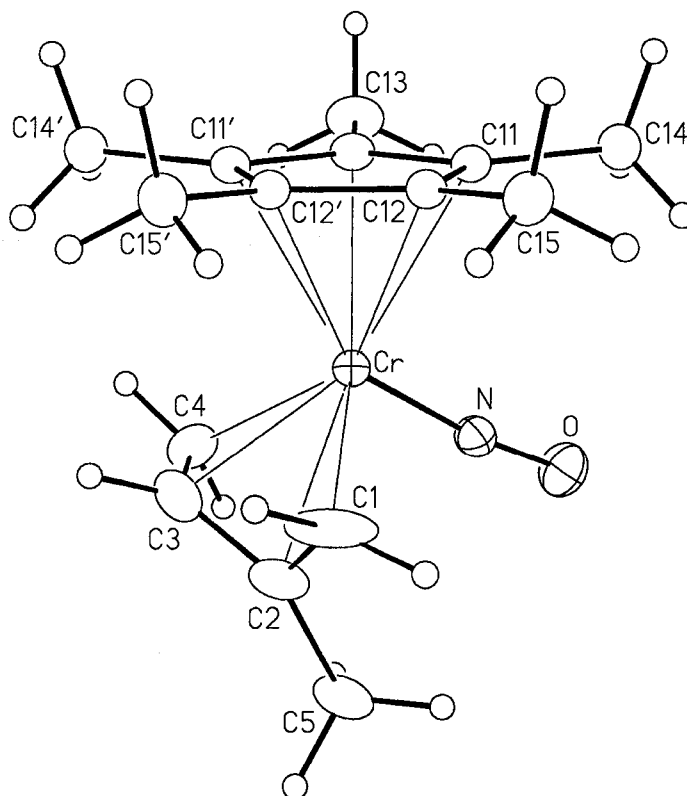


Figure 4.9. Solid-state molecular structure of *s-trans*-isoprene complex **112**. Non-hydrogen atoms are represented by Gaussian ellipsoids at the 20% probability level. Hydrogen atoms are shown with arbitrarily small thermal parameters. Selected bond lengths (Å) and angles (deg): Cr-N = 1.679(8), O-N = 1.208(9), Cr-C(1) = 2.188(4), Cr-C(2) = 2.146(6), Cr-C(3) = 2.080(6), Cr-C(4) = 2.245(12), C(1)-C(2) = 1.417(14), C(2)-C(3) = 1.356(11), C(2)-C(5) = 1.507(12), C(3)-C(4) = 1.317(15); Cr-N-O = 173.5(12), N-Cr-C(1) = 101.6(6), N-Cr-C(2) = 88.0(4), N-Cr-C(3) = 108.3(4), N-Cr-C(4) = 92.6(3), C(1)-C(2)-C(3) = 112.7(8), C(1)-C(2)-C(5) = 124.1(12), C(3)-C(2)-C(5) = 122.7(10), C(2)-C(3)-C(4) = 121.7(8), C(1)-C(2)-C(3)-C(4) = 125.2(11).

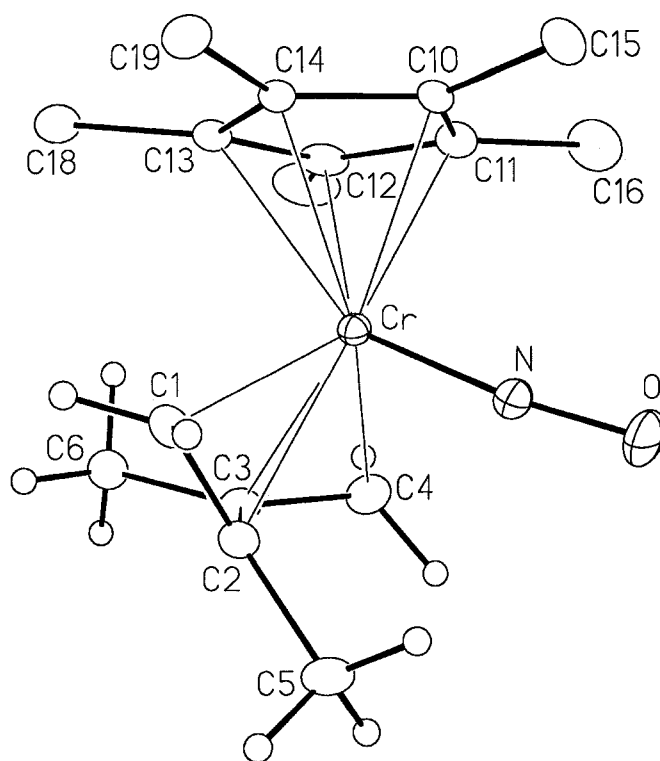


Figure 4.10: A side-on perspective of the solid-state molecular structure of *s-trans*-2,3-dimethylbutadiene complex **113**. Non-hydrogen atoms are represented by Gaussian ellipsoids at the 20% probability level. Hydrogen atoms are shown with arbitrarily small thermal parameters; hydrogen atoms of the Cp* ligand are omitted. Selected bond lengths (Å) and angles (deg): Cr-N = 1.667(3), O-N = 1.212(3), Cr-C(1) = 2.222(3), Cr-C(2) = 2.163(3), Cr-C(3) = 2.135(3), Cr-C(4) = 2.235(3), C(1)-C(2) = 1.386(4), C(2)-C(3) = 1.448(4), C(3)-C(4) = 1.401(5), C(2)-C(5) = 1.509(4), C(3)-C(6) = 1.513(4); Cr-N-O = 172.6(3), N-Cr-C(1) = 101.36(13), N-Cr-C(2) = 88.58(12), N-Cr-C(3) = 108.05(12), N-Cr-C(4) = 89.37(13), C(1)-C(2)-C(3) = 116.7(3), C(1)-C(2)-C(5) = 121.1(3), C(3)-C(2)-C(5) = 121.6(3), C(2)-C(3)-C(4) = 118.4(3), C(2)-C(3)-C(6) = 120.4(3), C(4)-C(3)-C(6) = 120.8(3), C(1)-C(2)-C(3)-C(4) = 119.3(3).

Aside from establishing the *s-trans* coordination mode, the crystal structures of η^4 -isoprene and η^4 -(2,3-dimethylbutadiene) complexes **112** and **113** are otherwise unremarkable; the torsional angle of the 1,3-diene ligand in both complexes is approximately 120°, typical of the heavier transition metal *s-trans*-(1,3-diene) complexes (see Table 4.1 for a detailed comparison, p. 95).

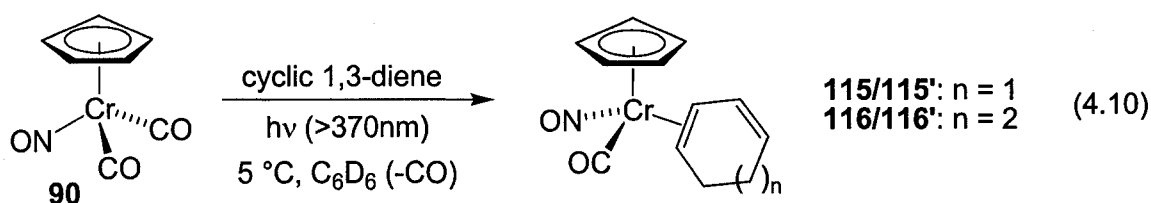
Given the isolation of unprecedented first-row *s-trans* 1,3-diene complexes **111-113**, we were curious to evaluate the efficacy of this photochemical method for the preparation of more sterically hindered 1,3-diene compounds. Unfortunately, photolysis of dicarbonyl complex **94** in the presence of 1,1,4,4-tetraphenylbutadiene fails to promote any observable product formation. Photo-substitution using 1,4-diphenylbutadiene does, however, lead to the expected *s-trans* complex **114** in approximately 60% yield. Isolation of this product in pure form was complicated by residual unreacted 1,3-diene, which could not be completely separated; the product, therefore, was characterized only by ^1H and ^{13}C NMR spectroscopy.

Photolysis of dicarbonyl complex **94** in the presence of the conjugated enyne, 4-phenyl-1-buten-3-yne,⁵² was also investigated. Although spectroscopic evidence for a transient η^2 -alkene-bound species was obtained, the final reaction mixture consisted of only decomposed organic starting material and intractable paramagnetic products.

D. Photolysis of Cp'CrNO(CO)₂ complexes in the presence of conjugated cyclic dienes

1. Formation of CpCrNO(CO)(η^2 -cyclic-1,3-diene) complexes

Given that the η^4 -(1,3-diene) complexes apparently adopt only the *s-trans* diene configuration, we were curious whether the photolysis of Cp'CrNO(CO)₂ complexes **90** and **94** in the presence of rigidly *s-cis* conjugated cyclic organic dienes would provide the corresponding *s-cis* η^4 -diene complexes. Small scale (~0.074 mmol) NMR-tube reactions revealed that upon irradiation CpCrNO(CO)₂ **90** binds 1,3-cyclohexadiene to give a 1 : 5 diastereomeric mixture of two CpCrNO(CO)(η^2 -C₆H₈) complexes **115** and **115'** (eq. 4.10). No evidence for the formation of a *s-cis* η^4 -diene complex was observed spectroscopically. The proton signals for the unbound olefin of the major η^2 -(1,3-cyclohexadiene) isomer, for example, appear at 6.04 and 5.56 ppm while the bound olefin signals are evident at 3.54 and 2.41 ppm. The strong correlation in the homonuclear COSY spectrum for the signals at 6.04 and 3.54 ppm clearly establishes the η^2 -bonding mode.

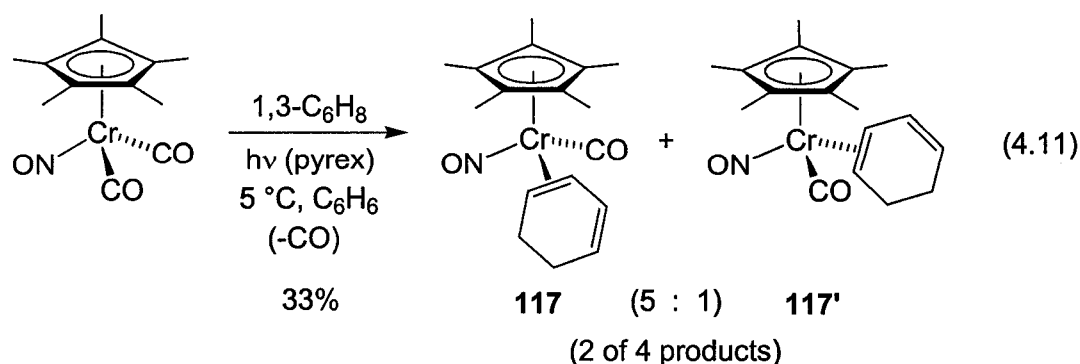


The corresponding η^2 -(1,3-cycloheptadiene) complexes **116** and **116'** were also prepared on a small scale and tentatively identified *in situ* by NMR spectroscopy (eq. 4.10); see the Experimental section for full details. Unfortunately, as observed for the

cyclopentadienyl η^4 -(1,3-diene) complexes, the cyclic η^2 -diene complexes **115** and **116** cannot be isolated in pure form and suffer loss of the diene ligand upon prolonged exposure to high vacuum.

4.3.2 Monomeric and dinuclear $[\text{Cp}^*\text{Cr}(\text{NO})(\text{CO})]_n(\eta^2\text{-cyclic-1,3-diene})$ complexes

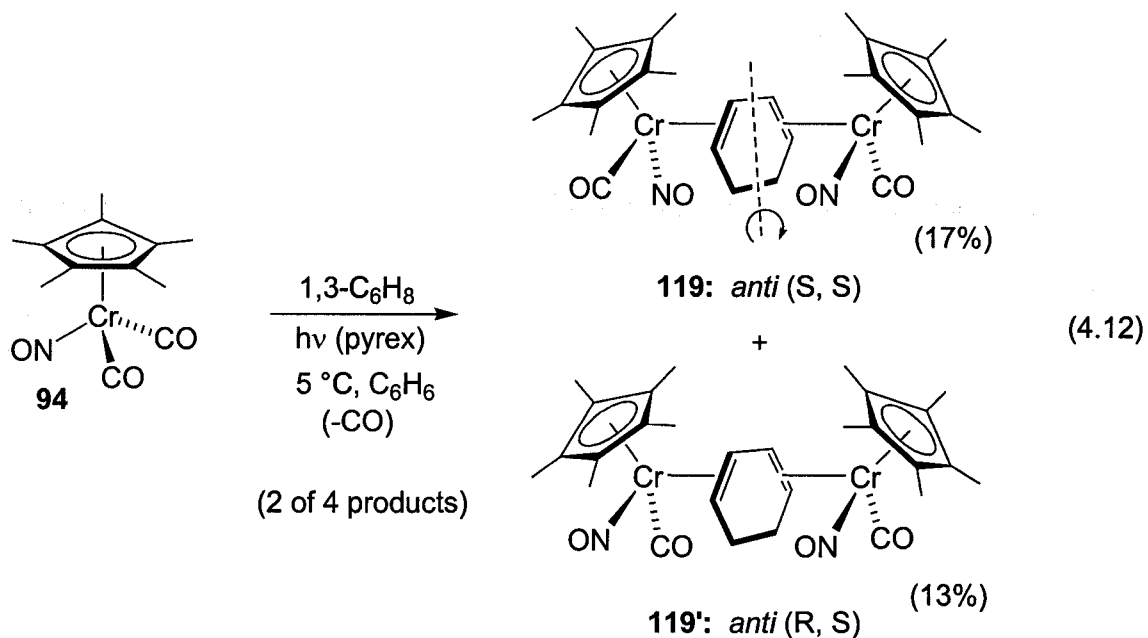
To inhibit the thermolability of cyclopentadienyl η^2 -(1,3-diene) complexes **115** and **116**, we again pursued the synthesis of the more sterically hindered permethylcyclopentadienyl analogues. In addition to being more thermally robust, we reasoned that this series may be more amenable to a second photo-assisted decarbonylation, to form the (ironically) elusive *s-cis* diene complexes. Thus, photolysis of $\text{Cp}^*\text{CrNO}(\text{CO})_2$ **94** in the presence of 1,3-cyclohexadiene yielded a number of products. Correlations among the ^1H NMR resonances between 3.0 and 3.5 ppm and the signals between 5.6 and 6.6 ppm, suggest that approximately half of the product mixture consists of the monomeric η^2 -cyclohexadiene complex, present as a 5 : 1 mixture of arbitrarily assigned diastereomers **117** and **117'**, and isolated in 33% yield by fractional crystallization from pentane (eq. 4.11, Table 4.6). Detailed NMR analysis of the minor isomer **117'** was not possible because of its very low abundance in the crude reaction mixture.



Analysis of the ^1H NMR data for the remaining two products reveals the formation of a 2 : 1 mixture, each bearing an η^4 -cyclohexadiene ligand. Fortunately, the major product is only slightly soluble in pentane and was selectively crystallized in low yield (~17%). Analysis of the ^1H NMR spectrum of this compound reveals a highly symmetrical chromium-bound cyclohexadiene ligand; only two inequivalent olefinic environments are apparent (see the Experimental section for details). Thus, this symmetric product could indeed be assigned as the expected *s-cis* η^4 -cyclohexadiene complex **118**. The infrared spectrum of this product, however, shows both intense carbonyl and nitrosyl absorptions at 1943 cm^{-1} and 1654 cm^{-1} . Additionally, careful integration of the ^1H NMR spectrum reveals that the relative ratio of Cp^* to η^4 -cyclohexadiene ligand is 2 : 1. These data are clearly inconsistent with assignment as a mononuclear *s-cis* η^4 -diene complex. To accommodate the NMR integration, an alternative structure is therefore assigned: a C_2 -symmetric dinuclear species consisting of two $\text{Cp}^*\text{CrNO}(\text{CO})$ fragments bridged by a 1,3-cyclohexadiene molecule. The relative position of the $\text{Cp}^*\text{CrNO}(\text{CO})$ fragments to each other may either be *syn* or *anti* (recall the related bonding modes E and G of acyclic conjugated dienes in Chart 4.2, p. 94). The *anti* diastereoisomer with (S, S) stereochemical designations at the chromium centres is assigned (*vide infra*) and illustrated in equation 4.12.

The minor product **119'**, isolated in approximately 13% yield by fractional crystallization, exhibits infrared absorptions identical to that of the major product; but due to reduced molecular symmetry, all four olefinic environments are inequivalent and appear as distinct resonance in the ^1H NMR spectrum (see the Experimental section for details). Furthermore, the resonances of the two Cp^* ligands of this minor product are

chemically inequivalent, appear at 1.55 and 1.51 ppm, while those of major complex **119** are isochronous at 1.56 ppm. The identity of **119'** may therefore be assigned as the (R, S) *anti* or *syn* diastereoisomer of complex **119** (eq. 4.12). Unfortunately, these assignments cannot be determined without X-ray crystallography.



The diene ligands of both η^2 - and μ - $\eta^2:\eta^2$ -(1,3-cyclohexadiene) complexes **117** and **119** are unfortunately labile in solution at ambient temperature. Nonetheless, X-ray quality crystals of the major isomer of complex **119** (as confirmed by ¹H NMR spectroscopy) were grown from pentane at low temperature and the solid-state molecular structure solved by X-ray crystallography (Fig. 4.11). Clearly, this structurally unprecedented molecule is the *anti* diastereomer (S, S at both chromium centres), having

a two-fold rotation axis that bisects the C(2)-C(2)' and C(4)-C(4)' bonds. Regrettably, single crystals of the minor isomer **119'** could not be obtained.

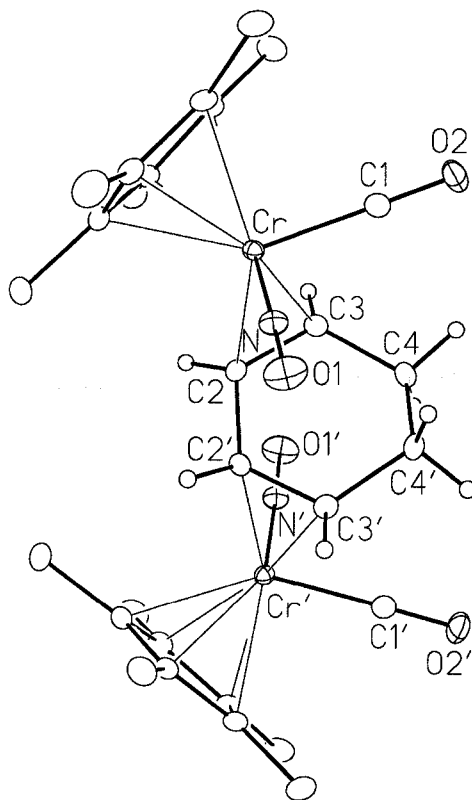
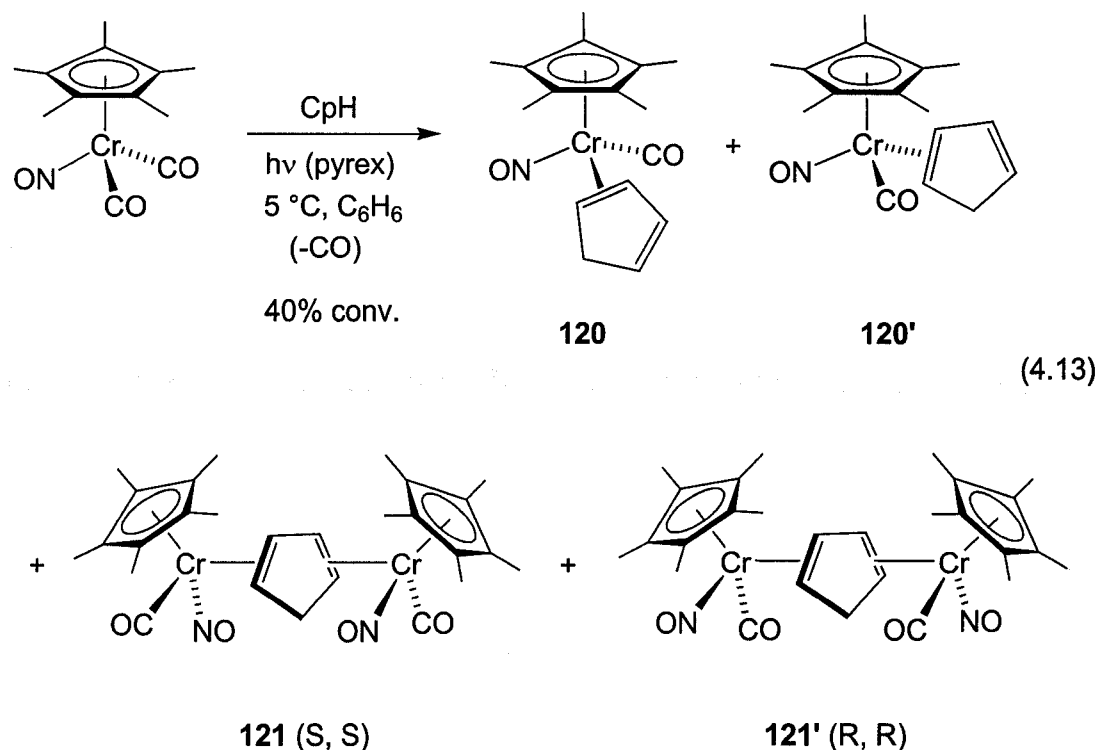


Figure 4.11: Solid-state molecular structure of the (S, S) diastereoisomers of $[(\eta^5\text{-C}_5\text{Me}_5)\text{carbonylnitrosylchromium}]_2(\mu\text{-}\eta^2\text{:}\eta^2\text{-1,3-cyclohexadiene})$ complex **119**. Non-hydrogen atoms are represented by Gaussian ellipsoids at the 20% probability level. Hydrogen atoms are shown with arbitrarily small thermal parameters; hydrogen atoms of the Cp* ligand are omitted. Primed atoms are related to unprimed ones via the crystallographic twofold rotational axis $(0, y, 1/4)$ passing through the midpoints of the C2–C2' and C4–C4' bonds. Selected bond lengths (Å) and angles (deg): Cr–N = 1.6743(16), Cr–C(1) = 1.851(2), Cr–C(2) = 2.2100(17), Cr–C(3) = 2.2415(18), O(1)–N = 1.196(2), O(2)–C(1) = 1.147(3), C(2)–C(2') = 1.477(4), C(2)–C(3) = 1.396(3), C(3)–C(4) = 1.510(3), C(4)–C(4') = 1.526(4); Cr–N–O(1) = 175.76(16), Cr–C(1)–O(2) = 178.41(18), Cr–C(2)–C(2') = 114.56(16), Cr–C(2)–C(3) = 72.95(10), Cr–C(3)–C(2) = 70.49(10), Cr–C(3)–C(4) = 122.34(12), C(2')–C(2)–C(3) = 120.50(11), C(2)–C(3)–C(4) = 119.41(16), C(3)–C(4)–C(4') = 113.02(12). C(3)–C(2)–C(2')–C(3') = 5.4(4).

Photolysis of $\text{Cp}^*\text{CrNO}(\text{CO})_2$ **94** in the presence of monomeric cyclopentadiene also provides a multitude of products; no clear evidence for the formation of an *s-cis* η^4 -cyclopentadiene complex was found (eq. **4.13**). Similar to the 1,3-cyclohexadiene chemistry, two η^2 -cyclopentadiene complexes **120** and **120'** were identified in solution, and detailed ^1H NMR data could only be obtained for the more abundant isomer. Interestingly, as many as four bridging cyclopentadiene complexes were tentatively identified, present as an approximate 4.5 : 2 : 4 : 1 mixture of stereoisomers, with the respective methylene proton resonances at 2.71, 2.62, 2.55, and 2.37 ppm. Unfortunately, due to the extensive overlap of the proton signals of these products, a clear interpretation of the NMR data is not possible. Nonetheless, the products with methylene signals at 2.71 and 2.37 ppm were isolated in small amounts, the consequent ^1H NMR spectra revealing in both cases highly symmetrical cyclopentadiene ligands, similar to the well-characterized symmetric bridging 1,3-cyclohexadiene ligand of complex **119**. The structures of these bridging complexes are therefore arbitrarily designated as the *anti* (S, S) and (R, R) diastereomers of complex **121** (as drawn in eq. **4.13**). The remaining unsymmetrical products may be comprised of *syn* diastereoisomers. Crystallographic determination of the structure of these unique complexes was impeded by low crystallinity and the thermal instability of the diene ligand in solution.

Attempts to promote selective formation of either the η^2 -(1,3-cyclohexdiene) product **117** or the bridging 1,3-cyclohexdiene product **119** met with little success. Addition of excess 1,3-cyclohexadiene, for example, does not provide greater quantities of monomeric product **117** while photolysis with just 0.5 equivalents of free diene fails to afford a greater proportion of dinuclear species **119**. In both cases the product ratio

remains approximately the same, possibly as a result of attaining a photostationary equilibrium.



Overall respective product ratio of **120**, **120'**, **121**, **121'**,
and two additional unknown products: 4.5 : 2 : 4.5 : 1 : 2 : 4

Despite the low yield and the thermolability of the bridging 1,3-diene complexes **119** and **121**, these products remain attractive for a number of reasons. The $\mu\text{-}\eta^2\text{:}\eta^2$ coordination mode of conjugated cyclic dienes, for example, has been identified crystallographically in only four other transition metal systems: an $[(\text{acac})\text{Cu}]_2(\mu\text{-}\eta^2\text{:}\eta^2\text{-1,3-cyclooctadiene})$ complex⁵³, an $[(\eta^6\text{-benzene})\text{osmiumcarbonyl}]_2[\mu\text{-}\eta^2\text{:}\eta^2\text{-1,3-cyclohexadiene}]$ cluster,⁵⁴ a $[(\kappa^2\text{-NO}_3)\text{Ag}]_2[\text{bis}(\mu\text{-}\eta^2\text{:}\eta^2\text{-1,3-cyclodecadiene})]$ complex,⁵⁵ and a $(\text{CpNi})_2(\mu\text{-}\eta^2\text{:}\eta^2\text{-cyclopentadiene})$ species.⁵⁶ Others have proposed the presence of

bridging cyclic 1,3-diene ligands in various nickel⁵⁷ and palladium⁵⁸ systems, as suggested by spectroscopic characterization. More interesting, however, is the fact that this coordination motif is unprecedented in organochromium chemistry, and this Cp*CrNO system strongly resists the formation of *s-cis* η^4 -(1,3-diene) complexes.

4.4 Electronic justification of preferential *s-trans* diene binding observed in the Cp'CrNO(1,3-diene) complexes

It is now clear that both the Cp and Cp* series of our acyclic η^4 -(1,3-diene) complexes exclusively adopt the *s-trans* diene coordination mode,⁵⁹ with the previously assigned *s-cis* η^4 -(2,3-dimethylbutadiene) complex **113'** (p. 118) actually existing as a dimeric bridged η^2 -diene species. Intriguingly, of the numerous *s-trans* 1,3-diene complexes reported over the last twenty-five years,^{21-23, 25, 26, 29, 30, 33, 38-43, 60} none have been discovered among chromium nor *any* of the other first-row transition metals. Previously reported η^4 -(conjugated diene) complexes of chromium adopt *only* the *s-cis* bonding mode; several of these complexes are also thermally unstable (Chart 4.3).⁶¹⁻⁷⁰

Contrary to that observed for many of the second- and third-row *s-trans* diene complexes, the Cp'CrNO(*s-trans*-diene) complexes **106-110** and **111-114** are not in equilibrium with their elusive *s-cis* counterparts. Moreover, the fact that photolysis of Cp*CrNO(CO)₂ **94** in the presence of cyclic conjugated dienes fails to afford *s-cis* η^4 -diene complexes, instead yielding the monomeric η^2 -diene species (**117**, **120**) and binuclear complexes (**119**, **121**), implies that there may be a strong electronic preference for *s-trans* coordination to the Cp'CrNO fragment.

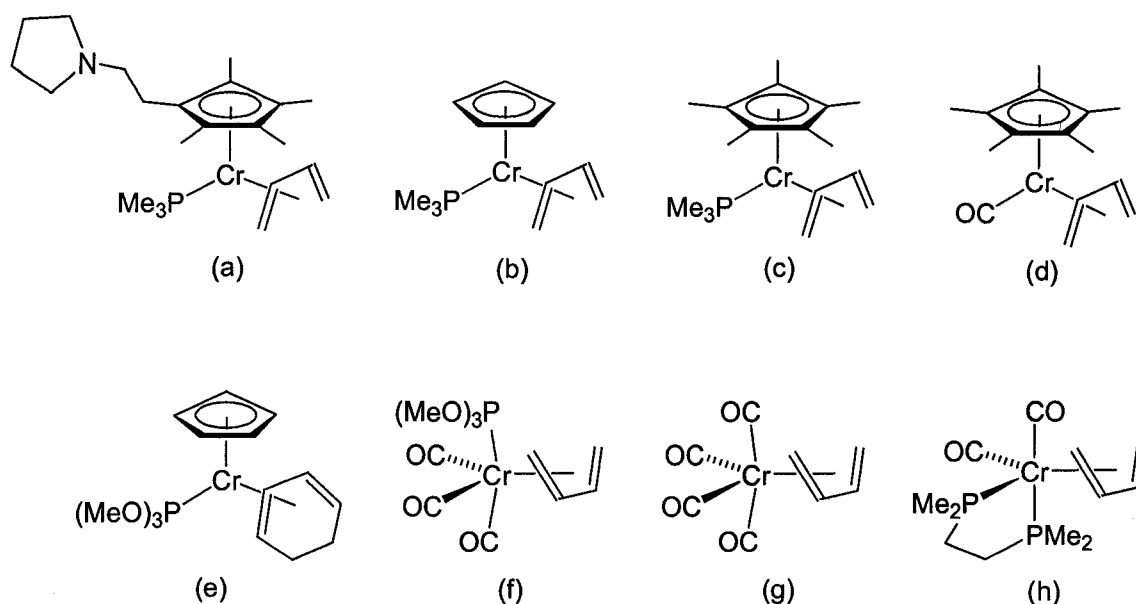


Chart 4.3: Selected examples of chromium *s-cis*-(1,3-diene) complexes. Unless noted otherwise, all complexes are stable at room temperature: (a) stable < -30 °C, ref. 61; (b) ref. 62; (c) stable < 0 °C, ref. 62; (d) stable < -30 °C, ref. 62; (e) stable < 25 °C, ref. 62; (f) ref. 63, 64 ; (g) ref. 65-68; (h) ref. 69, 70.

Indeed, both Legzdins⁷¹ and Nakamura^{19, 60} have proposed that electron deficient organometallic fragments favour *s-trans* 1,3-diene bonding over *s-cis*. This supposition has been supported by DFT calculations for the CpMo(NO) fragment (see Fig. 4.12 for the qualitative reproduction), the nitrosyl ligand of which is a strongly electron withdrawing π -acid. As seen in this molecular orbital analysis, the HOMO of the *s-trans* butadiene conformation (e) forms a lower energy MO (d) upon integration with the HOMO of the CpMo(NO) fragment (c); an MO of higher energy is formed (b) upon overlap with the HOMO of the *s-cis* butadiene conformation (a). Since chromium has less electron density than its second-row counterpart, it is reasonable to assume that the Cp'CrNO(η^4 -diene) complexes are more electron deficient than the molybdenum

analogues and therefore display an increased preference for *s-trans* diene coordination.

In the case of cyclic conjugated dienes, the observed bridging 1,3-diene dinuclear chromium species must also be of lower energy than the alternative *s-cis* coordinated chromium species. These assumptions are currently being evaluated via density functional theory.

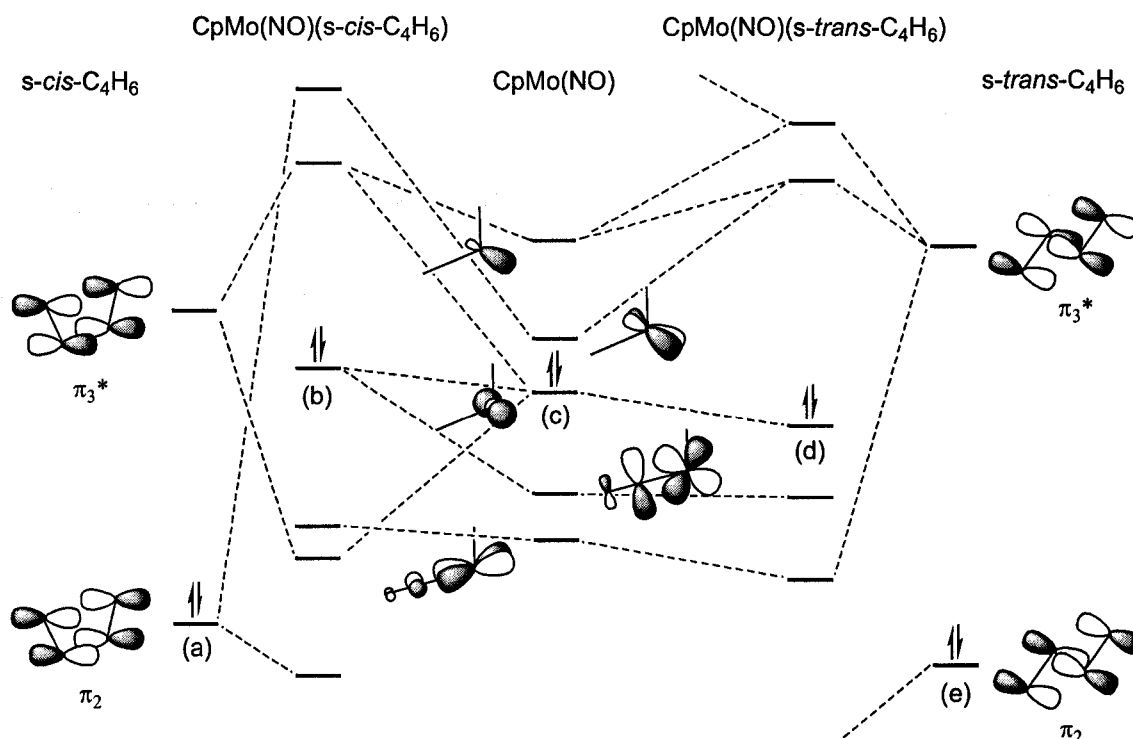


Figure 4.12: Qualitative molecular orbital energy diagram (reproduced from the DFT orbital analysis in ref. 16) showing the interaction of the π_2 and π_3^* orbitals of *s-cis* and *s-trans*-butadiene with the frontier orbitals of the CpMo(NO) fragment. The paired electrons indicate the HOMO of each species.

The fact that a second propene, allyltrimethylsilane, or 2-butyne molecule does not displace the remaining carbonyl ligand on the Cp'CrNO(CO) fragment implies that an electronic barrier to standard bis(alkene) bonding may also exist. Perhaps substitution

with a second olefin raises the subsequent HOMO of the corresponding product to an unfavourable energy level. Additionally, the lack of formation of an $\eta^2:\eta^2$ -(1,5-hexadiene) complex suggests that the highly selective formation of the reported chromium *s-trans* 1,3-diene complexes is dependent on the *conjugated* nature of the organic diene. In other words, the frontier molecular orbitals of a non-conjugated diene may also form an energetically unfavourable HOMO upon coordination to the $\text{Cp}^*\text{Cr}(\text{NO})$ fragment.

4.5 References

1. Christensen, N. J.; Legzdins, P. *Organometallics* **1991**, *10*, 3070.
2. Richter Addo, G. B.; Legzdins, P. *Metal Nitrosyls*. Oxford University Press: Oxford, 1992.
3. Richter Addo, G. B.; Legzdins, P.; Burstyn, J. *Chem. Rev.* **2002**, *102*, 857.
4. Hayton, T. W.; Legzdins, P.; Sharp, W. B. *Chem. Rev.* **2002**, *102*, 935.
5. McCleverty, J. A. *Chem. Rev.* **2004**, *104*, 403.
6. Koshland, D. E. *Science* **1992**, *258*, 1861.
7. Clarke, M. J.; Gaul, J. B. *Struct. Bonding. (Berlin)* **1993**, *81*, 147.
8. Legzdins, P.; Pang, C. C. Y.; Shaw, M. J. Compositions and Methods for Relaxing Smooth Muscles. U. S. Patent 5,631,284, May 20, 1997.
9. Legzdins, P.; Pang, C. C. Y.; Shaw, M. J. Compositions and Methods for Relaxing Smooth Muscles. U. S. Patent 5,811,463, September 22, 1998.
10. Works, C. F.; Ford, P. C. *J. Am. Chem. Soc.* **2000**, *122*, 7592.
11. Lang, D. R.; Davis, J. A.; Lopez, L. G. F.; Ferro, A. A.; Vasconcellos, L. C. G.; Franco, D. W.; Tfouni, E.; Wieraszko, A.; Clarke, M. J. *Inorg. Chem.* **2000**, *39*, 2294.

12. Patra, A. K.; Mascharak, P. K. *Inorg. Chem.* **2003**, *42*, 7363.
13. Weiner, W. P.; White, M. A.; Bergman, R. G. *J. Am. Chem. Soc.* **1981**, *103*, 3612.
14. Seidler, M. D.; Bergman, R. G. *Organometallics* **1983**, *2*, 1897.
15. Chang, J.; Seidler, M. D.; Bergman, R. G. *J. Am. Chem. Soc.* **1989**, *111*, 3258.
16. Legzdins, P.; Wassink, B. *J. Am. Chem. Soc.* **1986**, *108*, 317.
17. Legzdins, P.; Richter Addo, G. B.; Wassink, B.; Einstein, F. W. B.; Jones, R. H.; Willis, A. C. *J. Am. Chem. Soc.* **1989**, *111*, 2097.
18. Goldhaber, A.; Vollhardt, K. P. C.; Walborsky, E. C.; Wolfgruber, M. *J. Am. Chem. Soc.* **1986**, *108*, 516.
19. Tatsumi, K.; Yasuda, H.; Nakamura, A. *Isr. J. Chem.* **1983**, *23*, 145.
20. Reihlen, H.; Gruhl, A.; von Hessling, G.; Pfrengle, O. *Liebigs Ann. Chem.* **1930**, *482*, 161.
21. Erker, G.; Wicher, J.; Engel, K.; Rosenfeldt, F.; Dietrich, W.; Krüger, C. *J. Am. Chem. Soc.* **1980**, *102*, 6344.
22. Erker, G.; Wicher, J.; Engel, K.; Krüger, C. *Chem. Ber.* **1982**, *115*, 3300.
23. Yasuda, H.; Kajihara, Y.; Mashima, K.; Nagasuna, K.; Lee, K.; Nakamura, A. *Organometallics* **1982**, *1*, 388.
24. Mahima, K.; Nakamura, A. *J. Organomet. Chem.* **2002**, *663*, 5-12.
25. Erker, G.; Kehr, G.; Fröhlich, R. *Adv. Organomet. Chem.* **2004**, *51*, 109.
26. Erker, G.; Kehr, G.; Fröhlich, R. *J. Organomet. Chem.* **2004**, *689*, 4305.
27. Dahlman, M.; Erker, G.; Fröhlich, R.; Meyer, O. *Organometallics* **1999**, *18*, 4459.
28. Kai, Y.; Kanehisa, N.; Miki, K.; Kasai, N.; Mashima, K.; Nagasuna, K.; Yasuda, H.; Nakamura, A. *J. Chem. Soc., Chem. Commun.* **1982**, 191.
29. Hunter, A. D.; Legzdins, P.; Nurse, C. R. *J. Am. Chem. Soc.* **1985**, *107*, 1791.
30. Wang, L.-S.; Fettingner, J. C.; Poli, R. *J. Am. Chem. Soc.* **1997**, *119*, 4453.
31. Strauch, H. C.; Erker, G.; Fröhlich, R. *Organometallics* **1998**, *17*, 5746.

32. Sperry, C. K.; Rodriguez, G.; Bazan, G. C. *J. Organomet. Chem.* **1997**, 548, 1.
33. Fukumoto, H.; Mashima, K. *Organometallics* **2005**, 24, 3932.
34. Ernst, R. D.; Melendez, E.; Stahl, L.; Ziegler, M. L. *Organometallics* **1991**, 10, 3635.
35. Melendez, E.; Ilarraza, R.; Yap, G. P. A.; Rheingold, A. L. *J. Organomet. Chem.* **1996**, 522, 1.
36. Gemel, C.; Mereiter, K.; Schmid, R.; Kirchner, K. *Organometallics* **1997**, 16, 2623.
37. Christensen, N. J.; Hunter, A. D.; Legzdins, P. *Organometallics* **1989**, 8, 930.
38. Benyunes, S. A.; Green, M.; Grimshire, M. J. *Organometallics* **1989**, 8, 2268.
39. Beddows, C. J.; Box, M. R.; Butters, C.; Carr, N.; Green, M.; Kursawe, M.; Mahon, M. F. *J. Organomet. Chem.* **1998**, 550, 267.
40. Vong, W.-J.; S.-M., P.; Liu, R.-S. *Organometallics* **1990**, 9, 2187.
41. Poli, R.; Wang, L.-S. *J. Am. Chem. Soc.* **1998**, 120, 2831.
42. Wang, L.-S.; Fettingner, J. C.; Poli, R.; Meunier-Prest, R. *Organometallics* **1998**, 17, 2692.
43. Debad, J. D.; Legzdins, P.; Young, M. A. *J. Am. Chem. Soc.* **1993**, 115, 2051.
44. Ng, S. H. K.; Adams, C. S.; Hayton, T. W.; Legzdins, P.; Patrick, B. O. *J. Am. Chem. Soc.* **2003**, 125, 15210.
45. Legzdins, P.; McNeil, W. S.; Rettig, S. J.; Smith, K. M. *J. Am. Chem. Soc.* **1997**, 119, 3513.
46. Herberhold, M.; Alt, H.; Kreiter, C. G. *Liebigs Ann. Chem.* **1976**, 300.
47. Herberhold, M.; Alt, H. *J. Organomet. Chem.* **1972**, 42, 407.
48. Herberhold, M.; Alt, H.; Kreiter, C. G. *J. Organomet. Chem.* **1972**, 42, 413.
49. Hoyano, J. K.; Legzdins, P.; Malito, J. T. *Inorg. Synth.* **1978**, 18, 126.
50. Malito, J. T.; Dhakir, R.; Atwood, J. L. *J. Chem. Soc., Dalton Trans.* **1980**, 1253.

51. Templeton, J. *Adv. Organomet. Chem.* **1989**, 29, 1.
52. Kang, B.; Kim, D.; Do, Y.; Chang, S. *Org. Lett.* **2003**, 5, 3041.
53. Doyle, G.; Eriksen, K. A.; Van Engen, D. *Organometallics* **1985**, 4, 830.
54. Edwards, A. J.; Lewis, J.; Li, C.-K.; Morewood, C. A.; Raithby, P. R.; Shields, G. P. *Inorg. Chem. Commun.* **2003**, 6, 1291.
55. Coggon, P.; McPhail, A. T.; Sim, G. A. *J. Chem. Soc. B* **1970**, 1024.
56. Pasynkiewicz, S.; Buchowicz, W.; Poplawska, J.; Pietrzykowski, A.; Zachara, J. *J. Organomet. Chem.* **1995**, 490, 189.
57. Lehmkuhl, H.; Danowski, F.; Benn, R.; Mynott, R.; Schroth, G. *Chem. Ber.* **1986**, 119, 2542.
58. Murahasi, T.; Kanehisa, N.; Kai, Y.; Otani, T.; Kurosawa, H. *Chem. Commun.* **1996**, 825.
59. Norman, D. W.; Ferguson, M. J.; McDonald, R.; Stryker, J. M. *Organometallics* **2006**, 25, 2705.
60. Mashima, K.; Nakamura, A. *J. Organomet. Chem.* **2002**, 663, 5.
61. Döhring, A.; Gohre, J.; Jolly, P. W.; Kryger, B.; Rust, J.; Verhovnik, G. P. J. *Organometallics* **2000**, 19, 388.
62. Betz, P.; Döhring, A.; Emrich, R.; Goddard, R.; Jolly, P. W.; Krüger, C.; Romão, C.; Schönfelder, K. U.; Tsay, Y.-H. *Polyhedron* **1993**, 12, 2651.
63. Wang, N.-F.; Wink, D. J.; Dewan, J. C. *Organometallics* **1990**, 9, 335.
64. Kreiter, C. G.; Ozkar, S. *J. Organomet. Chem.* **1978**, 152, C13.
65. Kotzian, M.; Kreiter, C. G.; Ozkar, S. *J. Organomet. Chem.* **1982**, 229, 29.
66. Fischler, I.; Budzwait, M.; Koerner von Gustorf, E. A. *J. Organomet. Chem.* **1976**, 105, 325.
67. Koerner von Gustorf, E. A.; Jaenicke, O.; Wolfbeis, O.; Eady, C. R. *Angew. Chem. Int. Ed.* **1975**, 14, 278.
68. Koerner von Gustorf, E. A.; Jaenicke, O.; Polansky, O. E. *Angew. Chem. Int. Ed.* **1972**, 11, 532.

69. Kreiter, C. G.; Kotzian, M. *J. Organomet. Chem.* **1985**, 289, 295.
70. Kreiter, C. G. *Adv. Organomet. Chem.* **1986**, 26, 297.
71. Hunter, A. D.; Legzdins, P.; Einstein, F. W. B.; Willis, A. C.; Bursten, B. E.; Gatter, M. G. *J. Am. Chem. Soc.* **1986**, 108, 3843.

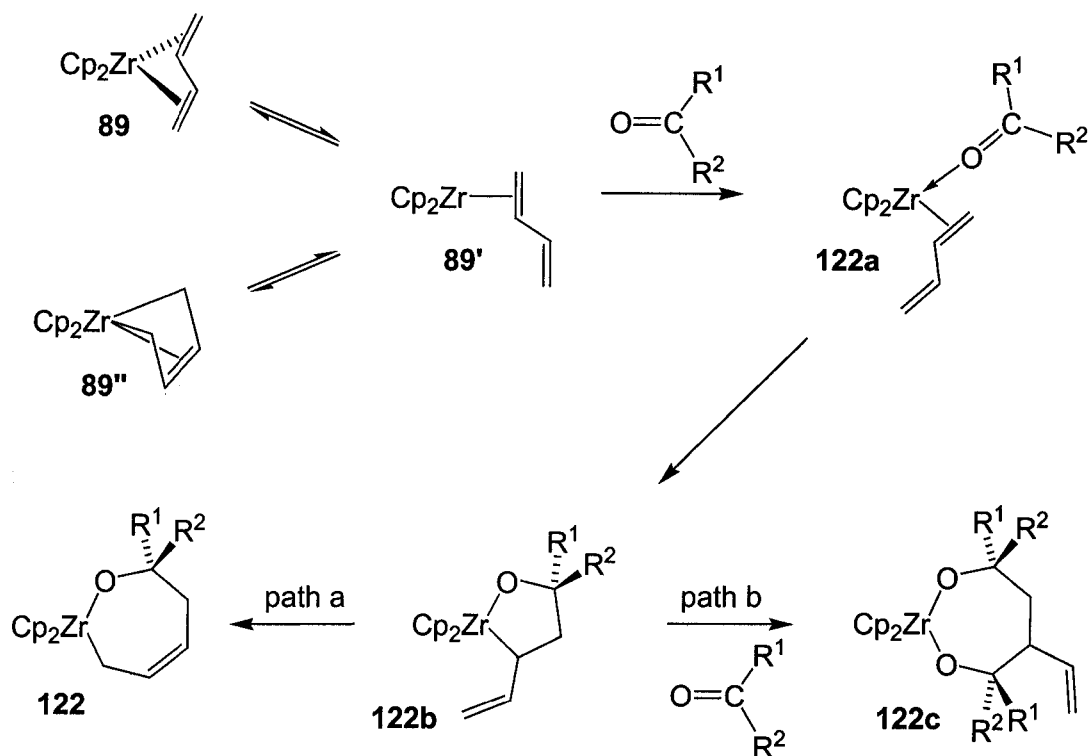
Chapter 5.

Reactivity of Cp'CrNO(1,3-diene) complexes: thermally stable η^3 -allyl compounds, novel zwitterionic complexes, and an η^2 -(hydrido-tin) species

5.0 Introduction

Although iron carbonyl η^4 -(1,3-diene) complexes have found widespread applications in the regio-, diastereo-, and enantioselective synthesis of organic compounds,¹⁻³ the unique reactivity demonstrated by the more recently discovered early metal η^4 -(1,3-diene) complexes were of more closely reflected our research goals.⁴⁻¹² The addition of carbonyl-containing organic molecules to *s-cis* and *s-trans* mixtures of zirconocene(butadiene) complex **89**, for example, affords the unique oxazirconacycles **122** and **122c** (Scheme 5.1).^{7, 8, 10-12} These reactions are thought to proceed via the unsaturated η^2 -butadiene intermediate **89'**, which exists in equilibrium with the *s-trans* η^4 -diene complex **89**. In the case of oxometallacycles **122**, synthesis of these products is initiated by coordination of the carbonyl compound to form the intermediate **122a**, then insertion to give vinyloxametallacyclopentane intermediate **122b**, followed by a rearrangement (path a) to yield the observed *cis*-cycloolefin product **122**. In some instances, usually in the case of diarylketones, a second equivalent of ketone adds to intermediate **122b** (path b) to provide dioxazirconacycloheptane complex **122c**.^{7, 11-13}

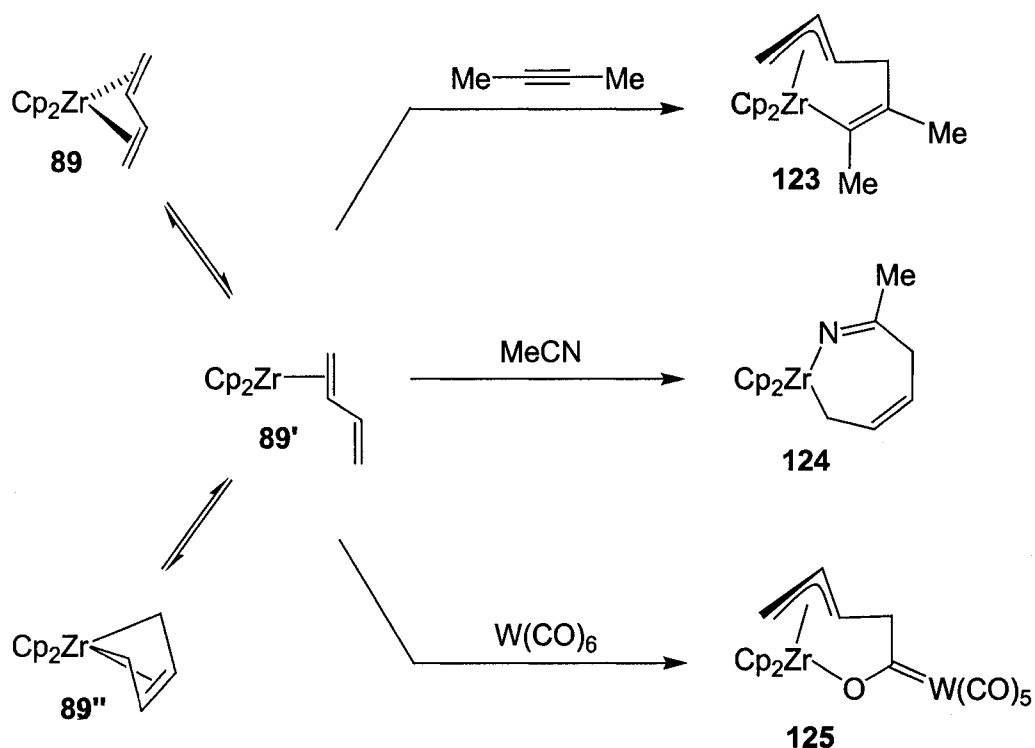
Scheme 5.1



Treatment of zirconocene η^4 -butadiene complex **89** with alkynes or acetonitrile provides the respective seven-membered zirconacycles **123** and **124** (Scheme 5.2).¹²

Complex **89** also undergoes insertion reactions with metal carbonyls [e.g., $\text{W}(\text{CO})_6$] to form the metallacyclic η^3 -allyl zirconoxycarbene complex **125**.^{9, 11-13}

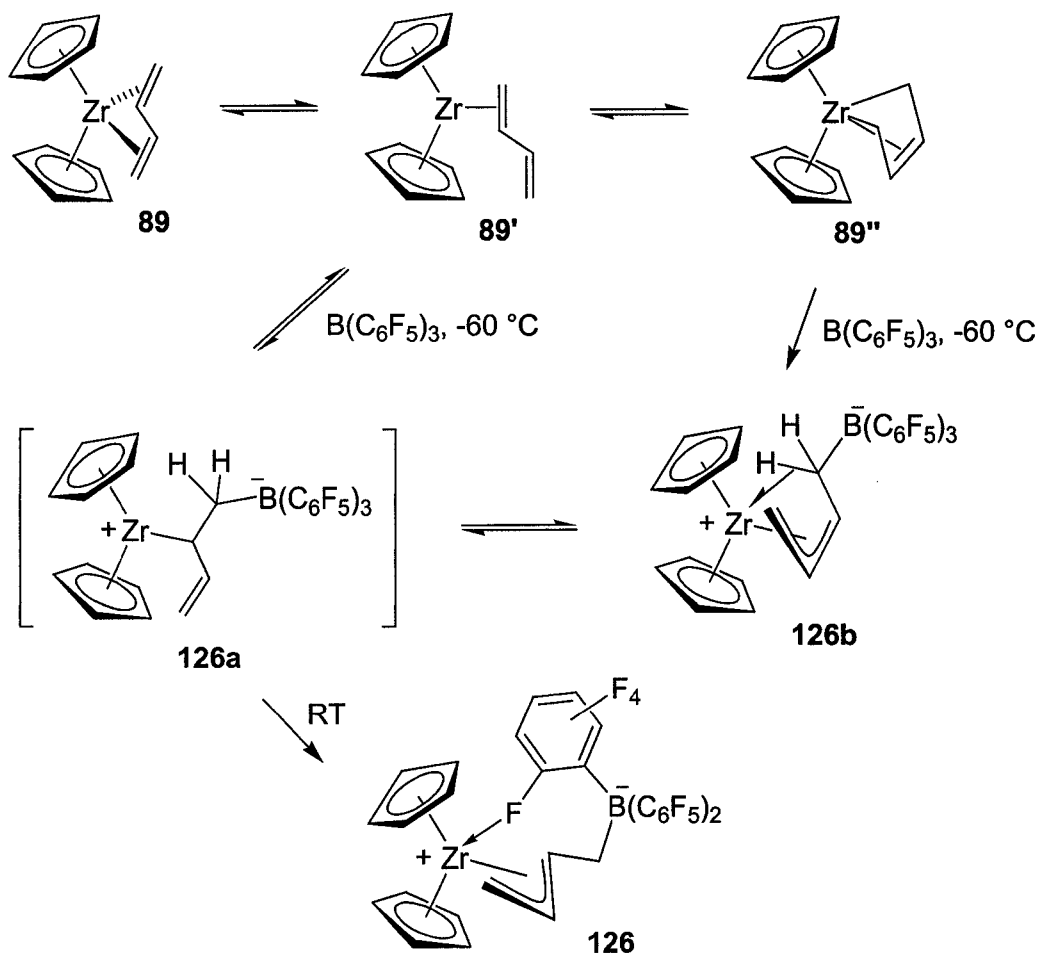
Scheme 5.2



Zirconocene(η⁴-1,3-diene) complexes also add a variety of inorganic or main group electrophiles at a terminal conjugated diene carbon atom. For instance, the strong Lewis acid tris(pentafluorophenyl)boron adds to *s-cis* and *s-trans* isomeric mixtures of zirconocene(η⁴-butadiene) **89** to generate the isolable dipolar zwitterionic complex **126**.^{11,}

¹² As depicted in Scheme 5.3, addition of B(C₆F₅)₃ at -60 °C to the η²-butadiene complex **89'** initially affords the kinetically preferred *cisoid* η³-allyl agostic complex **126b**. At ambient temperature this intermediate species rapidly rearranges to the more thermodynamically favoured *transoid* isomer **126**, presumably via the unsaturated intermediate **126a**.

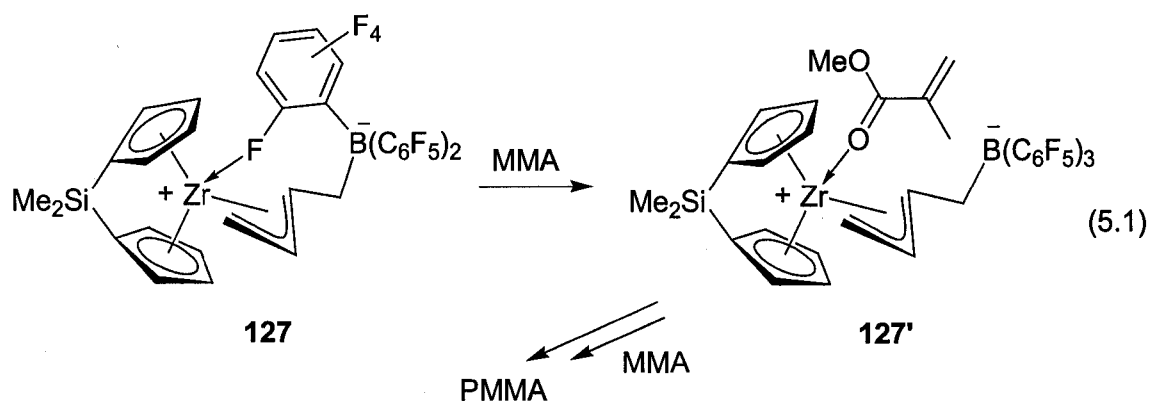
Scheme 5.3



The solid-state molecular structure of complex **126** reveals bridging of an *ortho*-fluorine atom of one of the C_6F_5 rings to the electropositive zirconium centre (Zr-F ca. 2.4 Å).¹¹⁻¹⁵ This interaction is also present in solution; indicated by a ^{19}F NMR resonance of the respective fluorine nucleus between -210 and -220 ppm, in contrast to the C_6F_5 ^{19}F resonances of unreacted $\text{B(C}_6\text{F}_5)_3$ between -130 and -170 ppm.

Due to this very weak (~8 Kcal/mol) Zr-ortho-F interaction, complexes such as **126** are susceptible to dissociation to an unsaturated intermediate followed by

coordination and insertion of α -olefins. Consequently, these complexes are very active single-component homogeneous Ziegler-Natta polymerization and co-polymerization catalysts.^{11-13, 16, 17} The *ansa*-zirconocene-derived complex **127**, for example, is an active catalyst for the polymerization of polar monomers such as methylmethacrylate (MMA) (eq. 5.1). Interestingly, the initial Lewis base adduct **127'** was identified spectroscopically, thus providing a reliable model for intermediates in the group IV catalyzed polymerization of polar monomers.

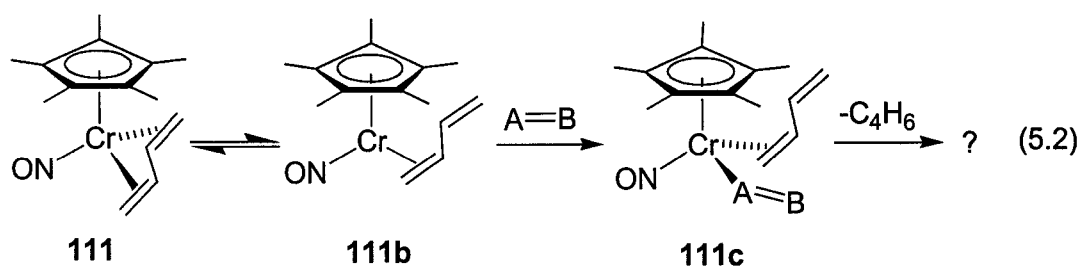


5.1 Attempted insertion reactions

Following the examples shown in Schemes 5.1 and 5.2, insertion reactions of the novel Cp*CrNO(*s-trans*-butadiene) complexes **106** and **111** were investigated. Regrettably, all attempted insertion reactions failed to afford any of the expected chromacyclic products; intractable mixtures were obtained in most cases. Treatment of pure Cp*CrNO(*s-trans*-butadiene) complex **111** with unsaturated organic compounds

such as 2-butyne, 2,6-dimethylphenylisonitrile, dimethylacetylenedicarboxylate (DMAD), acetone, or methacrolein (at room temperature in benzene- d_6 for 24 h) reveals only very broad signals in the resulting ^1H NMR spectra, indicating the formation of uncharacterized paramagnetic products. Moreover, a major component of these spectra is free butadiene, as determined by spectroscopic comparison to authentic material. No clear spectroscopic evidence for products similar to zirconacyclic complexes **122-124** was obtained. Equally disappointing reactivity is observed for similar reactions of the cyclopentadienyl analogue **106**.

Since the insertion of unsaturated organic compounds into metal-carbon bonds of zirconocene(η^4 -butadiene) **89** requires equilibration with a reactive η^2 -butadiene species **89'** (see Scheme 5.2, above), it is reasonable to assume that these decomposition reactions of chromium *s-trans*-butadiene complexes **106** and **111** are also initiated by a similar equilibrium. Thus, as shown for complex **111** in equation 5.3, isomerization to the 16-electron η^2 -butadiene species **111b** allows for coordination of an unsaturated organic molecule (denoted as $\text{A}=\text{B}$) to generate the 18-electron η^2 -butadiene complex **111c**, similar to zirconocene species **122a**. Unlike this latter species, however, complex **111c** is presumed to be thermally unstable, resulting in loss of butadiene and the formation of intractable chromium-containing product(s).



Given the thermal instability noted for $\text{CpCrNO(CO)}(\eta^2\text{-butadiene})$ **101** and the related permethylcyclopentadienyl complex **111a** (recall Ch. 4, p. 113), it is reasonable to assume that loss of butadiene from the structurally related complex **111c** is a thermodynamically preferred reaction pathway. Moreover, the fact that neither complex **101** nor complex **111a** form chromacyclobutanones, η^3 -allyl oxachromacycles, or chromacyclohexenones also implies that migratory insertion of unsaturated organic molecules is unlikely to occur using complexes of this type.

The irreversible loss of the diene ligand is even more pronounced upon addition of acetonitrile to complexes **106** or **111**. ^1H NMR analysis of reactions conducted in CD_3CN confirms that the starting complexes are completely consumed within several hours at room temperature; the diene ligands are ejected into solution along with the observation of considerably broad NMR signals. The identity of the chromium-containing product(s) remains unknown.

Addition of benzaldehyde to a solution of complex **111** in benzene- d_6 also leads to paramagnetic products, as evidenced by the increased broadness in the ^1H NMR spectrum and the formation of trace amounts of free butadiene. Unlike the above decomposition reactions, however, one product was isolated from this crude reaction mixture; slow evaporation (over twelve days under inert atmosphere) of the solvent

provides near-black crystals that were subsequently identified via X-ray crystallography as the bridging *benzyloxy chromium(I)* nitrosyl complex **128** (Fig. 5.1 and Scheme 5.4).

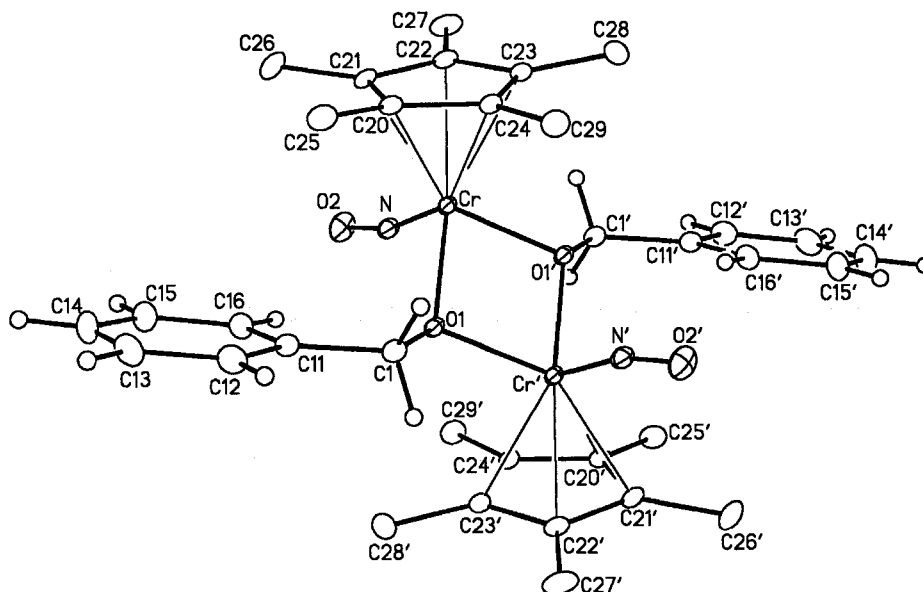
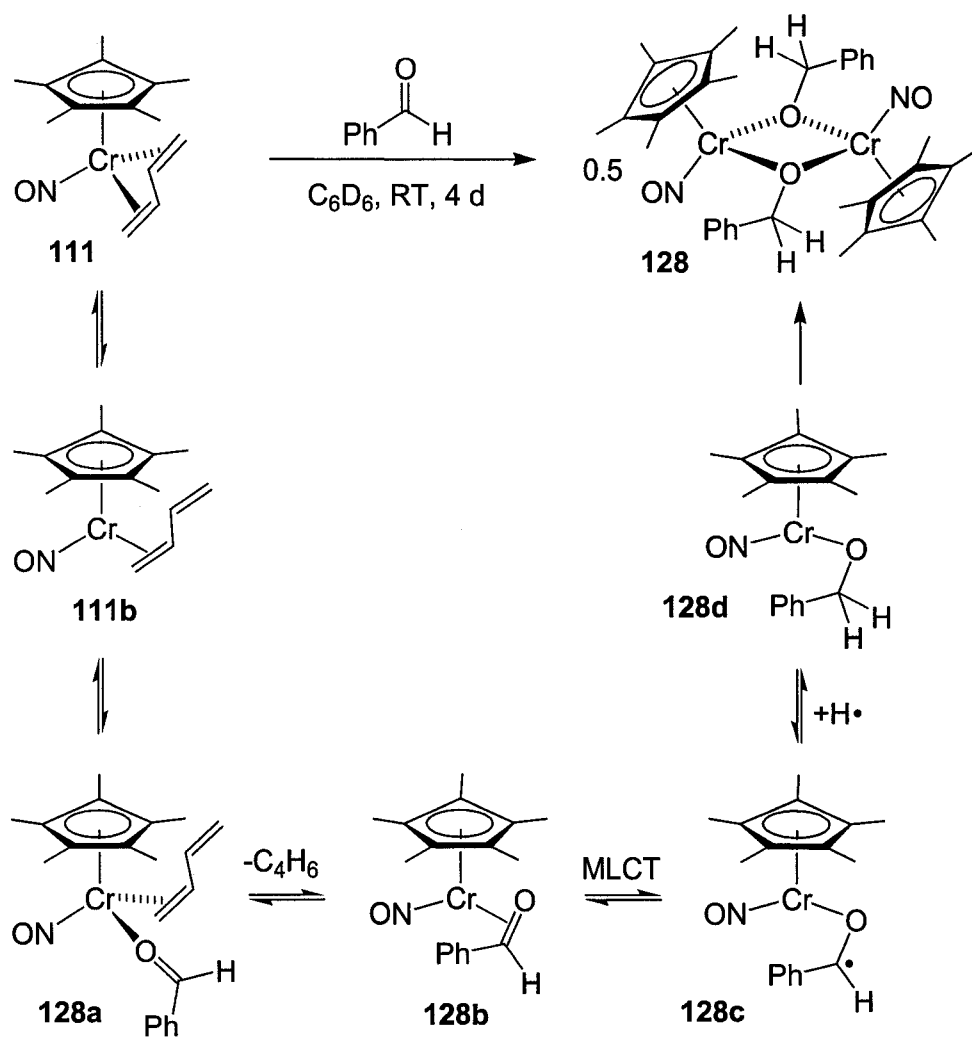


Figure 5.1: Solid-state molecular structure of $[\eta^5\text{-(C}_5\text{Me}_5\text{)Cr(NO)(}\mu\text{-OCH}_2\text{Ph)}]_2$ **128**. Non-hydrogen atoms are represented by Gaussian ellipsoids at the 20% probability level. Hydrogen atoms are shown with arbitrarily small thermal parameters for the benzyloxy groups, and are not shown for the pentamethylcyclopentadienyl groups. Primed atoms are related to the unprimed ones by the crystallographic inversion centre located at $(0, 1/2, 1/2)$. Selected bond lengths (Å) and angles (deg): Cr-O(1) = 1.9987(15), Cr-O(1') = 1.9844(15), Cr-N = 1.684(2), O(1)-C(1) = 1.416(3), O(2)-N = 1.214(2), C(1)-C(11) = 1.509(3), Cr-Cr' = 2.986; O(1)-Cr-O(1') = 82.88(7), O(1)-Cr-N = 98.56(8), Cr-O(1)-Cr' = 97.12(7), Cr-(O1)-C(1) = 128.67(13), Cr-N-O(2) = 166.50(17), O(1)-C(1)-C(11) = 113.04(19).

It is interesting that the Cr–N–O bond angle of this highly unexpected product is somewhat bent (166.5°), in contrast to the more linear arrangement of $\sim 173^\circ$ of our chromium(0) nitrosyl complexes, previously discussed in Chapter 4. It has been suggested by Legzdins¹⁸ that a similar decrease in the M–N–O angle of CpMo(NO)(*s-cis*-2,3-dimethylbutadiene) occurs as a result of increased $d \rightarrow \pi^*$ backbonding from the metal centre, effectively reducing the bond order of the nominally triple bonded NO functionality. In spite of the increased oxidation state of chromium(I) complex **128**, displacement of the somewhat π -acidic butadiene ligand of complex **111** by electron-donating alkoxy groups is consistent with this supposition.

A possible mechanism (Scheme 5.4) for the formation of this complex may involve initial η^4 - to η^2 - isomerization of the *s-trans* butadiene ligand of complex **111**. Coordination of benzaldehyde to the unsaturated η^2 -butadiene species **111b** then affords complex **128a**. As illustrated in eq. 5.2, this unstable intermediate may then lose butadiene to form the 16-electron chromium(0) species **128b**. Metal to ligand charge transfer (MLCT) from the chromium centre to the benzaldehyde ligand then forms the radical species **128c**. Each ketyl radical then abstracts a hydrogen atom from liberated butadiene or unreacted benzaldehyde to generate the observed 17-electron complex **128**. Due to the time required for this reaction (*e.g.*, up to four days at room temperature) and the apparent low yield (< 50%) of complex **128**, further investigation of the mechanism of formation and the possible utility of this complex were not pursued. Nonetheless, the mechanism proposed for the formation of complex **128** is not unreasonable given that other organometallic ketyls have been structurally characterized and employed in organic synthesis.¹⁹⁻²⁵

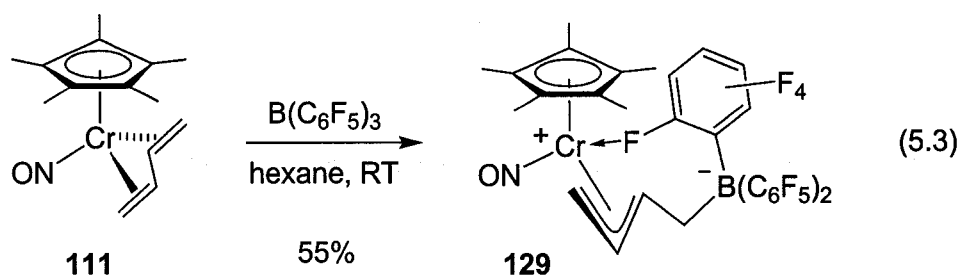
Scheme 5.4



5.2 Addition of strong Lewis acids

Given that $\text{B}(\text{C}_6\text{F}_5)_3$ converts zirconocene(butadiene) complexes into zwitterionic η^3 -allyl species, we proposed that similar treatment of $\text{Cp}^*\text{CrNO}(s\text{-trans-butadiene})$ complex **111** would provide analogous zwitterionic chromium nitrosyl products. Indeed, treatment of an orange solution of complex **111** in hexane with tris(perfluorophenyl)-boron leads to an immediate colour change to brick-red. Removal of the solvent and ^1H

NMR analysis of the subsequent residue reveals that the starting diene complex is completely consumed; the initial Cp* resonance at 1.49 ppm is replaced by that of the product at 1.09 ppm (Table 5.2). This product, initially assumed to be the zwitterionic allyl complex **129**, was obtained in 55% yield after recrystallization from hexane (eq. 5.3).



Unfortunately, complex **129** is thermally sensitive, irreversibly ejecting *free butadiene* into solution. This observation suggested that Lewis acid addition may not have occurred at the η^4 -diene ligand of complex **111** to form the expected η^3 -allyl-type ligand. Indeed, a Lewis acid-base adduct may have formed instead by reaction of $\text{B(C}_6\text{F}_5)_3$ and the nitrosyl ligand. Although the ^{19}F NMR spectrum of complex **129** revealed no evidence for a metal-coordinated *ortho*-fluorine atom, definitive determination of the chemoselectivity of the Lewis acid addition and the NO bonding mode via spectroscopic methods was complicated by several factors. Gradual thermal decomposition of complex **129** in solution (even at subzero temperatures) renders the ^1H NMR spectrum very low in resolution. In addition, an unidentified impurity (observed at 1.2 ppm in the ^1H NMR spectrum) could not be fully removed, even by recrystallization of complex **129**. Only five proton resonances for the diene (or possibly η^3 -allyl) ligand

are therefore clearly visible in the ^1H NMR spectrum (Table 5.1). The sixth proton, obscured by the impurity, was detected via indirect NMR methods. Thus, differentiating between an η^4 -butadiene ligand and a boron-substituted η^3 -allyl moiety is not possible via NMR spectroscopy. Equally frustrating is the infrared spectrum of complex **129**; the aromatic absorptions of the C_6F_5 groups obscure the region where terminal or Lewis acid-bound nitrosyl ligand absorptions are expected.²⁶⁻²⁹

Fortunately, this ambiguity over the chemoselectivity of the reaction with $\text{B}(\text{C}_6\text{F}_5)_3$ was resolved by an X-ray crystal structure of complex **129** (Fig. 5.3). Clearly, this novel zwitterionic complex is comprised simply of a $\text{B}(\text{C}_6\text{F}_5)_3$ group bound to the nitrosyl ligand. Moreover, given the *s-trans* coordination of the unreacted butadiene ligand (torsional angle = 123.5°), this intriguing species is a third structurally characterized member of this unprecedented family of first-row transition metal *s-trans*-diene complexes.

Since tris(perfluorophenyl)boron is a highly electron withdrawing oxophilic Lewis acid, it is no surprise that this compound forms a relatively strong polar covalent bond ($\text{B}-\text{O} = 1.57 \text{ \AA}$) with the nitrosyl ligand. As a result of this significant interaction, the nitrosyl moiety is expected to be an even stronger π -acidic ligand. The resulting increased demand for metal electron density, however, reduces the extent of π -back-donation to the diene ligand, rationalizing the observed increase in diene lability in solution.

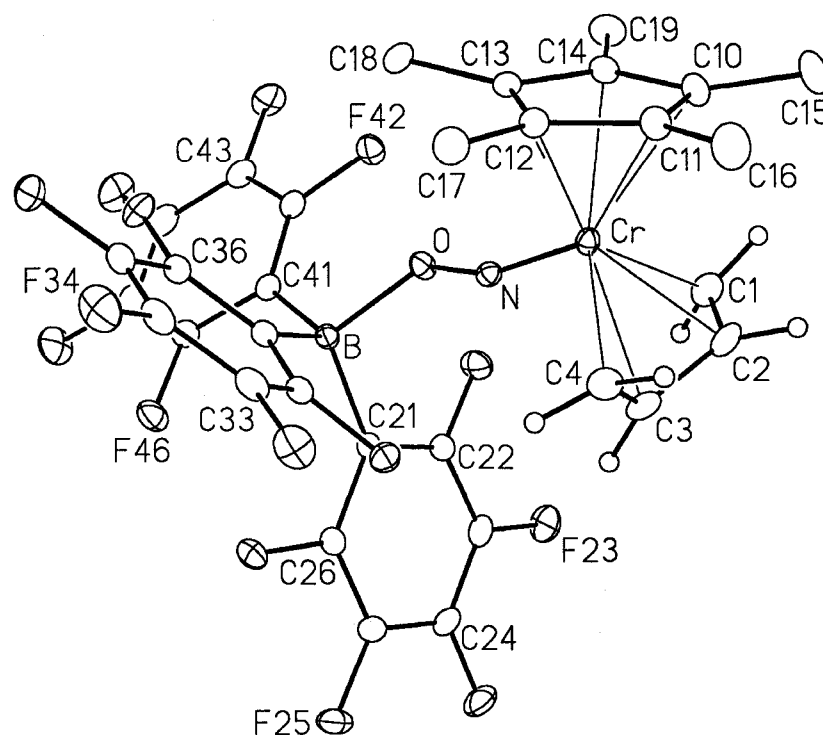
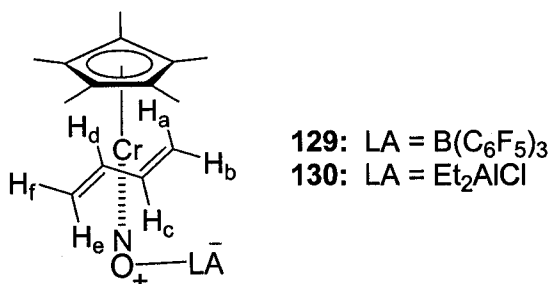


Figure 5.2: The solid-state molecular structure of $(\eta^5\text{-C}_5\text{Me}_5)\text{chromium}-(\eta^4\text{-s-trans-butadiene})\text{nitrosyl}[\text{tris(perfluorophenyl)boron}]$ **129**. Non-hydrogen atoms are represented by Gaussian ellipsoids at the 20% probability level. Hydrogen atoms of the butadiene ligand are shown with arbitrarily small thermal parameters, while those of the pentamethylcyclopentadienyl group are not shown. Selected bond lengths (Å) and angles (deg): Cr-N = 1.6527(14), Cr-C(1) = 2.2806(19), Cr-C(2) = 2.1294(19), Cr-C(3) = 2.1375(19), Cr-C(4) = 2.2531(18), N-O = 1.2749(18), O-B = 1.572(2), C(1)-C(2) = 1.382(3), C(2)-C(3) = 1.418(3), C(3)-C(4) = 1.390(3), C(21)-B = 1.639(2); N-O-B = 122.90(12), Cr-N-O = 159.96(12), C(1)-C(2)-C(3) = 120.3(2), C(2)-C(3)-C(4) = 118.5(2), O-B-C(21) = 106.59(13), C(1)-C(2)-C(3)-C(4) = 123.5(2).

Table 5.1: ^1H NMR data (ppm) for the boron-functionalized zwitterionic *s-trans* butadiene complexes **129** and the aluminum analogue **130**. Coupling constants (J) are in Hertz (Hz).



Complex	Cp*	H _a	H _b	H _c	H _d	H _e	H _f
129	1.09	3.11 (d, $J = 15.5$)	3.26 (dd, $J = 7.5, 1.5$)	3.61 (ddd, $J = 15.9, 12.0, 7.5$)	1.21 (ddd, $J = 15.0, 12.0, 7.5$) ^a	1.07 (br d, $J = 15.0$)	2.50 (dd, $J = 7.5, 0.7$)
130^b	1.28	3.43 (br d, $J = 14.1$)	3.57 (br d, $J = 5.7$)	4.14 (br m)	1.51 (br m)	1.38 (br d, $J = 14.4$)	2.59 (d, $J = 6.9$)

^aDetected indirectly via homonuclear COSY NMR spectroscopy; the coupling constants are based on those observed for the mutually coupled protons. ^bSignals for the ethyl protons appear at 1.46 ppm (br t, $J = 8.1$ Hz) and 0.34 ppm (br q, $J = 8.1$ Hz).

Surprisingly, the difference between the Cr–N–O angle in the solid-state molecular structures of the *s-trans*-isoprene complex **112** (Fig. 4.7) and 2,3-dimethylbutadiene complex **113** (Fig. 4.8) on the one hand and that of zwitterionic complex **129** on the other does not agree with this proposed increased π -backdonation to the nitrosyl ligand. The former two complexes have angles of approximately 173° while that of the latter is considerably more acute ($\sim 160^\circ$), although it should be closer to 180° . This discrepancy, however, is in agreement with the M–N–O angles of other structurally

characterized organometallic nitrosyl–boron adducts, and is attributed to the presence of sterically demanding substituents on the boron centre.^{28, 29}

The addition of diethylaluminum chloride to *s-trans* butadiene complex **111** in toluene- d_8 also affords a brick-red solution, the ^1H NMR spectrum of which reveals considerably broad signals similar in multiplicity and chemical shift to that of zwitterionic complex **129** (Table 5.1). The identity of this product is therefore tentatively assigned to be complex **130**, the Et_2AlCl adduct analogue of complex **129**.

Unfortunately, the stability of complex **130** in solution is much less than that of its boron-containing counterpart and isolation of this product in the solid-state was not possible.

Treatment of either the zwitterionic complexes **129** or **130** with a second equivalent of the respective Lewis acid fails to effect any detectable further reaction. Attempts to polymerize monomers such as ethylene, propene, or isoprene with these mixtures leads only to decomposition. The addition of nucleophiles such as Super-Hydride™ or potassium dimethylmalonate to the potentially electrophilic diene ligand of these zwitterionic complexes unfortunately also leads to decomposition.

5.3 Conversion of chromium(1,3-diene) and chromium(alkene) complexes to cationic η^3 -allyl derivatives

5.3.1 Protonation reactions of $\text{Cp}^*\text{Cr}(\text{NO})(s\text{-trans-butadiene})$

The preparation of the proposed Type I and Ic η^3 -allyl complexes via protonation of diene complex **111** was also investigated (recall Methods C and D in Scheme 2.1, p. 47). Treatment with HCl in diethyl ether at -78°C , for example, affords a yellow solution that, upon warming to room temperature, turns green and deposits a

paramagnetic green precipitate. Recrystallization of the precipitate from acetone affords deep green crystals, the solid-state molecular structure of which was determined by X-ray diffraction to be $[\text{Cp}^*\text{Cr}(\text{NO})\text{Cl}]_2$ **132** (Fig. 5.4). Prior characterization of this known complex was limited only to combustion and infrared analyses.³⁰

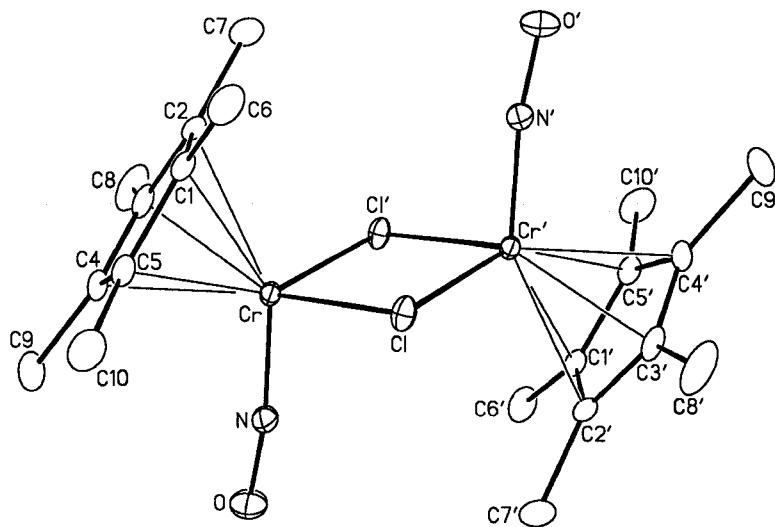
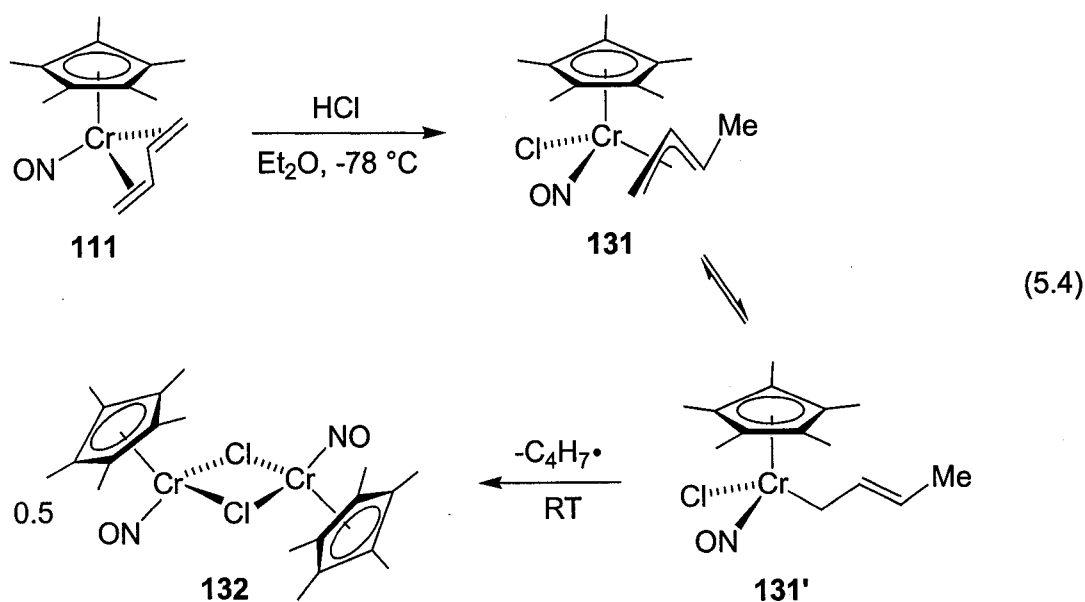


Figure 5.4: The solid-state molecular structure of $[\eta^5\text{-(C}_5\text{Me}_5\text{)Cr}(\text{NO})\text{Cl}]_2$ **132**. Non-hydrogen atoms are represented by Gaussian ellipsoids at the 20% probability level. Hydrogen atoms are not shown. Primed atoms are related to the unprimed ones by the crystallographic inversion centre at $(0, \frac{1}{2}, 0)$. Selected bond lengths (Å) and angles (deg): Cr-Cl = 2.3327(6), Cr-N = 1.6821(18), O-N = 1.200(2), Cr-Cr' = 3.104; Cl-Cr-Cl' = 96.618(19), Cl-Cr-N = 97.92(6), Cr-Cl-Cr' = 83.382(19), Cr-N-O = 171.94(17).

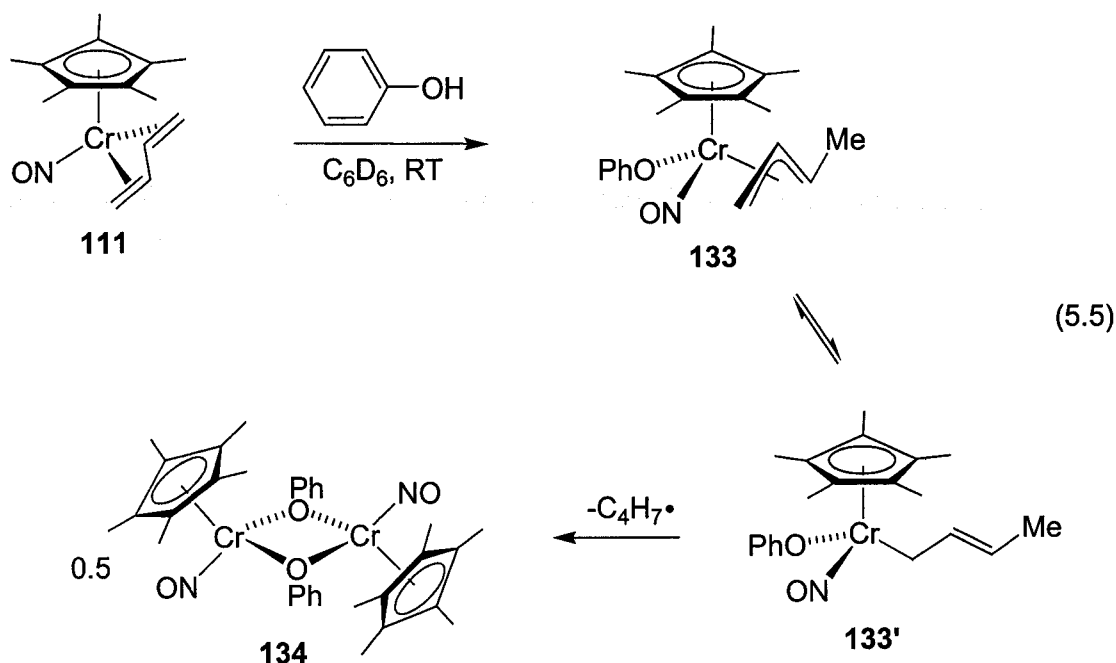
The formation of this dimer is presumably initiated by protonation of *s-trans* butadiene complex **111** to form the desired intermediate species $\text{Cp}^*\text{CrCl}(\text{NO})(\eta^3\text{-C}_4\text{H}_7)$ **131**. This complex is apparently thermally sensitive, decomposing upon warming into

dimeric complex **132** via a proposed Cr-allyl homolytic bond scission of the η^1 -crotyl intermediate **131'** (eq. 5.4). Indeed, monitoring this reaction by ^1H NMR spectroscopy in CD_2Cl_2 reveals that upon addition of HCl (4.0 M in dioxane) the starting complex **111** is quickly replaced by a species with unresolvable broad resonances. After warming to room temperature, however, several terminal vinyl signals emerge between 4.8 and 5.9 ppm that are correlated to a tentatively assigned methyl doublet at 1.64 ppm ($J = 4.69$ Hz). Hence, this unidentified volatile organic compound likely results from the coupling of crotyl radicals originating from the homolytic decomposition of intermediate species **131**.

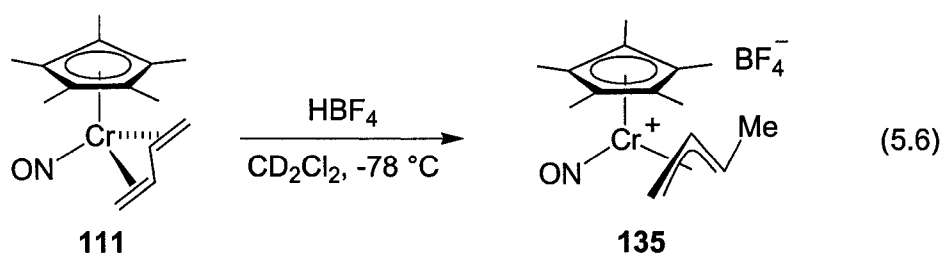


Addition of the more weakly acidic phenol ($\text{pK}_a \sim 10$) to the *s-trans* butadiene complex **111** unfortunately also provides discouraging results. The reaction occurs slowly over two days at room temperature in benzene- d_6 , providing a dark brown reaction mixture. ^1H NMR analysis of the product mixture reveals broad signals indicative of the

formation of paramagnetic products, as well as olefinic and methyl resonances similar to those of the organic product formed in equation 5.5. The identity of the paramagnetic organometallic product could not be determined, but is likely that of the phenoxy-bridged dimer **134**, similarly formed via the putative intermediate species **133** (eq. 5.6). Indeed, alkoxy bridged chromium(I) nitrosyl complexes are known.³¹

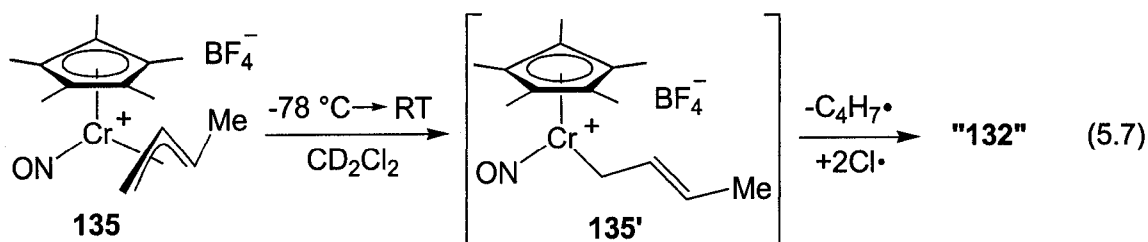


If the halo- and oxyacids indeed protonate diene complex **111** to generate a neutral 18-electron η^3 -crotyl intermediate (e.g., **131** or **133**), replacement of these acids with HBF_4 could provide the unsaturated cationic 16-electron η^3 -crotyl complex **135** (i.e., one of the Type I targets). Thus, the addition of ethereal tetrafluoroboric acid to a solution of complex **111** in deuterated dichloromethane at -78°C immediately elicits a colour change from orange to red. Variable temperature NMR analysis suggests that at -80°C the red species is indeed the desired cationic chromium(II) η^3 -crotyl nitrosyl complex **135** (eq. 5.6).



The low temperature ^1H NMR spectrum of this red product reveals distinct, albeit broad, signals for the central allyl proton at 6.05 ppm, the terminal protons at 4.88, 3.32, and 1.66 ppm, the methyl group at 1.64 ppm, and the Cp^* ligand at 1.72 ppm. The homonuclear COSY NMR spectrum corroborates these assignments by revealing strong correlations between the central and terminal protons as well as a weak interaction between the central and methyl protons. Moreover, the ^{13}C APT NMR spectrum clearly shows peaks for only one methylene group, two methine carbons, and one methyl group. The heteronuclear HMQC NMR spectrum confirms these assignments by revealing the expected ^1H - ^{13}C correlations.

Unfortunately, this intriguing complex suffers from severe thermal instability, quickly decomposing into a green solution above $-30\text{ }^\circ\text{C}$. Presumably, this decomposition entails equilibration to the σ -crotyl intermediate **135'** and homolytic cleavage of the unstable chromium-carbon bond (eq. 5.7). Accordingly, a volatile organic compound with ^1H NMR spectroscopic signatures identical to the organic compound formed in equation 5.4 was also detected in this green solution. The identity of the complementary organometallic product could not be determined, but is likely to be that of the previously observed chromium(I) nitrosyl species **132**, the chloride ligands arising from abstraction of the solvent.



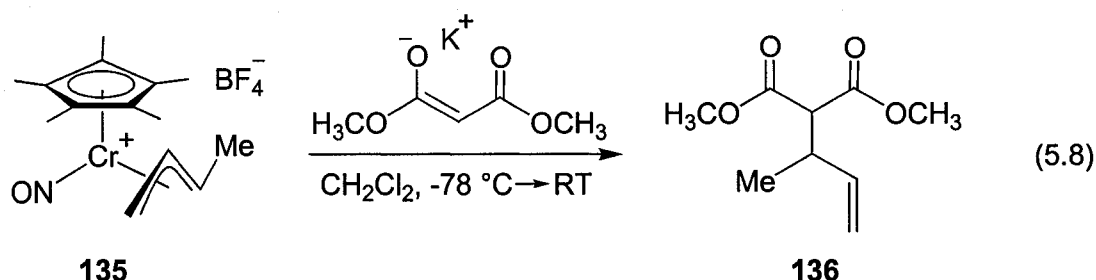
Altering the solvent conditions unfortunately does not improve the outcome of this reaction. Protonation of diene complex **111** with HBF_4 in diethyl ether or DME, for example, does not effect any colour change and only unreacted starting material is recovered. Reactions in THF lead only to decomposition and polymerization of the solvent after warming to room temperature.

Addition of HBF_4 to the *s-trans*-(2,3-dimethylbutadiene) complex **113** also affords a red solution at $-78\text{ }^\circ\text{C}$. VT NMR studies of this reaction, however, reveal that the presumed cationic η^3 -(1,1,2-trimethylallyl) species is much less stable than the parent η^3 -crotyl complex **135**; detailed spectroscopic characterization of this complex could not be performed due to rapid product decomposition, even at $-80\text{ }^\circ\text{C}$.

Despite the thermal instability of cationic η^3 -crotyl complex **135**, we were curious to evaluate the reactivity of this species in the presence of neutral or anionic ligands. Addition of potential dative ligands such as triphenylphosphine or IMes to complex **135**, unfortunately, leads only to the regeneration of *s-trans* diene complex **111** and the corresponding protonated salts of the potential ligand, clearly indicative of undesirable acid-base chemistry. Unsurprisingly, addition of NaI or Bu_4NCl to dichloromethane solutions of complex **135** leads only to intractable products.

Nucleophilic addition to the unsaturated η^3 -crotyl complex **135** was also investigated. Treatment of a freshly prepared solution of complex **135** in

dichloromethane at $-78\text{ }^{\circ}\text{C}$ with potassium dimethylmalonate, for example, affords a brown reaction mixture upon warming to room temperature. NMR analysis of this crude sample suggests that the nucleophile adds to the more hindered carbon of the crotyl moiety to form the organic product **136**, as determined by spectroscopic comparison to authentic material.³² Regrettably, the fate of the organometallic product remains unknown and there is no evidence for even transient formation of the desired chromacyclobutane species (eq. 5.8).

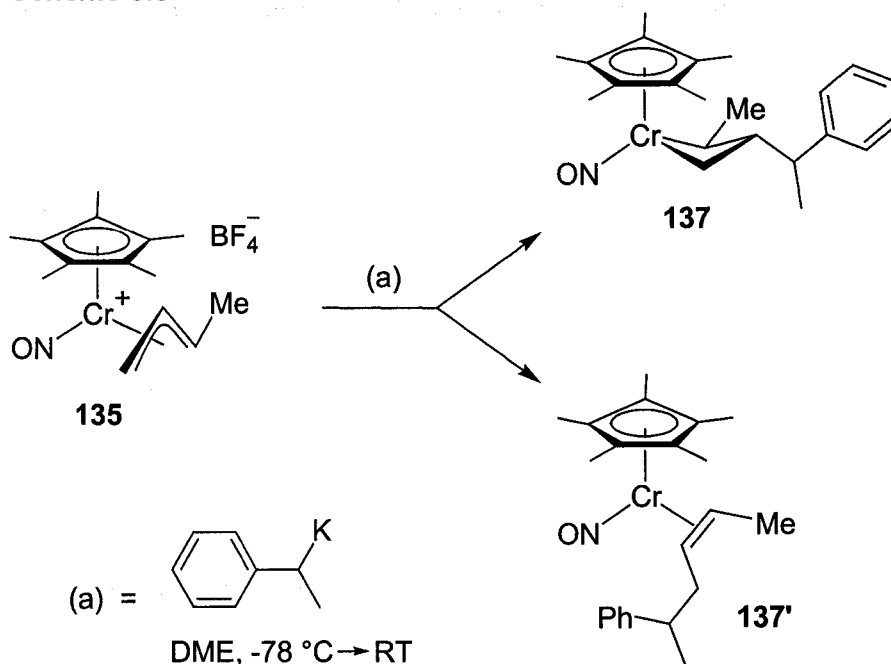


Addition of the benzylic potassium salt of ethylbenzene to diene complex **111** required more belaboured reaction conditions than the addition of malonate anion. Since this nucleophile is highly reactive toward halogenated solvents, the addition was conducted in DME. Prior to this, however, complex **135** must be generated in dichloromethane, the solvent then slowly removed at $-78\text{ }^{\circ}\text{C}$ under high vacuum ($\sim 10^{-5}$ torr), and the red residue finally re-dissolved in DME chilled to $-78\text{ }^{\circ}\text{C}$. Subsequent addition of the nucleophile to complex **135** and warming to room temperature provides a brown residue.

The ¹H NMR spectrum of this residue reveals new aromatic resonances between 6.89 and 7.12 ppm, and a broad singlet at 1.55 ppm, tentatively assigned to a new Cp*

ligand. More interesting, however, is a 1 : 1 ratio of two independent doublet of quartets at 2.75 ($J \approx 9.3, 4.7$ Hz) and 2.67 ($J \approx 8.2, 4.1$ Hz) ppm, which are respectively coupled to methyl doublets at 1.15 ($J \approx 7.0$ Hz) and 1.00 ($J \approx 6.5$ Hz). The discrepancy in the mutual coupling constants within these spin systems may be an artifact of low purity of the reaction residue and the resulting low resolution of the NMR spectrum. Nonetheless, these data suggest two possible structural types for this reaction product (Scheme 5.5).

Scheme 5.5



Both the chromacyclobutane complex **137** and the *cis* η^2 -alkene species **137'** could give rise to new aromatic resonances as well as two mutually exclusive doublets of quartets. Unfortunately, however, no evidence for the other three protons of these potential products could be found; there is considerable overlap of numerous multiplets in

the vicinity of the Cp* signal, but none of the associated protons reveal correlations with either of the doublet of quartets. Regrettably, numerous attempts to improve the yield and purity of these tantalizing complexes have, so far, been unsuccessful.

Although the cationic η^3 -crotyl species **135** may yet prove to be amenable to chromacyclobutane formation, we also investigated potential insertion reactions with this unsaturated complex. The introduction of excess carbon monoxide or a stoichiometric amount of 2,6-dimethylphenyl isonitrile to complex **135** in CD₂Cl₂ at –80 °C, for example, provides spectroscopic evidence that reaction does indeed occur. Regrettably, ¹H NMR spectra of the final reaction mixture at room temperature reveal considerably broad signals and no evidence for permethylcyclopentadienyl-bearing products. Addition of 2-butyne to complex **135** also fails to afford NMR-observable products.

5.3.2 Protonation reactions of Cp'CrNO(CO)(η^2 -1,3-diene) complexes

While exploring the reaction of various acids with *s-trans* butadiene complex **111**, we also investigated the corresponding reactivity of CpCrNO(CO)(η^2 -1,3-diene) complexes. As illustrated by Method F in eq. 4.3 (p. 98), protonation of complex **101** with haloacids should provide the neutral CpCr(NO)(η^3 -allyl)X **Ib** complexes. However, given the results discussed above, the products of such protonation reactions were not expected to be stable. Indeed the addition of a solution of HCl in dioxane to a freshly prepared mixture of CpCrNO(CO)(η^2 -butadiene) complex **101** and CpCrNO(*s-trans*-butadiene) **106** in diethyl ether at –78 °C provides a yellow solution, which presumably is comprised of CpCrCl(NO)(η^3 -crotyl) **132'**, that produces a green paramagnetic product upon warming to room temperatures. To avoid the deleterious effects of the inner sphere

halide ligand, we investigated the addition of tetrafluoroboric acid to complex **101**, which was expected to provide cationic carbonyl nitrosyl η^3 -allyl complexes (*i.e.*, Type **Ia**).

Treatment of a mixture of the η^2 - and η^4 -butadiene complexes **101** and **106** with HBF_4 in diethyl ether at -78°C provides a dark green precipitate that remains unchanged at room temperature. ^1H NMR analysis of this crude reaction product in acetone- d_6 reveals signals that clearly indicate the formation of the expected cationic η^3 -crotyl complex **138** (Fig. 5.5), the assignment of which is further supported by the appearance of CO and NO infrared stretching frequencies at 2066 and 1744 cm^{-1} , respectively. This product is obtained as a 1 : 1.5 : 5 : 22 mixture of four distinct diastereoisomers (a-d, Fig. 5.5), as determined by relative integration of the respective methyl doublets at $\delta 2.49$ ($J = 6.4\text{ Hz}$), 2.40 ($J = 6.4\text{ Hz}$), 2.32 ($J = 6.4\text{ Hz}$), and 2.58 ($J = 6.8\text{ Hz}$). Complete spectroscopic characterization could only be obtained for the two major isomers of complex **138** (Table 5.2). An intriguing aspect of these spectra is the near-perfect agreement between the corresponding ^1H NMR data of the tentatively assigned isomers of η^3 -crotyl complex **80**, obtained by the addition of NOPF_6 to $\text{CpCr(CO)}_2(\eta^3\text{-crotyl})$ **69** in a sealed system (eq. 3.2, p. 75).

Unfortunately, calculation of the yield of this reaction is impeded by the presence of an unidentified paramagnetic blue product, formed along with complex **138**, which cannot be fully separated from the desired product. This paramagnetic impurity also prevented the assignment of ligand orientation (*i.e.*, *endo* vs. *exo*) by NOE spectroscopy.

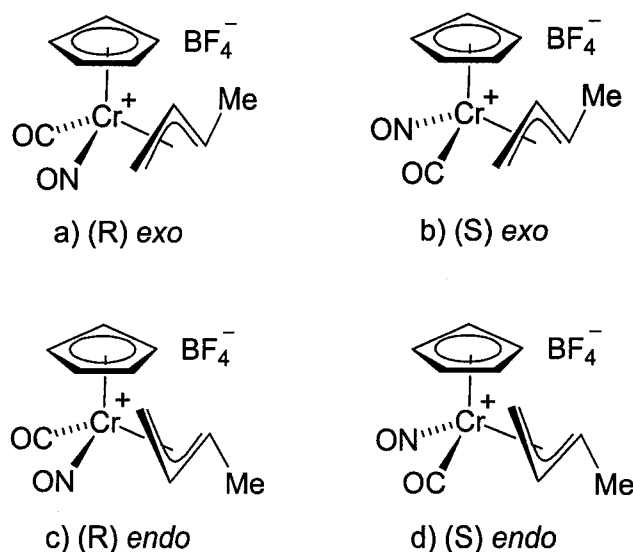


Figure 5.5: Tentatively assigned configurations of the four observed diastereoisomers of cationic η^3 -crotyl complex **138**.

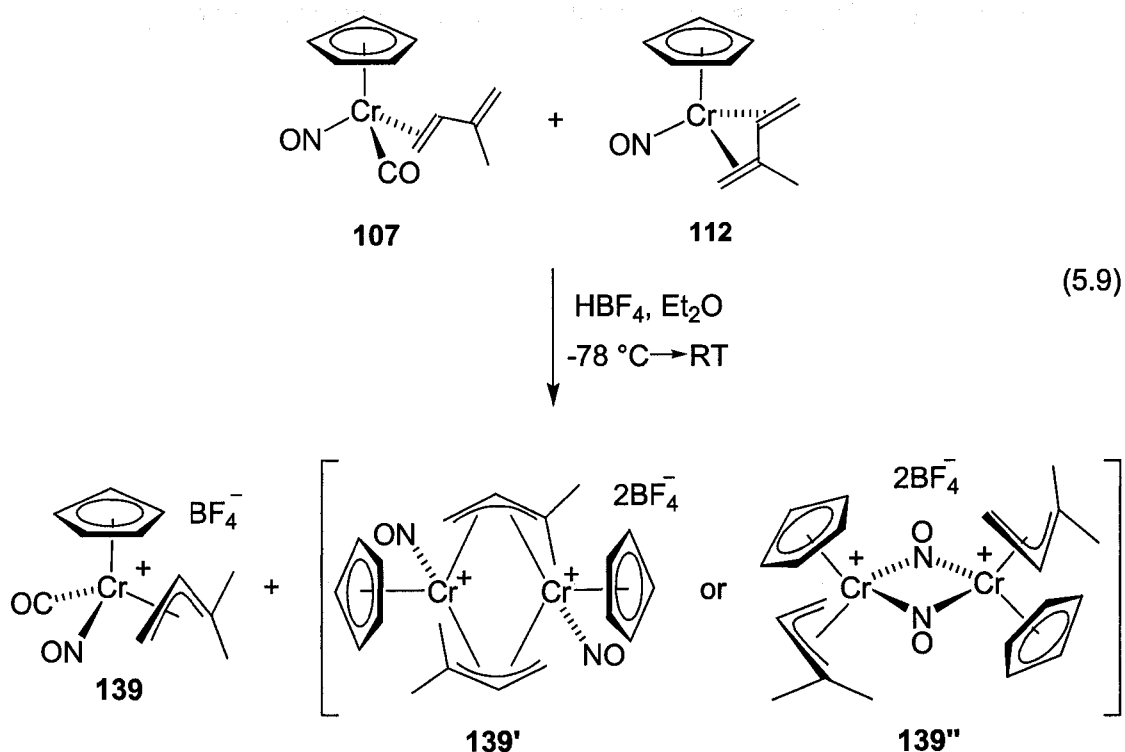
In contrast to the impure deep green solid obtained from the above reaction, addition of HBF_4 to a freshly prepared mixture of η^2 - and η^4 -isoprene complexes **102** and **107** in diethyl ether at -78°C affords a thermally stable orange, rather than deep green, powder. Spectroscopic and elemental analyses indicate that the product is indeed the η^3 -(1,1-dimethylallyl) complex **139** (eq. 5.9, Table 5.2), obtained in pure form but in 12% yield. Efforts to improve this yield met with little success. Although complex **139** also incorporates a stereogenic chromium centre, only one, as yet undetermined, diastereomer is present in solution.

A second product was also isolated from this protonation reaction. NMR analysis of this impure green material (Table 5.2) reveals ^1H resonances and coupling constants very similar to that of η^3 -(1,1-dimethylallyl) complex **139**, which is also present in this sample as a minor component. This may thus be a diastereomer of complex **139**. IR

spectroscopy, however, reveals two equal intensity nitrosyl absorptions at 1685 and 1657 cm^{-1} , with no evidence of a carbonyl ligand outside of that of the minor compound.

Given that the orange η^3 -(1,1-dimethylallyl) complex **139** arises from protonation of the η^2 -isoprene complex **107**, it is reasonable to propose that this green product arises from protonation of the η^4 -isoprene complex **112** present in the starting mixture, giving the novel dimeric allyl bridged complex **139'** or the nitrosyl bridged analogue **139''** (eq. 5.9).

These tentatively assigned structures unfortunately cannot be isolated in pure form.



An attempt to extend this reactivity to the cyclic η^2 -(1,3-diene) complexes **114**-**116** was not successful. The most frustrating aspect of this chemistry was avoiding acid-promoted oligomerization of residual unreacted diene. Removal of this high boiling fraction requires prolonged exposure to high vacuum. Unfortunately, the η^2 -diene

products are not stable under these conditions. Thus, the addition of HBF_4 to cyclic η^2 -diene complexes **114-116** in diethyl ether at -78°C , leads only to intractable product mixtures; no evidence for the desired endocyclic η^3 -allyl cations could be obtained.

Table 5.2: ^1H NMR (ppm) and IR (cm^{-1}) data of cationic η^3 -allyl complexes **138** and **139**. Coupling constants (J) are in Hertz (Hz).

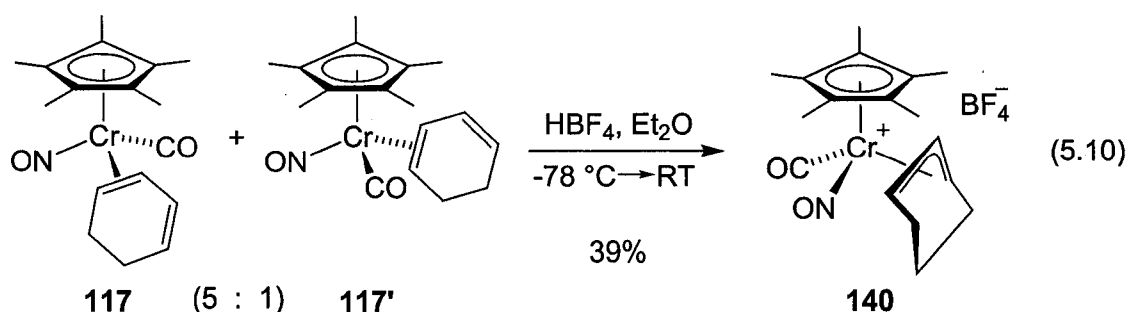
Complex	Cp	$\text{H}_{\text{central}}$	H_{anti}	H_{syn}	CH_3	ν_{CO}	ν_{NO}
1 st η^3 -crotyl, 138 ^a	5.96	5.35 (ddd, $J = 13.6, 12.8, 7.2$)	4.80 (dq, $J = 13.6, 6.8$); 2.81 (br d, $J = 12.8$)	4.37 (br d, $J = 7.2$)	2.58 (d, $J = 6.8$)	2066	1744
2 nd η^3 -crotyl, 138 ^a	6.04	5.11 (ddd, $J = 13.6, 13.2, 7.2$)	4.12 (dq, $J = 13.2, 6.4$); 3.46 (d, $J = 13.6$)	5.41 (d, $J = 7.2$)	2.32 (d, $J = 6.4$)	2066	1744
η^3 -(1,1-dimethylallyl), 139 ^b	5.69	4.85 (ddt, $J = 13.2, 7.8, 0.6$)	2.67 (dd, $J = 13.2, 3.0$)	3.90 (dd, $J = 7.8, 3.0$)	2.55 (d, $J = 0.6$); 1.58 (d, $J = 0.6$)	2066	1738
μ - η^3 -(1,1-dimethylallyl), 139 ^b	6.01	4.68 (dd, $J = 13.5, 7.2$)	3.91 (br d, $J = 13.5$)	5.46 (br d, $J = 7.2$)	2.54; 1.72	N/A	1685, 1657

^aRecorded in acetone- d_6 . ^bRecorded in acetonitrile- d_3 .

Protonation of an isomeric mixture of $\text{Cp}^*\text{CrNO}(\text{CO})(\eta^2\text{-1,3-cyclohexadiene})$ complex **117** with ethereal HBF_4 , fortunately, leads exclusively to the cationic η^3 -cyclohexenyl product **140**, isolated in 39% yield and present as a single isomer in solution (eq. 5.10). Infrared analysis of this complex reveals strong carbonyl and nitrosyl absorptions

at 2020 and 1727 cm^{-1} , while the ^1H NMR spectrum depicts resonances for all nine η^3 -cyclohexenyl protons, in contrast to the five signals observed for the more symmetric neutral $\text{CpCr}(\text{CO})_2(\eta^3\text{-cyclohexenyl})$ complex **72** (Chapter 2).

Unfortunately, given the low yield of the starting η^2 -diene complex **117**, the overall yield of η^3 -cyclohexenyl complex **140** cannot be increased to more than 13%. Two-dimensional NMR analysis was not possible given the amount of complex **140** available. Nonetheless, the structure of this product was confirmed in the solid-state via X-ray crystallography (Fig. 5.6).



Given the relative success of this reaction, we were curious to determine the outcome from protonation of the η^2 -(2-butyne), -acetylene, and -allyltrimethylsilane complexes **96-98**. Disappointingly, however, the addition of anhydrous HBF_4 to these complexes provides only intractable mixtures. As an aside, the addition of Bu_4NF to η^2 -allylTMS complex **96** fails to provide not only the anticipated anionic η^3 -allyl complex, but any tractable products, and neither decarbonylation of η^3 -allyl complexes **138-140** nor the controlled addition of nucleophiles has, as yet, been realized.

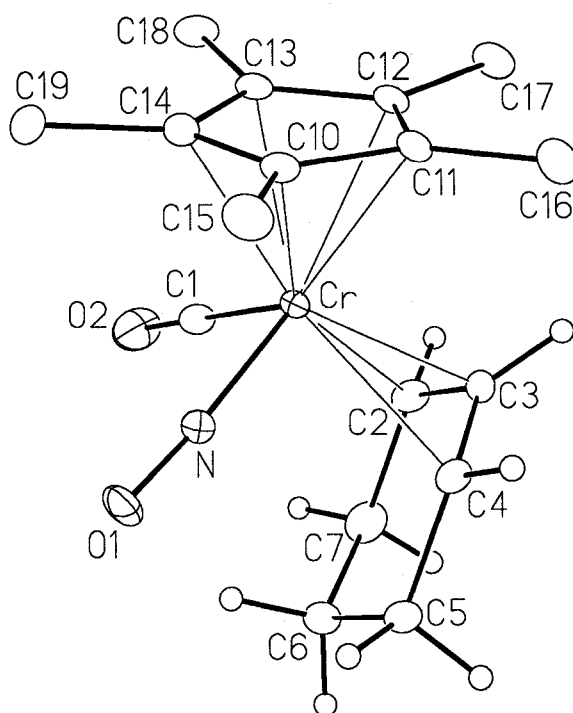
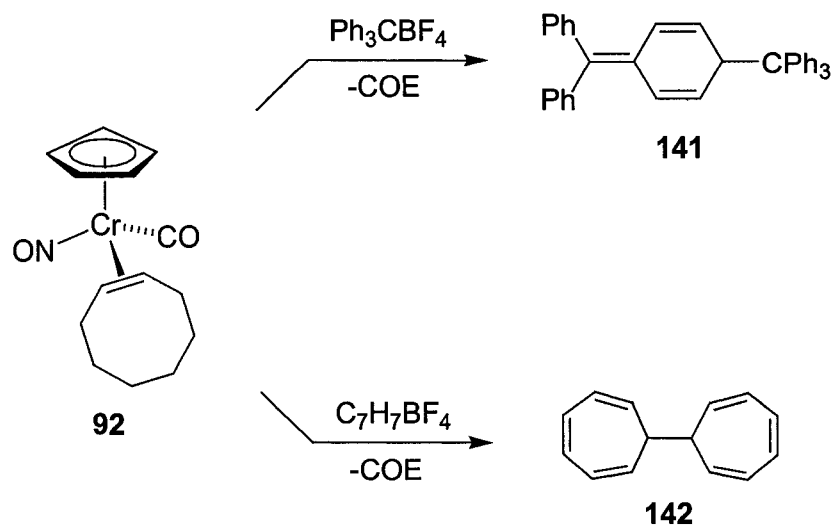


Figure 5.6: The solid-state molecular structure of $(\eta^5\text{-C}_5\text{Me}_5)\text{carbonylnitrosylchromium}(\eta^3\text{-cyclohexenyl})$ tetrafluoroborate complex **140**. Non-hydrogen atoms are represented by Gaussian ellipsoids at the 20% probability level. Hydrogen atoms are shown with arbitrarily small thermal parameters for the cyclohex-1-en-3-yl group, and are not shown for the pentamethylcyclopentadienyl group. Selected bond lengths (Å) and angles (deg): Cr-N = 1.713(3), Cr-C(1) = 1.839(4), Cr-C(2) = 2.325(4), Cr-C(3) = 2.143(3), Cr-C(4) = 2.374(4), O(1)-N = 1.179(4), O(2)-C(1) = 1.151(5), C(2)-C(3) = 1.389(5), C(2)-C(7) = 1.516(6), C(3)-C(4) = 1.391(5), C(4)-C(5) = 1.492(5), C(5)-C(6) = 1.517(6), C(6)-C(7) = 1.531(6); N-Cr-C(1) = 90.56(16), Cr-N-O(1) = 173.7(3), Cr-C(1)-O(2) = 176.9(4), C(2)-C(3)-C(4) = 118.9(3), C(3)-C(4)-C(5) = 121.0(3), C(5)-C(6)-C(7) = 113.7(3), C(2)-C(7)-C(6) = 114.3(3).

5.3.3 One-electron oxidation of Cp'CrNO(CO)(η^2 -alkene) complexes:

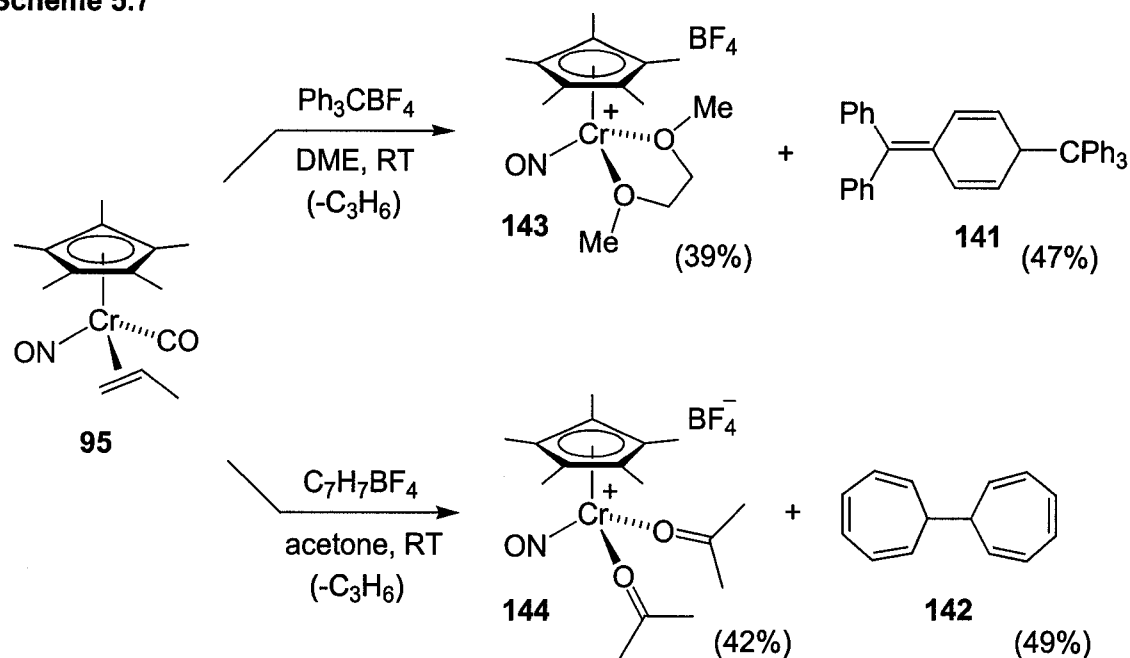
Given that the protonation of several Cp'CrNO(CO)(η^2 -1,3-diene) complexes yields cationic η^3 -allyl complexes of Type **1a**, we were hopeful that the related Cp'CrNO(CO)(η^2 -mono-olefin) complexes could be elaborated into analogous η^3 -allyl complexes by hydride abstraction from the coordinated alkene (recall eq. **4.3**, Method E, p. 98). Surprisingly, however, all attempts to convert the CpCrNO(CO)(η^2 -propene) and (η^2 -cyclooctene) complexes **91** and **92** to η^3 -allyl cationic species via hydride abstraction leads to one-electron rather than two-electron chemistry. Upon treatment with potential hydride abstraction agents such as the trityl or tropylium cation, both the η^2 -cyclooctene and η^2 -propene complexes **91** and **92** are converted to intractable paramagnetic green materials. In accordance with the formation of odd-electron organometallic products, trityl dimer **141** or ditropyl **142**, are also isolated from these reaction mixtures, as determined by electron impact mass spectrometry and spectroscopic comparison to authentic materials.³³ Moreover, as shown for the η^2 -cyclooctene complex **92** (Scheme **5.6**), liberated alkene is observed in the ^1H NMR spectra of the final product mixture. Similar one-electron chemistry is suspected to occur for reactions conducted in acetone, dichloromethane and THF solvents. The strong Lewis acidic character of the unidentified paramagnetic products eventually polymerizes THF over a twelve hour period.

Scheme 5.6



Treatment of the $\text{Cp}^*\text{CrNO}(\text{CO})(\eta^2\text{-propene})$ complex **95** with either Ph_3CBF_4 or $\text{C}_7\text{H}_7\text{BF}_4$ in DME or acetone also affords the respective organic dimers **141** and **142** and a green paramagnetic product. Reactions in THF lead to solvent polymerization, in addition to paramagnetic products. Importantly, treatment of *s-trans* butadiene complex **111** with trityl, tropylium, or ferricinium salts in DME or acetone also affords the same paramagnetic chromium products, as well as free butadiene. Crystals of each of these green paramagnetic products were obtained from the reactions in DME and acetone, respectively, and the structures identified via X-ray crystallography (Scheme 5.7, and Figs. 5.7 and 5.8, respectively).

Scheme 5.7



The 17-electron three-legged piano stool organometallic complex **143**, isolated from reaction conducted in DME, is comprised of a cationic chromium(I) centre chelated by a single DME ligand. Similar to that of the benzyloxy chromium(I) nitrosyl complex **128**, the nitrosyl ligand in complex **143** is also slightly bent ($\text{Cr-N-O}(1) = 166.2^\circ$), perhaps as a result of increased $d \rightarrow \pi^*$ backdonation. The structurally related bis(acetone) adduct **144**, isolated from reactions conducted in acetone, incorporates two acetone ligands in place of the DME ligand; the nitrosyl ligand is similarly slightly bent ($\text{Cr-N-O}(1) = 166.8^\circ$). Upon standing in THF for several hours at room temperature, solutions of either complex leads to the formation of a solid translucent polymer, presumed to be poly(tetrahydrofuran).

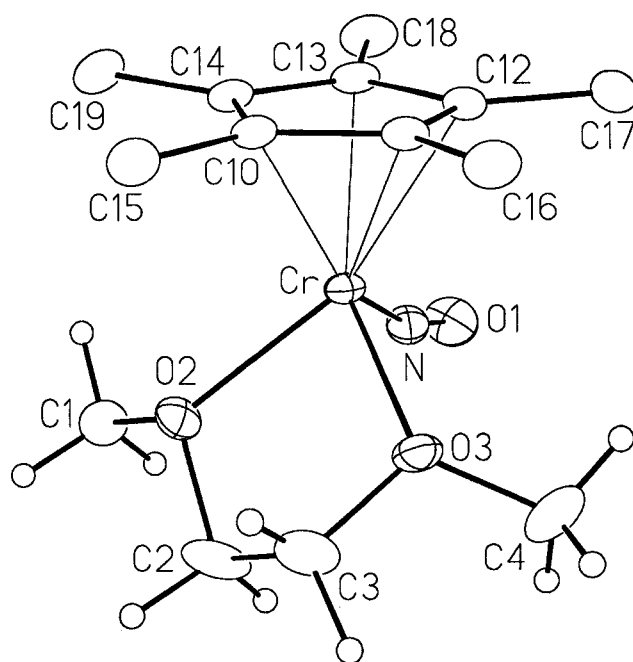


Figure 5.7: The solid-state molecular structure of the $(\eta^5\text{-C}_5\text{Me}_5)\text{Cr}(\text{NO})(\kappa^2\text{-1,2-dimethoxyethane})$ tetrafluoroborate complex **143**. Non-hydrogen atoms are represented by Gaussian ellipsoids at the 20% probability level. Hydrogen atoms are shown with arbitrarily small thermal parameters for the 1,2-dimethoxyethane ligand; hydrogens of the pentamethylcyclopentadienyl group are not shown. Selected bond lengths (Å) and angles (deg): C-O(2) = 2.067(2), Cr-O(3) = 2.059(2), Cr-N = 1.683(3), O(1)-N = 1.200(4), O(2)-C(2) = 1.467(4), C(2)-C(3) = 1.433(6); O(2)-Cr-O(3) = 79.20(9), O(2)-Cr-N = 100.98(11), Cr-N-O(1) = 166.2(3), O(2)-C(2)-C(3) = 107.2(3), O(3)-C(3)-C(2) = 109.8(3), O(2)-C(2)-C(3)-O(3) = 51.6(5).

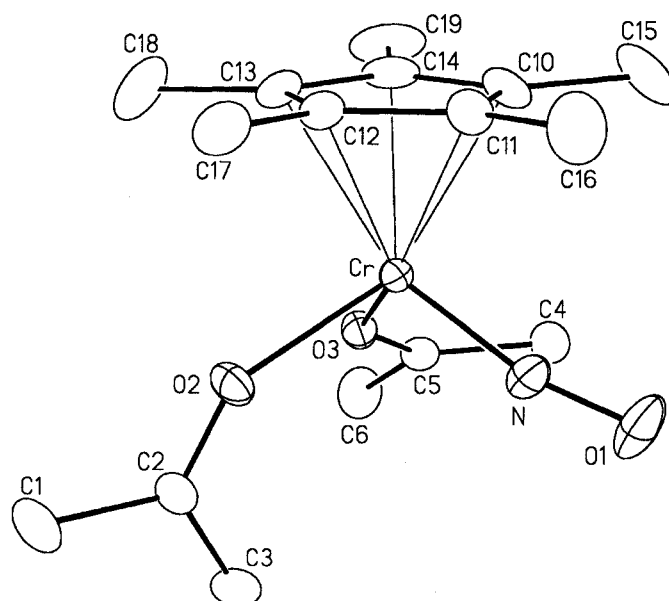


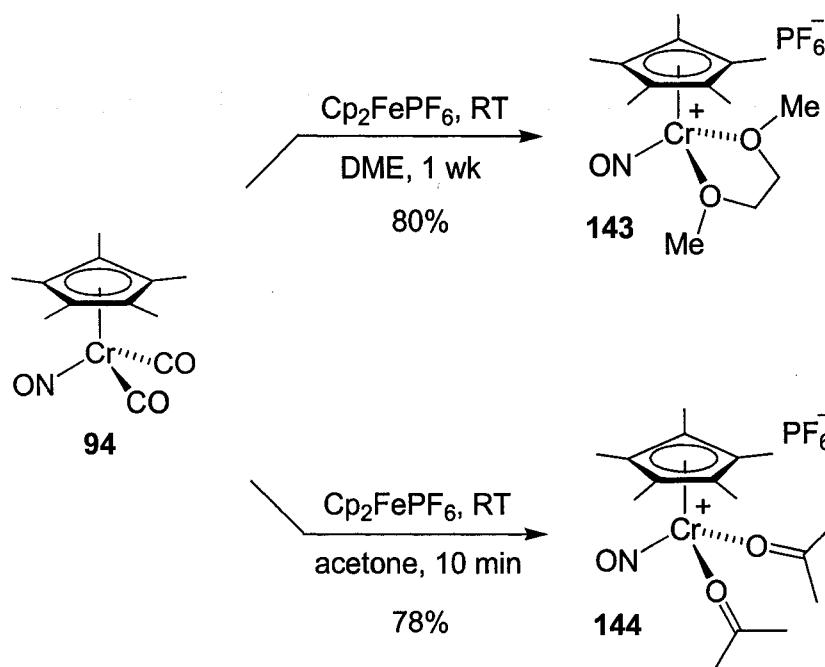
Figure 5.8: The solid-state molecular structure of the $(\eta^5\text{-C}_5\text{Me}_5)\text{Cr}(\text{NO})$ -bis(acetone) tetrafluoroborate complex **144**. Non-hydrogen atoms are represented by Gaussian ellipsoids at the 20% probability level. Hydrogen atoms are not shown. Selected bond lengths (Å) and angles (deg): Cr-O(2) = 2.0147(14), Cr-O(3) = 2.0159(14), Cr-N = 1.6837(19), O(1)-N = 1.201(3), O(2)-C(2) = 1.228(3), O(3)-C(5) = 1.232(2); O(2)-Cr-O(3) = 88.22(6), Cr-N-O(1) = 166.8(2), O(2)-C(2)-O(1) = 119.0(2), O(3)-C(5)-C(6) = 118.6(2).

Complexes **143** and **144** are the first members of a new class of paramagnetic dative oxygen-donor chromium nitrosyl complexes. The related paramagnetic nitrogen-donor complexes have been previously reported.³⁴⁻³⁶ Investigation of the reactivity of donor complexes is discussed in Chapter 6.

The PF_6^- analogues of O-donor complexes **143** and **144** are prepared in high yield by adapting the synthetic method used for the preparation of the related N-donor complexes (Scheme 5.8). Thus, stirring a mixture of ferricinium hexafluorophosphate

and $\text{Cp}^*\text{CrNO}(\text{CO})_2$ **94** in DME for one week affords complex **143** in 80% yield after filtration and removal of solvent. Similar treatment of complex **94** in acetone forms complex **144** in comparable yield, but in far less time (10 min). The markedly shorter reaction time is attributed to the far greater solubility of Cp_2FePF_6 in acetone than in DME.

Scheme 5.8

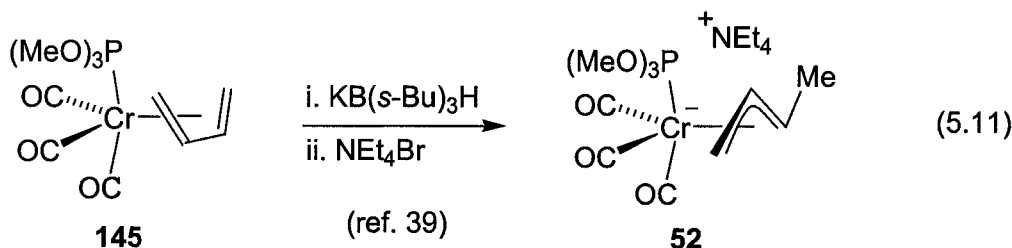


5.4 Addition of tin reagents to $\text{Cp}^*\text{CrNO}(\text{s-trans-butadiene})$

5.4.1 Formation of unique η^3 -crotyl chromium-tin complexes via tin-hydride addition

Wink and co-workers^{37, 38} have shown that hydride addition from K-Selectride™ [$\text{KB}(\text{sec-butyl})_3\text{H}$] to $\text{Cr}(\text{CO})_3(\text{P}(\text{OR})_3)(\text{s-cis-butadiene})$ **145** affords the thermally stable anionic η^3 -crotyl species **52** (eq. 5.11). Since the stability of this chromate complex presumably arises from the electron withdrawing ability of the π -acidic carbonyl ligands,

we surmised that the strongly π -acidic nitrosyl ligand of $\text{Cp}^*\text{CrNO}(\text{s-trans-butadiene})$ **111** might also support similar “ate” complex formation.

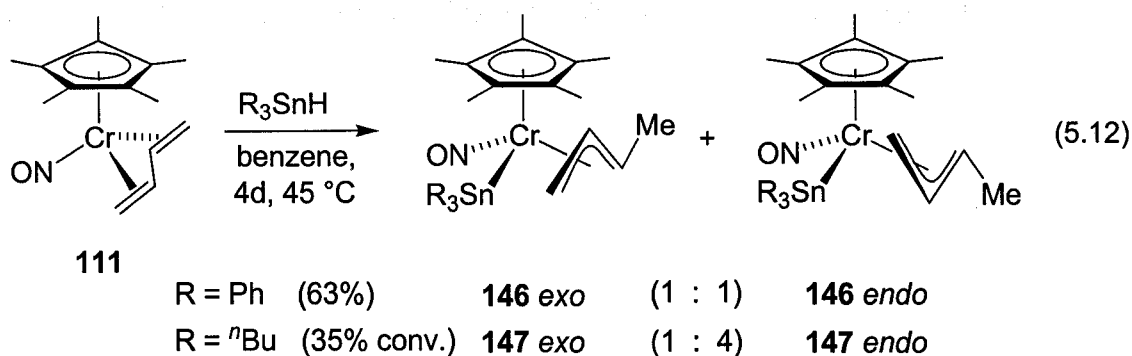


Unfortunately, the addition of K-Selectride or other hydride reagents such as sodium borohydride or Super-Hydride™ (LiEt_3BH) to a solution of complex **111** in benzene- d_6 leads only to rapid degradation of the starting materials. Interestingly, however, this decomposition is not observed upon the addition of triphenyltin hydride (eq. 5.12). After five days at room temperature in benzene- d_6 , ^1H NMR analysis (Table 5.3, entries 1 and 2) reveals approximately 70% conversion to the diamagnetic η^3 -crotyl-containing species **146**, formed as a 1 : 1 mixture of stereoisomers. The relative position of each proton resonance is markedly different for each isomer, with the central proton of one isomer being apparent at 2.19 ppm while that of the second is found at 3.35 ppm. Such differences in chemical shift undoubtedly result from the magnetic anisotropy of the aromatic Cp^* ring and/or the chromium centre, the effects of which are quite pronounced in *endo* and *exo* isomers of η^3 -allyl complexes.³⁹⁻⁴⁴

The rate of this reaction can be somewhat increased by heating the reaction to 45 °C (safely below the 60 °C decomposition point of butadiene complex **111**). In this way, a 100 mg scale reaction of diene complex **111** with Ph_3SnH in benzene is converted

to complex **146** in four days. Purification of the crude product on silica-gel and crystallization from diethyl ether then affords the η^3 -crotyl complex in 63% yield.

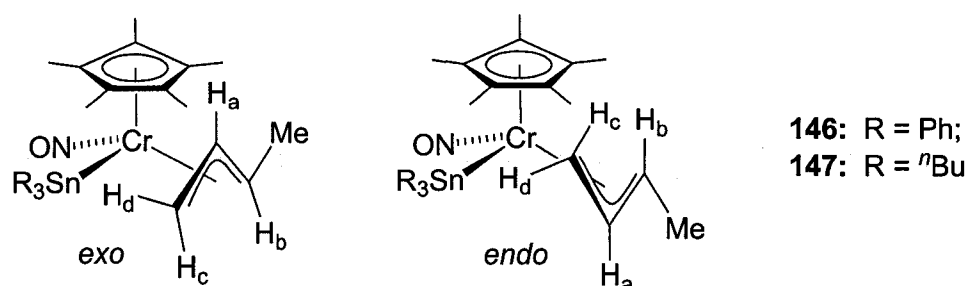
Given the high solubility of this product in benzene and diethyl ether, we anticipated that the adduct must be neutral and incorporate a covalently bound triphenyltin ligand, leading to the assignment of the product as *endo* and *exo* isomers of $\text{Cp}^*\text{CrNO}(\text{SnPh}_3)(\eta^3\text{-crotyl})$ **146** (eq. 5.12). Combustion and mass spectrometric analyses are consistent with the assigned molecular composition.



The presence of the triphenyltin ligand is apparent in the ^1H NMR spectrum of both isomers of complex **146**: tin satellites arising from three- and four-bond tin-hydrogen coupling are observed at the base of several of the η^3 -crotyl ^1H NMR resonances. This level of multinuclear coupling is expected given that both ^{119}Sn and ^{117}Sn isotopes possess a nuclear magnetic spin of $\frac{1}{2}$ and are 8.56% and 7.61% abundant.⁴⁵ Since ^{119}Sn -H coupling constants are typically of greater magnitude than the corresponding ^{117}Sn -H coupling constants,⁴⁵ we had expected to observe discreet doublets arising from proton coupling with each isotope. The observed tin satellites are, however, insufficiently resolved to measure both coupling constants. We therefore report

the tin-proton coupling constant of complex **146** and related complexes (*vide infra*) as an average of both ^{119}Sn and ^{117}Sn proton coupling constants.

Table 5.3: ^1H NMR data (ppm) of the neutral η^3 -crotyl chromium-tin complexes **146** and **147**. Coupling constants (J) are in Hertz (Hz).^a



Entry	Complex	Cp*	H _a	H _b	H _c	H _d	Me
1	146 <i>exo</i>	1.36	2.19 (dt, J = 14.5, 8.5)	4.08 (br dq, J = 7.0, 1.0)	1.56 (br dd, J = 14.5, 3.0)	3.33 (dd, J = 7.0, 3.0)	0.96 (d, J = 7.0), (br d, $J_{\text{Sn-H}} = 15.5$)
2	146 <i>endo</i>	1.42	3.35 (ddd, J = 14.5, 11.0, 7.0)	1.89 (dq, J = 11.0, 6.0)	0.14 (br d, J = 14.5), (br d, $J_{\text{Sn-H}} = 24.0$)	4.29 (dd, J = 7.0, 2.0), (br d, $J_{\text{Sn-H}} = 26.0$)	1.85 (d, J = 6.0)
3	147 <i>exo</i>	<i>b</i>	2.03 (dt, J = 13.9, 8.1)	4.01 (app quint, J = 7.2)	1.41 ^c	2.60 (dd, J = 8.1, 1.8)	1.09 ^c
4	147 <i>endo</i>	1.50	3.35 (m)	1.91 (m)	-0.27 (dd, J = 14.2, 2.7)	3.85 (dd, J = 6.9, 2.7), (br d, $J_{\text{Sn-H}} = 20$)	1.95 (br s)

^aThe aromatic and *n*-butyl proton resonances have been omitted, see the Experimental Procedures section for full spectroscopic details. ^bDue to sample impurities, the Cp* and *n*-butyl proton resonances could not be identified. ^cDetected via homonuclear COSY NMR spectroscopy; obscured by impurities in the 1D ^1H NMR spectrum.

The ambiguity over the orientation of the crotyl ligand was resolved by selective crystallization of what turned out to be the *endo* isomer. X-ray crystallography clearly shows the methyl group and central carbon of the crotyl ligand pointing away from the Cp* ring (Fig. 5.9). Moreover, the bond between the two metal centres (Cr–Sn = 2.67 Å) is clearly evident and consistent with other chromium–tin bond lengths.⁴⁶ The nitrosyl ligand, with an infrared absorption at 1636 cm⁻¹, has a slightly bent geometry (Cr–N–O = 170.8°).

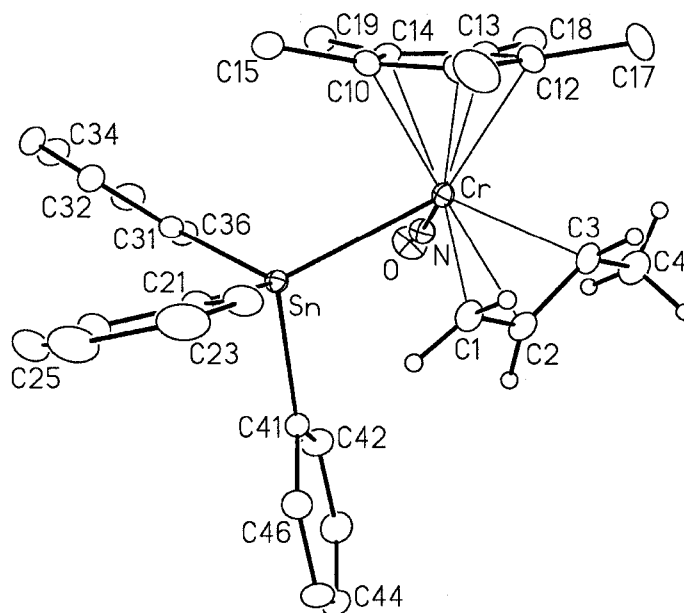


Figure 5.9: The solid-state molecular structure of the *endo* isomer of (η^5 -C₅Me₅)(NO)(Ph₃Sn)Cr(η^3 -crotyl) complex **146**. Non-hydrogen atoms are represented by Gaussian ellipsoids at the 20% probability level. Hydrogen atoms of the crotyl group are shown with arbitrarily small thermal parameters, while phenyl and pentamethylcyclopentadienyl hydrogens are not shown. Selected bond lengths (Å) and angles (deg): Sn–Cr = 2.6755(4), Sn–C(21) = 2.171(3), Cr–N = 1.673(2), Cr–C(1) = 2.282(3), Cr–C(2) = 2.204(3), Cr–C(3) = 2.241(3), O–N = 1.205(3), C(1)–C(2) = 1.383(4), C(2)–C(3) = 1.389(4), C(3)–C(4) = 1.504(5); Cr–Sn–C(21) = 124.27(7), Sn–Cr–N = 81.55(8), Cr–N–O = 170.8(2), C(1)–C(2)–C(3) = 120.5(3), C(2)–C(3)–C(4) = 120.7(3).

As noted for the *endo* and *exo* isomers of $\text{CpCr(CO)}_2(\eta^3\text{-2-methylallyl})$ complex **70** (p. 57), there appears to be no interconversion between the related isomers of complex **146**. ^1H NMR analysis of a sample containing the pure *endo* isomer does not provide visible evidence for conversion to the *exo* isomer, even upon heating to reflux in toluene. This complex also exhibits remarkable stability toward air for several days in the solid-state and up to twelve hours in solution.

Addition of tributyltin hydride to butadiene complex **111** also affords a chromium-tin η^3 -crotyl adduct, formed as a 4 : 1 mixture of geometrical isomers. The stereochemical assignment of *endo* and *exo* isomers of $\text{Cp}^*\text{CrNO(SnBu}_3)(\eta^3\text{-crotyl)}$ **147** is derived from spectroscopic comparison to the analogous isomers of complex **146** (Table 5.3, entries 3 and 4). Unfortunately, only the *endo* isomer can be clearly identified in the ^1H NMR spectrum of the mixture; isolation of this product in high yield and purity has not been accomplished.

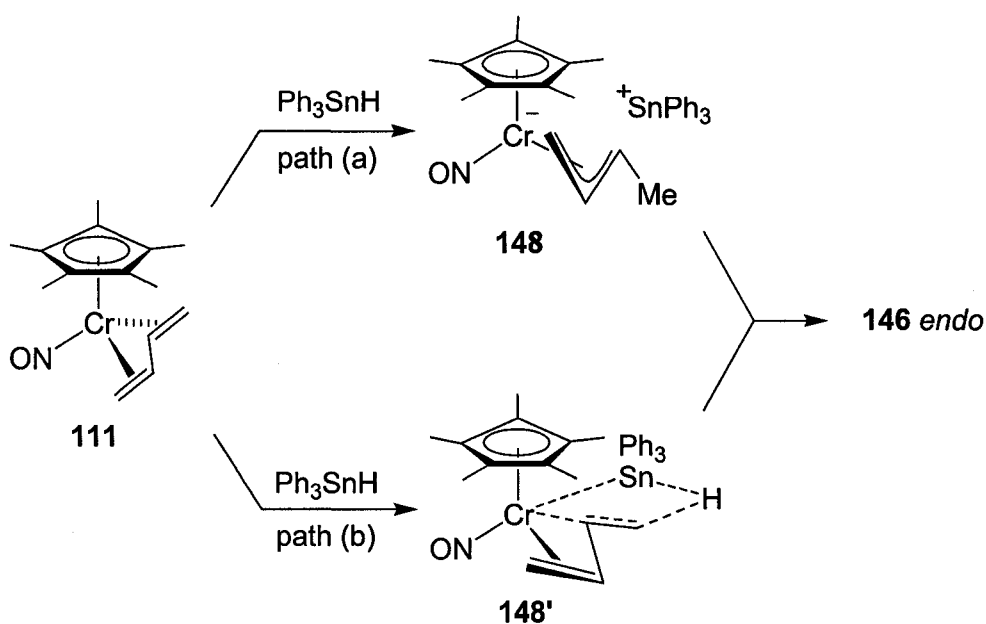
5.4.2 Proposed mechanisms for the formation of the η^3 -crotyl chromium-tin complexes

Although the η^3 -crotyl complex **146** arises from a formal oxidative addition of a Sn-H bond across the chromium-butadiene fragment, the exact mechanism of this transformation remains poorly understood. We have determined, however, that this addition reaction probably does not involve a radical initiation process. The diene to crotyl transformation, for example, occurs at the same rate in the absence of light and is not accelerated upon exposure of the reaction mixture to UV light. Moreover, the addition of radical initiators such as AIBN fails to accelerate the formation of complex **146**, instead leading to the formation of intractable organochromium products. Running

the reaction in THF appears to slightly reduce the reaction time to three days, suggesting a more polar reaction process.

We therefore surmise that, in the case of the structurally characterized *endo* isomer of η^3 -crotyl complex **146**, the hydride addition is triggered by heterolytic hydride transfer from Ph_3SnH to form the transient ionic species **148**, which upon ion association affords the neutral η^3 -crotyl complex **146** (Scheme 5.9, path a). Alternatively, the formation of η^3 -crotyl complex **146** may proceed in a concerted fashion via the five-centred transition state **148'** (Scheme 5.9, path b). Inspection of the crystal structure of the *endo* isomer of complex **146** (Fig. 5.9), however, reveals that the methyl group of the η^3 -crotyl ligand is *trans* to the Ph_3Sn ligand. Since pathway (b) can only provide a kinetic product in which these two ligands are mutually *cis*, this mechanism is unlikely to be involved in the formation of the *endo* isomer of complex **146** unless a subsequent rearrangement ensues. Pathway (a), however, involves a non-coordinated triphenyltin cation which can coordinate *trans* to the more sterically congested substituted position of the η^3 -crotyl ligand.

Scheme 5.9



The tricoordinate organotin(IV) cation, Bu_3Sn^+ , is known to be moderately stable at room temperature in the presence of non-coordinating counterions and donor solvents,⁴⁷ while treatment of Ph_3SnH with $\text{B}(\text{C}_6\text{F}_5)_3$ is reported to provide the thermally stable hydride reagent $[\text{Ph}_3\text{Sn}][\text{HB}(\text{C}_6\text{F}_5)_3]$.⁴⁸ Although neither of these R_3Sn^+ moieties exist as ‘pure’ tetravalent stannyl cations, these relatively stable species nonetheless provide support for the transient existence of a similar positively charged ion in intermediate complex **148**. Lambert⁴⁹ has recently reported the preparation of $[\text{tris}(2,4,6\text{-triisopropylphenyl})\text{stannyl}][\text{B}(\text{C}_6\text{F}_5)_4]$, the stannyl cation component of which is entirely free of solvent and anion interactions, as determined by X-ray crystallography.

We have also obtained empirical evidence, albeit serendipitously, that also supports the existence of the triphenyltin cation in intermediate species **148**. For instance, in one of the recrystallized samples of the *endo* isomer of η^3 -crotyl complex

146, a trace amount of green crystals was found. X-ray crystallography of this minor impurity revealed the structure of a peculiar dimeric chromium(I) complex $[\text{Cp}^*\text{Cr}(\text{NO})(\mu\text{-O})(\mu\text{-OH})(\text{SnPh}_2)_2]_2$ **149** (Fig. 5.10).

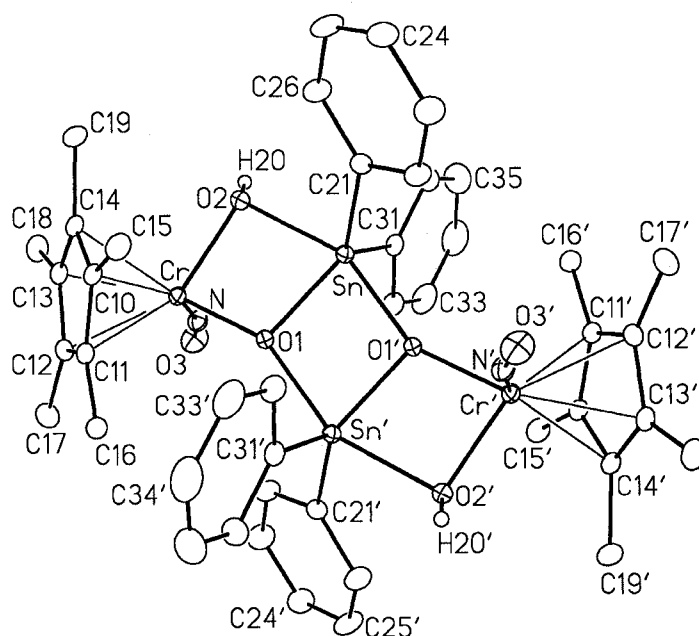


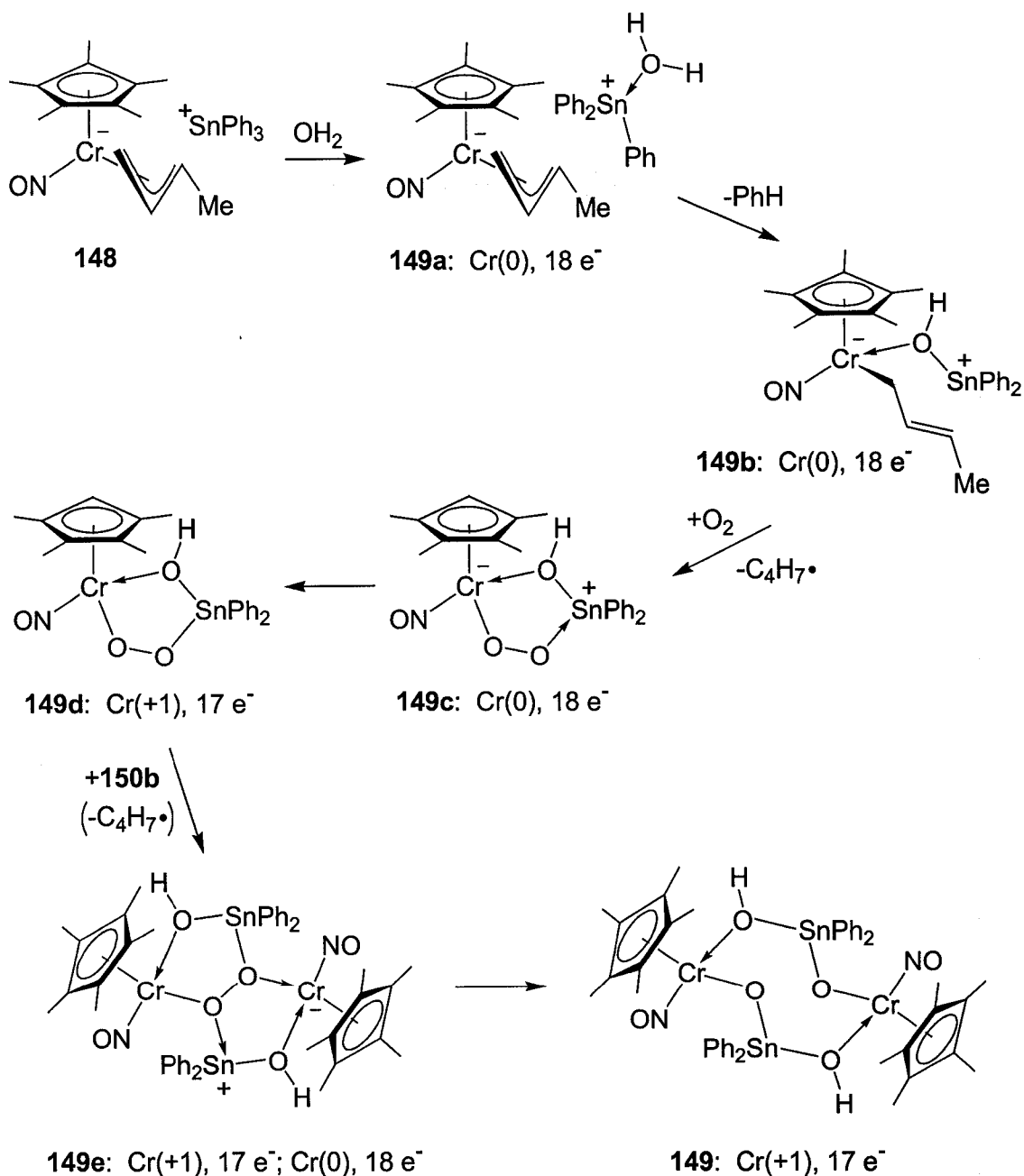
Figure 5.10: The solid-state molecular structure of $[(\eta^5\text{-C}_5\text{Me}_5)\text{Cr}(\text{NO})(\mu\text{-O})(\mu\text{-OH})(\text{SnPh}_2)_2]_2$ **149**. Non-hydrogen atoms are represented by Gaussian ellipsoids at the 20% probability level. Hydroxyl hydrogen atoms are shown with arbitrarily small thermal parameters; all other hydrogens are not shown. Selected bond lengths (Å) and angles (deg): Sn-O(1) = 2.0178(15), Sn-O(1') = 2.1044(15), Sn-O(2) = 2.1767(17), Sn-C(21) = 2.128(2), Sn-C(31) = 2.127(2), Cr-O(1) = 2.0137(15), Cr-O(2) = 2.0028(16), Cr-N = 1.690(2), O(3)-N = 1.207(3), O(2)-H2O = 0.78(3), Sn-Sn' = 3.198, O(1)-O(1') = 2.602, Cr-Sn = 3.161; O(1)-Sn-O(1') = 78.26(6), O(1)-Sn-O(2) = 76.11(6), O(1)-Cr-O(2) = 80.26(6), Sn-O(2)-Cr = 98.18(7), Cr-N-O(3) = 165.2(2).

Since we have already established that purified samples of η^3 -crotyl chromium-tin complex **146** are remarkably stable toward air and moisture, this dimeric species must arise from air and water exposure *during* the formation of η^3 -crotyl complex **146**. As shown in Scheme 5.10, we propose that the formation of dimeric complex **149** is initiated by the coordination of a contaminant water molecule to the Ph_3Sn^+ cation of intermediate η^3 -crotyl species **148**, which affords complex **149a**; loss of benzene then leads to a hydroxyldiphenyltin cation. Subsequent dative coordination of this cation to the metal centre then promotes η^3 - to η^1 - isomerization of the η^3 -crotyl ligand, to provide the σ -crotyl species **149b**. Homolytic scission of the thermally unstable Cr-crotyl bond then reduces the metal centre by one-electron. At the same time, reaction of a contaminant oxygen molecule with the chromium centre and coordination to the tin centre provides the 18-electron intermediate **149c**. Internal reorganization of electrons then generates covalent Cr–O and Sn–O bonds, providing the chromacyclic species **149d**. Dative coordination of the bridging peroxo ligand to the chromium and tin centres of another molecule of complex **149b**, with prior or concomitant loss of crotyl radical, then forms the mixed-valent species **149e**. Reorganization of electrons then completely cleaves the O–O linkage to provide the observed neutral chromium(I) dimeric product **149**. We have yet to determine if the addition of one equivalent of oxygenated water to a mixture of butadiene complex **111** and triphenyltin hydride will provide complex **149** in higher yield; however, it is clear that this product can be avoided in reactions run under more rigorously inert and anhydrous conditions.

Although the tetranuclear species $[\text{CpCr}(\mu\text{-O})]_4$ is known,⁵⁰ complex **149** is the first example of a mixed-metal chromium system with bridging 2-electron oxo ligands.

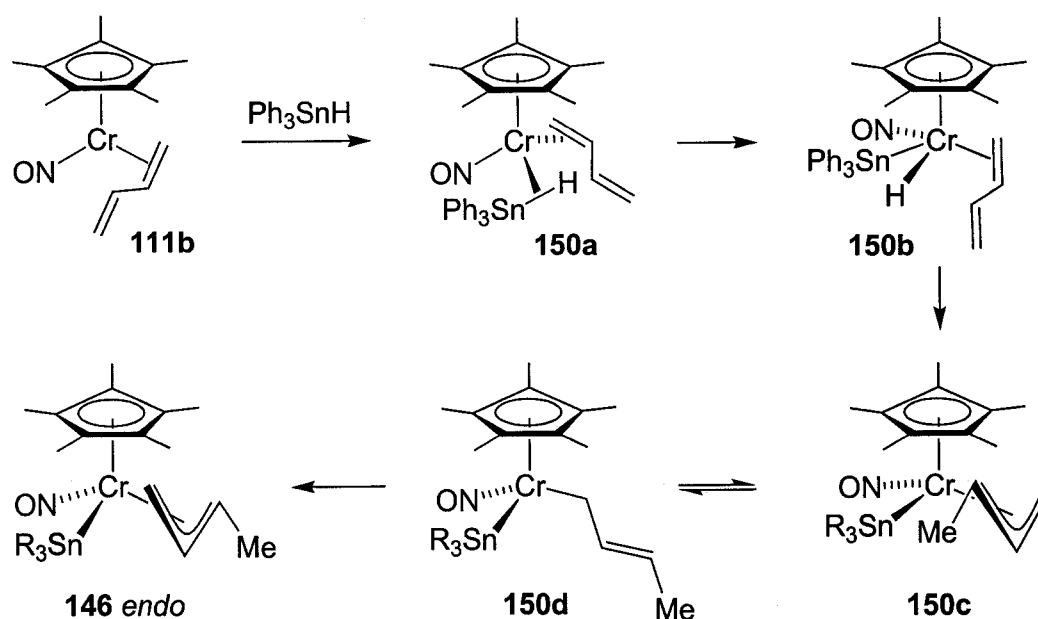
All other oxygen-containing chromium complexes are mononuclear and possess either 4-electron oxo or η^2 -peroxo ligands,⁵¹⁻⁵⁵ providing support for at least the transient existence of peroxo intermediates **149c-149d**.

Scheme 5.10



In addition to the ionic and concerted pathways proposed for the formation of η^3 -crotyl complex **146**, a third mechanism may also be possible (Scheme 5.11). Equilibration of butadiene complex **111** to the unsaturated intermediate **111b** followed by coordination of triphenyltin hydride, for example, would provide the η^2 -(hydrido-stannane) species **150a**. Oxidative addition of the tin-hydride bond and insertion of the diene ligand into the consequent Cr–H bond would then afford the *endo* η^3 -crotyl intermediate **150c**. The more energetically favourable isomer of **146** *endo* is then formed

Scheme 5.11



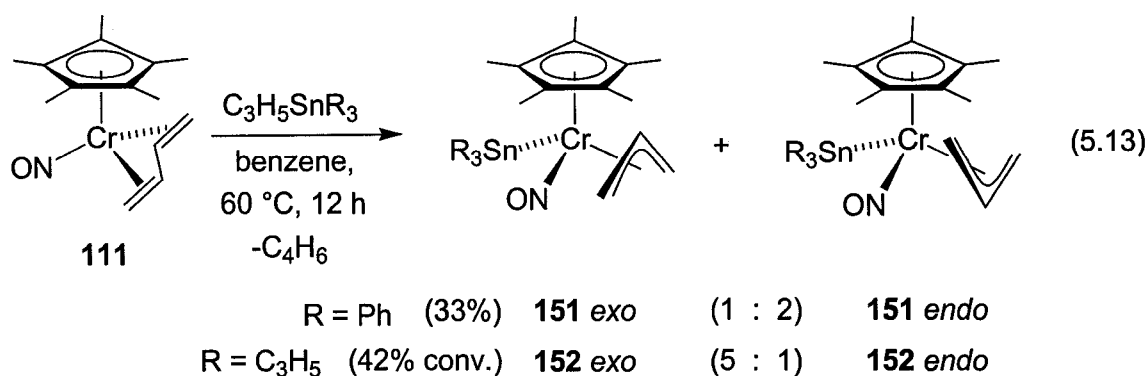
via an $\eta^3 \rightarrow \eta^1 \rightarrow \eta^3$ isomerization of the crotyl ligand, placing the crotyl methyl group *trans* to the triphenyltin ligand.⁵⁶ The η^1 -crotyl intermediate **150d** might also give rise to the *exo* isomer of complex **146** via a 180° rotation of the crotyl ligand followed by η^3 -crotyl coordination.⁵⁶ Interestingly, complexes **150a–150c** are structurally similar to

the proposed intermediates for the previously discussed catalytic hydrosilylation of conjugated dienes (recall Scheme 1.8, p. 23).

The preparation of an unprecedented class of η^3 -allyl chromium(II) complexes has thus been developed. Perhaps more importantly, the methodology itself is also unique: the oxidative addition of tin-hydride bonds across a metal-diene fragment is completely unprecedented. Reactions involving transition metals and tin-hydride reagents typically involve oxidative addition to a metal employed in the catalytic hydrostannylation of unsaturated organic compounds.⁵⁷⁻⁶⁰

5.4.3 Oxidative addition of allyltriphenyltin

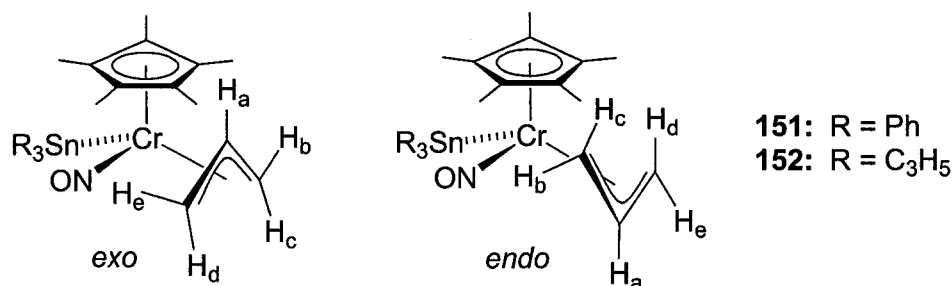
In light of this apparent tendency of Ph_3SnH to react at the butadiene ligand of $\text{Cp}^*\text{CrNO}(\text{s-trans-butadiene})$ **111**, we proposed to investigate the potential for a similar oxidative addition of Sn–C bonds to afford alkyl-substituted η^3 -allyl chromium-tin nitrosyl complexes. As determined by ^1H NMR analysis (Table 5.4, entries 1 and 2), the reaction of butadiene complex **111** with allyltriphenyltin proceeds over three days at room temperature in benzene- d_6 to provide a product bearing both Ph_3Sn and η^3 -allyl ligands. The proton resonances of this reaction mixture, however, reveal an *unsubstituted* η^3 -allyl ligand as well as liberated butadiene. Given the similarity of chemical shifts and the ^1H - ^1H and ^1H -Sn coupling constants of this complex with those of the η^3 -crotyl complex **146**, the structure of this product has been identified as complex **151**, formed as a 2 : 1 mixture of stereoisomers (eq. 5.13). Increasing the temperature of reaction to 60 °C for twelve hours affords complex **151** in 33% yield after silica-gel column chromatography and recrystallization from diethyl ether.



Assignment of the η^3 -allyl ligand configuration of the minor isomer of complex **151** as *exo* was accomplished by TROESY which revealed a strong NOE between the proton resonance of the Cp* ligand at 1.35 ppm and that of the minor isomer central η^3 -allyl proton at 2.37 ppm. This correlation is absent from the TROESY data of the major isomer, which is tentatively assigned to be in the *endo* configuration.

Spectroscopic analysis of the thermolysis of diene complex **111** in the presence of tetraallyltin reveals the formation of Cp*CrNO(η^3 -allyl)[Sn(allyl)₃] **152** as a 5 : 1 mixture of isomers (eq. 5.13). Unfortunately, this product could not be isolated as a pure solid but the yield (42%) was determined by ¹H NMR spectroscopy. Nonetheless, full spectroscopic characterization of the major isomer of this complex clearly identifies the unsubstituted η^3 -allyl ligand (Table 5.4, entry 3). By a similar analysis, the minor isomer of complex **152** is assigned as the *endo* isomer. Unfortunately, the considerable overlap of proton signals from both the major isomer and unreacted starting material renders spectroscopic characterization of the minor isomer very tentative (Table 5.4, entry 4).

Table 5.4: ^1H NMR data (ppm) of the neutral η^3 -allyl chromium-tin complexes **148**. Coupling constants (J) are in Hertz (Hz).^a



Entry	Complex	Cp*	H _a	H _b	H _c	H _d	H _e
1	151 <i>exo</i>	1.35	2.37 (app tt, $J = 13.6, 7.6$)	4.41 (br d, $J = 6.8$), (br d, $J_{\text{Sn-H}} = 27.2$)	1.82 (br d, $J = 13.6$)	1.41 (br d, $J = 13.6$)	3.12 (br dd, $J = 7.6, 2.4$), (br d, $J_{\text{Sn-H}} = 25.6$)
2	151 <i>endo</i>	1.41	3.54 (dddd, $J = 13.6, 12.0, 7.2, 6.8$)	3.32 (dt, $J = 7.6, 2.4$), (br d, $J_{\text{Sn-H}} = 22.4$)	1.26 (br d, $J = 12.0$)	0.28 (br d, $J = 13.6$)	3.26 (br dd, $J = 7.2, 2.8$), (br d, $J_{\text{Sn-H}} = 20.8$)
3	152 <i>exo</i>	1.36	2.30 ^b	3.07 (br dd $J = 7.2, 1.8$), (br d, $J_{\text{Sn-H}} = 20.0$)	1.73 (br d, $J = 8.1$)	1.18 (br d, $J = 13.2$)	2.67 (br dt, $J = 8.1, 2.1$), (br d, $J_{\text{Sn-H}} = 33.0$)
4	152 <i>endo</i>	1.41	3.56 ^c	4.14 (br dt, $J = 6.6, 5.0$)	1.41 ^c	0.21 (br d, $J = 12.5$)	3.24 (br d, $J = 6.6$ Hz)

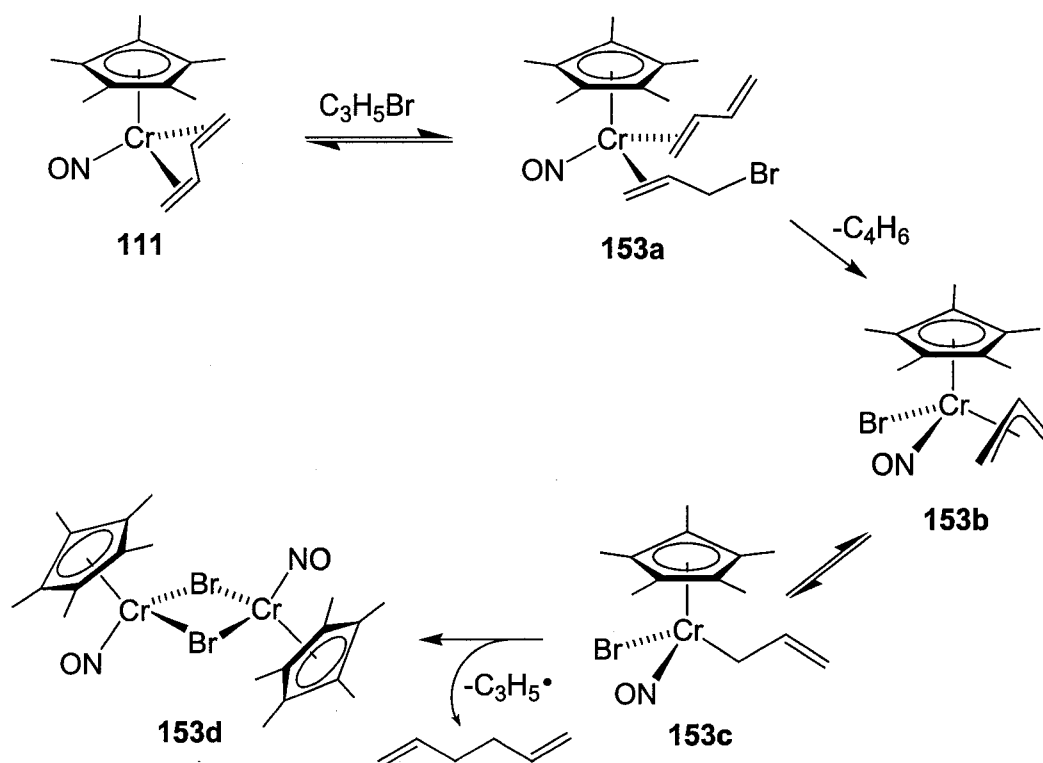
^aThe proton resonances of the tin substituents have been omitted, see the Experimental Section for full spectroscopic details. ^bDetected via homonuclear COSY NMR spectroscopy; obscured by other product signals in the 1D ^1H NMR spectrum.

It is reasonable to assume that the thermal loss of butadiene or simply η^4 - to η^2 -equilibration provides an unsaturated chromium(0) centre that is capable of oxidative cleavage of the allyl–Sn bond. We therefore explored the reactivity of other compounds

containing polarized bonds toward butadiene complex **111**. Disappointingly, however, addition of 9-BBN, Et₃SiH, (TMS)₃SiH, CHCl₃, (CH₃)₃Cl, or Ph₆Sn₂ to complex **111** in benzene-d₆ fails to effect any reaction, even after ten days at room temperature. A gradual increase in reaction temperature to 80 °C or exposure of the reaction mixture to ultraviolet light leads only to decomposition to intractable products. Hydrogen also fails to react with butadiene complex **111**.

The addition of allyl bromide, however, cleanly provides free butadiene and a second organic compound, identified as 1,5-hexadiene by spectroscopic comparison to authentic material. The identity of the paramagnetic chromium-containing byproduct(s) is unknown. As shown in Scheme 5.12, we propose that the formation of the two organic products is initiated by η^4 - to η^2 - isomerization of the butadiene ligand followed by π -coordination of allyl bromide to form the intermediate species **153a**. Oxidative addition of the η^2 -(allyl bromide) ligand and concomitant loss of butadiene then affords the neutral chromium(II) η^3 -allyl complex **153b**. Isomerization of the allyl ligand to the η^1 -coordination mode then affords the σ -allyl complex **153c**, which undergoes σ -bond homolysis to provide the allyl radical. Although the final organochromium product could not be isolated, it is likely to be the paramagnetic chromium(I) dimer [Cp*Cr(NO)Br]₂ **153d**.

Scheme 5.12



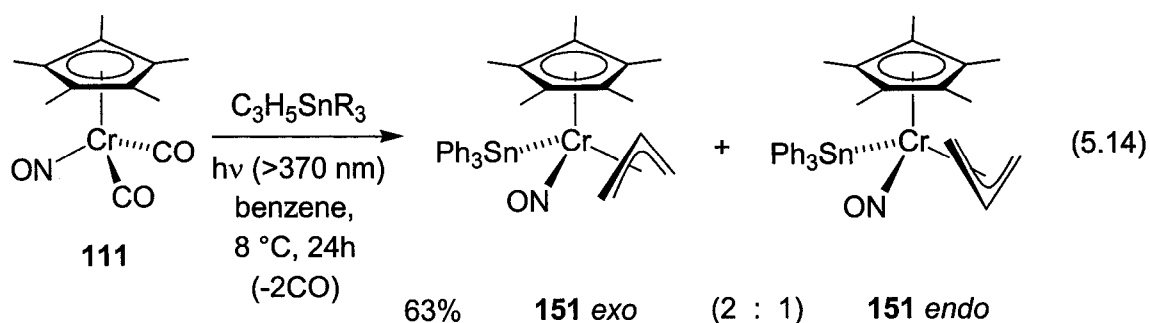
As a control experiment for this reaction, we also investigated the addition of allyl bromide to $\text{Cp}^*\text{CrNO}(\text{CO})_2$ **94**. Unlike the interaction between diene complex **111** and allyl bromide, heating a mixture of complex **94** and allyl bromide in benzene- d_6 fails to effect any reaction. This is presumably a result of the robust nature of the chromium–CO bonds, which prevents thermal decarbonylation. Consistent with the photolytic diene synthesis (Chapter 4), photolysis of dicarbonyl complex **94** in the presence of allyl bromide leads to nearly complete consumption of the starting materials and the formation of 1,5-hexadiene and an unidentified green paramagnetic product that we assume to be complex **153d**.

5.5 Photolytic decarbonylation of $\text{Cp}^*\text{CrNO}(\text{CO})_2$ in the presence of tin reagents

5.5.1 Preparation of $\text{Cp}^*\text{CrNO}(\eta^3\text{-allyl})(\text{SnPh}_3)$

By combining the photo-initiated activation of $\text{Cp}^*\text{CrNO}(\text{CO})_2$ **94** with the use of allyltin reagents, we discovered a tantalizing direct method for the preparation of η^3 -allyl chromium-tin complexes **151** and **152**. Photolysis (450 Watt, Hg Hanovia) of dicarbonyl complex **94** in the presence of allyltriphenyltin in benzene- d_6 provides $\text{Cp}^*\text{CrNO}(\eta^3\text{-allyl})(\text{SnPh}_3)$ **151** as a 1 : 3 mixture of *endo* and *exo* isomers in 48% conversion, as ascertained by ^1H NMR spectroscopy. A trace amount of 1,5-hexadiene was also detected, along with two unassigned Cp^* signals at 1.42 and 1.40 ppm. Further photolysis only increases the relative amount of these impurities. Since many alkyltin reagents are prone to photo-induced radical decomposition,⁶¹ we attribute the formation of 1,5-hexadiene and the unidentified Cp^* -containing impurities to the radical-mediated decomposition of allyltriphenyltin.

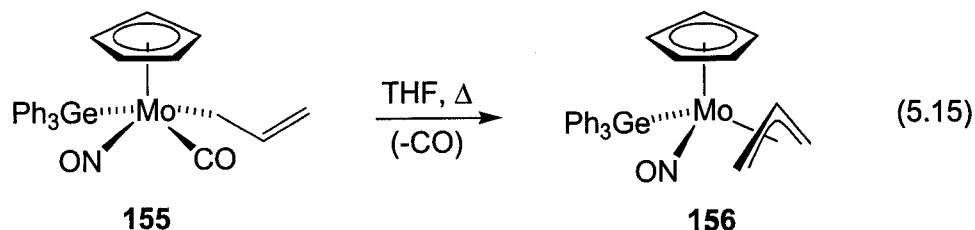
To avoid this competitive reaction pathway, we reintroduced the 370 nm cutoff filter to the photolysis apparatus. In this way, photolysis of complex **94** in the presence of allyltriphenyltin at 8 °C in benzene- d_6 for 24 h affords η^3 -allyl complex **151** in much higher conversion (72%) and with considerably lower formation of organic and organochromium impurities. The selectivity of this reaction is further improved upon the introduction of a nitrogen purge. Passing the resulting reaction mixture through a silica-gel column and recrystallization from diethyl ether ultimately provides allyl complex **151** in 63% yield and high purity (eq. 5.14). Changing the reaction solvent to toluene and lowering the reaction temperature to -20 °C does not improve the yield of this product.



Unfortunately, extending this methodology to the preparation of η^3 -allyl complex **152** is less successful, producing the desired product in lower yield and purity than with the analogous triphenyltin complex **151**. Even using the 370 nm cutoff filter and a vigorous nitrogen purge, the photolysis of a mixture of tetraallyltin and $\text{Cp}^*\text{CrNO}(\text{CO})_2$ **94** for 24 h at 8°C leads to a 1 : 1.5 mixture of *endo* and *exo* isomers of complex **152** in only 33% yield. This product could not be separated from the unassigned organochromium byproducts.

Despite the apparent simplicity of the chemistry shown in equation 5.14, there is no literature precedent for the formation of *isolable* η^3 -allyl complexes via the oxidative addition of allyl tin compounds to any transition metal. However, the palladium-catalyzed carboxylation of allyl stannanes is known and is believed to proceed via intermediate $(\text{R}_3\text{Sn})\text{Pd}(\text{II})\text{L}(\eta^3\text{-allyl})$ (L = neutral two-electron donor) complexes.^{62, 63} There are, in fact, very few examples of the oxidative addition of any type of Sn–C bonds to a transition metal centre.^{64–66} The only literature that reflects some of the principles involved in this chemistry is one report of the formation of $\text{CpMo}(\text{NO})(\text{GePh}_3)(\eta^3\text{-allyl})$ **156** via thermal decarbonylation of $\text{CpMo}(\text{NO})(\text{CO})(\text{GePh}_3)(\eta^1\text{-allyl})$ **155** (eq. 5.15); the precursor is prepared via the nucleophilic attack of $[\text{CpMo}(\text{NO})(\text{CO})(\text{GePh}_3)][\text{Et}_4\text{N}]$ **154** on allyl bromide.⁶⁷ Thus, provided it can be generalized, our photolytic strategy for the

formation of $\text{Cp}^*\text{Cr}(\text{NO})(\eta^3\text{-allyl})(\text{SnR}_3)$ complexes represents a novel and compelling route to a new class of stable allylchromium nitrosyl complexes.



5.5.2 Spectroscopic identification of $\text{Cp}^*\text{CrNO}(\text{CO})\eta^2\text{-(H-SnPh}_3\text{)}$

After it became clear that allylstannanes add oxidatively to $\text{Cp}^*\text{CrNO}(\text{CO})_2$ **94** via photo-labilization of the carbonyl ligands, the reactivity of Ph_3SnH was investigated under similar reaction conditions. If successful, this reaction would provide an entry route into an otherwise unknown series of unsaturated chromium hydride complexes, which may be amenable to synthetically useful insertion reactions, including those of dienes.

Thus, broad spectrum UV irradiation of a mixture of dicarbonyl complex **94** in the presence of one equivalent of triphenyltin hydride under a nitrogen purge provides ^1H NMR spectroscopic evidence for the formation of a 10 : 1 mixture of isomeric chromium hydride complexes **157** (δ Cr-H: -3.62 and -3.82 , respectively). Closer analysis of this reaction mixture, however, reveals that the hydride signal at -3.62 ppm is flanked by two doublets arising from $^{119}\text{Sn-H}$ ($J = 360$ Hz) and $^{117}\text{Sn-H}$ ($J = 344$ Hz) coupling (Fig. 5.11); the lower concentration of the minor isomer prevents detection of the tin satellites for the signal at -3.82 .

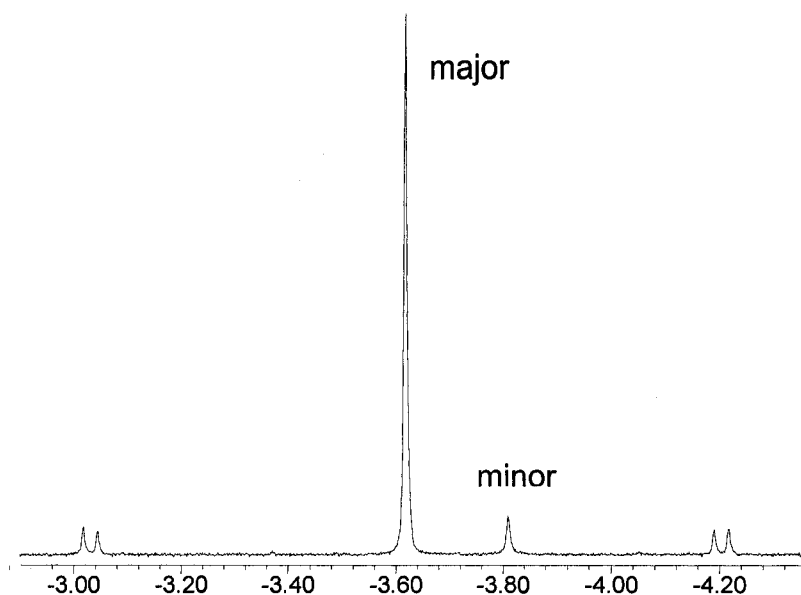
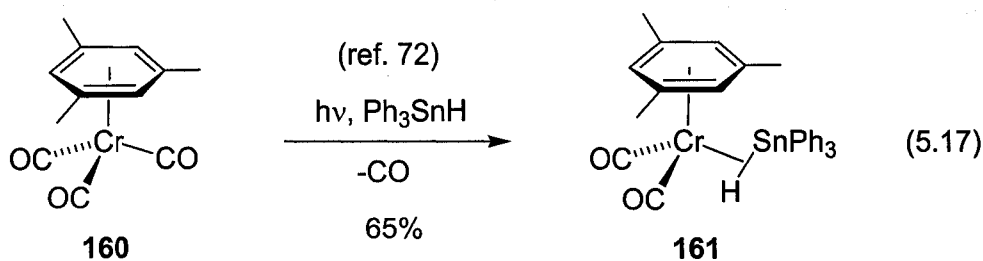
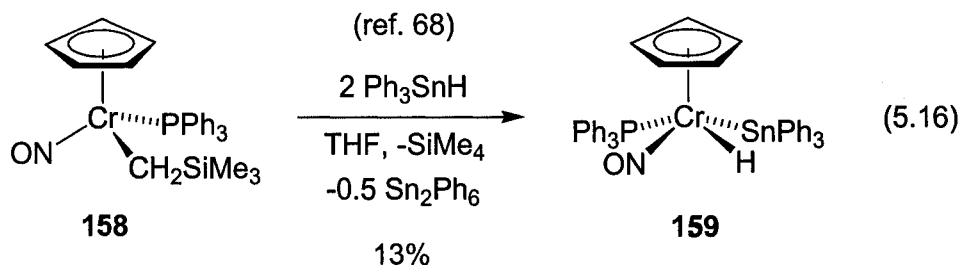


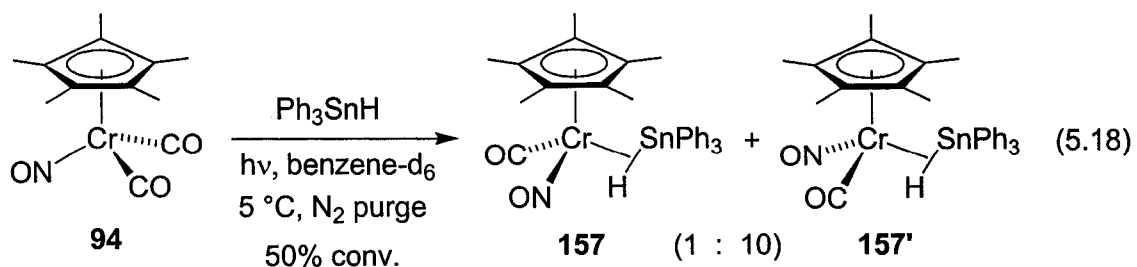
Figure 5.11: Expansion of the hydrido region of the ^1H NMR spectrum of complex **157**.

It is known that the magnitude of the Sn–H coupling constant is proportional to the amount of direct Sn–H bonding present in transition metal tin-hydride complexes.⁶⁸⁻⁷¹ In complexes where there is an agostic interaction between the transition metal and the Sn–H bond, the value of $J_{\text{Sn-H}}$ ranges from 1500 to 1800 Hz. Transition metal tin-hydride complexes possessing a three-centred two-electron Sn–M–H bond, however, exhibit ^{119}Sn -H coupling constants ranging from 328 to 338 Hz, while complexes with discrete M–Sn and M–H bonds can have ^{119}Sn -H coupling constants anywhere between 0 and 150 Hz.⁶⁹⁻⁷² The structurally characterized complex $\text{CpCr}(\text{NO})(\text{PPh}_3)(\text{H})(\text{SnPh}_3)$ **159**, for example, elicits a ^{119}Sn -H coupling constant of only 23.7 Hz and is therefore considered to be a nominally chromium(II) hydride species (eq. 5.16).⁶⁸ On the other hand, $(\eta^6\text{-arene})\text{Cr}(\text{CO})_2(\text{HSnPh}_3)$ complexes are reported to have ^{119}Sn -H coupling constants ranging from 328 to 338 Hz;^{69, 72} this three-centred two-electron, or η^2 -(hydrido-

stannane), interaction has been confirmed in the solid-state for the η^6 -(mesityl) complex **161** (eq. 5.17).^{69, 72}



Given the similarity between the ¹¹⁹Sn-H coupling constant of the η^2 -(hydrido-stannane) complex **161** with that of the above photolysis product, we tentatively assigned the structure of complex **157** as possessing an η^2 -(Sn-H) ligand (eq. 5.18).



Unfortunately, we have yet to isolate complex **157** or optimize the yield of the reaction. At room temperature, for example, the reaction produces only a trace amount of the desired product. Once isolated, the infrared spectrum should provide additional evidence for the three-centred two-electron bond; the structurally similar (η^6 -arene)- $\text{Cr}(\text{CO})_2(\text{HSnPh}_3)$ complexes, for example, reveal diagnostic Cr–H stretching frequencies in the range of 1918 to 1950 cm^{-1} .⁶⁹

Despite our current inability to isolate η^2 -stannane complex **157** from solution, this nonetheless introduces another class of potentially useful complexes into the relatively under-studied area of chromium-tin(IV) chemistry. To the best of our knowledge, all other examples of chromium-tin complexes consist of a tricoordinate tin moiety and a chromiumcarbonyl fragment.^{73, 74} Moreover, the η^3 -allyl chromium-tin complexes **146**, **147**, **151**, and **152** are the first examples of tin(IV)-chromium(II) compounds possessing both alkyl and nitrosyl ligands.

5.6 References

1. Knolker, H.-J. *Chem. Rev.* **2000**, *100*, 2941, and references therein.
2. Pearson, A. J. *Iron Compounds in Organic Synthesis*. Academic Press: London, 1992.
3. Pearson, A. J. *Acc. Chem. Res.* **1980**, *13*, 463.
4. Erker, G.; Wicher, J.; Engel, K.; Rosenfeldt, F.; Dietrich, W.; Krüger, C. *J. Am. Chem. Soc.* **1980**, *102*, 6344.
5. Erker, G.; Wicher, J.; Engel, K.; Krüger, C. *Chem. Ber.* **1982**, *115*, 3300.

6. Yasuda, H.; Kajihara, Y.; Mashima, K.; Nagasuna, K.; Lee, K.; Nakamura, A. *Organometallics* **1982**, *1*, 388.
7. Erker, G.; Engel, K.; Atwood, J. L.; Hunter, W. E. *Angew. Chem. Int. Ed.* **1983**, *22*, 494.
8. Yasuda, H.; Nakamura, A. *Angew. Chem. Int. Ed.* **1987**, *26*, 723.
9. Christensen, N. J.; Legzdins, P. *Organometallics* **1991**, *10*, 3070.
10. Mashima, K.; Nakamura, A. *J. Organomet. Chem.* **2002**, *663*, 5.
11. Erker, G.; Kehr, G.; Fröhlich, R. *Adv. Organomet. Chem.* **2004**, *51*, 109.
12. Erker, G.; Kehr, G.; Fröhlich, R. *J. Organomet. Chem.* **2004**, *689*, 4305.
13. Mahima, K.; Nakamura, A. *J. Organomet. Chem.* **2002**, *663*, 5-12.
14. Temme, B.; Erker, G.; Karl, J.; Luftmann, H.; Fröhlich, R.; Kotila, S. *Angew. Chem. Int. Ed.* **1995**, *34*, 1755.
15. Dahlman, M.; Erker, G.; Fröhlich, R.; Meyer, O. *Organometallics* **2000**, *19*, 2956.
16. Yasuda, H.; Yamamoto, H.; Yamashita, M.; Yokota, K.; Nakamura, A.; Miyake, S.; Kai, Y.; Kanehisa, N. *Macromolecules* **1993**, *26*, 7134.
17. Bolig, A. D.; Chen, E. Y.-X. *J. Am. Chem. Soc.* **2002**, *124*, 5612.
18. Hunter, A. D.; Legzdins, P.; Einstein, F. W. B.; Willis, A. C.; Bursten, B. E.; Gatter, M. G. *J. Am. Chem. Soc.* **1986**, *108*, 3843.
19. Hou, Z.; Fujita, A.; Koizumi, T.; Yamazaki, H.; Wakatsuki, Y. *Organometallics* **1999**, *18*, 1979.
20. Hou, Z.; Fujita, A.; Zhang, Y.; Miyano, T.; Yamazaki, H.; Wakatsuki, Y. *J. Am. Chem. Soc.* **1998**, *120*, 754.
21. Hou, Z.; Jia, X.; Hoshino, M.; Wakatsuki, Y. *Angew. Chem. Int. Ed.* **1997**, *36*, 1292.
22. Hou, Z.; Fujita, A.; Yamazaki, H.; Wakatsuki, Y. *J. Am. Chem. Soc.* **1996**, *118*, 2053.
23. Hou, Z.; Fujita, A.; Yamazaki, H.; Wakatsuki, Y. *J. Am. Chem. Soc.* **1996**, *118*, 7843.

24. Hou, Z.; Miyano, T.; Yamazaki, H.; Wakatsuki, Y. *J. Am. Chem. Soc.* **1995**, *117*, 4421.
25. Covert, K. J.; Wolczanski, P. T.; Hill, S. A.; Krusic, P. J. *Inorg. Chem.* **1992**, *31*, 66.
26. Richter Addo, G. B.; Legzdins, P. *Metal Nitrosyls*. Oxford University Press: Oxford, 1992.
27. Richter Addo, G. B.; Legzdins, P.; Burstyn, J. *Chem. Rev.* **2002**, *102*, 857.
28. Sharp, W. B.; Legzdins, P.; Patrick, B. O. *J. Am. Chem. Soc.* **2001**, *123*, 8143.
29. Lee, K. E.; Arif, A. M.; Gladysz, J. A. *Inorg. Chem.* **1990**, *29*, 2885.
30. Legzdins, P.; McNeil, W. S.; Rettig, S. J.; Smith, K. M. *J. Am. Chem. Soc.* **1997**, *119*, 3513.
31. Legzdins, P.; Nurse, C. R. *Inorg. Chem.* **1985**, *24*, 327.
32. Minami, I.; Shimizu, I.; Tsuji, J. *J. Organomet. Chem.* **1985**, *296*, 269.
33. Adams, H.; Bailey, N. A.; Willett, D. G.; Winter, M. J. *J. Organomet. Chem.* **1987**, *333*, 61.
34. Legzdins, P.; McNeil, W. S. *J. Am. Chem. Soc.* **1994**, *116*, 6021.
35. Legzdins, P.; McNeil, W. S.; Batchelor, R. J.; Einstein, F. W. B. *J. Am. Chem. Soc.* **1995**, *117*, 10521.
36. Chin, T. T.; Legzdins, P.; Trotter, J.; Yee, V. C. *Organometallics* **1992**, *11*, 913.
37. Wang, N.-F.; Wink, D. J.; Dewan, J. C. *Organometallics* **1990**, *9*, 335.
38. Wink, D. J.; Wang, N.-F.; Springer, J. P. *Organometallics* **1989**, *8*, 259.
39. Norman, D. W.; Ferguson, M. J.; Stryker, J. M. *Organometallics* **2004**, *23*, 2015.
40. Older, C. M.; Stryker, J. M. *Organometallics* **2000**, *19*, 2661.
41. Bi, S.; Ariafield, A.; Jia, G.; Lin, Z. *Organometallics* **2005**, *24*, 680.
42. Ariafield, A.; Bi, S.; Lin, Z. *Organometallics* **2005**, *24*, 2241.

43. Xue, P.; Bi, S.; Sung, H. H. Y.; Williams, I. D.; Lin, Z.; Jia, G. *Organometallics* **2004**, *23*, 4735.
44. van Staveren, D. R.; Bill, E.; Bothe, E.; Buhl, M.; Weyhermüller, T.; Metzler-Nolte, N. *Chem. Eur. J.* **2002**, *8*, 1649.
45. Kennedy, J. D.; McFarlane, W. Silican, Germanium, Tin, and Lead. In *Multinuclear NMR*, Mason, J., Ed., Plenum: New York, 1987; Ch. 11.
46. Holt, M. S.; Wilson, W. L.; Nelson, J. H. *Chem. Rev.* **1989**, *89*, 11.
47. Lambert, J. B.; Zhao, Y.; Wu, H.; Tse, W. C.; Kuhlmann, B. *J. Am. Chem. Soc.* **1999**, *121*, 5001.
48. Lambert, J. B.; Kuhlmann, B. *J. Chem. Soc., Chem. Commun.* **1992**, 931.
49. Lambert, J. B.; Lin, L.; Keinan, S.; Muller, T. *J. Am. Chem. Soc.* **2003**, *125*, 6022.
50. Bottomley, F.; Paez, D. E.; Sutin, L.; White, P. S.; Köhler, F. H.; Thompson, R. C.; Westwood, N. P. C. *Organometallics* **1990**, *9*, 2443.
51. Cramer, C. J.; Tolman, W. B.; Theopold, K. H.; Rheingold, A. L. *PNAS* **2003**, *100*, 3635.
52. Hess, J. S.; Leelasubcharoen, S.; Rheingold, A. L.; Doren, D. J.; Theopold, K. H. *J. Am. Chem. Soc.* **2002**, *124*, 2454.
53. Qin, K.; Incarvito, C. D.; Rheingold, A. L.; Theopold, K. H. *J. Am. Chem. Soc.* **2002**, *124*, 14008.
54. Qin, K.; Incarvito, C. D.; Rheingold, A. L.; Theopold, K. H. *Angew. Chem. Int. Ed.* **2002**, *41*, 2333.
55. Hess, A.; Hörz, M. R.; Liable-Sands, L. M.; Lindner, D. C.; Rheingold, A. L.; Theopold, K. H. *Angew. Chem. Int. Ed.* **1999**, *38*, 166.
56. Faller, J. W.; Rosan, A. M. *J. Am. Chem. Soc.* **1976**, *98*, 3388.
57. Kazmaier, U.; Lucas, S.; Klein, M. *J. Org. Chem.* **2006**, *71*, 2429.
58. Braune, S.; Pohlman, M.; Kazmaier, U. *J. Org. Chem.* **2004**, *69*, 468.
59. Christoffers, J.; Werner, T.; Baro, A.; Fischer, P. *J. Organomet. Chem.* **2004**, *689*, 3550.
60. Smith, N. D.; Mancuso, J.; Lautens, M. *Chem. Rev.* **2000**, *100*, 3257.

61. Takuwa, A.; Kanaue, T.; Yamashita, K.; Nishigaichi, Y. *J. Chem. Soc., Perkin Trans. 1* **1998**, 1309.
62. Matsubara, T. *Organometallics* **2003**, 22, 4286.
63. Shi, M.; Nicholas, K. M. *J. Am. Chem. Soc.* **1997**, 119, 5057.
64. Schubert, U.; Grubert, S.; Schulz, U.; Mock, S. *Organometallics* **1992**, 11, 3163.
65. Müller, C.; Schubert, U. *Chem. Ber.* **1991**, 124, 2181.
66. Butler, G.; Eaborn, C.; Pidcock, A. *J. Organomet. Chem.* **1979**, 181, 47.
67. Carre, F.; Colomer, E.; Corriu, R. J. P.; Vioux, A. *Organometallics* **1984**, 3, 970.
68. Legzdins, P.; Shaw, M. J. *Organometallics* **1995**, 14, 4721.
69. Khaleel, A.; Klabunde, K. J. *Inorg. Chem.* **1996**, 35, 3223.
70. Schubert, U.; Kunz, E.; Harkers, B.; Willnecker, J.; Meyer, J. *J. Am. Chem. Soc.* **1989**, 111, 2572.
71. Schubert, U. *Adv. Organomet. Chem.* **1990**, 30, 151.
72. Piana, H.; Kirchgassner, U.; Schubert, U. *Chem. Ber.* **1991**, 124, 743.
73. Wagner, H.; Baumgartner, J.; Marschner, C. *Organometallics* **2005**, 24, 4649.
74. Patil, H. R. H.; Graham, W. A. G. *Inorg. Chem.* **1966**, 5, 1401.

Chapter 6.

Non-carbonyl sources of chromium: alternative strategies for the preparation of *pseudo*-tetrahedral η^3 -allyl chromium complexes

6.0 Overview

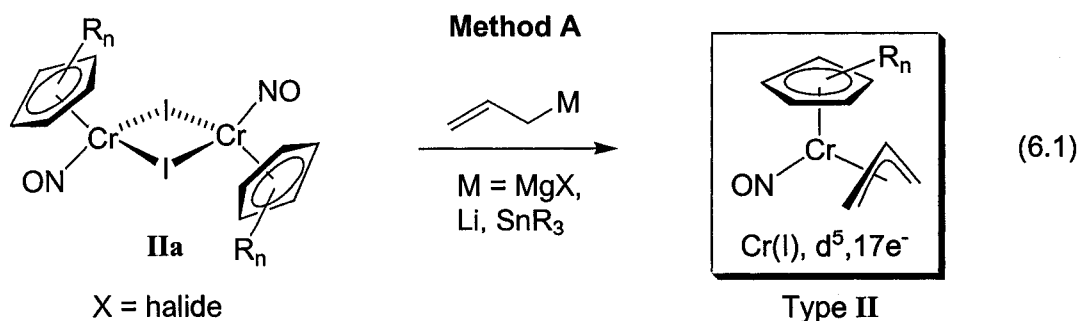
The previous chapters have focused on the development of chromium η^3 -allyl complexes bearing π -acidic ligands. Although several new classes of thermally stable η^3 -allyl complexes have been introduced, we have yet to convert these half-sandwich complexes into the desired *pseudo*-tetrahedral analogues. The biggest obstacle to these transformations is the presence of carbonyl ligands that cannot be removed or exchanged from the metal centre without unwanted loss or functionalization of the allyl ligand; we have yet to determine the reactivity of the R_3Sn ligands in the more recently discovered η^3 -allyl chromium-tin complexes.

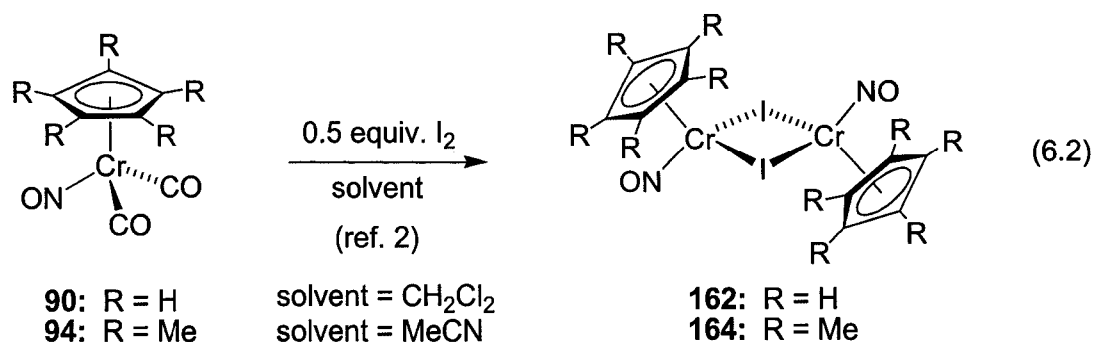
Thus, we have also explored the preparation of the proposed Type II-V chromium η^3 -allyl target molecules (outlined in Chapter 1, pp. 34-36) from *non-carbonyl* sources of chromium. Each of the following sections of this chapter therefore consists of an introduction to the proposed strategies for the synthesis of these *pseudo*-tetrahedral complexes, followed by a discussion of the corresponding experimental results.

6.1 Attempted synthesis of chromium(I) nitrosyl η^3 -allyl complexes

6.1.1 Introduction

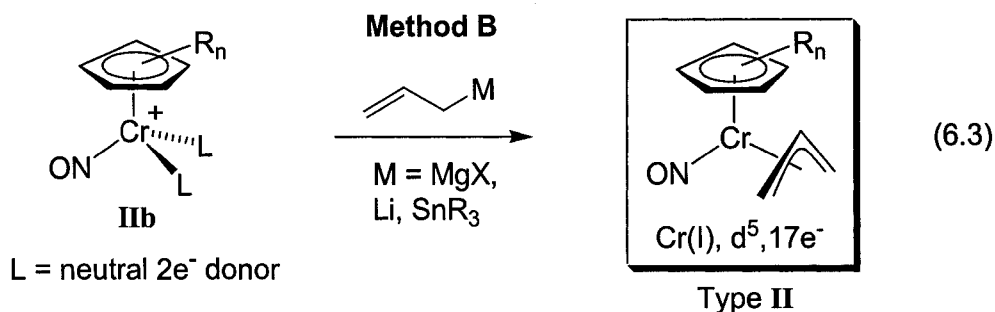
We originally envisioned the synthesis of the Type II 17-electron η^3 -allyl chromium nitrosyl complexes via allylation of dimeric monohalochromium nitrosyl complexes **IIa**, the iodo- analogues of which are well known (eq. 6.1).^{1,2} The dimeric complex $[\text{CpCr}(\text{NO})\text{I}]_2$ **162**, for example, is obtained from the addition of half an equivalent of iodine to $\text{CpCrNO}(\text{CO})_2$ **90** in dichloromethane; a full equivalent of iodine leads to the formation of the dinitrosyl complex $\text{CpCr}(\text{NO})_2\text{I}$ **163** (eq. 6.2) rather than the expected $\text{CpCr}(\text{NO})\text{I}_2$ product.¹ Similar treatment of the more hindered permethylcyclopentadienyl complex $\text{Cp}^*\text{CrNO}(\text{CO})_2$ **94** leads only to the dinitrosyl species $\text{Cp}^*\text{Cr}(\text{NO})_2\text{I}$ **165**. Conducting this oxidation reaction in acetonitrile, however, avoids this disproportionation product and provides the desired dimeric iodo- complex $[\text{Cp}^*\text{Cr}(\text{NO})\text{I}]_2$ **164** (eq. 6.2).² The formation of the bromo- analogues of the Type **IIa** complexes has not been reported, while the only known chloro- analogue $[\text{Cp}^*\text{Cr}(\text{NO})\text{Cl}]_2$ **132** is prepared from dicarbonyl complex **94** and PCl_5 in acetonitrile.²



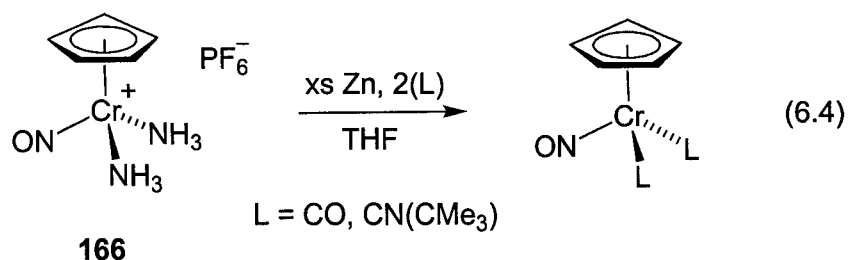


Interestingly, the alkylation of moniodo- complex **162** is successful only upon the addition of trimethylsilyl Grignard reagents in the presence of a stabilizing phosphine or amine ligand.³⁻⁵ The unique stability of the resulting CpCr(NO)(L)(CH₂SiMe₃) complexes presumably results from the steric bulk of the alkyl ligand and the lack of β -hydrogen atoms. Surprisingly, the addition of allyl-containing reagents to complex **162** has yet to be reported and there are no reports of *any* reactivity of the more hindered [Cp*Cr(NO)I]₂ complex **164**.

An alternative approach to the preparation of the Type II η^3 -allyl complexes relies on the allylation of cationic bis(donor) chromium(I) nitrosyl complexes **IIb** (eq. 6.3). Several bis(N-donor) members of this class of complexes are known,⁶⁻⁸ while we have prepared the structurally related DME and bis(acetone) complexes **143** and **144** (recall Chapter 5, pp. 168-172).



We were also interested in the reduction of the cationic N- and O-donor complexes in the presence of conjugated dienes, the desired outcome of which would provide an alternative method for preparing the $\text{Cp}'\text{CrNO}(\text{s-trans-1,3-diene})$ complexes, discussed previously in Chapter 4 and 5. Indeed, Legzdins has demonstrated related reactions in which the cationic bis(ammonia) complex **166** is slowly reduced by zinc powder under a CO atmosphere or in the presence of an isocyanide to provide neutral $\text{CpCrNO}(\text{L})_2$ ($\text{L} = \text{CO}, \text{CNR}$) complexes (eq. 6.4).⁸



6.1.2 Halo-bridged dimers as chromium nitrosyl sources

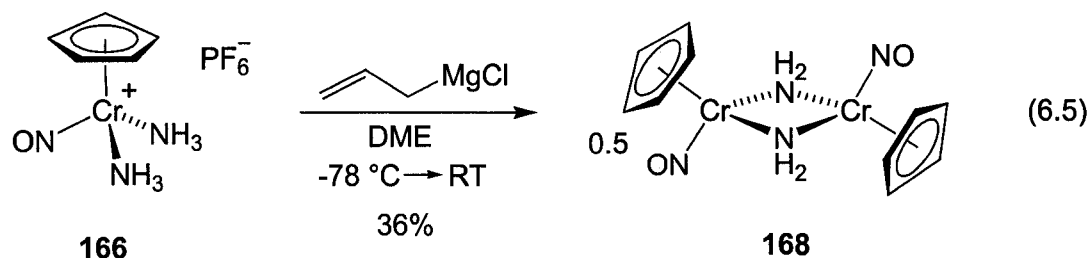
We therefore began the investigation of non-carbonyl sources of chromium by exploring allyl anion addition to $[\text{CpCr}(\text{NO})\text{I}]_2$ **162**. Unfortunately, however, treatment of this complex with reagents such as allylmagnesium bromide or chloride, allyllithium or tetraallyltin at low temperature provides only brown intractable products; infrared

analysis of these reaction mixtures revealed a multitude of tentatively assigned nitrosyl ligand absorptions between 1700 and 1600 cm^{-1} . Addition of the more hindered cinnamyl lithium reagent also provides an intractable reaction mixture, as does allyl anion addition in the presence of PPh_3 . We attribute this undesirable reactivity to the thermal instability of the putative $\text{Cp}^*\text{Cr}(\text{NO})(\eta^1\text{-allyl})$ intermediates.

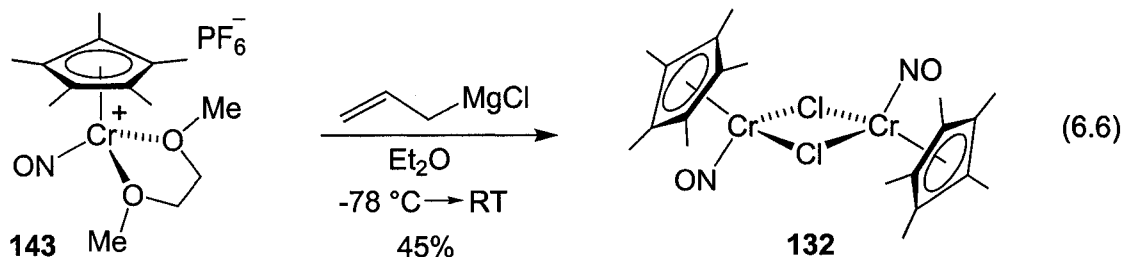
Unfortunately, the addition of allylating reagents to the permethylcyclopentadienyl analogue of complex **162**, $[\text{Cp}^*\text{Cr}(\text{NO})\text{I}]_2$ **164**, could not be studied. In our hands, the preparation of this starting material did not result in the expected green crystalline product,² but only a brown intractable powder. The addition of the allyl anion to $[\text{Cp}^*\text{Cr}(\text{NO})\text{Cl}]_2$ **132** affords only intractable reaction mixtures.²

6.1.3 Reactivity of cationic bis(donor) chromium(I) nitrosyl complexes

The addition of various allyl anion sources to the $[\text{CpCr}(\text{NO})\text{bis}(\text{acetonitrile})]\text{PF}_6$ complex **167** also leads to the formation of intractable brown mixtures. Interestingly, however, the reaction between allylmagnesium chloride and the related bis(ammonia) complex **166** provides a red product, which upon recrystallization from diethyl ether provides red crystals of the known bridging amido $[\text{CpCr}(\text{NO})(\mu\text{-NH}_2)]_2$ complex **168**, as determined by X-ray crystallographic comparison of the previously reported compound⁹ (eq. 6.5). The formation of this unexpected product is presumably initiated via the deprotonation of an ammonia ligand of complex **166** by the Grignard reagent, with concomitant loss of the remaining ammonia ligand.



In all but one case, the addition of allyl magnesium chloride or bromide to the O-donor complexes **143** and **144** leads to the formation of intractable products; the exception being the reaction between allylmagnesium chloride and a suspension of DME complex **143** (in diethyl ether at -78°C). Initially, a colour change from green to brown was observed, followed by the formation of a green precipitate upon warming to room temperature, subsequently determined to be the dimeric $[\text{Cp}^*\text{Cr}(\text{NO})\text{Cl}]_2$ complex **132**, formed in 45% yield (eq. **6.6**).



Equally disappointing results were obtained from zinc reduction of the N-donor complexes **166** and **167** and the O-donor complexes **143** and **144** in the presence of a large excess of butadiene or isoprene. In all cases only intractable yellow-brown products were obtained. Other reductants, such as magnesium powder or sodium-mercury amalgam, also leads to the formation of similar product mixtures. No

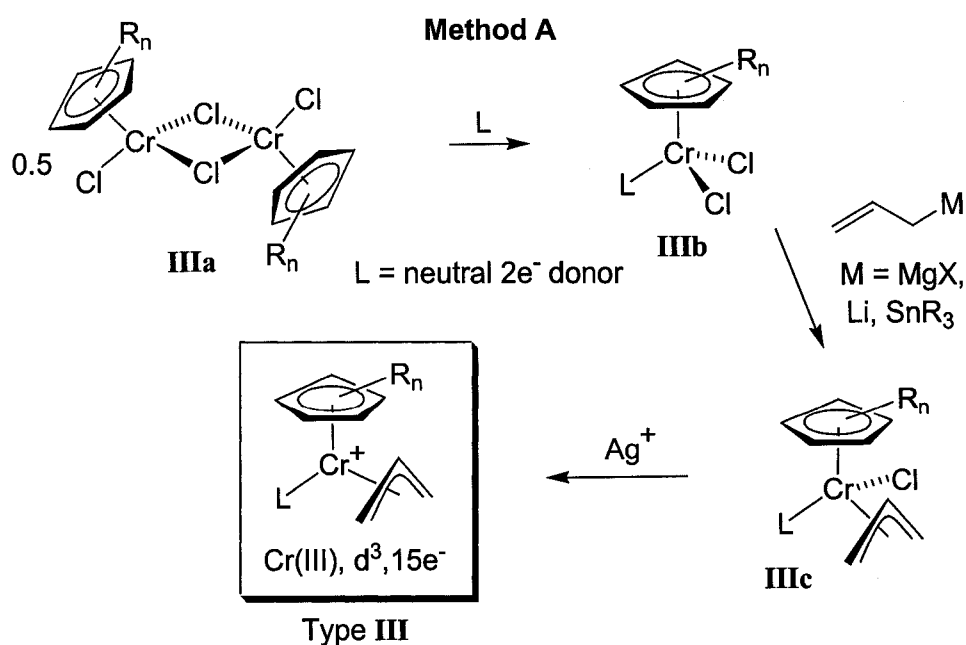
spectroscopic evidence for the presence of any η^2 -diene or η^4 -diene complexes was obtained.

6.2 Synthesis and reactivity of dihalochromium complexes bearing neutral ligands

6.2.1 Introduction

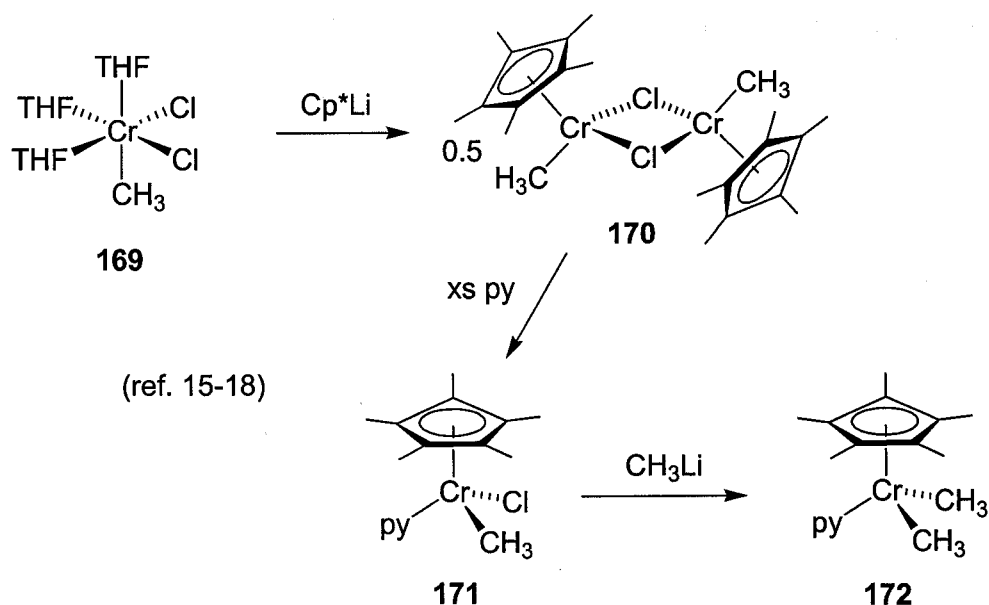
Since a number of groups have employed $\text{Cp}'\text{Cr}(\text{L})\text{Cl}_2$ (L = donor ligand) complexes in the synthesis of bis(alkyl) chromium(III) complexes,¹⁰⁻¹⁴ we proposed that these complexes should also be amenable to allyl anion addition. For example, initial splitting of dimeric dichlorochromium complexes **IIIa** by a neutral donor molecule, followed by treatment with allylating reagents to give the consequent Type **IIIb** 17-electron complex would provide the allyl-containing species **IIIc** (Scheme 6.1) or its η^1 -analogue. Subsequent electrophilic dehalogenation of this complex may then afford the desired cationic Type **III** *pseudo*-tetrahedral η^3 -allyl products.

Scheme 6.1



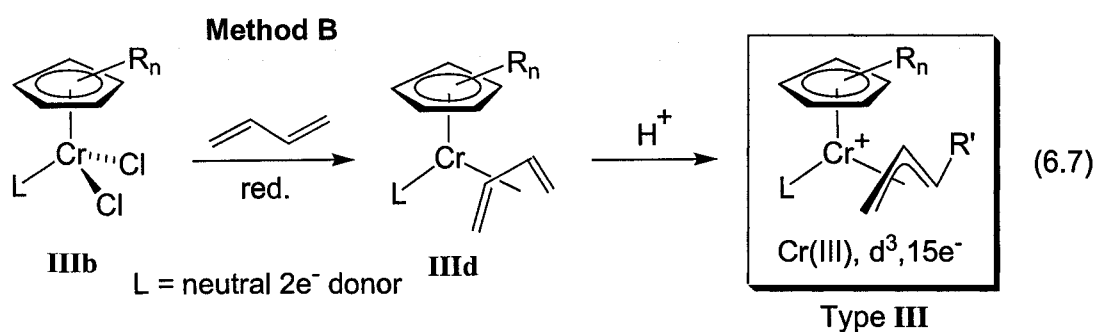
Reversing the order of addition of the donor ligand and the allyl anion may also provide the requisite Type **IIIc** allylchromium complexes. Indeed, a similar approach has been employed in the preparation of the monomethyl and dimethyl pyridine complexes **171** and **172** (Scheme 6.2).^{15, 16} In this case, however, the starting alkyl complex **170** is prepared via the addition of Cp*Li to the preformed methyl-containing chromium(III) dichloro complex **169**.^{17, 18}

Scheme 6.2

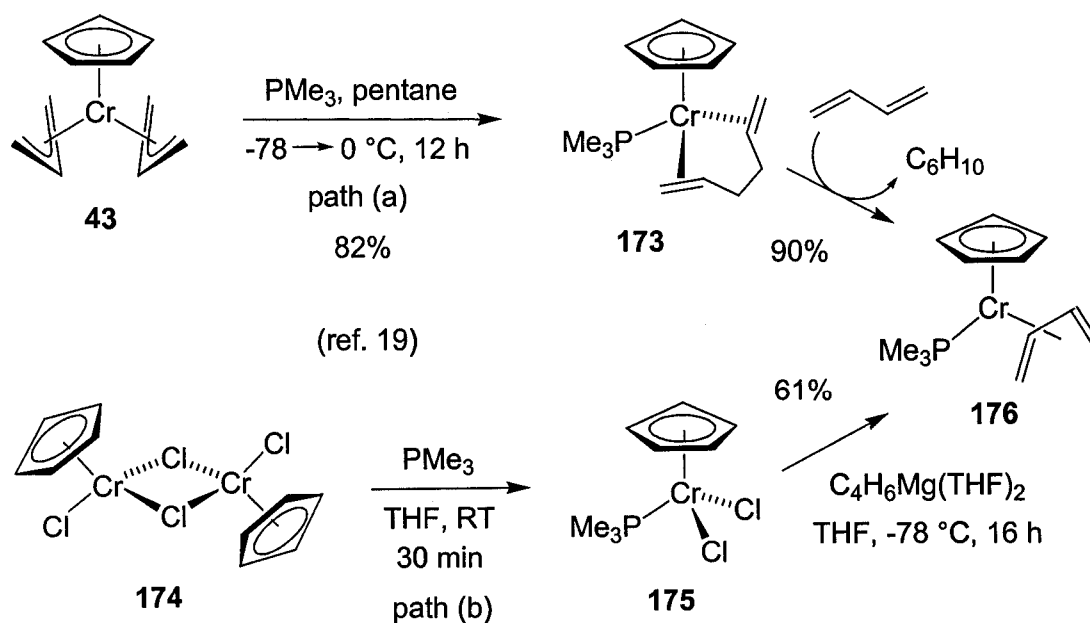


The preparation of the Type **III** η^3 -allyl target complexes may also be possible simply via the protonation of known 17-electron chromium(I) η^4 -diene complexes **IIIId**, the syntheses of which entail the reduction of Cp'Cr(L)Cl₂ (L = donor ligand) complexes in the presence of conjugated dienes (eq. 6.7).¹⁹ The thermally stable CpCr(PMe₃)(η^4 -butadiene) complex **176**, for example, is prepared via initial trimethylphosphine-induced

reductive coupling of the allyl ligands in $\text{CpCr}(\eta^3\text{-allyl})_2$ complex **43**, followed by exchange of the consequent $\eta^2:\eta^2$ -(1,5-hexadiene) ligand with butadiene (Scheme 6.3, path a).¹⁹ This complex is also obtained via the addition of PMe_3 to $[\text{CpCrCl}_2]_2$ **174**,¹⁹ followed by treatment with magnesium butadienide²⁰ (Scheme 6.3, path b). The thermally sensitive permethylcyclopentadienyl analogue (complex **177**) of diene complex **176** is prepared via an extension of this latter approach.¹⁹



Scheme 6.3



6.2.2 Addition of sterically hindered donor ligands to $[\text{Cp}^*\text{CrCl}_2]_2$

Our initial attempts to prepare the Type **III** η^3 -allyl complexes began with the coordination of sterically hindered ancillary ligands to the dimeric dichloro species $[\text{Cp}^*\text{CrCl}_2]_2$ **178**.^{15, 21} The addition of 2,4,6-trimethylpyridine (PyMe_3) or IMes to blue solutions of complex **178** in THF, however, failed to effect a colour change, indicative of a lack of coordination. Indeed, combustion analysis of the recrystallized residue from the reaction of complex **178** with PyMe_3 revealed the presence of only unreacted organochromium starting material.

Similar analysis of the product from the reaction of complex **178** with IMes reveals only trace amounts of nitrogen in the sample, indicative of very little conversion to the tentatively assigned $\text{Cp}^*\text{Cr}(\text{IMes})\text{Cl}_2$ **179**, which could not be isolated in sufficient yield or purity. Treatment of $[\text{Cp}^*\text{CrCl}_2]_2$ **178** with allylmagnesium bromide or chloride followed by the addition of PyMe_3 or IMes, on the other hand, provides in each case a brown reaction mixture. Unfortunately, these products could not be isolated or identified.

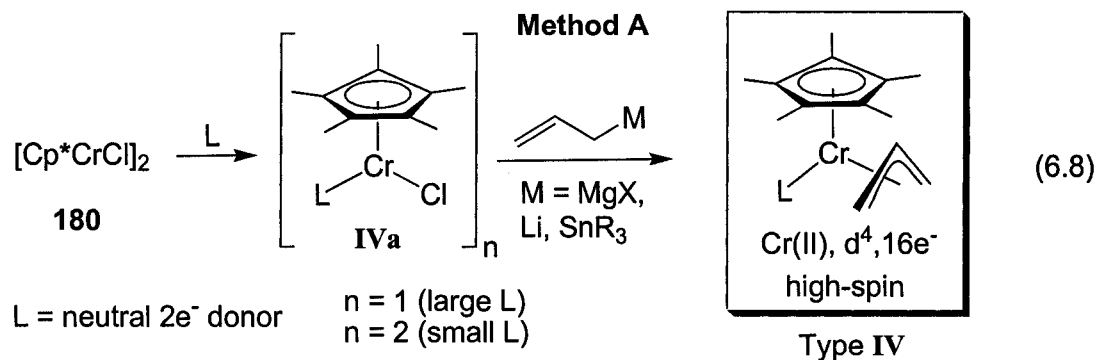
6.2.3 Protonation of chromium(I) η^4 -butadiene complexes

Given the discouraging results from these preliminary investigations, we focused on the alternative method for the synthesis of the Type **III** η^3 -allyl complexes. Regrettably, however, the addition of tetrafluoroboric acid to $\text{CpCr}(\text{PMe}_3)(\eta^4\text{-butadiene})$ **176** and the permethylcyclopentadienyl analogue **177** failed to provide the desired cationic η^3 -allyl derivatives. In each case, protonation of the red diene complex at low temperature leads to the isolation of blue powders, the identity of which could not be ascertained via elemental analysis.

6.3 Monohalo chromium(II) complexes as η^3 -allyl and η^4 -(1,3-diene) precursors

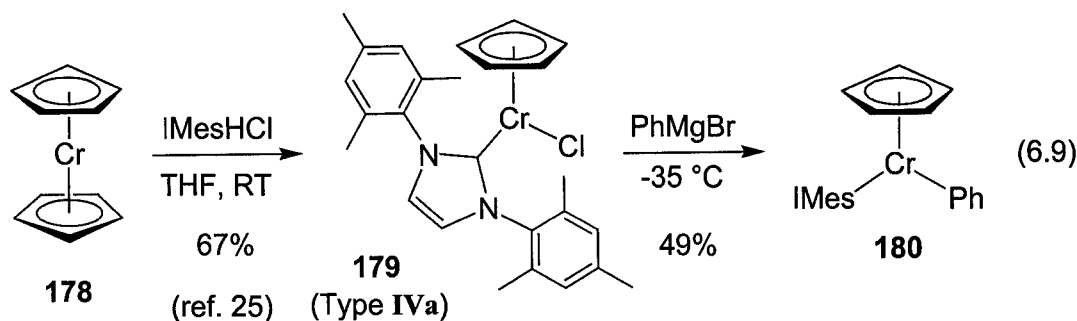
6.3.1 Introduction

Although, prior to our work, the addition of neutral donor molecules to the dimeric $[\text{Cp}^*\text{CrCl}]_2$ complex **180**²² had yet to be reported, we proposed that this strategy might nonetheless afford 14-electron Type IVa complexes. Subsequent allylation may then provide the paramagnetic 16-electron Type IV η^3 -allyl complexes (eq. 6.8). Since the cyclopentadienyl analogue of complex **180** readily disproportionates to form chromocene and chromous chloride,^{22, 23} this approach to prepare the Type IV complexes is presumably limited to the permethylcyclopentadienyl analogues.

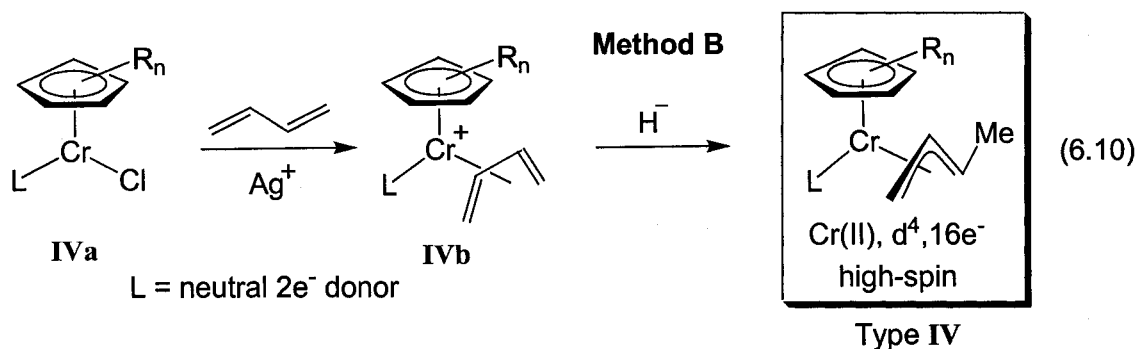


The formation of the sterically less encumbered Type IV $\text{CpCr}(\text{L})(\eta^3\text{-allyl})$ complexes may be accomplished by exploiting the work of Tilset, in which the reaction of the mildly acidic²⁴ IMesHCl salt with chromocene **178** affords the 14-electron complex $\text{CpCrCl}(\text{IMes})$ **179** in good yield.²⁵ Treatment of this complex with PhMgCl provides the thermally stable phenyl derivative **180** (eq. 6.9). Thus, the addition of allyl Grignard in place of PhMgCl may provide $\text{CpCr}(\text{IMes})(\eta^3\text{-allyl})$. This methodology

cannot be extended to decamethylchromocene **181**, which upon exposure to IMesHCl , instead forms $[\text{Cp}^*\text{CrCl}_3][\text{IMes}^+]$ **182** in undisclosed yield.²⁵

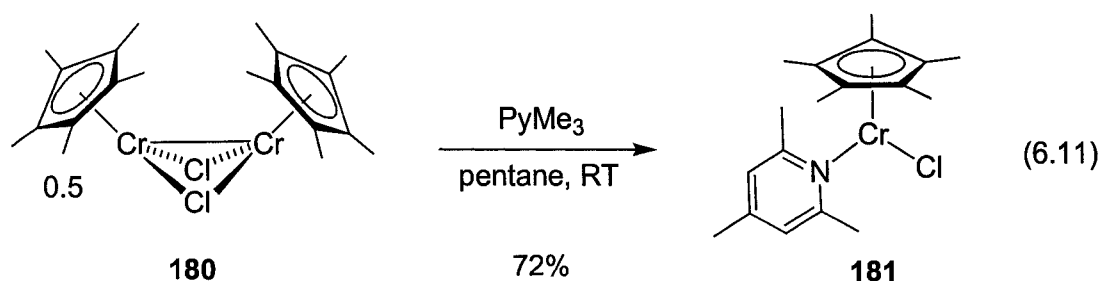


A second approach to prepare the Type IV η^3 -allyl complexes entails the coordination of conjugated dienes to cationic derivatives of Type IVa 14-electron complexes. Subsequent hydride attack on the consequent η^4 -diene ligand may then afford the desired chromium(I) η^3 -crotyl complexes (eq. 6.10). Indeed, similar chemistry has been demonstrated for the conversion of cationic $[\text{Co}(\text{CO})_3(\eta^4\text{-1,3-diene})]^+$ and $[\text{CpMo}(\text{CO})_2(\eta^4\text{-1,3-diene})]^+$ complexes to the neutral η^3 -allyl products.²⁶⁻²⁸



6.3.2 Synthesis and reactivity of a 14-electron 2,4,6-trimethylpyridine complex

In contrast to the addition of 2,4,6-trimethylpyridine to the chromium(III) complex $[\text{Cp}^*\text{CrCl}_2]_2$ **178**, similar treatment of the chromium(II) complex $[\text{Cp}^*\text{CrCl}]_2$ **180** leads immediately to the formation of a dark pink precipitate, isolated in 72% yield and subsequently identified as $\text{Cp}^*\text{Cr}(\text{PyMe}_3)\text{Cl}$ **181** by X-ray crystallography of crystals grown from toluene (eq. 6.10 and Fig. 6.1).



Further characterization of this novel complex via electron impact mass spectrometry was unfortunately ambiguous; only the PyMe_3 and Cp^*CrCl fragment ions could be identified in the mass spectrum. Combustion analysis of complex **181** also failed to provide accurate elemental composition data even when performed on X-ray quality crystals. It is therefore apparent that the hindered pyridine ligand of this complex is only weakly bound to the metal centre. Indeed, heating a solution of complex **181** in THF to 60 °C results in decomposition and the formation of intractable materials. In spite of this thermal lability, the closest known structural analogue of this complex is the trivalent $\text{Cp}^*\text{Cr}(\text{pyridine})\text{Cl}_2$ species.²⁹ Indeed, to the best of our knowledge, complex **181** is the first example of a divalent $\text{Cp}^*\text{Cr}(\text{donor})\text{Cl}$ species derived from $[\text{Cp}^*\text{CrCl}]_2$.

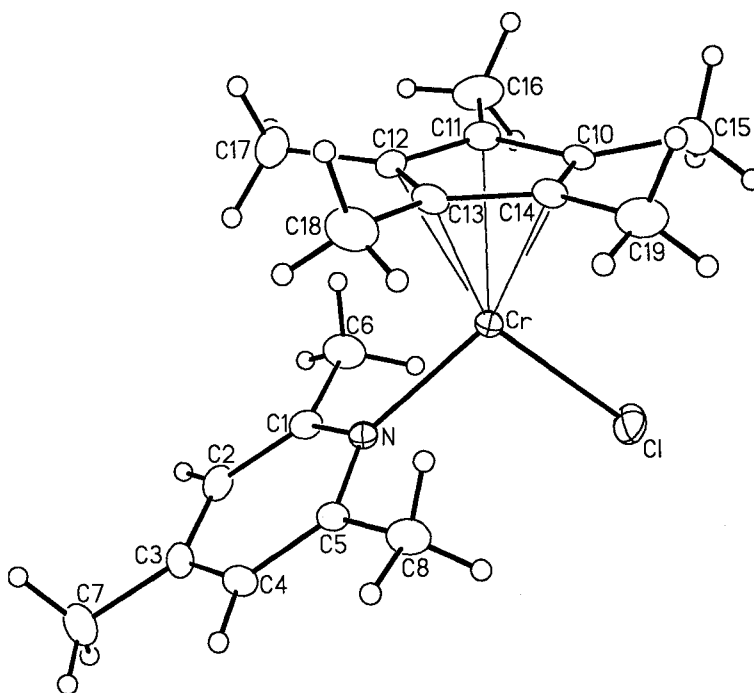


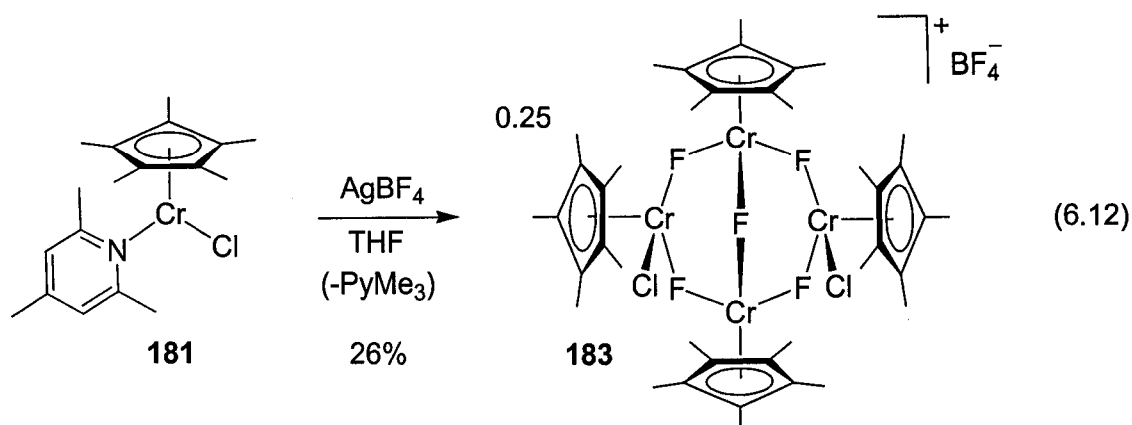
Figure 6.1: The solid-state molecular structure of $[(\eta^5\text{-C}_5\text{Me}_5)\text{CrCl}(2,4,6\text{-trimethylpyridine})]$ **181**. Non-hydrogen atoms are represented by Gaussian ellipsoids at the 20% probability level. Hydrogen atoms are shown with arbitrarily small thermal parameters. Selected bond lengths (Å) and angles (deg): Cr-Cl = 2.2938(13), Cr-N = 2.103(3), N-C(1) = 1.350(5), N-C(5) = 1.365(5); Cl-Cr-N = 98.69(9), Cr-N-C(1) = 121.3(3), Cr-N-C(5) = 117.8(3).

Despite the novelty of this complex, attempts to convert it into an η^3 -allyl bearing species met with no success. Addition of allyl Grignard reagents or tetraallyltin, for example, leads only to the formation of intractable brown products, resulting perhaps from Cr-allyl bond homolysis of the putative $\text{Cp}^*\text{Cr}(\text{PyMe}_3)(\text{allyl})$ intermediate **182**. To improve the stability of this unidentified species, it may thus be necessary to incorporate isopropyl or *tert*-butyl substituents at the 2- and 6- position of the pyridine ligand, but we have yet to explore this possibility.

We also studied the reaction between allyl chloride and complex **181**, which, in theory, could provide a 1 : 1 mixture of $[\text{Cp}^*\text{CrCl}_2]_2$ **178** and the unknown desired chromium(III) allyl complex $\text{Cp}^*\text{CrCl}(\eta^3\text{-allyl})$. Thus, heating an equimolar mixture of allyl chloride and complex **181** in THF to 40 °C results in a colour change from purple to blue. Unfortunately, however, the product of this reaction was determined to be $[\text{Cp}^*\text{CrCl}_2]_2$ **178** alone, formed in near-quantitative yield, via combustion analysis. Although 1,5-hexadiene may have formed as a by-product, we did not analyze the reaction mixture for the presence of this molecule.

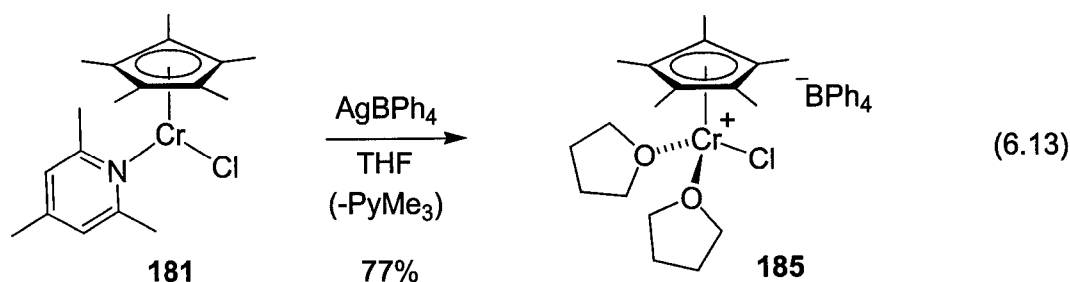
6.3.3 Attempted coordination of conjugated dienes to $\text{Cp}^*\text{CrCl}(\text{PyMe}_3)$

The addition of conjugated dienes to $\text{Cp}^*\text{CrCl}(\text{PyMe}_3)$ complex **181** in the presence of silver salts provided isolable, albeit highly unexpected, products. Treatment of a mixture of complex **181** and excess isoprene in THF with AgBF_4 , for example, leads to an immediate colour change from purple to blue along with the formation of a grey precipitate. Single crystals were obtained from a solution of the blue product in a 1 : 1 mixture of THF and diethyl ether and the molecular structure identified to be that of the trivalent tetranuclear complex $[\text{Cp}^*_4\text{Cr}_4(\mu\text{-F})_5\text{Cl}_2]\text{BF}_4$ **183** via X-ray crystallography (eq. 6.9). The previously reported PF_6^- analogue of this complex is formed by means of a gradual decomposition of the ethylene polymerization catalyst $[\text{Cp}^*\text{Cr}(\text{CH}_3)(\text{THF})_2]\text{PF}_6$ **184** in dichloromethane.³⁰⁻³² Since the respective bond lengths and angles of the cations of both salts of complex **183** are identical, we did not perform a complete structural analysis of the BF_4^- congener.



The mechanism of formation of this unexpected product remains unclear. It is apparent, however, that one-electron oxidation of the PyMe_3 complex **181** is a more energetically favourable reaction pathway than the desired dehalogenation reaction. Moreover, this oxidation to chromium(III) clearly promotes rapid degradation of the BF_4^- and PF_6^- counterions. We therefore questioned if this decomposition pathway could be avoided via treatment of complex **181** with AgBPh_4 , which is devoid of abstractable halogen.

Thus, the addition of one equivalent of silver tetraphenylborate to a solution of complex **181** in THF immediately generates a deep blue solution and a grey precipitate. Subsequent crystallization of the blue product afforded needle-like crystals of the novel cationic bis(THF) complex **185** in 77% yield, as determined by X-ray crystallography (eq. 6.13 and Fig. 6.2).



As noted for the tetranuclear complex **183**, the three-legged piano stool complex **185** clearly arises as a result of oxidation of the metal centre along with concomitant loss of the bulky pyridine ligand. However, since fluoride ions are absent in this reaction, the chromium(III) centre in this case coordinates two solvent molecules to form a stable, nominally 15-electron complex. Interestingly, all other examples of known cationic trivalent cyclopentadienyl bis(THF) chromium complexes possess alkyl or alkoxide ligands rather than halides.^{31, 33, 34}

The use of silver tetraphenylborate thus avoids the formation of multinuclear chromium halide complexes, however, it fails to remove the chloride ligand from complex **181**, preferring instead to oxidize the metal centre. Moreover, addition of isoprene to this reaction fails to provide any evidence of even transient diene coordination. Further research in this area therefore requires the use of non-oxidative halide abstraction reagents.

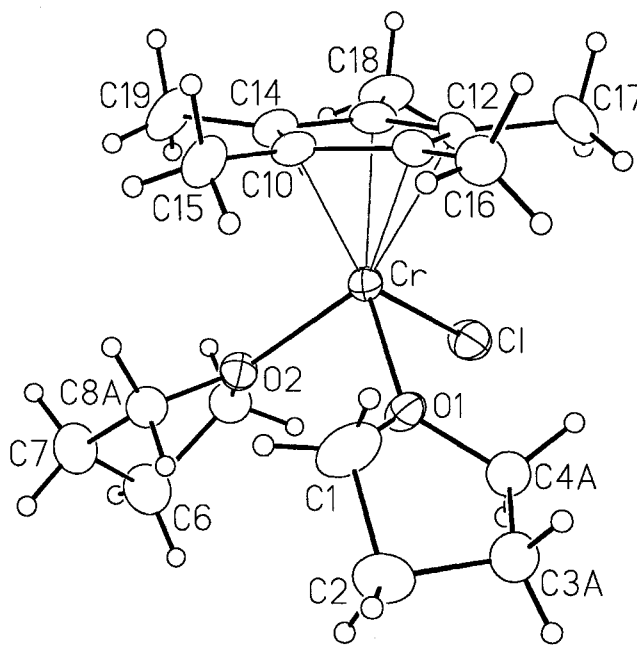


Figure 6.2: The solid-state molecular structure of $[\text{Cp}^*\text{Cr}(\text{THF})_2\text{Cl}][\text{BPh}_4] \cdot \text{C}_4\text{H}_8\text{O}$ **185**. The BPh_4^- anion and the interstitial THF molecule are omitted. Non-hydrogen atoms are represented by Gaussian ellipsoids at the 20% probability level. Hydrogen atoms are shown with arbitrarily small thermal parameters. Selected bond lengths (Å) and angles (deg): $\text{Cr}-\text{Cl} = 2.2934(17)$, $\text{Cr}-\text{O}(1) = 2.053(3)$, $\text{Cr}-\text{O}(2) = 2.057(3)$, $\text{O}(1)-\text{C}(1) = 1.407(7)$, $\text{O}(1)-\text{C}(4\text{A}) = 1.447(10)$, $\text{O}(2)-\text{C}(5\text{A}) = 1.421(13)$, $\text{O}(2)-\text{C}(8\text{A}) = 1.443(12)$, $\text{C}(1)-\text{C}(2) = 1.495(9)$, $\text{C}(2)-\text{C}(3\text{A}) = 1.550(12)$, $\text{C}(3\text{A})-\text{C}(4\text{A}) = 1.517(13)$, $\text{C}(5\text{A})-\text{C}(6) = 1.595(13)$, $\text{C}(6)-\text{C}(7) = 1.464(9)$, $\text{C}(7)-\text{C}(8\text{A}) = 1.507(13)$; $\text{Cl}-\text{Cr}-\text{O}(1) = 93.97(11)$, $\text{Cl}-\text{Cr}-\text{O}(2) = 94.55(11)$, $\text{O}(1)-\text{Cr}-\text{O}(2) = 87.04(15)$.

6.3.4 Synthesis and reactivity of $\text{Cp}'\text{Cr}(\text{IMes})\text{Cl}$ complexes

Although $\text{Cp}^*\text{Cr}(\text{PyMe}_3)\text{Cl}$ **181** qualifies as a Type **IVa** complex, it is not amenable to allyl anion addition and possesses a thermally labile donor ligand. We were therefore hopeful that allylation of the structurally similar $\text{CpCr}(\text{IMes})\text{Cl}$ complex **179**,²⁵ which possesses a more thermally robust dative bond,^{35, 36} would alleviate the lability

problem. Unfortunately, however, the addition of allyl Grignard, -lithium, or -tin reagents to this unsaturated complex leads only to the formation of intractable products.

Given the probability that this is likely a result of reduction of the metal centre via Cr-allyl σ -bond homolysis or bimolecular decomposition via ligand exchange, we targeted allylation of the permethylcyclopentadienyl analogue of complex **179**. The presence of the more sterically hindered ancillary C_5Me_5 ligand in this complex might inhibit the bimolecular decomposition process via kinetic control or reduce the rate of homolysis via greater electronic stabilization of the chromium(II) σ -allyl intermediate. Unfortunately, the procedure for the synthesis of $\text{Cp}^*\text{Cr}(\text{IMes})\text{Cl}$ **187**, as reported in a patent,³⁷ via the addition of IMes to $[\text{Cp}^*\text{CrCl}]_2$ **180** does not provide data to support the formation or the identity of this complex; in our hands, reproducing this procedure provides no isolable products.

Because the reaction between IMesHCl and decamethylchromocene **181** affords only $[\text{Cp}^*\text{CrCl}_3][\text{IMes}^+]$ **182**,²⁵ we speculated that similar treatment of pentamethylchromocene **186** might provide $\text{Cp}^*\text{Cr}(\text{IMes})\text{Cl}$ **187** by way of selective protonation of the less hindered cyclopentadienyl ligand. Surprisingly, however, no procedure for the synthesis of the necessary mixed chromocene has been reported. The previously reported $\text{CpCr}(\eta^5\text{-ethyltetramethylcyclopentadienyl})$ complex, however, is prepared in under 40% yield via the addition of NaCp to $[\eta^5\text{-(C}_5\text{Me}_4\text{Et)CrCl}]_2$, prepared *in situ*.³⁸ A modification of this procedure therefore provided us with Cp^*CrCp **186** in very good yield (eq. 6.14). X-ray crystallography of crystals grown from pentane reveals the structure of a typical mixed sandwich complex, displaying only a 4.27° deviation between the planes formed by the Cp and Cp^* rings (Fig. 6.3).³⁹

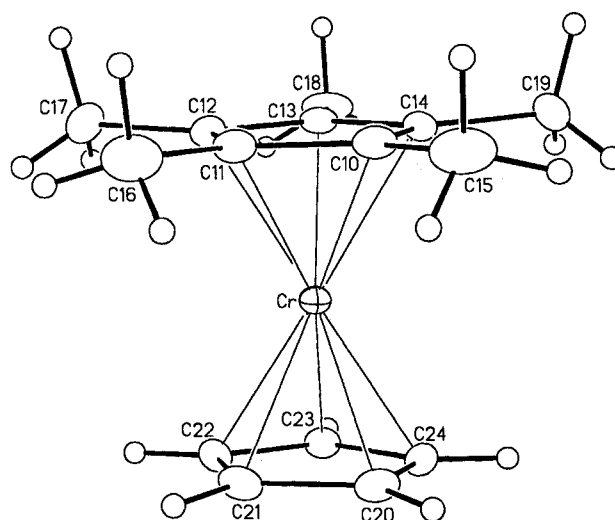
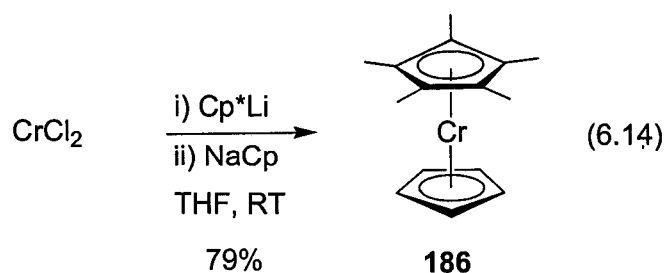
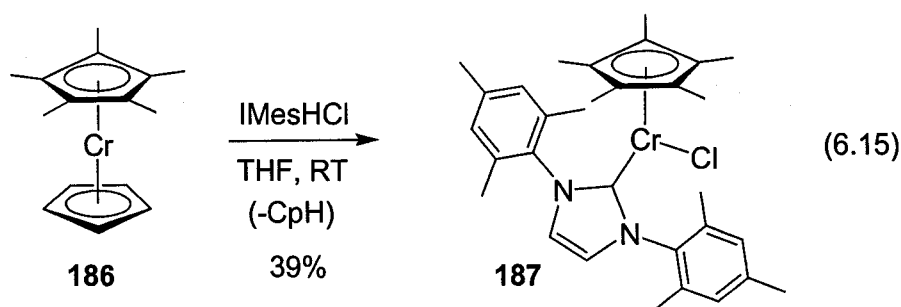


Figure 6.3: The solid-state molecular structure of $(\eta^5\text{-C}_5\text{Me}_5)\text{Cr}(\eta^5\text{-C}_5\text{H}_5)$ **186**. Non-hydrogen atoms are represented by Gaussian ellipsoids at the 20% probability level. Hydrogen atoms are shown with arbitrarily small thermal parameters. Selected bond lengths (Å): Cr-C(10) = 2.146(2), Cr-C(11) = 2.134(2), Cr-C(12) = 2.151(2), Cr-C(13) = 2.169(2), Cr-C(14) = 2.165(2), Cr-C(20) = 2.144(2), Cr-C(21) = 2.139(2), Cr-C(22) = 2.160(2), Cr-C(23) = 2.184(2), Cr-C(24) = 2.174(2).

The addition of IMesHCl to a solution of the mixed chromocene **186** indeed provides the desired complex $\text{Cp}^*\text{Cr}(\text{IMes})\text{Cl}$ **187** in 39% yield, after recrystallization

from diethyl ether (eq. 6.15). Characterization of this novel adduct by high resolution electron impact mass spectrometry reveals the expected molecular ion of $m/z = 526.22026$; however, combustion analysis failed to afford data consistent with the elemental composition of this extremely air and moisture sensitive compound. Nonetheless, single crystals of complex **187** were obtained and the structure confirmed by X-ray crystallography (Fig. 6.4).



The crystal structure of this monomeric 14-electron complex clearly reveals the skewed orientation of the carbene mesityl groups which, in conjunction with the methyl groups of the permethylcyclopentadienyl ligand, forms a sterically imposing enclosure around the chloride ligand. Unfortunately, despite this sterically shielded environment, addition of allylating reagents to complex **187** leads only to the formation of intractable product mixtures.

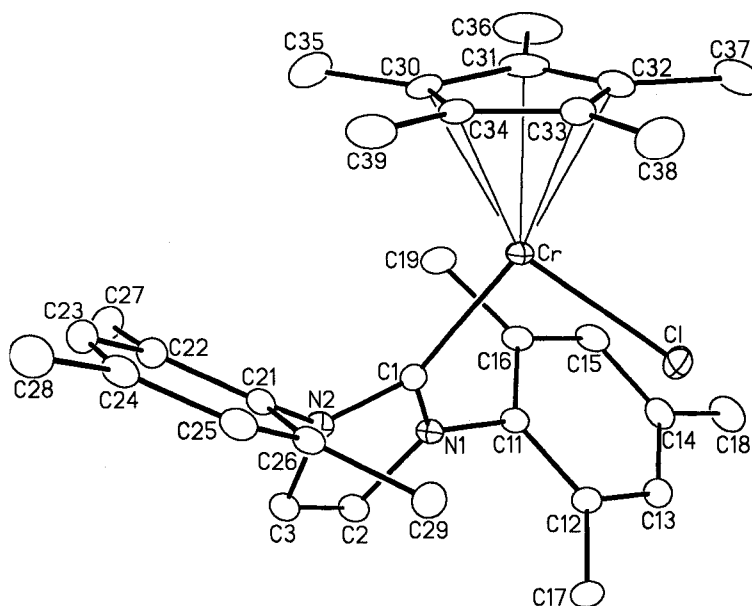
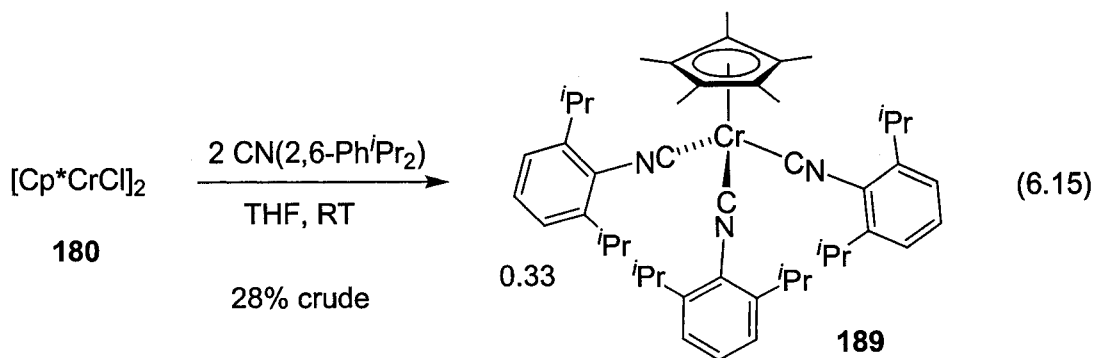


Figure 6.4: The solid-state molecular structure of $(\eta^5\text{-Me}_5\text{C}_5)(1,3\text{-dimesitylimidazoline-2-ylidene})\text{chlorochromium(II)}$ **187**. Non-hydrogen atoms are represented by Gaussian ellipsoids at the 20% probability level. Hydrogen atoms are not shown. Selected bond lengths (Å) and angles (deg): Cr-Cl = 2.3001(10), Cr-C(1) = 2.127(3), N(1)-C(1) = 1.369(4), N(1)-C(2) = 1.388(4), N(1)-C(11) = 1.447(4), C(2)-C(3) = 1.333(5); Cl-Cr-C(1) = 95.53(9), N(1)-C(1)-N(2) = 103.4(3), C(1)-N(1)-C(11) = 127.4(3), C(1)-N(2)-C(21) = 127.5(3).

6.3.5 Formation of a tris(2,6-diisopropylphenyl isocyanide)chromium(I) complex

As a final effort directed toward the synthesis of $\text{Cp}^*\text{Cr(L)Cl}$ complexes amenable to allyl anion addition, we explored the synthesis of complexes in which the donor ligand (L) is a sterically encumbered isocyanide molecule. Isocyanides are isoelectronic with CO, and capable of both ligand-to-metal σ -donation and metal-to-ligand π -backbonding,⁴⁰ and thus may lead to the formation of isolable $\text{Cp}^*\text{Cr(CNR)}(\eta^3\text{-allyl})$ complexes.

Relatively few chromium isocyanide complexes have been reported; none possess the $\text{Cp}^*\text{Cr}(\text{CNR})\text{X}$ (X = halide) structure suitable for our goals.^{29, 41-46} Our first attempt to prepare these 14-electron complexes began with the addition of one equivalent of 2,6-diisopropylphenylisocyanide,^{47, 48} to a solution of $[\text{Cp}^*\text{CrCl}]_2$ **180** in THF. Removal of the solvent and trituration of the red residue with pentane left behind a blue powder, the identity and yield of which have yet to be determined. Subsequent cooling of the pentane extracts deposited an orange-red powder. Surprisingly, analysis of this product via high resolution electron impact mass spectrometry provided no evidence for the presence of a chloride ligand; a molecular ion with $m/z = 748.46561$ and two daughter fragment ions with $m/z = 561.3303$ and 374.19405 suggested the presence of Cp^*Cr species bearing three, two, and one isocyanide ligand(s), respectively. The source of these ions was tentatively attributed to the unexpected neutral complex $\text{Cp}^*\text{Cr}[\text{CN}(2,6\text{-Ph}^i\text{Pr}_2)]_3$ **189** (eq. 6.15).



Verification of the composition of this unusual molecule was impeded by persistent impurities; combustion analysis provided only tenuous data. Fortunately, however, crystals of this complex were grown from pentane and the proposed structure

confirmed by X-ray crystallography (Fig. 6.5). Although the low resolution of this crystal structure prevents detailed analysis, the molecular composition and connectivity of this unprecedented 17-electron complex was nonetheless obtained.

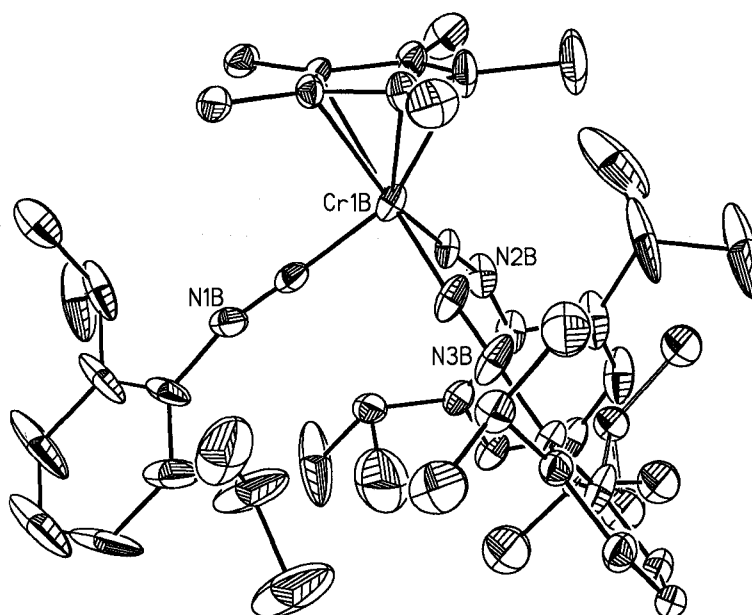
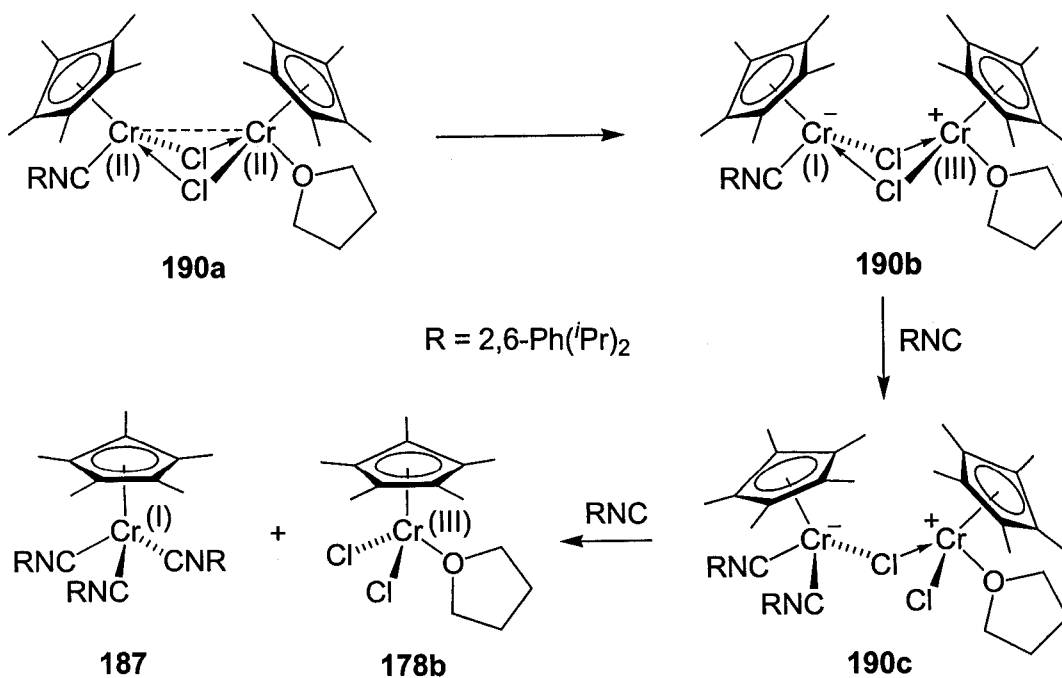


Figure 6.5: The solid-state molecular structure of the tris(2,6-diisopropylphenyl isocyanide)(η^5 -C₅Me₅)chromium(I) complex **189**. Due to the poorly diffracting crystal, accurate structural data could not be obtained.

The formation of this unexpected paramagnetic chromium(I) product may be rationalized by a redox disproportionation mechanism (Scheme 6.4), initiated by the formation of the unsymmetrical dinuclear species **190a**, with coordination of an isocyanide to one of the chromium centres of dimer **180** and coordination of solvent to the remaining chromium centre. As a result of the isocyanide π -acidity, the relatively

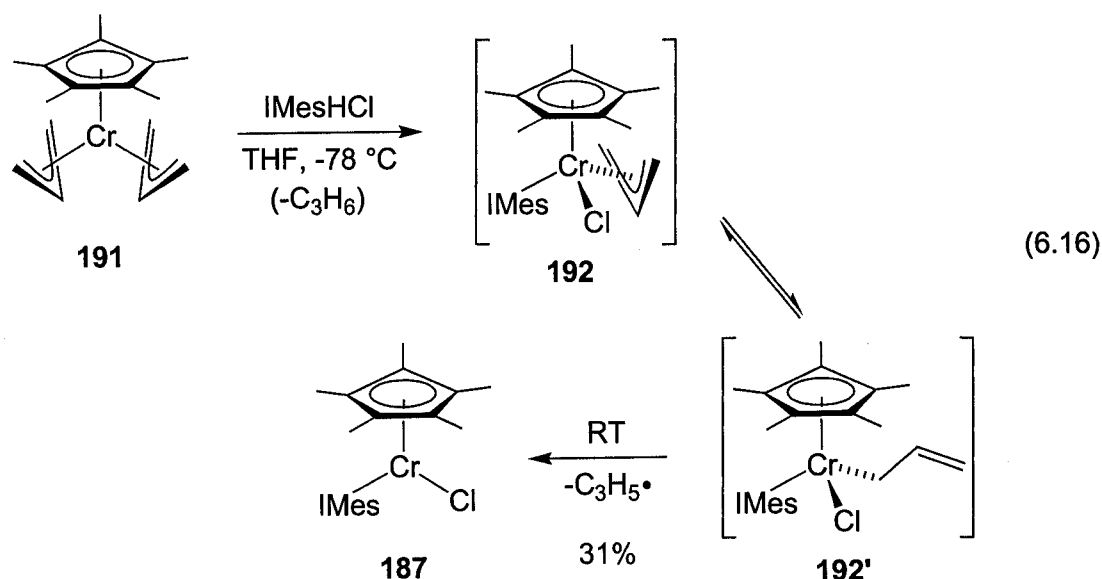
electron poor isocyanide-bearing chromium centre is reduced internally by the THF-coordinated metal centre, to form the mixed-valent intermediate **190b**. Successive coordination of two additional isocyanide molecules to the chromium(I) centre along with heterolytic cleavage of the remaining Cr(I)–Cl bond then affords complex **187** and, possibly, $\text{Cp}^*\text{Cr}(\text{THF})\text{Cl}_2$ **178b**. The latter complex is known to exist in solution, while in the solid-state forming the blue chromium(III) dimer $[\text{Cp}^*\text{CrCl}_2]_2$,¹⁹ identical in colour to that of the blue residue isolated from this reaction. Further support for this tenuous mechanism is the apparent low yield (~28%) of complex **187**, which approaches the maximum theoretical yield of 33% for reaction of one equivalent of isocyanide (per chromium) with $[\text{Cp}^*\text{CrCl}_2]_2$. Unfortunately, the addition of excess isocyanide fails to provide a significantly increased yield of this unusual product.

Scheme 6.4

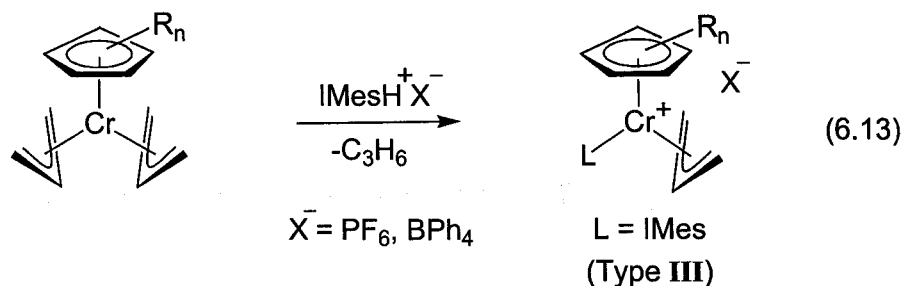


6.3.6 The reaction of imidazolium salts with $\text{Cp}^*\text{Cr}(\eta^3\text{-allyl})_2$

Although our attempts to prepare Type IV $\eta^3\text{-allyl}$ complexes were unsuccessful, the pursuit of $\text{Cp}^*\text{Cr}(\text{IMes})\text{Cl}$ complexes **179** and **187** prompted us to consider other allylchromium precursors potentially amenable to protonation by IMesHCl . Thus, the addition of this imidazolium salt to the thermally unstable chromium(III) complex $\text{Cp}^*\text{Cr}(\eta^3\text{-allyl})_2$ **191** was investigated, targeting the corresponding trivalent complex $\text{Cp}^*\text{Cr}(\text{IMes})(\eta^3\text{-allyl})\text{Cl}$ **192**. Unfortunately, however, this reaction provides only the previously characterized divalent complex $\text{Cp}^*\text{Cr}(\text{IMes})\text{Cl}$ **187**, as determined by mass spectrometry and X-ray crystallography. The formation of **187** presumably proceeds via homolysis of the $\sigma\text{-allyl}$ intermediate **192'** (eq. 6.16).



The nominally seven-coordinate geometry of the proposed η^3 -allyl intermediate **192** is unfavourable for many cyclopentadienyl organochromium complexes.⁴¹ To avoid this steric congestion imidazolium salts bearing non-coordinating counterions were introduced, hopefully leading to Type **III** η^3 -allyl complexes (eq. 6.17).

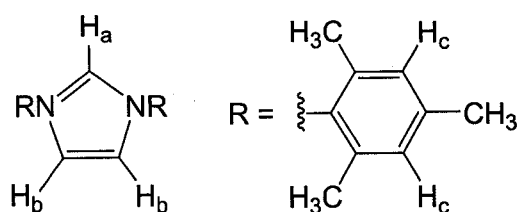


IMesH⁺PF₆[−] was therefore prepared according to the literature procedure⁴⁹ and IMesH⁺BPh₄[−] via a modification thereof. Surprisingly, however, the addition of either of these salts to bis(allyl) complex **192** failed to effect any reaction; thermal decomposition of the starting complex proceeds as if IMesH⁺X[−] was absent. Equally unexpectedly, these salts also fail to react either with chromocene **178** or pentamethylchromocene **186**, even upon heating to 60 °C.

These observations imply that the Brønsted acidity of the unreactive imidazolium salts is significantly lower than that of the chloride analogue. A comparison of the ¹H NMR data for all three IMesHX salts reveals that the chemical shift of the acidic imidazolium proton is markedly dependent on the counterion, with relatively little difference between the shifts of the other proton resonances (Table 6.1). Since hydrogen bonding increases the acidity of carbon acids⁵⁰ and chloride ion is a classical hydrogen bond acceptor, it is reasonable to assume that the reactive nature of IMesHCl, as well as

the relatively downfield chemical shift of the acidic proton, is a direct result of a corresponding hydrogen-chloride bonding interaction. Although the crystal structure of this compound is known,⁵¹ the position of the acidic proton has not been refined, thus preventing corroboration of this proposed interaction.

Table 6.1: ¹H NMR data (ppm) of the IMesHX (X = Cl[−], PF₆[−], BPh₄[−]) salts in CDCl₃. The labeling scheme is shown below.



X =	H _a	H _b	H _c	<i>ortho</i> -CH ₃	<i>para</i> -CH ₃
Cl [−]	11.02 (t, <i>J</i> = 1.5 Hz)	7.58 (d, <i>J</i> = 1.5 Hz)	7.04 (s)	2.20 (s)	2.32 (s)
PF ₆ [−]	8.68 (t, <i>J</i> = 1.5 Hz)	7.53 (d, <i>J</i> = 1.5 Hz)	7.02 (s)	2.01 (s)	2.34 (s)
^a BPh ₄ [−]	6.97 (t, <i>J</i> = 1.8 Hz)	6.19 (d, <i>J</i> = 1.8 Hz)	7.04 (s)	1.90 (s)	2.40 (s)

^aThe proton resonances of the BPh₄[−] anion have been omitted, refer to the Experimental Section for full characterization data of this imidazolium salt.

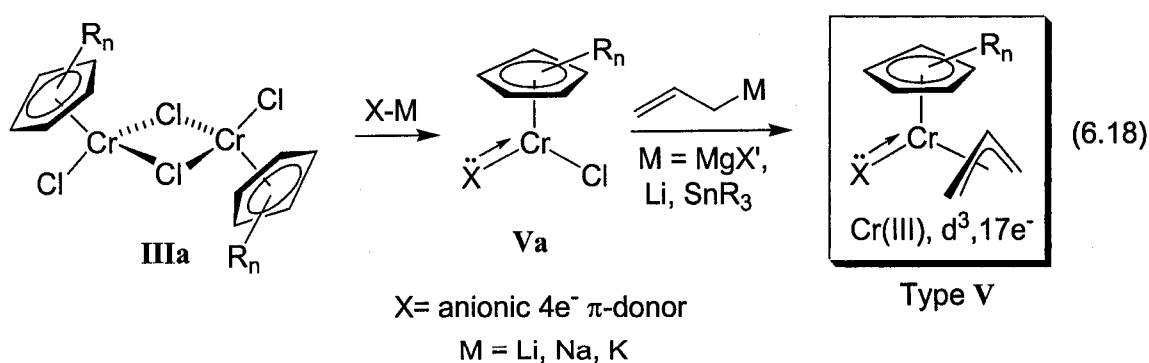
The relative unreactivity of the noncoordinating IMes salts is thus attributed to the lack of hydrogen bonding between the counterions and the acidic proton. The minor discrepancies between the chemical shifts of several of the protons of the BPh₄[−] salt and those of the PF₆[−] congener can be attributed to either magnetic anisotropic shielding from

the phenyl rings of the BPh_4^- anion and/or the presence of a relatively weak hydrogen bonding interaction between the acidic proton and a fluorine atom of the PF_6^- anion. To the best of our knowledge, there have been no other discussions of this phenomenon among acidic N-heterocyclic carbene precursors and its effect on the reactivity of imidazolium salts toward organometallic compounds.

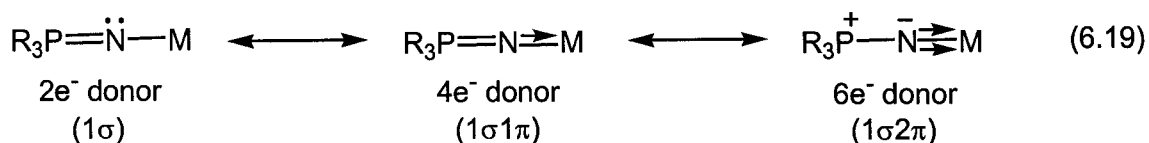
6.4 Phosphinimide chromium complexes as η^3 -allyl precursors

6.4.1 Introduction

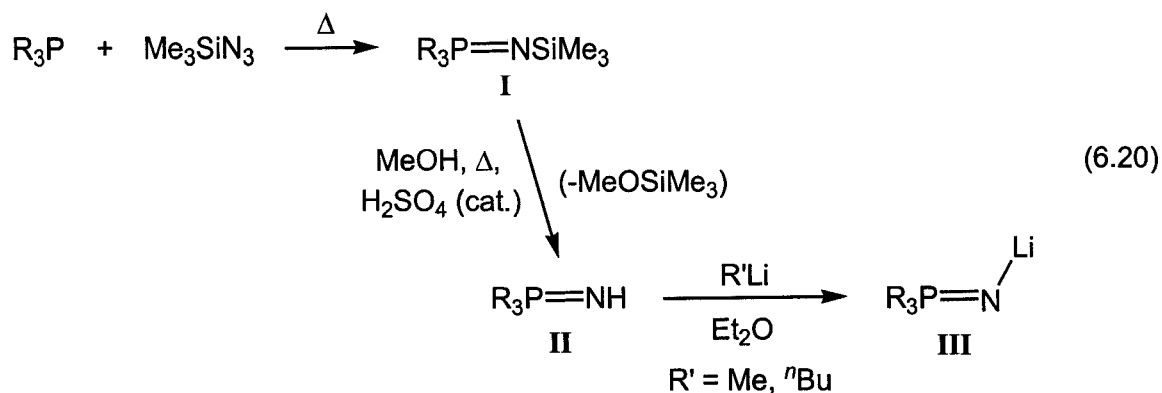
Our final approach to the synthesis of *pseudo*-tetrahedral chromium η^3 -allyl complexes via non-carbonyl sources entailed the preparation of nominally 17-electron chromium(III) Type V target complexes via allylation of Type Va complexes (eq. 6.18). Preparation of such coordinatively unsaturated 15-electron precursor complexes may be possible via a metathesis of alkali metal salts of π -donating X-type molecules and dimeric $[\text{Cp}'\text{CrCl}_2]_2$ complexes (eq. 6.18).



Given the recent demonstration of phosphinimide ligands in organotitanium chemistry, particularly in the area of catalytic olefin polymerizations,⁵²⁻⁵⁹ we were curious to evaluate the effect of incorporating such strongly electron donating ligands in the proposed Type **Va** organochromium complexes. In addition to stabilizing electronically unsaturated transition metal complexes by donating up to six electrons to the metal centre via (1σ2π)-type donation (eq. 6.19),⁶⁰ these nitrogen-bound ligands are considered to be steric analogues of cyclopentadienyl ligands.⁵² If this is indeed the case, then a Type **V** η³-allyl chromium complex bearing a phosphinimide ligand would be a very close structural analogue of the metallacyclobutane precursors Cp'₂Ti(η³-allyl), discussed previously in Chapter 1 (p. 14). Moreover, the successful formation of such chromium phosphinimide complexes would represent the first examples of the Cp'Cr(N=PR₃)X (X = halide) structural class.

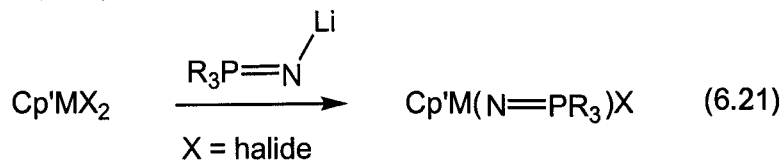


One established synthesis of phosphinimide ligand precursors entails the initial oxidation of tertiary phosphines by tosyl azide to provide the trimethylsilyl phosphinimine product **I** (eq. 6.20).⁶¹ Subsequent desilylation in acidic methanol results in the amine derivative **II**,⁶² which upon treatment with an alkyl lithium reagent affords the lithiated phosphinimide **III**.^{63, 64}

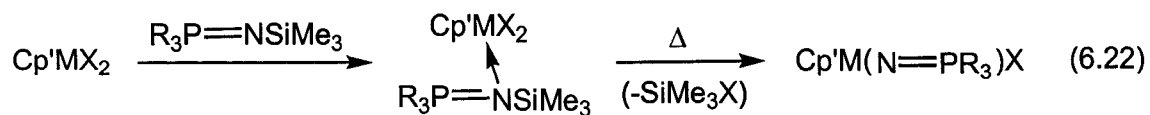


One general synthesis of transition metal phosphinimide complexes involves the addition of the lithio-phosphinimide compound **III** to the requisite metal halide (Method A, eq. 6.21).⁵² Phosphinimide complexes can also be prepared via the addition of trimethylsilyl phosphinimine **I** to organometallic halides via elimination of Me_3SiX ($\text{X} =$ halide) from the Lewis base adduct (Method B, eq. 6.22).⁵²

Method A



Method B



There are no examples of the preparation of chromium phosphinimide complexes via either of these approaches; however, the formation of $\text{CrCl}_2(\text{Me}_3\text{Si}-\text{N}=\text{PMe}_3)_2$ **193** has been reported. This complex fails to lose Me_3SiCl upon heating to reflux in dichloromethane.⁶⁵ The trivalent pincer-phosphinimine complex $[\text{HC}(\text{Ph}_2\text{P}=\text{N}-\text{SiMe}_3)_2\text{Cr}(\mu-\text{Cl})_2]$ **194** is prepared from $[\text{HC}(\text{Ph}_2\text{P}=\text{N}-\text{SiMe}_3)]\text{Li}$ and $\text{CrCl}_2(\text{THF})_2$.⁶⁶

6.4.2 Disproportionation of a phosphinimide ligand

To provide steric protection for the targeted $\text{Cp}^*\text{Cr}(\text{N}=\text{PR}_3)(\eta^3\text{-allyl})$ complexes and resistance to reduction at chromium by $\eta^1\text{-allyl}$ bond homolysis, we chose to use phosphinimide ligands possessing *tert*-butyl substituents. Unfortunately, however, we could not reproduce the published procedure for the requisite lithium phosphinimide.^{63, 64} All attempts to prepare $t\text{-Bu}_3\text{P}=\text{N}-\text{Li}$ resulted in the formation of a multitude of phosphorus containing salts, as ascertained by ^1H and ^{31}P NMR spectroscopy.

We therefore investigated the coordination of one equivalent of $t\text{-Bu}_3\text{P}=\text{N}(\text{TMS})$ to each chromium centre of $[\text{Cp}^*\text{CrCl}_2]_2$ **178**, hoping to induce the loss of Me_3SiCl in a subsequent step. This reaction provided two products after trituration into ether and THF and evaporation to dryness. Fortunately, crystallization of the purple-blue product from toluene provided crystals suitable for X-ray diffraction and the structure was identified to be the organochromium salt $[\text{Cp}^*\text{CrCl}_3^-][t\text{-Bu}_3\text{PNH}_2^+]$ **195** (Fig. 6.6); the yield of the purple-blue powder was subsequently determined to be 48% based on the amount of chromium present. The identity and yield of the second product from this reaction could not be determined.

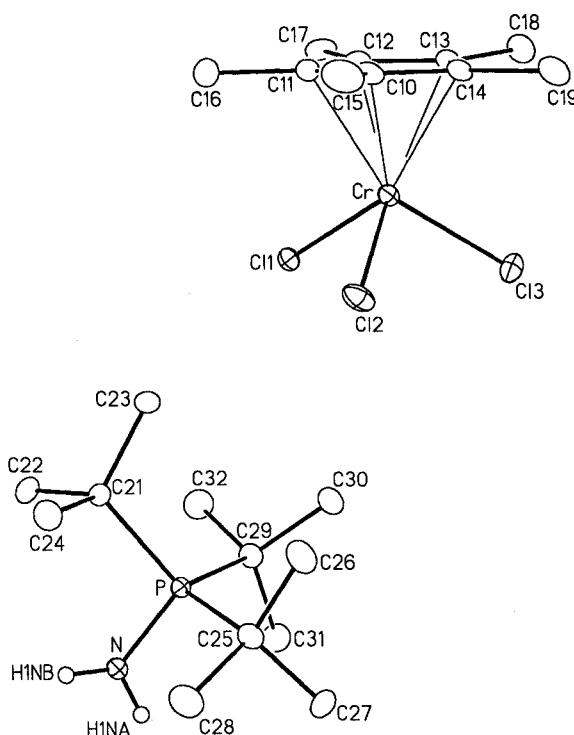


Figure 6.6: The solid-state molecular structure of $[\text{Cp}^*\text{CrCl}_3][{}^t\text{Bu}_3\text{PNH}_2]$ **195**. Non-hydrogen atoms are represented by Gaussian ellipsoids at the 20% probability level. Hydrogen atoms are shown with arbitrarily small thermal parameters for the amino group; the remaining hydrogen atoms are not shown. Selected bond lengths (Å) and angles (deg): Cr-Cl(1) = 2.3557(9), Cr-Cl(2) = 2.2934(9), Cr-Cl(3) = 2.3315(9), P-N = 1.638(3), P-C(21) = 1.863(3), P-C(25) = 1.866(3), P-C(29) = 1.871(3), N-H(1NA) = 0.79(3), N-H(1NB) = 0.89(3); N-P-C(21) = 103.86(15), N-P-C(25) = 109.42(14), N-P-C(29) = 113.58(15), H(1NA)-N-H(1NB) = 112(3), H(1NA)-N-P = 114(3), H(1NB)-N-P = 111(2).

Although the constituent $[\text{Cp}^*\text{CrCl}_3]^-$ and $[{}^t\text{Bu}_3\text{PNH}_2]^+$ ions of complex **195** are not unprecedented,^{25, 63, 67-70} we cannot provide a mechanistic rationale for the formation of this unexpected compound. Intriguingly, however, the same distribution of products is obtained upon conducting the addition reaction in a silanized glass reaction vessel, excluding the potential involvement of boro-silicate surface silanol residues in this

chemistry. Conducting this reaction using $[\text{Cp}^*\text{CrCl}_2]_2$ **174** results in the isolation of two unidentified products identical in colour to the products obtained from reaction with the complex $[\text{Cp}^*\text{CrCl}_2]_2$ **178**, but still unidentified. The addition of $t\text{Bu}_3\text{PN}(\text{TMS})$ to $\text{CrCl}_2(\text{THF})$, followed by treatment with Cp^*Li also provides a mixture of unidentified blue and purple-blue products.

Thus, our attempts to prepare Type V η^3 -allyl complexes from phosphinimide chromium sources have so far been unsuccessful. The synthesis of these targeted complexes may therefore require the use of the elusive $t\text{Bu}_3\text{P}=\text{N}-\text{Li}$ salt, or the use of phosphinimine ligands less prone to disproportionation reactions..

6.5 Conclusions

Our efforts to prepare Types II-V *pseudo*-tetrahedral η^3 -allyl complexes have, unfortunately, been unsuccessful. The addition of allyl-containing reagents to the chromium(I) nitrosyl complexes, for example, leads only to the formation of intractable products. Given the thermal stability of the bis $[\eta^3-(1,3\text{-trimethylsilyl})\text{allyl}]$ complexes prepared by Hanusa,^{71, 72} future investigations in this area may benefit from the use of hindered 1,3-disubstituted allyl reagents.

The addition of the sterically hindered neutral donor molecules 2,4,6-trimethylpyridine and IMes to $[\text{Cp}^*\text{CrCl}_2]$ provides little evidence for coordination to the metal centre. Thus, continued work in this area may be successful in preparing the targeted $\text{Cp}^*\text{Cr}(\text{L})\text{Cl}_2$ complexes by tethering the donor and permethylcyclopentadienyl ligands, a strategy employed by other research groups.^{10-13, 73} In contrast, 2,4,6-trimethylpyridine readily coordinates to the chromium(II) dimer $[\text{Cp}^*\text{CrCl}]_2$ to provide $\text{Cp}^*\text{Cr}(\text{PyMe}_3)\text{Cl}$ in

good yield. Unfortunately, however, subsequent allylation provides only intractable products. Future work in this area may also benefit from the incorporation of sterically encumbered 1,3-disubstituted allyl ligands.

Given that the chromium(III) product resulting from the addition of silver tetrafluoroborate to $\text{Cp}^*\text{Cr}(\text{PyMe}_3)\text{Cl}$ in the presence of conjugated dienes results in degradation of the BF_4^- ion, the unidentified product obtained from the addition of tetrafluoroboric acid to the $\text{CpCr}(\text{PMe}_3)(\eta^4\text{-butadiene})$ complex **176** may also result from a similar anion degradation. Successful conversion of this η^4 -diene complex to a trivalent η^3 -allyl chromium species may therefore require the use of protic acids containing more chemically inert counterions.⁷⁴

In spite of these setbacks, our efforts to synthesize 16-electron $[\text{Cp}'\text{Cr}(\text{NO})(\eta^3\text{-allyl})]^+$ complexes of Type I have resulted in the discovery of several interesting classes of organochromium complexes. For example, a reasonably general procedure for the synthesis of unprecedented $\text{CpCr}(\text{CO})_2(\eta^3\text{-allyl})$ complexes has been developed,⁷⁵ while oxidation of these neutral complexes with the nitrosonium ion provided the chromium(III) η^3 -allyl redox isomers in high yield. These complexes are the first reported examples of thermally stable chromium(III) η^3 -allyl complexes.⁷⁶

The introduction of a 370 nm cutoff filter to the photolysis of $\text{CpCrNO}(\text{CO})_2$ in the presence of olefins resulted in significantly improved yields of the previously reported $\text{CpCr}(\text{NO})(\text{CO})(\eta^2\text{-alkene})$ complexes. Preparation of the previously unknown permethylcyclopentadienyl series, however, does not require the use of this filter.⁷⁷ A series of $\text{CpCr}(\text{NO})(\text{CO})(\eta^2\text{-1,3-diene})$ and $\text{CpCrNO}(\eta^4\text{-s-trans-1,3-diene})$ complexes have also been prepared from >370 nm UV irradiation of $\text{CpCrNO}(\text{CO})_2$ in the presence

of conjugated dienes. Interestingly, synthesis of the permethylcyclopentadienyl analogues results in the formation of *only* the *s-trans* complexes. Unlike the less hindered cyclopentadienyl analogues, these $\text{Cp}^*\text{Cr}(\text{NO})(\eta^4\text{-1,3-diene})$ complexes do not require the use of the 370 nm filter and can be isolated and characterized in the solid-state.⁷⁷ The *s-trans* coordination mode of these complexes is completely unprecedented among the first-row transition metals. Moreover, all known examples of other chromium $\eta^4\text{-(1,3-diene)}$ complexes exclusively adopt the *s-cis* diene orientation.

Interestingly, photolysis of both $\text{CpCrNO}(\text{CO})_2$ and $\text{Cp}^*\text{CrNO}(\text{CO})_2$ in the presence of rigidly *s-cis* cyclic organic 1,3-dienes does not provide *s-cis* $\eta^4\text{-diene}$ complexes. Monomeric $\text{Cp}'\text{Cr}(\text{NO})(\text{CO})(\eta^2\text{-cyclic-1,3-diene})$ products were identified in both cases, as well as unexpected $[\text{Cp}^*\text{Cr}(\text{NO})(\text{CO})]_2(\mu\text{-}\eta^2\text{:}\eta^2\text{-cyclic-1,3-diene})$ complexes. We tentatively attribute this aversion to *s-cis* $\eta^4\text{-(1,3-diene)}$ coordination and the thermodynamic preference for *s-trans*- or $\eta^2\text{-(1,3-diene)}$ coordination to an energetically unfavourable interaction between the frontier molecular orbitals of the *s-cis* conjugated dienes and the Cp^*CrNO fragment. Corroboration of this assumption via computational methods is currently in progress in collaboration with Professor M. Klobukowski of the University of Alberta.

Reactivity studies have shown that protonation of both the $\text{CpCr}(\text{NO})(\text{CO})\text{-(}\eta^2\text{-1,3-diene)}$ and $\text{Cp}^*\text{Cr}(\text{NO})(\text{CO})(\eta^2\text{-cyclic-1,3-diene})$ series of complexes provides thermally stable $\eta^3\text{-allyl}$ products. More interesting, however, is the addition of tetravalent tin-hydride reagents to the $\text{Cp}^*\text{CrNO(s-trans-butadiene)}$ complex, which provided an unprecedented class of bimetallic $\text{Cp}^*(\text{R}_3\text{Sn})\text{Cr}(\text{NO})(\eta^3\text{-crotyl})$ complexes. The $\eta^3\text{-allyl}$ congener was prepared either by the thermal assisted oxidative addition of

allyltriphenyltin to the *s-trans* butadiene complex or from the photo-assisted double decarbonylation of $\text{Cp}^*\text{CrNO}(\text{CO})_2$ in the presence of allyltriphenyltin. Both of these methods are unprecedented procedures for the preparation of transition metal-tin η^3 -allyl complexes.

Clearly, the scope of this methodology must be investigated. Future work in this area should explore the use of substituted allyltin reagents as well as vinyl-, alkynyl-, and allenyltin compounds. Moreover, the addition of triphenyltin hydride to the η^4 -isoprene and η^4 -(2,3-dimethylbutadiene) congeners of the *s-trans* butadiene complex should also be investigated. These η^3 -allyl chromium-tin complexes may also be useful in nucleophilic reactions with carbonyl-containing organic compounds. Preliminary results suggest, however, that solutions of the η^3 -crotyl complex in benzene are unreactive toward benzaldehyde.

Preliminary investigations have also shown that the photolysis of $\text{Cp}^*\text{CrNO}(\text{CO})_2$ in the presence of triphenyltin hydride provides an unprecedented $\text{Cp}^*\text{Cr}(\text{NO})(\text{CO})$ -(η^2 -hydrido-stannane) species. Since we have only tentatively identified this product *in situ*, further research in this area will require isolation and full characterization of this complex. The insertion of unsaturated organic molecules into the 'Cr-H' bond of this tantalizing complex should also be studied.

Finally, the *s-trans* butadiene complex was found to undergo protonation by HBF_4 to provide the 16-electron species $[\text{Cp}^*\text{Cr}(\text{NO})(\eta^3\text{-allyl})]\text{BF}_4$, the first *pseudo*-tetrahedral allylchromium complex to be reported. Unfortunately, the severe thermal instability of this complex prevented a thorough study of potential central carbon alkylation reactions. Although this complex possesses a strongly π -acidic nitrosyl ligand to help maintain the

allyl moiety in the η^3 -coordination mode, the steric unsaturation about the metal centre may still allow for bimolecular decomposition. Improving the stability of this complex may therefore require the use of more sterically demanding ancillary ligands. Indeed, the so-called “tetrahedral enforcer” ligand, hydrotris(3-*tert*-butyl-5-methyl-pyrazolyl)-borate ($\text{Tp}^{t\text{Bu}, \text{Me}}$),⁷⁸ has been used in the synthesis of highly unsaturated thermally stable monomeric ($\text{Tp}^{t\text{Bu}, \text{Me}}$)CrR (R = Et, Ph, CH_2SiMe_3) complexes.⁷⁹ Thus, if ($\text{Tp}^{t\text{Bu}, \text{Me}}$)-Cr(NO)(η^4 -1,3-diene), or perhaps slightly less hindered analogues, could be prepared and then protonated with tetrafluoroboric acid, a series of *pseudo*-tetrahedral η^3 -allyl complexes with considerably more convenient thermal sensitivity might be obtained.

6.6 References

1. Legzdins, P.; Nurse, C. R. *Inorg. Chem.* **1985**, *24*, 327.
2. Legzdins, P.; McNeil, W. S.; Rettig, S. J.; Smith, K. M. *J. Am. Chem. Soc.* **1997**, *119*, 3513.
3. Legzdins, P.; Shaw, M. J. *Organometallics* **1995**, *14*, 4721.
4. Legzdins, P.; McNeil, W. S.; Shaw, M. J. *Organometallics* **1994**, *13*, 562.
5. Legzdins, P.; Shaw, M. J. *J. Am. Chem. Soc.* **1994**, *116*, 7700.
6. Chin, T. T.; Legzdins, P.; Trotter, J.; Yee, V. C. *Organometallics* **1992**, *11*, 913.
7. Legzdins, P.; McNeil, W. S. *J. Am. Chem. Soc.* **1994**, *116*, 6021.
8. Legzdins, P.; McNeil, W. S.; Batchelor, R. J.; Einstein, F. W. B. *J. Am. Chem. Soc.* **1995**, *117*, 10521.
9. Hames, B. W.; Legzdins, P.; Oxley, J. C. *Inorg. Chem.* **1980**, *19*, 1565.
10. Theopold, K. H. *Eur. J. Inorg. Chem.* **1998**, 15.
11. Liang, Y.; Yap, G. P. A.; Rheingold, A. L.; Theopold, K. H. *Organometallics* **1996**, *15*, 5284.
12. Döhring, A.; Gohre, J.; Jolly, P. W.; Kryger, B.; Rust, J.; Verhovnik, G. P. J. *Organometallics* **2000**, *19*, 388.
13. Döhring, A.; Jensen, V. R.; Jolly, P. W.; Thiel, W.; Weber, J. C. *Organometallics* **2001**, *20*, 2234.
14. Heintz, R. A.; Leelasubcharoen, S.; Liable-Sands, L. M.; Rheingold, A. L.; Theopold, K. H. *Organometallics* **1998**, *17*, 5477, and references therein.
15. Richeson, D. S.; Mitchell, J. F.; Theopold, K. H. *Organometallics* **1989**, *8*, 2570.
16. Noh, S. K.; Sendlinger, S. C.; Janiak, C.; Theopold, K. H. *J. Am. Chem. Soc.* **1989**, *111*, 9127.
17. Nishimura, K.; Kuribayashi, H.; Yamamoto, A.; Ikeda, S. *J. Organomet. Chem.* **1972**, *37*, 317.
18. Kurras, E. *Naturwissenschaften* **1959**, *46*, 171.

19. Betz, P.; Döhring, A.; Emrich, R.; Goddard, R.; Jolly, P. W.; Krüger, C.; Romão, C.; Schönfelder, K. U.; Tsay, Y.-H. *Polyhedron* **1993**, *12*, 2651.
20. Fujita, K.; Ohnuma, Y.; Yasuda, H.; Tani, H. *J. Organomet. Chem.* **1976**, *113*, 201.
21. Benn, H.; Wilke, G.; Henneberg, D. *Angew. Chem. Int. Ed.* **1973**, *12*, 1001.
22. Heintz, R. A.; Ostrander, R. L.; Rheingold, A. L.; Theopold, K. H. *J. Am. Chem. Soc.* **1994**, *116*, 11387.
23. Hermans, P. M. J. A.; Scholten, A. B.; Van den Beuken, E. K.; Bussard, H. C.; Roeloffsen, A.; Metz, B.; Reijerse, E. J.; Beurskens, P. T.; Bosman, W. P.; Smits, J. M.; Heck, J. *Chem. Ber.* **1993**, *126*, 533.
24. Amyes, T. L.; Diver, S. T.; Richard, J. P.; Rivas, F. M.; Toth, K. *J. Am. Chem. Soc.* **2004**, *126*, 4366.
25. Voges, M. H.; Romming, C.; Tilset, M. *Organometallics* **1999**, *18*, 529.
26. Pankayatselvan, R.; Nicholas, K. M. *J. Organomet. Chem.* **1990**, *384*, 361.
27. Faller, J. W.; Rosan, A. M. *J. Am. Chem. Soc.* **1977**, *99*, 4858.
28. Faller, J. W.; Murray, H. H.; White, M. A.; Chao, K. H. *Organometallics* **1983**, *2*, 400.
29. Braunlein, B.; Köhler, F. H.; Strauss, W.; Zeh, H. *Z. Naturforsch.* **1995**, *50b*, 1739.
30. Thomas, B. J.; Mitchell, J. F.; Theopold, K. H. *J. Organomet. Chem.* **1988**, *348*, 333.
31. Thomas, B. J.; Theopold, K. H. *J. Am. Chem. Soc.* **1988**, *110*, 5902.
32. Theopold, K. H. *Eur. J. Inorg. Chem.* **1998**, 15.
33. White, P. A.; Calabrese, J. C.; Theopold, K. H. *Organometallics* **1996**, *15*, 5743.
34. Bhandari, G.; Kim, Y.; McFarland, J. M.; Rheingold, A. L.; Theopold, K. H. *Organometallics* **1995**, *14*, 738.
35. Herrmann, W. A. *Angew. Chem. Int. Ed. Engl.* **2002**, *41*, 1290.
36. Herrmann, W. A. *Adv. Organomet. Chem.* **2002**, *48*, 1.

37. Voges, M. H.; Tilset, M.; Blom, R.; Froeseth, M.; Jens, K. J. *European, WO0001739*, January 13, 2000.
38. Köhler, F. H.; Cao, R. D.; Gisbert, M. *Inorg. Chim. Acta* **1984**, L1.
39. Long, N. J. *Metallocenes: An Introduction to Sandwich Complexes*. Blackwell Science: Oxford, 1998.
40. Collman, J. P.; Hegedus, L. S.; Norton, J.; Finke, R. G. *Principles and Applications of Organotransition Metal Chemistry*. University Science Books: Mill Valley, CA, 1987.
41. Heigl, O. M.; Herdtweck, E.; Grasser, S.; Köhler, F. H.; Strauss, W.; Zeh, H. *Organometallics* **2002**, 21, 3572.
42. Bohling, D. A.; Mann, K. R. *Inorg. Chem.* **1983**, 22, 1561.
43. Bohling, D. A.; Evans, J. F.; Mann, K. R. *Inorg. Chem.* **1982**, 21, 3546.
44. Wigley, D. E.; Walton, R. A. *Inorg. Chem.* **1983**, 22, 3138.
45. Lemke, F. R.; Wigley, D. E.; Walton, R. A. *J. Organomet. Chem.* **1983**, 248, 321.
46. Basoto, M.; Michelin, R. A.; Mozzon, M.; Sgarbossa, P.; Tassan, A. J. *Organomet. Chem.* **2005**, 690, 5414.
47. Weber, W. P.; Gokel, G. W.; Ugi, I. K. *Angew. Chem. Int. Ed.* **1972**, 11, 530.
48. Kamer, P. C. J.; Nolte, R. J. M.; Drenth, W. *J. Am. Chem. Soc.* **1988**, 110, 6818.
49. Arduengo, A. J., III; Gamper, S. F.; Tamm, M.; Calabrese, J. C.; Davidson, F.; Craig, H. A. *J. Am. Chem. Soc.* **1995**, 117, 572.
50. Loudon, G. M. *Organic Chemistry, 3rd. Edition*. Benjamin/Cummings: Redwood City, 1995, p. 357.
51. Arduengo, A. J., III; Harlow, R. L.; Kline, M. *J. Am. Chem. Soc.* **1991**, 113, 361.
52. Stephan, D. W. *Organometallics* **2005**, 24, 2548.
53. Graham, T. W.; Kickham, J.; Courtenay, S.; Wei, P.; Stephan, D. W. *Organometallics* **2004**, 23, 3309.
54. Kickham, J. E.; Guerin, F.; Stephan, D. W. *J. Am. Chem. Soc.* **2002**, 124, 11486.

55. Guerin, F.; Beddie, C. L.; Stephan, D. W.; Spence, R. E. v. H.; Wurz, R. *Organometallics* **2001**, *20*, 3466.
56. Guerin, F.; Stewart, J. C.; Beddie, C.; Stephan, D. W. *Organometallics* **2000**, *19*, 2994.
57. Sung, R. C. W.; Courtenay, S.; McGarvey, B. R.; Stephan, D. W. *Inorg. Chem.* **2000**, *39*, 2542.
58. Stephan, D. W.; Stewart, J. C.; Guerin, F.; Spence, R. E. v. H.; Xu, W.; Harrison, D. G. *Organometallics* **1999**, *18*, 1116.
59. Stephan, D. W.; Guerin, F.; Spence, R. E. v. H.; Koch, L.; Gao, X.; Brown, S. J.; Swabey, J. W.; Wang, Q.; Xu, W.; Zoricak, P.; Harrison, D. G. *Organometallics* **1999**, *18*, 2046.
60. Siemeling, U.; Kolling, L.; Kuhnert, O.; Neumann, B.; Stammmler, A.; Stammmler, H. G.; Fink, G.; Kaminski, E.; Kiefer, A.; Schrock, R. R. *Z. Anorg. Allg. Chem.* **2003**, *629*, 781.
61. Stephan, D. W.; Stewart, J. C.; Guerin, F.; Courtenay, S.; Kickham, J.; Hollink, E.; Beddie, C.; Hoskin, A.; Graham, T.; Wei, P.; Spence, R. E. v. H.; Xu, W.; Koch, L.; Gao, X.; Harrison, D. G. *Organometallics* **2003**, *22*, 1937.
62. Wolfsberger, W. Z. *Z. Naturforsch. B* **1978**, *33*, 1452.
63. Courtenay, S.; Wei, P.; Stephan, D. W. *Can. J. Chem.* **2003**, *81*, 1471.
64. Schmidbaur, H.; Jonas, G. *Chem. Ber.* **1967**, *100*, 1120.
65. Miekisch, T.; Mai, H. J.; Meyer zu Kocker, R.; Dehnicke, K. *Z. Anorg. Allg. Chem.* **1996**, *622*, 583.
66. Wei, P.; Stephan, D. W. *Organometallics* **2002**, *21*, 1308.
67. Aldrige, S.; Shang, M.; Fehlner, T. P. *Acta. Cryst. C* **1998**, *C54*, 47.
68. Cristau, H. J.; Chiche, L.; Kadoura, J.; Torreilles, E. *Tet. Lett.* **1988**, *29*, 3931.
69. Anfang, S.; Seybert, G.; Harms, K.; Gerseler, G.; Massa, W.; Dehnicke, K. *Z. Anorg. Allg. Chem.* **1998**, *624*, 1187.
70. Cristau, H. J. *J. Chem. Rev.* **1994**, *94*, 1299.
71. Carlson, C. N.; Smith, J. D.; Hanusa, T. P.; Brennessel, W. W.; Young, V. G. *J. Organomet. Chem.* **2003**, *683*, 191.

72. Smith, J. D.; Hanusa, T. P.; Young, V. G. *J. Am. Chem. Soc.* **2001**, *123*, 6455.
73. Enders, M.; Fernandez, P.; Ludwig, G.; Pritzkow, H. *Organometallics* **2001**, *20*, 5005.
74. Strauss, S. H. *Chem. Rev.* **1993**, *93*, 927.
75. Norman, D. W.; Ferguson, M. J.; Stryker, J. M. *Organometallics* **2004**, *23*, 2015.
76. Norman, D. W.; McDonald, R.; Stryker, J. M. *Organometallics* **2005**, *24*, 4461.
77. Norman, D. W.; Ferguson, M. J.; McDonald, R.; Stryker, J. M. *Organometallics* **2006**, *25*, 2705.
78. Trofimenko, S.; Calabrese, J. C.; Thompson, J. S. *Inorg. Chem.* **1987**, *26*, 1507.
79. Kersten, J. L.; Kucharczyk, R. R.; Yap, G. P. A.; Rheingold, A. L.; Theopold, K. H. *Chem. Eur. J.* **1997**, *3*, 1668.

Experimental procedures, spectroscopic and analytical data

General: All manipulations on air sensitive compounds were performed under a nitrogen atmosphere using standard Schlenk techniques, or in a nitrogen filled drybox equipped with a freezer maintained at $-35\text{ }^{\circ}\text{C}$. Unless stated otherwise, all reactions were carried out under a nitrogen atmosphere. The high vacuum line (10^{-5} mm Hg) was used to add solvent and volatile reagents to reaction mixtures at $-198\text{ }^{\circ}\text{C}$ via vacuum transfer and to remove volatile compounds from reaction mixtures. Photolysis reactions were conducted in Pyrex vessels, cooled with a $5\text{ }^{\circ}\text{C}$ circulating ethanol bath and irradiated with a Hanovia 450 Watt high pressure mercury lamp placed six inches from the reaction vessel, all in an enclosed photolysis chamber. Photolysis reaction mixtures containing $\text{CpCrNO}(\text{CO})_2$ **90** or tin reagents were jacketed by a GWV 370 nm cutoff filter. IR spectra were recorded on a Nicolet Magna IR 750 or a Nicolet 20SX spectrophotometer and are reported in reciprocal wave numbers (cm^{-1}) calibrated to the 1601 cm^{-1} absorption of polystyrene. All infrared measurements were obtained either in solution (KBr solution cells) or in the solid-state (as Nujol mulls on KBr disks). Celite filtration in the drybox was performed using a plug of Hyflo Super CelTM (Fisher) over glass wool in a disposable pipette or through a sintered glass funnel under reduced pressure. Chromatographic separation of all organometallic products was performed in the drybox. Cylindrical medium-walled Pyrex vessels equipped with Kontes K-826510 Teflon vacuum stopcocks are referred to as solvent or reaction bombs.

Nuclear magnetic resonance spectra (^1H NMR and ^{13}C NMR) were recorded on Varian Inova 300 (^1H , 300 MHz), Varian Inova 400 (^1H , 400 MHz; ^{13}C , 100 MHz), Varian Mercury 400 (^1H , 400 MHz; ^{13}C , 100 MHz), and Varian Inova 500 (^1H , 500 MHz; ^{13}C , 125 MHz) spectrometers. ^{31}P , ^{11}B , and ^{19}F NMR spectra were recorded on the Varian Inova 400 (^{31}P , 162 MHz, ^{11}B 159.8 MHz, ^{19}F 376 MHz) spectrometer. Chemical shifts are reported in the δ scale, referenced to residual protiated solvent. In ^1H NMR spectral data, values of the coupling constants are either obtained directly from the spectrum, or inferred from the coupling constants of mutually coupled nuclei. Although generally measured to ± 0.1 Hz, J values are self-consistent only to ± 0.5 Hz. Multiplicities are reported as observed. Data for the ^1H - ^1H COSY is presented such that correlations are listed only once. In ^{13}C APT NMR spectral data “+” denotes a quaternary or methylene carbon (*i.e.*, C or CH_2), “-” denotes a methine or methyl carbon (*i.e.*, CH or CH_3). HMQC experiments are recorded at the ^1H frequency. In the assignment of several ^1H NMR and ^{13}C NMR spectra, the numbering or lettering scheme used is included with the illustration of the corresponding molecule. In complexes where aromatic resonances overlap and cannot be assigned a ubiquitous designation of “Ph” is used.

High resolution mass spectra (HRMS) were obtained on a Kratos MS-50 spectrometer in electron impact mode operating at 40 eV. The m/z ratio for the most abundant ion is given for each organometallic complex analyzed by HRMS. Elemental analyses were performed by the University of Alberta Microanalysis Laboratories. All air sensitive compounds (2-3 mg) were first wrapped in a thin-walled pre-weighed aluminum boat and then further wrapped in second pre-weighed aluminum boat and kept in nitrogen-filled

one-dram vials prior to analysis. Due to the high volatility of some samples or problematic combustion, several compounds failed to afford consistent elemental analysis even when using highly purified crystalline samples suitable for X-ray crystallography. For a comment on this problem, common to certain classes of early transition metal complexes, see the supporting information in reference 1.

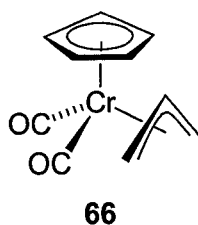
X-ray crystallography intensity data were collected on either a Bruker P4/RA/SMART 1000 CCD or a Bruker PLATFORM/SMART 1000 CCD at -80°C with $\text{MoK}\alpha$ radiation. In each case a semi-empirical absorption correction was applied to the data. All crystal structures were solved using direct methods (SHELXS-86 or DIRDIF-96)^{2,3} and refined against F^2 using SHELXL-93.⁴ All non-hydrogen atoms were refined anisotropically.

Materials: Unless indicated otherwise, solvents and reagents were purchased from commercial vendors, distilled or passed down a plug of neutral or basic alumina and degassed prior to use by repeated freeze-pump-thaw cycles on a vacuum line. Toluene, benzene, tetrahydrofuran, diethyl ether, 1,2-dimethoxyethane, hexane and pentane were distilled from sodium/benzophenone ketyl or potassium/benzophenone ketyl. Methylene chloride and acetonitrile were distilled from calcium hydride and degassed prior to use. Acetone was dried over boric anhydride and degassed prior to use.

Experimental details for Chapter 2:

Improved preparation of tris(acetonitrile)tricarbonylchromium 67:⁵

A suspension of chromiumhexacarbonyl (24.0 g, 0.109 mol) in acetonitrile (350 mL) was heated to reflux with vigorous stirring for eight days, or for three days following the complete consumption of the starting material. To facilitate removal of liberated CO, the reflux condenser was connected to a nitrogen bubbler filled with one inch of mineral oil. To reintroduce sublimed $\text{Cr}(\text{CO})_6$ to the solution, the reaction flask was shaken manually at approximately 12 h intervals. The cloudy orange solution was then cooled to room temperature, transferred via cannula to a frit layered with Celite, and filtered into a Schlenk flask. The filtration flask was then placed in a hot water bath and both the solvent and residual $\text{Cr}(\text{CO})_6$ were removed *in vacuo* to provide $(\text{CH}_3\text{CN})_3\text{Cr}(\text{CO})_3$ **67** as a bright yellow powder (24.89 g, 88%). IR (cm^{-1} , NUJOL): $\nu_{\text{CN}} = 2280$ (w); $\nu_{\text{CO}} = 1914$ (s), 1794 (s), 1774 (s). Note: this compound is pyrophoric.



$(\eta^5\text{-Cyclopentadienyl})(\eta^3\text{-allyl})\text{dicarbonylchromium 66, method A:}$

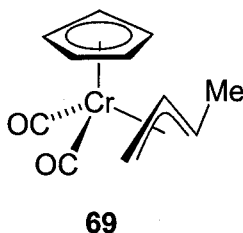
To a solution of sodium tricarbonyl(η^5 -cyclopentadienyl)chromate **67**⁶ [100 mg, 0.446 mmol; prepared *in situ* via a 12 h reflux of NaCp and $\text{Cr}(\text{CO})_6$] in THF (20 mL) cooled to $-30\text{ }^\circ\text{C}$ was added allyl tosylate (104 mg, 0.49 mmol) slowly via syringe. After

stirring for 2 h, a solution of trimethylamine *N*-oxide (165 mg, 2.23 mmol) in methanol (5 mL) was added via cannula and the dark orange solution warmed to room temperature. After 30 min of additional stirring, the solvent was removed *in vacuo* and the orange-green residue triturated with pentane until the extracts remained colourless. The orange extracts were then combined and filtered through a sintered glass funnel layered with a short plug of Celite and the filtrate evaporated *in vacuo* to provide η^3 -allyl complex **66** as a light orange powder (19.1 mg, 20%). Characterization data is provided below.

(η^5 -Cyclopentadienyl)(η^3 -allyl)dicarbonylchromium **66, method B:**

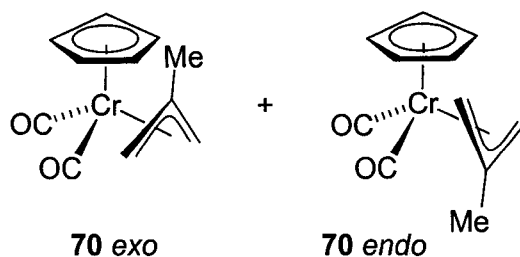
To a solution of tris(acetonitrile)tricarbonylchromium **67** (100 mg, 0.386 mmol) in acetonitrile (20 mL) cooled to $-30\text{ }^{\circ}\text{C}$ was added allyl bromide (33.4 μL , 0.386 mmol), resulting in an immediate colour change from yellow to red. After stirring for 1 h, a solution of sodium cyclopentadienide⁷ (34.0 mg, 0.386 mmol) in acetonitrile (10 mL) was added slowly via cannula and the dark orange mixture warmed to room temperature over a period of 15 min. The solvent was then removed *in vacuo* and the residue triturated with pentane until the extracts remained colourless. The orange extracts were then combined and filtered through a sintered glass funnel layered with a short plug of Celite. The filtrate was then passed through a 1 x 10 cm neutral alumina(I) column and eluted with hexane. The first five 20 mL fractions were combined and the solvent removed under reduced pressure to provide η^3 -allyl complex **66** as a light orange powder (62 mg, 75%). IR (ν_{CO} , cm^{-1} , THF): 1939, 1869. ^1H NMR (500 MHz, C_6D_6): δ 3.97 (s, 5H, C_5H_5), 3.73 (tt, $J = 11.1, 7.0\text{ Hz}$, 1H, $\text{H}_{\text{central}}$), 2.67 (dt, $J = 7.0, 1.1\text{ Hz}$, 2H, H_{syn}), 0.48 (dt, $J = 10.9, 1.1\text{ Hz}$, 2H, H_{anti}). ^{13}C NMR (125 MHz, C_6D_6): δ 247.1, 87.9, 71.0,

47.0. HRMS calcd for $C_{10}H_{10}CrO_2$: m/z 214.0083; found: 214.00887. Anal. calcd for $C_{10}H_{10}CrO_2$: C, 56.08; H, 4.71; found: C, 55.83; H, 4.82. Crystals suitable for X-ray crystallography were grown from a concentrated solution of complex **66** in methylcyclohexane at -35°C . Details are provided in Appendix A, part 1.



(η^5 -Cyclopentadienyl)(η^3 -3-methyl-allyl)dicarbonylchromium **69:**

As per the procedure for η^3 -allyl complex **66**, method B, except crotyl bromide (35.2 μL , 0.386 mmol) was used as the substrate. Yield: 64.3 mg (73%) of a bright yellow powder. IR (ν_{CO} , cm^{-1} , THF): 1932, 1863. ^1H NMR (500 MHz, C_6D_6): δ 4.04 (s, 5H, C_5H_5), 3.65 (dtq, $J = 10.5, 7.0, 0.5$ Hz, 1H), 2.51 (ddd, $J = 7.0, 2.0, 0.5$ Hz, 1H), 1.52 (d, $J = 6.5$ Hz, 3H), 1.03 (br dq, $J = 10.0, 6.5$ Hz, 1H), 0.36 (ddd, $J = 10.0, 2.0, 0.5$ Hz, 1H). ^{13}C NMR (125 MHz, C_6D_6): δ 249.9, 246.6, 88.1, 72.8, 68.9, 41.6, 19.5. HRMS calcd for $C_{11}H_{12}CrO_2$: m/z 228.02425; found: 228.02453. Anal. calcd for $C_{11}H_{12}CrO_2$: C, 57.89; H, 5.30; found: C, 57.73; H, 5.02.

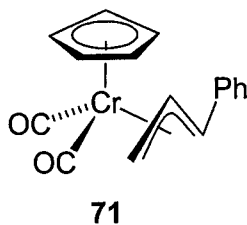


(η^5 -Cyclopentadienyl)(η^3 -2-methyl-allyl)dicarbonylchromium 70:

As per the procedure for η^3 -allyl complex **66**, method B, except 2-methyl-3-bromopropene (38.9 μ L, 0.386 mmol) was used as the substrate and the time allowed for oxidative addition was 6 h. Yield: 62.5 mg (71%) of a dark orange powder comprised of a 2 : 1 mixture of *endo* and *exo* isomers of η^3 -(2-methyl-allyl) complex **70**. IR (ν_{CO} , cm^{-1} , THF): 1943, 1938, 1880, 1870. Anal. calcd for $\text{C}_{11}\text{H}_{12}\text{CrO}_2$: C, 57.89; H, 5.30; found: C, 56.99; H, 5.21. HRMS calcd for $\text{C}_{11}\text{H}_{12}\text{CrO}_2$: m/z 228.02425; found: 228.02423. Crystals suitable for X-ray crystallography studies were grown of the *exo* isomer from a solution of complex **70** in methylcyclohexane at -35°C . Details are provided in Appendix A, part 2.

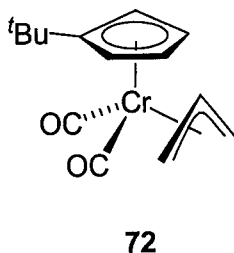
NMR data for the *endo* isomer of complex **70**: ^1H NMR (500 MHz, C_6D_6): δ 4.08 (s, 5H), 2.88 (s, 2H), 1.72 (s, 2H), 1.46 (s, 3H). ^{13}C NMR (125 MHz, C_6D_6): δ 252.8, 104.6, 87.8, 47.8, 23.5.

NMR data for the *exo* isomer of complex **70**: ^1H NMR (500 MHz, C_6D_6), assignments based on similarities of chemical shift and J values to that of complex **66**: δ 4.06 (s, 5H), 2.59 (s, 2H), 1.46 (s, 3H), 0.54 (s, 2H). ^{13}C NMR (125 MHz, C_6D_6): δ 247.8, 115.0, 88.4, 48.4, 25.8.



(η^5 -Cyclopentadienyl)(η^3 -3-phenylallyl)dicarbonylchromium 71:

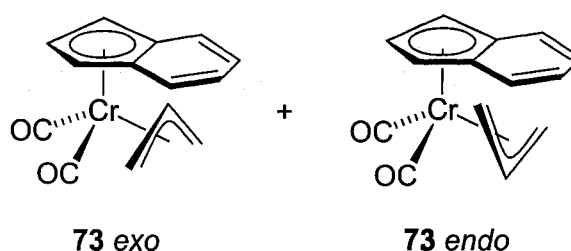
As per the procedure for η^3 -allyl complex **66**, method B, except cinnamyl bromide (571 μ L, 3.86 mmol), tris(acetonitrile)tricarbonylchromium (1.00 g, 3.86 mmol), and sodium cyclopentadienide (0.408 g, 4.63 mmol) were used and the time allowed for oxidative addition was 2 h. Yield: 683 mg (61%) of a dark orange powder. IR (ν_{CO} , cm^{-1} , THF): 1936, 1869. ^1H NMR (500 MHz, C_6D_6): δ 7.18 (m 2H, H), 7.09 (m, 2H, H), 7.0 (tt, $J = 7.0, 2.5$ Hz, 1H, H), 4.55 (dt, $J = 10.5, 7.0$ Hz, 1H), 3.94 (s, 5H), 2.72 (dd, $J = 7.0, 2.0$ Hz, 1H, H), 1.90 (d, $J = 11.0$ Hz, 1H, H), 0.60 (ddd, $J = 10.5, 2.0, 0.5$ Hz, 1H). ^{13}C NMR (125 MHz, C_6D_6): δ 250.6, 246.9, 128.7, 128.5, 126.7, 125.9, 89.2, 69.9, 69.2, 42.4. HRMS calcd for $\text{C}_{16}\text{H}_{14}\text{CrO}_2$: m/z 290.03989; found: 290.04022. Anal. calcd for $\text{C}_{16}\text{H}_{14}\text{CrO}_2$: C, 66.20; H, 4.86; found: C, 65.54; H, 4.72.



(η^5 -*tert*-Butylcyclopentadienyl)(η^3 -allyl)dicarbonylchromium 72:

As per the procedure for η^3 -allyl complex **66** except lithium *tert*-butylcyclopentadienide (49.5 mg, 0.386 mmol) was used as the ancillary ligand source. Yield: 72.0 mg

(69%) of a light orange powder. IR (ν_{CO} , cm^{-1} , THF): 1931, 1863. ^1H NMR (500 MHz, C_6D_6): δ 4.15 (t, $J = 2.0$ Hz, 2H), 3.83 (tt, $J = 11.0, 7.0$ Hz, 1H), 3.65 (t, $J = 2.5$ Hz, 2H), 2.77 (br d, $J = 7.0$ Hz, 2H), 1.14 (s, 9H), 0.52 (br d, $J = 11.0$ Hz, 2H). ^{13}C NMR (125 MHz, C_6D_6): δ 247.6, 120.0, 88.9, 84.8, 71.4, 47.7, 31.5, 31.4. HRMS calcd for $\text{C}_{14}\text{H}_{18}\text{CrO}_2$: m/z 270.07120; found: 270.07171. Anal. calcd for $\text{C}_{14}\text{H}_{18}\text{CrO}_2$: C, 62.21; H, 6.71; found: C, 61.75; H, 6.63.



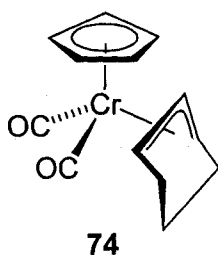
(η^5 -Indenyl)(η^3 -allyl)dicarbonylchromium 73:

As per the procedure for η^3 -allyl complex **66**, method B, except indenyllithium (47.0 mg, 0.386 mmol) was used as the ancillary ligand source. Yield: 25.5 mg (25%) of a bright red powder comprised of the *exo* isomer of complex **73** and a trace amount of the tentatively assigned *endo* isomer. An analytical sample was prepared by recrystallization from pentane. IR (ν_{CO} , cm^{-1} , THF): 1938, 1871. HRMS calcd for $\text{C}_{14}\text{H}_{12}\text{CrO}_2$: m/z 264.02423, found 264.02439. Anal. calcd for $\text{C}_{14}\text{H}_{12}\text{CrO}_2$: C, 63.64; H, 4.58; found: C, 62.83; H, 3.99.

NMR data for the *exo* isomer of complex **73**: ^1H NMR (500 MHz, C_6D_6): δ 6.44 (m, second order, 4H), 5.12 (d, $J = 2.5$ Hz, 2H), 4.64 (t, $J = 2.5$ Hz, 1H), 2.50 (dt, $J = 7.0, 1.0$

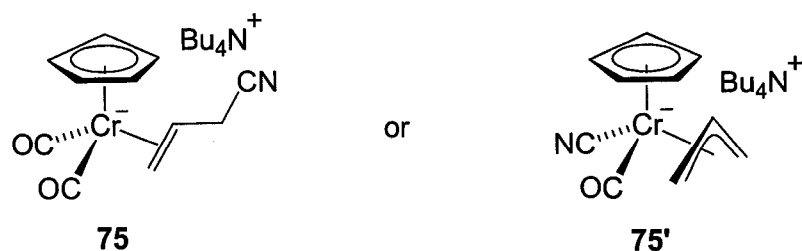
Hz, 2H), 0.58 (dt, $J = 11.5, 1.0$ Hz, 2H), -0.11 (tt, $J = 11.7$ Hz, 7.5 Hz, 1H). ^{13}C NMR (100 MHz, C_6D_6): δ 248.6, 125.7, 124.7, 106.8, 86.2, 84.1, 79.1, 55.8.

NMR data for the *exo* isomer of complex **73**, partial data only: δ 3.59 (d, $J = 7.0$ Hz, 2H), -0.63 (d, $J = 12.0$ Hz, 2H).



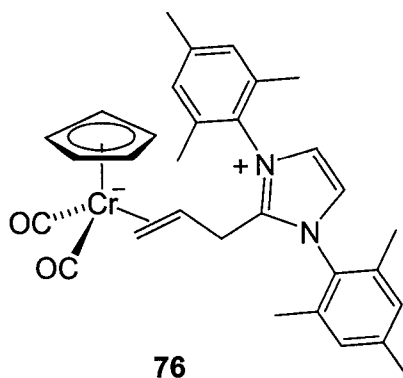
(η^5 -Cyclopentadienyl)(η^3 -cyclohexenyl)dicarbonylchromium **74:**

As per the procedure for η^3 -allyl complex **66**, method B, except 3-bromocyclohexene (44.4 μL , 0.386 mmol) was used as the substrate and the time allowed for oxidative addition was 12 h. Yield: 12.0 mg (12%) of a light orange powder. IR (ν_{CO} , cm^{-1} , THF): 1923, 1860. ^1H NMR (500 MHz, C_6D_6): δ 4.09 (s, 5H), 4.02 (t, $J = 7.5$ Hz, 1H), 3.47 (complex m, FWHM = 14.2 Hz, 2H), 1.79 (complex m, FWHM = 19.4 Hz, 4H), 0.77 (complex m, FWHM = 26.0 Hz, 1H_{eq}), 0.38 (dddd, by appearances nearly a dtt, $J = 14.1, 10.8, 10.6, 7.4, 7.3$ Hz, 1H_{ax}). ^{13}C NMR (125 MHz, C_6D_6): δ 246.0, 88.8, 63.4, 61.4, 22.3, 18.7. HRMS calcd for $\text{C}_{13}\text{H}_{14}\text{CrO}_2$: m/z 254.03989; found: 254.03987. Anal. calcd for $\text{C}_{13}\text{H}_{14}\text{CrO}_2$: C, 61.41; H, 5.55; found: C, 61.07; H, 5.55. Crystals suitable for X-ray crystallography were grown from a concentrated solution of complex **74** in pentane at -35°C . Details are provided in Appendix A, part 3.



Addition of tetrabutylammonium cyanide to η^3 -allyl complex **66:**

To a solution of (η^5 -C₅H₅)Cr(CO)₂(C₃H₅) **66** (20.0 mg, 0.093 mmol) in 5 mL of THF was added a solution of tetrabutylammonium cyanide (24.0 mg, 0.09 mmol) also in 5 mL of THF. After stirring for 15 h at room temperature, the mixture was filtered through Celite, and the filtrate evaporated *in vacuo*. Unreacted η^3 -allyl complex **66** was removed via trituration with 2 x 10 mL of pentane and the residue dried to give 9.5 mg of a yellow powder (contaminated with inseparable [Bu₄N]CN). ¹H NMR (300 MHz, acetone-d₆), partial data only: δ 4.12 (s, 5H, C₅H₅); 3.02 (dd, J = 17.1, 3.9 Hz, 1H); 2.07 (m, 1H); 1.60 (dd, J = 8.1, 2.0 Hz, 1H); 1.44 (br m, Bu₄N⁺); 0.98 (br m, Bu₄N⁺); 0.45 (dd, J = 9.3, 2.0, 2.0 Hz, 1H).

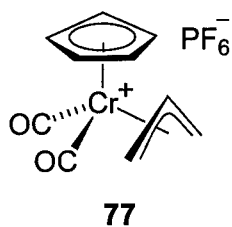


(η^5 -Cyclopentadienyl)dicarbonylchromium[η^2 -3-(1,3-dimesitylimidazolyl)-propene] **76:**

To a solution of (η^5 -C₅H₅)Cr(CO)₂(C₃H₅) **66** (17.6 mg, 0.082 mmol) in benzene was added 1,3-bis-(2,4,6-trimethylphenyl)imidazolin-2-ylidene (IMes)⁸ (25 mg, 0.082 mmol) dissolved in a minimum of benzene. After standing for 3 h at room temperature, light red crystals had deposited. The supernatant was decanted and the crystals washed with 2 x 5 mL diethyl ether. Drying under vacuum provided the zwitterionic complex **76** (41 mg, 89%). IR (ν_{CO} , cm⁻¹, acetone): 1845, 1757. ¹H NMR (500 MHz, acetone-d₆): δ 7.84 (s, 2H, NCHCHN); 7.22 (br s, 2H, H_{meta}); 7.16 (br s, 2H, H_{meta}); 3.86 (s, 5H, C₅H₅); 3.63 (dd, J = 15.0, 2.5 Hz, 1H, CH₂); 2.39 (s, 6H, CH_{3-para}); 2.26 (s, 6H, CH_{3-ortho}); 2.14 (s, 6H, CH_{3-ortho}); 1.69 (m, 1H, H_{central}); 1.44 (dd, J = 15.0, 11.5 Hz, 1H, CH₂); 1.32 (dd, J = 8.0, 2.0 Hz, 1H, H_{syn}); -0.19 (dd, J = 9.5, 2.0 Hz, 1H, H_{anti}). ¹³C NMR (125 MHz, C₆D₆): δ 258.3 (CO); 258.1 (CO); 153.2 (NCN); 141.9 (C_{para}); 135.9 (C_{ortho}); 135.5 (C_{ortho}); 132.0 (C_{ipso}); 130.8 (C_{meta}); 130.5 (C_{meta}); 123.7 (NCCN); 85.9 (C₅H₅); 35.9 (C_{methylene}); 34.6 (C_{central}); 29.5 (C_{terminal}); 21.1 (para-CH₃); 18.1 (ortho-CH₃); 17.8 (ortho-CH₃). COSY (600 MHz, acetone-d₆): δ 7.22 \leftrightarrow δ 2.39; δ 7.22 \leftrightarrow δ 2.26; δ 7.22 \leftrightarrow δ 2.14; δ 7.16 \leftrightarrow δ 2.39; δ 7.16 \leftrightarrow δ 2.26; δ 7.16 \leftrightarrow δ 2.14; δ 3.63 \leftrightarrow δ 1.69; δ 3.63 \leftrightarrow δ 1.44; δ 1.69 \leftrightarrow δ 1.44; δ 1.69 \leftrightarrow δ 1.32; δ 1.69 \leftrightarrow δ -0.19; δ 1.32 \leftrightarrow δ -0.19. HMQC

(500 MHz, acetone- d_6): δ 7.84 \leftrightarrow δ 123.7; δ 7.22 \leftrightarrow δ 130.5; δ 7.16 \leftrightarrow δ 130.5; δ 3.86 \leftrightarrow δ 85.9; δ 3.63 \leftrightarrow δ 35.9; δ 2.39 \leftrightarrow δ 21.1; δ 2.26 \leftrightarrow δ 18.1; δ 2.14 \leftrightarrow δ 17.8; δ 1.69 \leftrightarrow δ 34.6; δ 1.44 \leftrightarrow δ 35.9; δ 1.32 \leftrightarrow δ 29.5; δ -0.19 \leftrightarrow δ 29.5. HMBC (600 MHz, acetone- d_6): δ 7.84 \leftrightarrow δ 153.2; δ 7.84 \leftrightarrow δ 123.7; δ 7.22 \leftrightarrow δ 132.0; δ 7.22 \leftrightarrow δ 130.5; δ 7.22 \leftrightarrow δ 21.1; δ 7.22 \leftrightarrow δ 18.1; δ 7.16 \leftrightarrow δ 132.0; δ 7.16 \leftrightarrow δ 130.8; δ 7.16 \leftrightarrow δ 21.1; δ 7.16 \leftrightarrow δ 17.8; δ 3.86 \leftrightarrow δ 85.9; δ 3.63 \leftrightarrow δ 153.2; δ 3.63 \leftrightarrow δ 34.6; δ 3.63 \leftrightarrow δ 29.5; δ 2.39 \leftrightarrow δ 141.9; δ 2.39 \leftrightarrow δ 130.8; δ 2.26 \leftrightarrow δ 135.9; δ 2.26 \leftrightarrow δ 132.0; δ 2.14 \leftrightarrow δ 135.9; δ 2.14 \leftrightarrow δ 132.0; δ 1.44 \leftrightarrow δ 153.2; δ 1.44 \leftrightarrow δ 34.6; δ 1.44 \leftrightarrow δ 29.5; δ 1.32 \leftrightarrow δ 35.9; δ -0.19 \leftrightarrow δ 35.9; δ -0.19 \leftrightarrow δ 258.1. Anal. calcd for $C_{31}H_{34}CrN_2O_2$: C, 71.79; H, 5.40; N, 6.61; found: C, 71.21; H, 5.22; N, 6.83. Crystals suitable for X-ray crystallography were grown from an equimolar mixture of η^3 -allyl complex **66** and IMes in THF upon standing at RT for 12 h, providing zwitterion complex **76** as the 0.5 THF solvate. Details of the crystallography are provided in Appendix A, part 4.

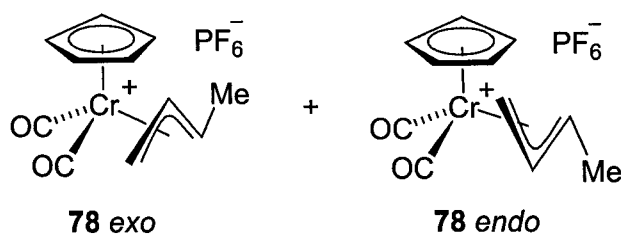
Experimental details for Chapter 3:



$[(\eta^5\text{-Cyclopentadienyl})(\eta^3\text{-allyl})\text{dicarbonylchromium}]\text{PF}_6\cdot(\text{DME})_{0.5}$ **77:**

To a solution of $(\eta^5\text{-C}_5\text{H}_5)\text{Cr}(\text{CO})_2(\text{C}_3\text{H}_5)$ **66** (405 mg, 1.89 mmol) in 20 mL of DME cooled to 0 °C was added a cold (0 °C) solution of NOPF_6 (331 mg, 1.89 mmol) in

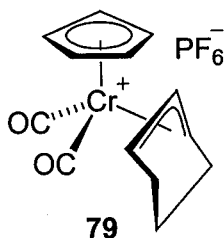
15 mL of DME via cannula. An immediate colour change from orange to green was observed along with effervescence and the formation of a green precipitate. After stirring for 20 min, the suspension was warmed to room temperature and 20 mL of diethyl ether added. The precipitate was collected on a frit, washed with 2 x 10 mL diethyl ether and dried to give allylchromium complex **77** as a green DME solvate (625 mg, 82%). IR (ν_{CO} , cm^{-1} , NUJOL): 2070, 2032. Anal. Calcd. for $\text{C}_{10}\text{H}_{10}\text{CrO}_2\text{PF}_6 \cdot 0.5\text{DME}$: C, 35.66; H, 3.74; found: C, 34.87; H, 3.80. Crystals suitable for X-ray crystallography were grown from a dilute (~ 46 mM) equimolar solution of η^3 -allyl complex **66** and NOPF_6 in DME, upon standing at RT for 16 h. Details of the crystallography are provided in Appendix A, part 4.



$[(\eta^5\text{-Cyclopentadienyl})(\eta^3\text{-crotyl})\text{dicarbonylchromium}]\text{PF}_6$ **78:**

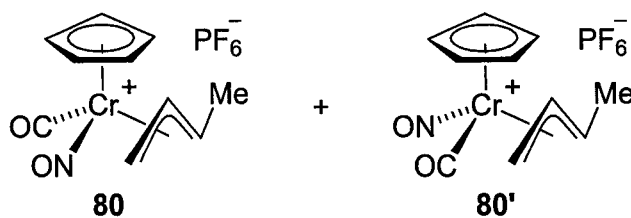
To a solution of $(\eta^5\text{-C}_5\text{H}_5)\text{Cr}(\text{CO})_2(\text{C}_4\text{H}_7)$ **69** (46 mg, 0.202 mmol) in 5 mL of DME cooled to 0 °C was added a solution of NOPF_6 (35 mg, 0.202 mmol) in 10 mL of cold (0 °C) DME via cannula. A colour change from yellow to light green was immediately observed along with concomitant effervescence and the formation of a light green precipitate. After stirring for 20 min, the suspension was warmed to room temperature and 10 mL of diethyl ether added. The precipitate was collected on a frit, washed with 2 x 5 mL diethyl ether and dried to give crotylchromium complex **78** as an

analytically pure yellow-green powder (53 mg, 70%). On the basis of the four carbonyl absorptions, this product is tentatively as a mixture of two unidentified isomers. IR (ν_{CO} , cm^{-1} , NUJOL): 2065, 2040, 2031, 2022. Anal. Calcd. for $\text{C}_{11}\text{H}_{12}\text{CrO}_2\text{PF}_6$: C, 35.40; H, 3.24; found: C, 35.34; H, 2.92.



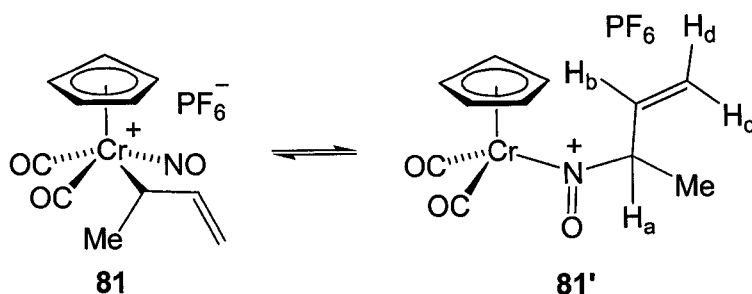
$[(\eta^5\text{-Cyclopentadienyl})(\eta^3\text{-cyclohexenyl})\text{dicarbonylchromium}]\text{PF}_6$ **79:**

To a solution of $(\eta^5\text{-C}_5\text{H}_5)\text{Cr}(\text{CO})_2(\text{C}_6\text{H}_9)$ **72** (46 mg, 0.180 mmol) in 5 mL of DME cooled to 0 °C was added a solution of NOPF_6 (35 mg, 0.197 mmol) in 10 mL of cold (0 °C) DME via cannula. A colour change from yellow to orange was immediately observed along with concomitant effervescence and the formation of an orange-red precipitate. After stirring for 20 min, the suspension was warmed to room temperature and 10 mL of diethyl ether added. The precipitate was collected on a frit, washed with 2 x 5 mL diethyl ether and dried to give cyclohexenylchromium complex **79** as an orange-red powder (69 mg, 96%). IR (ν_{CO} , cm^{-1} , NUJOL): 2039, 2002. Anal. calcd. for $\text{C}_{13}\text{H}_{14}\text{CrO}_2\text{PF}_6$: C, 39.11; H, 3.53; found: C, 38.60; H, 3.42.



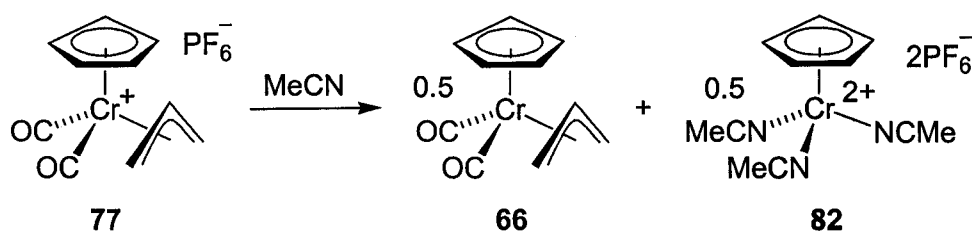
Addition of NOPF₆ to the η^3 -crotyl dicarbonyl complex **69 in a sealed system:**

In a solvent bomb, the η^3 -crotyl dicarbonyl complex **69** (85.0 mg, 0.0372 mmol) was dissolved in 20 mL of DME and cooled to 0 °C. A solution of NOPF₆ (65.0 mg, 0.0372 mmol) in 10 mL of DME was then added from the sidearm of the solvent bomb; the Teflon stopcock was sealed immediately after addition. After warming to room temperature, the mixture was stirred for 2 h then transferred to a frit layered with Celite and filtered. The filtrate was evaporated *in vacuo* and the dark orange residue dissolved in 0.8 mL of acetone-d₆. ¹H NMR analysis of this sample reveals a 3.5 : 1.0 mixture of two isomers, tentatively attributed to the unassigned diastereoisomers of the [CpCrNO(CO)(η^3 -crotyl)]PF₆ complex **80**. The yield could not be determined. ¹H NMR (500 MHz, acetone-d₆), major isomer: δ 5.96 (s, 5H, η^5 -C₅H₅); 2.58 (d, J = 6.8 Hz, 3H, CH₃); minor isomer: 6.04 (s, 5H, η^5 -C₅H₅); 2.32 (d, J = 6.4 Hz, 3H, CH₃).



Addition of gaseous nitric oxide to the cationic η^3 -crotyl dicarbonyl complex 77:

A Schlenk flask containing the cationic η^3 -crotyl dicarbonyl complex 77 (16.0 mg, 0.0043 mmol) was purged for 10 min with nitric oxide then 0.8 mL of acetone- d_6 added to form a dark orange solution, comprised of the tentatively assigned product 81 or 81'. NMR analysis of the sample after 2 h shows evidence of four different crotyl methyl signals: ^1H NMR (500 MHz, acetone- d_6): δ 1.61 (d, $J = 6.8$ Hz); 1.45 (d, $J = 6.4$ Hz); 1.41 (d, $J = 6.4$ Hz); 1.16 (d, $J = 6.4$ Hz); 3.4 : 6.8 : 1.0 : 8.7 ratio, respectively. HMQC (500 MHz, C_6D_6): δ 1.61 \leftrightarrow δ 18.8; δ 1.45 \leftrightarrow δ 20.0; δ 1.41 \leftrightarrow δ undetectable; δ 1.16 \leftrightarrow δ 23.1. NMR analysis of the sample after 24 h; equilibration to just one isomer: ^1H NMR (500 MHz, acetone- d_6): δ 6.24 (s, 5H, C_5H_5); 5.88 (ddd, $J = 17.0, 10.5, 5.5$ Hz, 1H, H_b); 5.15 (d, $J = 17.0$ Hz, 1H, H_d); 4.93 (d, $J = 10.5$ Hz, 1H, H_c); 4.20 (br dq, $J = 6.5, 5.5$ Hz, 1H, H_a); 1.16 (d, $J = 6.5$ Hz, 3H, CH_3). COSY (500 MHz, acetone- d_6): δ 5.88 \leftrightarrow δ 5.15; δ 5.88 \leftrightarrow δ 4.93; δ 5.88 \leftrightarrow δ 4.20; δ 5.15 \leftrightarrow δ 4.93; δ 5.15 \leftrightarrow δ 4.20; δ 4.93 \leftrightarrow δ 4.20; δ 4.20 \leftrightarrow δ 1.16. ^{13}C NMR (125 MHz, acetone- d_6): δ 234.2 (CO); 143.8 (CH_b); 111.9 (CH_2); 105.5 (C_5H_5); 67.9 (CH_a); 23.1 (CH_3). HMQC (500 MHz, acetone- d_6): δ 6.24 \leftrightarrow δ 105.5; δ 5.88 \leftrightarrow δ 143.8; δ 5.15 \leftrightarrow δ 111.9; δ 4.93 \leftrightarrow δ 111.9; δ 4.20 \leftrightarrow δ 67.9; δ 1.16 \leftrightarrow δ 23.1. This compound could not be isolated from solution.



Addition of acetonitrile to the cationic η^3 -allyl complex 77:

Allylchromium(III) complex **77** (22 mg, 0.061 mmol) was dissolved in 5 mL of acetonitrile. Upon stirring for 3 h, a color change from green to burgundy was observed. The volatile components of this solution were then isolated via vacuum transfer and subjected to GC analysis, which established the presence of 1,5-hexadiene (*vide infra*). The reaction residue was then triturated with 3 x 5 mL diethyl ether, the extracts combined, and the solvent removed *in vacuo* to provide the neutral chromium η^3 -allyl complex **66** as a yellow-orange powder (6 mg, 47%), identified spectroscopically by comparison to authentic material. The remaining purple residue was recrystallized from a 1 : 1 mixture acetonitrile/diethyl ether at -35°C to give $[(\eta^5\text{-C}_5\text{H}_5)\text{Cr}(\text{NCCH}_3)_3](\text{PF}_6)_2$ **82** (14 mg, 43%), as determined by comparison of the infrared spectrum and combustion analysis to authentic material from independent synthesis, given below.

Independent synthesis of $[(\eta^5\text{-Cyclopentadienyl})\text{tris}(\text{acetonitrile})\text{chromium}](\text{PF}_6)_2$ **82**:

To a solution of $[(\eta^5\text{-C}_5\text{H}_5)\text{CrCl}_2]_2$ **174** (50 mg, 0.133 mmol) in 20 mL of acetonitrile was added a solution of silver hexafluorophosphate (134 mg, 0.532 mmol) in 10 mL acetonitrile. A colour change from green to dark purple was observed along with the formation of a white precipitate. After stirring for 2 h, the suspension was filtered through a frit layered with Celite and the filtrate layered with 15 mL of diethyl ether.

After two days at $-35\text{ }^{\circ}\text{C}$, deep purple crystals were deposited. The supernatant was then removed and the crystals washed with 2 x 10 mL of diethyl ether and dried to give the tris(acetonitrile) complex **82** (102 mg, 72%). IR (ν_{CN} , cm^{-1} , NUJOL): 2325, 2296. Anal. calcd for $\text{C}_{11}\text{H}_{14}\text{CrN}_3\text{P}_2\text{F}_{12}$: C, 24.92; H, 2.66; N, 7.93; found: C, 25.42; H, 2.50; N, 7.71.

Gas chromatography parameters and measurements used to detect 1,5-hexadiene from the reaction of the cationic η^3 -allyl complex **77 with acetonitrile:**

Column: HP-5, 25 m x 0.32 mm x 0.52 μm

GC Instrument: HP-5890-FID

Carrier gas: Helium

Initial Temperature: 60 $^{\circ}\text{C}$

Initial Time: 0.5 min

Rate: 10 $^{\circ}\text{C}/\text{min}$

Final Temperature: 280 $^{\circ}\text{C}$

Injector Temperature: 280 $^{\circ}\text{C}$

Detector Temperature: 300 $^{\circ}\text{C}$

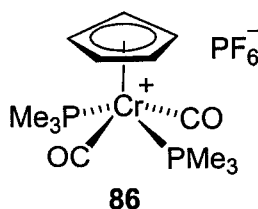
Manual Injection: 1 μL injected

Split Ratio: 1 : 1

Carrier Gas Flow: 3 mL/min

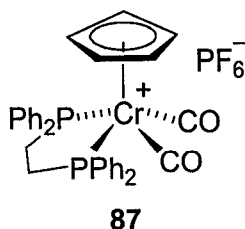
Retention times (min) of the control and reaction samples:

- 1,5-hexadiene: 1.97
- acetonitrile: 1.75
- 1 : 100 mixture of 1,5-hexadiene and acetonitrile: 1.70 and 1.98
- volatile fraction from the reaction of **77** with acetonitrile: 1.70 and 1.96



$[(\eta^5\text{-Cyclopentadienyl})\text{bis}(\text{trimethylphosphine})\text{dicarbonylchromium}]\text{PF}_6$ **86:**

To a suspension of $(\eta^5\text{-C}_5\text{H}_5)\text{Cr}(\text{CO})_2(\text{C}_3\text{H}_5)]\text{PF}_6 \cdot (\text{DME})_{0.5}$ **77** (111 mg, 0.275 mmol) in 20 mL of DME was added PMe_3 (577 μL , 1.0 M in THF, 0.577 mmol) via syringe. The colour of the mixture immediately turned from dark green to light green and light green precipitate formed. After 30 min the solid was collected on a frit, washed with 2 x 10 mL diethyl ether and dried to give complex **86** as a yellow-green powder (48 mg, 33%). Cooling the filtrate to -35°C for 24 h then provided the known¹⁰ allyl-trimethylphosphonium PF_6 salt as an off-white powder (10.8 mg, 15%). Characterization data for complex **86**: IR (ν_{CO} , cm^{-1} , NUJOL): 1959, 1885. ^1H NMR (400 MHz, acetone- d_6): δ 5.25 (t, $J = 2.0$ Hz, 5H, C_5H_5); 1.84 (2nd order m, 18 H, PMe_3). ^{31}P NMR (162 MHz, acetone- d_6): 52.94 (s, PMe_3); -138.03 (sept, $J = 708.1$ Hz, PF_6). ^{13}C NMR (100 MHz, acetone- d_6): δ 245.8 (t, $J = 51.1$ Hz, CO); 91.0 (s, C_5H_5); 19.6 (dd, $J = 15.6$ 2.0 Hz, PMe_3). Anal. calcd for $\text{C}_{13}\text{H}_{23}\text{CrO}_2\text{P}_3\text{F}_6$: C, 29.9; H, 4.44; found: C, 30.84; H, 4.29. Crystals suitable for X-ray crystallography were grown from a solution of complex **86** in acetone at -35°C . Details are provided in Appendix A, part 6.



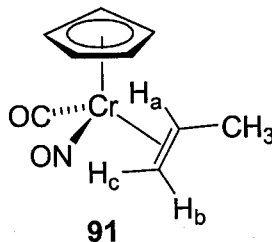
{(η^5 -Cyclopentadienyl)[1,2-bis(diphenylphosphino)ethane]dicarbonyl-chromium} PF_6 **87:**

To a suspension of (η^5 -C₅H₅)Cr(CO)₂(C₃H₅)]PF₆ • (DME)_{0.5} **77** (125 mg, 0.309 mmol) in 20 mL of DME was added dppe (117 mg, 0.294 mmol). The colour of the mixture immediately turned from dark green to light green. After 30 min the solvent was removed *in vacuo* and the residue triturated with 2 x 10 mL of pentane. The pentane insoluble material was dissolved in 10 mL of acetone, 5 mL of diethyl ether added and the mixture stored at -35 °C for 12 h to yield a yellow precipitate. The solid was collected on a frit, washed with 2 x 10 mL diethyl ether and dried to give complex **87** as a yellow powder (45 mg, 21%). Cooling the filtrate to -35 °C for 24 h then provided the doubly allylated phosphonium PF₆ salt as an off-white powder (32 mg, 10%).

Characterization data for complex **87**: IR (ν_{CO} , cm⁻¹, NUJOL): 1971, 1917. ¹H NMR (500 MHz, acetone-d₆): δ 7.83 (m, 5H, Ph); 7.62 (m, 6H, Ph); 7.33 (m, 5H, Ph); 7.23 (m, 4H, Ph); 4.86 (t, J = 1.5 Hz, 5H, C₅H₅); 3.43 (2nd order m, 2H, CH₂); 3.12 (2nd order m, 2H, CH₂). ³¹P NMR (162 MHz, acetone-d₆): 106.78 (s, dppe); -137.93 (sept, J = 708.1 Hz, PF₆). ¹³C NMR (100 MHz, acetone-d₆): δ 249.0 (t, J = 28.7 Hz, CO); 137.6 (t, J = 24.6 Hz, C_{ipso}); 133.6 (t, J = 3.9 Hz, C_{meta}); 133.4 (t, J = 22.2 Hz, C_{ipso}); 132.2 (s, C_{para}); 132.1 (s, C_{para}); 131.5 (t, J = 3.9 Hz, C_{meta}); 130.4 (t, J = 5.1 Hz, C_{ortho}); 129.6 (t, J = 4.8 Hz, C_{ortho}); 93.2 (s, C₅H₅); 28.7 (dd, J = 39.8 Hz, CH₂CH₂). Anal. calcd for C₃₃H₂₉CrO₂P₃F₆: C, 55.32; H, 4.08; found: C, 55.14; H, 4.11. Crystals suitable for X-ray crystallography

were grown from a solution of complex **87** in a 1 : 1 mixture of acetone and diethyl ether at $-35\text{ }^{\circ}\text{C}$. Details are provided in Appendix A, part 7.

Experimental details for Chapter 4:

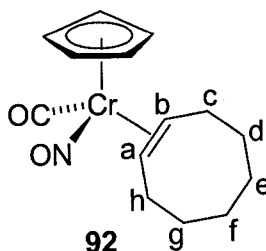


Improved synthesis and characterization of $(\eta^5\text{-cyclopentadienyl})(\eta^2\text{-propene})\text{-nitrosylchromium } \mathbf{91}$:¹¹

In a solvent bomb, a solution of $\text{CpCrNO}(\text{CO})_2$ **90** (164 mg, 0.81 mmol) in 5 mL of benzene was frozen in liquid nitrogen and ~ 5 mL of propene added via vacuum transfer. The atmosphere of the reaction vessel was removed *in vacuo* while the starting materials remained frozen. The reaction vessel was then sealed and the solution warmed to $5\text{ }^{\circ}\text{C}$ and irradiated for 10 h. The yellow-brown reaction mixture was then warmed to room temperature, excess propene removed by warming the solution and venting to a nitrogen line, and the solvent removed *in vacuo*. The residue was then dissolved in 10 mL of pentane and cooled to $-35\text{ }^{\circ}\text{C}$ to provide complex **91** as a yellow-brown powder (136 mg, 70%), present in solution as a 1 : 1.5 mixture of two structurally unassigned isomers. IR (THF, cm^{-1}): $\nu_{\text{CO}} = 1957$, $\nu_{\text{NO}} = 1656$. The compound was insufficiently stable for further purification or characterization.

NMR analysis of the major isomer: ^1H NMR (400 MHz, C_6D_6): δ 4.32 (s, 5H, C_5H_5); 3.14 (ddd, $J = 12.8, 9.2, 6.0$ Hz, 1H, H_a); 2.11 (d, $J = 12.8$ Hz, 1H, H_b); 2.02 (d, $J = 9.2$ Hz, 1H, H_c); 1.44 (d, $J = 6.0$ Hz, 3H, CH_3). COSY (400 MHz, C_6D_6): δ 3.14 \leftrightarrow δ 2.11; δ 3.14 \leftrightarrow δ 2.02; δ 3.14 \leftrightarrow δ 1.44; δ 2.11 \leftrightarrow δ 1.44.

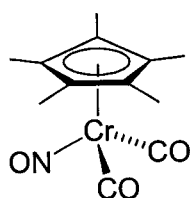
NMR analysis of the minor isomer: ^1H NMR (400 MHz, C_6D_6): δ 4.31 (s, 5H, C_5H_5); 2.67 (ddd, $J = 13.2, 9.2, 6.0$ Hz, 1H, H_a); 2.2 (d, $J = 13.2$ Hz, 1H, H_b); 2.04 (d, $J = 9.2$ Hz, 1H, H_c); 1.68 (d, $J = 6.0$ Hz, 3H, CH_3). COSY (400 MHz, C_6D_6): δ 2.67 \leftrightarrow δ 2.2; δ 2.67 \leftrightarrow δ 2.04; δ 2.67 \leftrightarrow δ 1.68; δ 2.2 \leftrightarrow δ 1.68; δ 2.04 \leftrightarrow δ 1.68



Improved synthesis and characterization of $(\eta^5\text{-cyclopentadienyl})(\eta^2\text{-cyclooctene})\text{-nitrosylcarbonylchromium } \mathbf{92}$:¹¹

In a Schlenk tube, a solution of $\text{CpCrNO}(\text{CO})_2$ **90** (420 mg, 2.07 mmol) in neat cyclooctene (20 mL) was cooled to 5 °C and irradiated for 9 h. During the photolysis, ~22 mL of $\text{CO}_{(\text{g})}$ was released (as monitored by an inverted graduated water column) and a colour change from orange to red-brown was observed. Residual starting material was then removed *in vacuo* and the remaining material recrystallized from pentane to provide the $\eta^2\text{-cyclooctaene}$ complex **92** as a yellow-brown powder (370 mg, 63%). IR (THF, cm^{-1}): $\nu_{\text{CO}} = 1957$, $\nu_{\text{NO}} = 1661$. ^1H NMR (500 MHz, CD_3CN): δ 5.01 (s, 5H, C_5H_5);

3.39 (dddd, $J = 11.5, 10.0, 3.9$ Hz, 1H, H_a); 2.95 (dddd, $J = 11.0, 10.0, 3.9$ Hz, 1H, H_b); 2.51 (dt, $J = 10.0, 3.9$ Hz, 1H, H_c); 2.43 (dq, $J = 14.0, 3.6$ Hz, 1H, H_h); 1.82 to 1.64 (ov m, 5H, H_h and H_d to H_g); 1.56 to 1.37 (ov m, 5H, H_c and CH_d to CH_g). COSY (500 MHz, CD_3CN): $\delta 3.39 \leftrightarrow \delta 2.59$; $\delta 3.39 \leftrightarrow \delta 2.43$; $\delta 3.39 \leftrightarrow \delta 1.77$; $\delta 2.95 \leftrightarrow \delta 2.51$; $\delta 2.95 \leftrightarrow \delta 1.52$; $\delta 2.51 \leftrightarrow \delta 1.80$; $\delta 2.51 \leftrightarrow \delta 1.54$; $\delta 2.43 \leftrightarrow \delta 1.77$; $\delta 2.43 \leftrightarrow \delta 1.49$; $\delta 1.80 \leftrightarrow \delta 1.48$; $\delta 1.76 \leftrightarrow \delta 1.49$; $\delta 1.70 \leftrightarrow \delta 1.44$. ^{13}C APT NMR (125 MHz, CD_3CN): δ 249.4 (+, CO); 93.1 (–, C_5H_5); 72.8 (–, CH_b); 68.2 (–, CH_a); 33.3 (+, CH_2); 33.2 (+, CH_2); 30.0 (+, CH_{2-h}); 29.9 (+, CH_{2-c}); 27.3 (+, CH_2); 27.2 (+, CH_2). HMQC (500 MHz, CD_3CN): $\delta 5.01 \leftrightarrow \delta 93.1$; $\delta 3.39 \leftrightarrow \delta 68.2$; $\delta 2.95 \leftrightarrow \delta 72.8$; $\delta 2.51 \leftrightarrow \delta 29.9$; $\delta 1.51 \leftrightarrow \delta 29.9$; $\delta 2.43 \leftrightarrow \delta 30.0$; $\delta 1.77 \leftrightarrow \delta 30.0$; $\delta 1.81 \leftrightarrow \delta 33.3$; $\delta 1.47 \leftrightarrow \delta 33.3$; $\delta 1.71 \leftrightarrow \delta 33.2$; $\delta 1.52 \leftrightarrow \delta 33.2$; $\delta 1.72 \leftrightarrow \delta 27.3$; $\delta 1.45 \leftrightarrow \delta 27.3$; $\delta 1.69 \leftrightarrow \delta 27.2$; $\delta 1.51 \leftrightarrow \delta 27.2$. HRMS calcd for $C_{14}H_{19}CrNO_2$: m/z 285.08209; found: 285.08167. This compound did not afford consistent combustion analysis data.

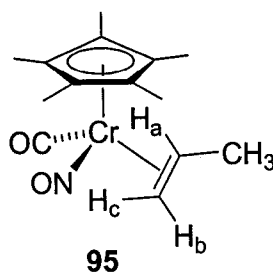


94

Improved procedure for the preparation of (η^5 -permethylcyclopentadienyl)-dicarbonylnitrosylchromium 94:¹²

To a suspension of $(CH_3CN)_3Cr(CO)_3$ **67** (2.77 g, 10.7 mmol) in 80 mL of THF was added a suspension of Cp^*Li (1.52 g, 10.7 mmol) in 10 mL of THF. Upon stirring for 20 min at room temperature, a deep red solution formed. A solution of *N*-methyl-*N*-

nitroso-*p*-toluene sulfonamide (Diazald) (2.29 g, 10.7 mmol) in 30 mL of THF was then added via cannula. Upon stirring for 5 h, a pale brown precipitate formed. The solid was then removed by filtration through Celite, the filtrate evaporated *in vacuo* and the residue triturated with 3 x 50 mL of pentane. The extracts were then combined and the solvent removed *in vacuo* to provide dicarbonyl complex **94** as red crystals (2.5 g, 85%). IR (cm⁻¹, THF): $\nu_{\text{CO}} = 2001, 1928$, $\nu_{\text{NO}} = 1681$. ¹H NMR (400 MHz, C₆D₆): δ 1.51 (s, 15H, C₅Me₅). ¹³C APT NMR (100 MHz, C₆D₆): δ 240.7 (CO); 102.1 (C₅Me₅); 9.7 (C₅Me₅). HRMS calcd for C₁₂H₁₅CrNO₃: m/z 273.04572; found: 273.04626. An extension of this procedure provides CpCrNO(CO)₂ **90** in 90% yield.



(η^5 -Permethylcyclopentadienyl)(η^2 -propene)carbonylnitrosylchromium **95:**

In a Schlenk tube, Cp*CrNO(CO)₂ **94** (510 mg, 1.87 mmol) was dissolved in 50 mL of benzene and ~1 mL (12.4 mmol) of propene added via bubbling. The solution was then cooled to 5 °C and irradiated for 24 h. The resulting brown solution was then passed through a 1 x 5 cm silica-gel column and eluted with benzene. The dark orange eluent was then evaporated *in vacuo* and the residue dissolved in 10 mL of pentane. Several crystallizations at -35 °C then afforded η^2 -propene complex **95** as a yellow powder (355 mg, 66%), present in solution as a 1 : 1 mixture of structurally unassigned isomers. IR (cm⁻¹, THF): $\nu_{\text{CO}} = 1948$, $\nu_{\text{NO}} = 1654$. HRMS calcd for C₁₄H₂₁CrNO₂: m/z 287.09775;

found: 287.09855. Anal. calcd for $C_{14}H_{21}CrNO_2$: C, 58.52; H, 7.37; N, 4.88; found: C, 58.15; H, 7.42; N, 4.93.

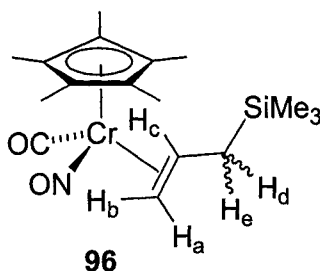
NMR analysis of the static isomer of complex **95** at 27 °C. 1H NMR (400 MHz, toluene- d_8): δ 2.29 (d, J = 13.2 Hz, 1H, H_b); 2.19 (ov m, 1H, H_a); 1.79 (d, J = 6.0 Hz, 3H, CH_3); 1.45 (ov s, 15H, C_5Me_5); 1.3 (d, J = 8.8 Hz, 1H, H_c). COSY (400 MHz, toluene- d_8): δ 2.29 \leftrightarrow δ 2.19; δ 2.19 \leftrightarrow δ 1.79; δ 2.19 \leftrightarrow δ 1.31. ^{13}C APT NMR (100 MHz, toluene- d_8): δ 247.9 (+, CO); 101.8 (+, C_5Me_5); 68.3 (−, CH); 48.9 (+, CH_2); 22.2 (−, CH_3); 9.3 (−, C_5Me_5). HMQC (400 MHz, toluene- d_8): δ 2.29 \leftrightarrow δ 48.9; δ 2.19 \leftrightarrow δ 68.3; δ 1.79 \leftrightarrow δ 22.2; δ 1.45 \leftrightarrow δ 9.3; δ 1.31 \leftrightarrow δ 48.9.

NMR analysis of the fluxional isomer of complex **95** at 27 °C. 1H NMR (400 MHz, toluene- d_8): δ 2.44 (br m, 1H, H_b); 2.22 (ov m, 1H, H_a); 1.66 (d, J = 6.0 Hz, 3H, CH_3); 1.45 (ov s, 15H, C_5Me_5); no signal detectable for H_c . COSY (400 MHz, toluene- d_8): δ 2.44 \leftrightarrow δ 1.66. ^{13}C APT NMR (100 MHz, toluene- d_8): δ 248.6 (+, CO); 101.9 (+, C_5Me_5); 64.3 (−, br, CH); 53.3 (+, br, CH_2); 21.6 (−, CH_3); 9.4 (−, C_5Me_5). HMQC (400 MHz, toluene- d_8): δ 1.66 \leftrightarrow δ 21.6; δ 1.45 \leftrightarrow δ 9.4. Due to the broad signals at this temperature, assignments for this isomer are tenuous and many expected 2D correlations are not observed.

NMR analysis of the static isomer of complex **95** at −80 °C. 1H NMR (400 MHz, toluene- d_8): δ 2.38 (d, J = 12.8 Hz, 1H, H_b); 2.01 (br m, 1H, H_a); 1.88 (ov d, J \approx 5.0 Hz, 3H, CH_3); 1.39 (s, 15H, C_5Me_5); 1.27 (d, J = 8.8, 1H, H_c). COSY (400 MHz, toluene- d_8):

$\delta 2.38 \leftrightarrow \delta 2.01$; $\delta 2.38 \leftrightarrow \delta 1.88$; $\delta 2.01 \leftrightarrow \delta 1.88$; $\delta 2.01 \leftrightarrow \delta 1.27$. ^{13}C APT NMR (100 MHz, toluene- d_8): $\delta 248.1$ (+, CO); 101.5 (+, C_5Me_5); 67.3 (–, CH); 47.6 (+, CH_2); 22.5 (–, CH_3); 9.2 (–, C_5Me_5). HMQC (400 MHz, toluene- d_8): $\delta 2.38 \leftrightarrow \delta 47.6$; $\delta 2.01 \leftrightarrow \delta 67.3$; $\delta 1.88 \leftrightarrow \delta 22.5$; $\delta 1.39 \leftrightarrow \delta 9.2$; $\delta 1.27 \leftrightarrow \delta 47.6$.

NMR analysis of the fluxional isomer of complex **95** at -80°C . ^1H NMR (400 MHz, toluene- d_8): $\delta 2.51$ (d, $J = 12.0$ Hz, 1H, H_b); 2.17 (br m, 1H, H_a); 1.88 (ov d, $J \approx 5.0$ Hz, 3H, CH_3); 1.41 (s, 15H, C_5Me_5); 1.07 (d, $J = 8.4$ Hz, 1H, H_c). COSY (400 MHz, toluene- d_8): $\delta 2.51 \leftrightarrow \delta 2.17$; $\delta 2.51 \leftrightarrow \delta 1.88$; $\delta 2.51 \leftrightarrow \delta 1.07$; $\delta 2.17 \leftrightarrow \delta 1.88$; $\delta 2.17 \leftrightarrow \delta 1.07$. ^{13}C APT NMR (100 MHz, toluene- d_8): $\delta 248.8$ (+, CO); 101.3 (+, C_5Me_5); 61.7 (–, CH); 53.3 (+, CH_2); 22.5 (–, CH_3); 9.4 (–, C_5Me_5). HMQC (400 MHz, toluene- d_8): $\delta 2.51 \leftrightarrow \delta 53.3$; $\delta 2.17 \leftrightarrow \delta 61.7$; $\delta 1.88 \leftrightarrow \delta 22.5$; $\delta 1.41 \leftrightarrow \delta 9.4$; $\delta 1.07 \leftrightarrow \delta 53.3$.



(η^5 -Permethylcyclopentadienyl)[η^2 -(1-trimethylsilyl-prop-2-ene)]carbonylnitrosyl-chromium **96:**

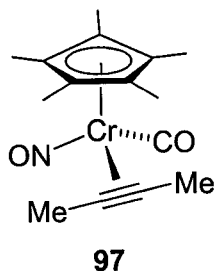
In a Schlenk tube, $\text{Cp}^*\text{CrNO}(\text{CO})_2$ **94** (250 mg, 0.915 mmol) was dissolved in 50 mL of benzene and 150 μL (0.944 mmol) of allyltrimethylsilane added via syringe. The solution was then cooled to 5°C and irradiated for 22 h. The resulting brown solution was then passed through a 1 x 5 cm silica-gel column and eluted with benzene. The dark

orange eluent was then evaporated *in vacuo* and the residue dissolved in 10 mL of pentane. Several crystallizations at $-35\text{ }^{\circ}\text{C}$ then provided the allyltrimethylsilane complex as an orange powder (158 mg, 48%), present in solution as a 2 : 3 mixture of unassigned isomers. Crystals suitable for X-ray crystallography were grown from a solution of complex **96** in pentane over two days at $-35\text{ }^{\circ}\text{C}$. Details are provided in Appendix A, part 8. IR (cm^{-1} , THF): $\nu_{\text{CO}} = 1942$, $\nu_{\text{NO}} = 1652$. HRMS calcd for $\text{C}_{17}\text{H}_{29}\text{CrNSiO}_2$: m/z 359.13727; found: 359.13761. Anal. calcd for $\text{C}_{17}\text{H}_{29}\text{CrNSiO}_2$: C, 56.8; H, 8.13; N, 3.9; found: C, 56.46; H, 8.13; N, 4.00.

NMR analysis of the static isomer of complex **96**. ^1H NMR (400 MHz, C_6D_6): δ 2.62 (dddd, $J = 13.2, 12.0, 9.0, 3.2\text{ Hz}$, 1H, H_c); 2.29 (d, $J = 13.2\text{ Hz}$, 1H, H_a); 2.12 (dd, $J = 14.0, 3.2\text{ Hz}$, 1H, H_d/H_e); 1.51 (br s, 15H, C_5Me_5); 1.29 (br d, $J = 9.0\text{ Hz}$, 1H, H_b); 0.77 (dd, $J = 14.0, 12.0\text{ Hz}$, 1H, H_d or H_e); 0.07 (s, $J = 9\text{H}$, SiMe_3). COSY (400 MHz, C_6D_6): δ 2.62 \leftrightarrow δ 2.29; δ 2.62 \leftrightarrow δ 2.12; δ 2.62 \leftrightarrow δ 1.29; δ 2.62 \leftrightarrow δ 0.77; δ 2.12 \leftrightarrow δ 0.77. ^{13}C APT NMR (100 MHz, C_6D_6): δ 248.8 (+, CO); 101.6 (+, C_5Me_5); 73.4 (−, C_2); 47.8 (+, C_1); 26.7 (+, C_3); 9.6 (−, C_5Me_5); −1.8 (−, SiMe_3). HMQC (400 MHz, C_6D_6): δ 2.62 \leftrightarrow δ 73.4; δ 2.29 \leftrightarrow δ 47.8; δ 2.12 \leftrightarrow δ 26.7; δ 1.51 \leftrightarrow δ 9.6; δ 1.29 \leftrightarrow δ 47.8; δ 0.77 \leftrightarrow δ 26.7; δ 0.07 \leftrightarrow δ −1.8.

NMR analysis of the fluxional isomer of complex **96**. ^1H NMR (400 MHz, C_6D_6): δ 2.71 (br m, 1H, H_c); 2.1 (br d, $J = 12.0\text{ Hz}$, 1H, H_a); 1.8 (dd, $J = 14.0, 2.8\text{ Hz}$, 1H, H_d/H_e); 1.53 (br d, $J \approx 8.4\text{ Hz}$, 1H, H_b); 1.5 (br s, 15H, C_5Me_5); 0.72 (br t, $J = 12.8$, 1H, H_d/H_e); 0.07 (s, $J = 9\text{H}$, SiMe_3). COSY (400 MHz, C_6D_6): δ 2.71 \leftrightarrow δ 2.10; δ 2.71 \leftrightarrow δ 1.8; δ

2.71 \leftrightarrow δ 1.53; δ 1.8 \leftrightarrow δ 0.72. ^{13}C APT NMR (100 MHz, C_6D_6): δ 250.0 (+, CO); 101.8 (+, C_5Me_5); 68.6 (–, br, C_2); 51.8 (+, br, C_1); 26.1 (+, C_3); 9.7 (–, C_5Me_5); –1.7 (–, SiMe_3). HMQC (400 MHz, C_6D_6): δ 2.71 \leftrightarrow δ 68.6; δ 2.10 \leftrightarrow δ 51.8; δ 1.8 \leftrightarrow δ 26.1; δ 1.53 \leftrightarrow δ 51.8; δ 0.72 \leftrightarrow δ 26.1; δ 1.5 \leftrightarrow δ 9.67; δ 0.07 \leftrightarrow δ –1.7.



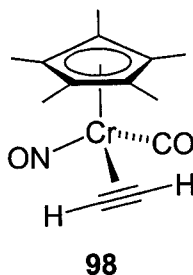
(η^5 -Permethylcyclopentadienyl)(η^2 -2-butyne)carbonylnitrosylchromium **97:**

In a Schlenk tube, $\text{Cp}^*\text{CrNO}(\text{CO})_2$ **94** (250 mg, 0.915 mmol) was dissolved in 50 mL of benzene and 2-butyne (100 μL , 1.28 mmol) added via syringe. The solution was then cooled to 5 $^\circ\text{C}$ and irradiated for 20 h. The resulting red-brown solution was then passed through a 1 x 5 cm silica-gel column and eluted with benzene. The dark red eluent was then evaporated *in vacuo* and the residue dissolved in 10 mL of pentane. Several crystallizations at –35 $^\circ\text{C}$ then provided 2-butyne complex **97** as dark red crystals (134 mg, 49%). The structure of these crystals was established by X-ray crystallography. Details are provided in Appendix A, part 9. IR (cm^{-1} , THF): ν_{CO} = 1942, ν_{NO} = 1646. ^1H NMR (400 MHz, C_6D_6): δ 2.33 (q, J = 1.5 Hz, 3H, CH_3); 2.19 (q, J = 1.5 Hz, 3H, CH_3); 1.55 (s, 15H, C_5Me_5). ^{13}C NMR (100 MHz, C_6D_6): δ 245.1 (CO); 103.4 (C_5Me_5); 94.2 (CCH_3); 77.6 (CCH_3); 12.5 (CCH_3); 10.6 (CCH_3); 9.7 (C_5Me_5). HMQC (400 MHz, C_6D_6): δ 2.33 \leftrightarrow δ 12.5; 2.19 \leftrightarrow 10.6; 1.55 \leftrightarrow 9.7. HMBC (400 MHz, C_6D_6): δ 2.33 \leftrightarrow

$\delta 94.2$; $\delta 2.33 \leftrightarrow \delta 77.6$; $\delta 2.19 \leftrightarrow \delta 94.2$; $\delta 2.19 \leftrightarrow \delta 77.6$; $\delta 1.55 \leftrightarrow \delta 103.4$. HRMS

calcd for $C_{15}H_{21}CrNO_2$: m/z 299.09775; found: 299.09803. Anal. calcd for

$C_{15}H_{21}CrNO_2$: C, 60.19; H, 7.07; N, 4.68; found: C, 59.83; H, 7.36; N, 4.69.



(η^5 -Permethylcyclopentadienyl)(η^2 -acetylene)carbonylnitrosylchromium 98:

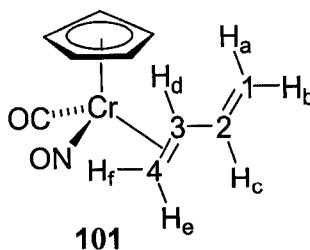
In an NMR tube, $Cp^*CrNO(CO)_2$ complex **94** (35 mg, 0.128 mmol) was dissolved in 0.7 ml of toluene- d_8 , cooled to $-78^\circ C$ and the solution saturated with acetylene via bubbling for 15 min. The solution was then sealed, warmed to $5^\circ C$ and irradiated for 20 h to provide acetylene complex **98** with $\sim 40\%$ conversion. The product could not be isolated as a solid compound. NMR analysis of the resulting red-brown solution: 1H NMR (400 MHz, toluene- d_8): δ 6.28 (s, 1H, C_2H_2); 5.8 (s, 1H, C_2H_2); 1.47 (s, 15H, C_5Me_5). ^{13}C NMR (100 MHz, toluene- d_8): δ 242.4 (CO); 103.9 (C_5Me_5); 101.5 (C_2H_2); 85.4 (C_2H_2); 10.1 (C_5Me_5). HMQC (400 MHz, toluene- d_8): δ 6.28 \leftrightarrow δ 101.5; δ 5.8 \leftrightarrow δ 85.4; δ 1.47 \leftrightarrow δ 10.1.

Conjugated diene complexes:

Note: the relative connectivity of the diene protons of the *s-trans*-(1,3-diene) products could be clearly determined by multidimensional NMR spectroscopy; however, the assignment of exactly which protons are nearer to the cyclopentadienyl ligand is purely arbitrary.

Photolysis of $\text{CpCrNO}(\text{CO})_2$ in the presence of 1,3-butadiene:

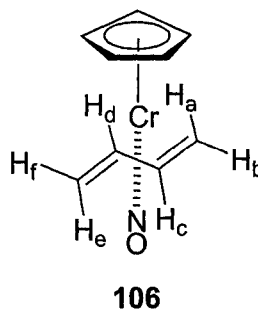
In an NMR tube, $\text{CpCrNO}(\text{CO})_2$ **90** (40 mg, 0.197 mmol) was dissolved in 0.7 mL of benzene- d_6 and ~ 50 μL (0.639 mmol) of 1,3-butadiene added via vacuum transfer. The solution was then cooled to 5 $^\circ\text{C}$ and irradiated for 18 h. Spectroscopic analysis of the resulting red-brown solution revealed the presence of a 1 : 1 : 12 mixture of two unassigned isomers of η^2 -butadiene complex **101** and one isomer of η^4 -butadiene complex **106**, respectively. A pure sample of η^4 -butadiene complex **106** by irradiating the reaction mixture without the 370 nm filter for three days. IR (THF, cm^{-1}) of the product mixture: complex **101**, $\nu_{\text{CO}} = 1973$, $\nu_{\text{NO}} = 1639$; complex **106**, $\nu_{\text{NO}} = 1670$. IR (THF, cm^{-1}) of pure η^4 -butadiene complex **106**: $\nu_{\text{NO}} = 1670$.



NMR analysis of the first isomer of η^2 -butadiene complex **101**. ^1H NMR (400 MHz, C_6D_6): δ 5.22 (dd, $J = 16.8, 1.2$ Hz, 1H, H_c); 5.17 (br m, 1H, H_a); 4.72 (dd, $J = 6.0, 0.4$

Hz, 1H, H_b); 4.33 (s, 5H, C₅H₅); 3.6 (2nd order m, 1H, H_d); 2.18 (dd, $J = 12.4, 1.2$ Hz, 1H, H_e); 2.11 (br d, $J = 8.4$ Hz, 1H, H_f). COSY (400 MHz, C₆D₆): $\delta 5.22 \leftrightarrow \delta 3.6$; $\delta 5.17 \leftrightarrow \delta 4.72$; $\delta 5.17 \leftrightarrow \delta 3.6$; $\delta 4.72 \leftrightarrow \delta 3.6$; $\delta 3.6 \leftrightarrow \delta 2.18$; $\delta 3.6 \leftrightarrow \delta 2.11$. ¹³C APT NMR (100 MHz, C₆D₆): $\delta 243.3$ (+, CO); 142.1 (–, C₂); 110.5 (+, C₁); 90.2 (–, C₅H₅); 68.4 (–, br, C₃); 46.3 (+, br, C₄). HMQC (400 MHz, C₆D₆): $\delta 5.22 \leftrightarrow \delta 142.1$; $\delta 5.17 \leftrightarrow \delta 110.5$; $\delta 4.72 \leftrightarrow \delta 110.5$; $\delta 4.39 \leftrightarrow \delta 90.2$; $\delta 3.6 \leftrightarrow \delta 68.4$; $\delta 2.18 \leftrightarrow \delta 46.3$; $\delta 2.11 \leftrightarrow \delta 46.3$.

NMR analysis of the second isomer of η^2 -butadiene complex **101**. ¹H NMR (400 MHz, C₆D₆): $\delta 5.74$ (ddd, $J = 18.0, 8.0, 6.8$ Hz, 1H, H_c); 5.37 (2nd order m, 1H, H_a); 4.89 (dd, $J = 10.4, 1.2$ Hz, 1H, H_b); 4.37 (s, 5H, C₅H₅); 3.21 (2nd order m, 1H, H_d); 2.29 (d, $J = 13.2$, 1H, H_e); 2.15 (d, $J = 8.4$ Hz, 1H, H_f). COSY (400 MHz, C₆D₆): $\delta 5.74 \leftrightarrow \delta 4.89$; $\delta 5.74 \leftrightarrow \delta 2.15$; $\delta 5.37 \leftrightarrow \delta 4.89$; $\delta 5.37 \leftrightarrow \delta 3.21$; $\delta 4.89 \leftrightarrow \delta 3.21$; $\delta 3.21 \leftrightarrow \delta 2.29$; $\delta 3.21 \leftrightarrow \delta 2.15$. ¹³C APT NMR (100 MHz, C₆D₆): $\delta 242.7$ (+, CO); 143.8 (–, C₂); 111.7 (+, C₁); 93.1 (–, C₅H₅); 69.3 (–, C₃); 44.4 (+, C₄). HMQC (400 MHz, C₆D₆): $\delta 5.74 \leftrightarrow \delta 143.8$; $\delta 5.37 \leftrightarrow \delta 111.7$; $\delta 4.89 \leftrightarrow \delta 111.7$; $\delta 4.37 \leftrightarrow \delta 93.1$; $\delta 3.21 \leftrightarrow \delta 69.3$; $\delta 2.29 \leftrightarrow \delta 44.4$; $\delta 2.15 \leftrightarrow \delta 44.4$.

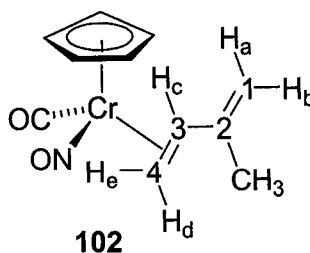


NMR analysis of the *s-trans* η^4 -butadiene complex **106**: ^1H NMR (400 MHz, C_6D_6): δ 4.54 (s, 5H, C_5H_5); 3.44 (dd, $J = 6.8, 1.2$ Hz, 1H, H_f or H_b); 3.18 (ddd, $J = 13.6, 10.7, 6.8$ Hz, 1H, H_d or H_c); 3.0 (dd, $J = 6.8, 0.8$ Hz, H_b or H_f); 2.74 (br d, $J = 14.0$ Hz, H_a or H_e); 2.32 (dddd, $J = 14.0, 10.7, 6.8, 0.4$ Hz, H_c or H_d); 2.08 (dt, $J = 13.6, 1.2$ Hz, H_e or H_a). COSY (400 MHz, C_6D_6): $\delta 3.44 \leftrightarrow \delta 3.18$; $\delta 3.44 \leftrightarrow \delta 3.0$; $\delta 3.44 \leftrightarrow \delta 2.08$; $\delta 3.18 \leftrightarrow \delta 2.74$; $\delta 3.18 \leftrightarrow \delta 2.32$; $\delta 3.18 \leftrightarrow \delta 2.08$; $\delta 3.0 \leftrightarrow \delta 2.74$; $\delta 3.0 \leftrightarrow \delta 2.32$; $\delta 2.74 \leftrightarrow \delta 2.32$; $\delta 2.32 \leftrightarrow \delta 2.08$. ^{13}C APT NMR (100 MHz, C_6D_6): δ 102.8 (–, CH); 92.5 (–, C_5H_5); 87.5 (–, CH); 65.4 (+, CH_2); 62.5 (+, CH_2). HMQC (400 MHz, C_6D_6): $\delta 4.54 \leftrightarrow \delta 92.5$; $\delta 3.44 \leftrightarrow \delta 65.4$; $\delta 3.0 \leftrightarrow \delta 62.5$; $\delta 2.74 \leftrightarrow \delta 62.5$; $\delta 2.08 \leftrightarrow \delta 65.4$; due to the extensive coupling of the butadiene methine protons, the associated 2D correlations were not observed.

Photolysis of $\text{CpCrNO}(\text{CO})_2$ in the presence of 2-methylbutadiene:

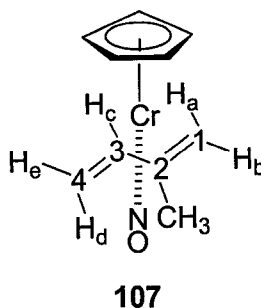
In an NMR tube, $\text{CpCrNO}(\text{CO})_2$ **90** (40 mg, 0.197 mmol) was dissolved in 0.7 mL of benzene- d_6 and 50 μL (0.5 mmol) of 2-methylbutadiene added via syringe. The solution was then cooled to 5 $^\circ\text{C}$ and irradiated for 18 h. Spectroscopic analysis of the resulting red-brown solution revealed the formation of a 1 : 1 : 6 mixture of two unassigned isomers of η^2 -isoprene complex **102** and one isomer of η^4 -isoprene complex

107, respectively. IR (THF, cm^{-1}) of the product mixture: complex **106**, $\nu_{\text{CO}} = 1972$, $\nu_{\text{NO}} = 1644$; complex **107**, $\nu_{\text{NO}} = 1672$; assignments are based on those made for complexes **101** and **106**.



NMR analysis of the first isomer of η^2 -isoprene complex **102**. ^1H NMR (300 MHz, C_6D_6): δ 5.0 (br m, 1H, H_a/H_b); 4.77 (br m, 1H, H_a or H_b); 4.34 (s, 5H, C_5H_5); 3.88 (dd, $J = 13.2, 9.3$ Hz, 1H, H_c); 2.41 (dd, $J = 13.2, 2.1$, 1H, H_d); 1.83 (br dd, $J = 9.3, 1.5$ Hz, 1H, H_e); 1.49 (br s, 3H, CH_3). COSY (300 MHz, C_6D_6): δ 5.0 \leftrightarrow δ 4.77; δ 5.0 \leftrightarrow δ 3.88; δ 5.0 \leftrightarrow δ 1.49; δ 4.77 \leftrightarrow δ 1.49; δ 3.88 \leftrightarrow δ 2.41; δ 3.88 \leftrightarrow δ 1.83; δ 2.41 \leftrightarrow δ 1.83. ^{13}C APT NMR (100 MHz, C_6D_6): δ 93.5 (–, C_5H_5); no other observable signals. HMQC (300 MHz, C_6D_6): δ 4.34 \leftrightarrow δ 93.5; no other observable correlations.

NMR analysis of the second isomer of η^2 -isoprene complex **102**: ^1H NMR (300 MHz, C_6D_6): δ 5.14 (br m, 1H, H_a/H_b); 4.78 (br m, 1H, H_a or H_b); 4.3 (s, 5H, C_5H_5); 3.19 (dd, $J = 14.1, 9.3$ Hz, 1H, H_c); 2.3 (dd, $J = 14.1, 0.7$, 1H, H_d); 2.24 (br d, $J = 9.3$ Hz, 1H, H_e); 1.49 (br s, 3H, CH_3). COSY (300 MHz, C_6D_6): δ 5.19 \leftrightarrow δ 4.78; δ 5.14 \leftrightarrow δ 3.19; δ 5.14 \leftrightarrow δ 1.49; δ 3.19 \leftrightarrow δ 2.3; δ 3.19 \leftrightarrow δ 2.24. ^{13}C APT NMR (100 MHz, C_6D_6): δ 93.3 (–, C_5H_5); no other observable signals. HMQC (300 MHz, C_6D_6): δ 4.34 \leftrightarrow δ 93.3; no other detectable correlations.



NMR analysis of the *s-trans* η^4 -isoprene complex **107**: ^1H NMR (300 MHz, C_6D_6):

δ 4.51 (s, 5H, C_5H_5); 3.3 (d, $J = 1.2$ Hz, 1H, H_b); 3.09 (dd, $J = 7.2, 1.2$ Hz, 1H, H_e); 3.0 (dd, $J = 14.1, 1.5$ Hz, H_d); 2.16 (dd, $J = 14.1, 7.2$ Hz, H_c); 1.88 (t, $J = 1.1$ Hz, H_a); 1.45 (br s, 3H, CH_3). COSY (300 MHz, C_6D_6): δ 3.3 \leftrightarrow δ 3.09; δ 3.3 \leftrightarrow δ 1.88; δ 3.3 \leftrightarrow δ

1.45; δ 3.09 \leftrightarrow δ 3.0; δ 3.09 \leftrightarrow δ 2.16; δ 3.0 \leftrightarrow δ 2.16; δ 2.16 \leftrightarrow δ 1.88; δ 2.16 \leftrightarrow δ

1.45. ^{13}C APT NMR (100 MHz, C_6D_6): δ 92.8 (–, C_5H_5); 91.8 (+, C_2); 85.7 (–, C_3); 63.8

(+, C_1); 61.7 (+, C_4); 18.5 (–, CH_3). HMQC (300 MHz, C_6D_6): δ 4.51 \leftrightarrow δ 92.8; δ 3.3 \leftrightarrow

δ 63.8; δ 3.09 \leftrightarrow δ 61.7; δ 3.0 \leftrightarrow δ 61.7; δ 2.16 \leftrightarrow δ 85.7; δ 1.88 \leftrightarrow δ 63.8; δ 1.45 \leftrightarrow δ

18.5.

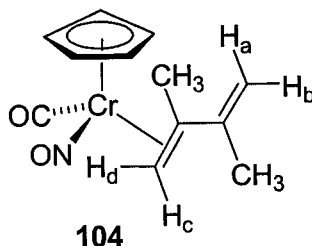
***In situ* preparation and characterization of the η^2 -(1,3-diene) complexes **103-105** and the *s-trans* η^4 -(1,3-diene) complexes **108-110**:**

As per the procedure for the formation of butadiene complexes **101** and **106**. In an NMR tube, approximately two molar equivalents of the organic 1,3-diene were added via syringe to a solution of $\text{CpCrNO}(\text{CO})_2$ **90** (20 mg, 0.098 mmol) in 0.7 mL benzene- d_6 . The solution was then cooled to 5 °C and irradiated for 17 h. Only the η^2 -(2,3-dimethylbutadiene) complex **104**, the *s-trans* η^4 -(2,3-dimethylbutadiene) complex **109**, and the η^4 -(2,4-dimethylbutadiene) complex **110** could be identified via 300 MHz ^1H NMR spectroscopy. Due to extensive overlap with residual starting material signals,

many of the ^1H NMR signals assigned for the diene ligands of complexes **103**, **105**, **108**, and **110** were detected indirectly via homonuclear COSY NMR spectroscopy. The low resolution of the product signals and prevented clear determination of the corresponding multiplicities and coupling constants.

η^2 -(1,3-Pentadiene) complexes **103 and **103'**:** Cp resonances located at 4.36 and 4.33 ppm. The ^1H NMR chemical shifts of the diene protons could only be identified for one isomer at 5.76, 5.2, 3.34, 2.33, 2.07 ppm.

***s-Trans* η^4 -(1,3-pentadiene) complex **108** and **108'**:** Cp resonances located at 4.56 and 4.48 ppm. The ^1H NMR chemical shifts of the diene protons could only be identified for one isomer at 3.08, 2.90, 2.82, 2.75, 2.14 ppm.

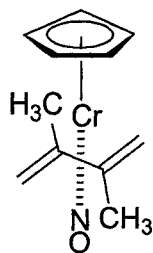


η^2 -(2,3-Dimethylbutadiene) complex **104:** present as a 1 : 1.3 mixture of isomers.

Major isomer: ^1H NMR (300 MHz, C_6D_6): δ 5.25 (d, $J = 1.3$ Hz, 1H, H_a or H_b); 5.08 (dq, $J = 2.6, 1.3$ Hz, 1H, H_a or H_b); 4.40 (s, 5H, C_5H_5); 2.56 (br s, 1H, H_c or H_d); 2.18 (br s, 1H, H_c or H_d); 1.58 (br d, $J = 1.1$ Hz, 3H, CH_3); 1.20 (br s, 3H, CH_3). COSY (300

MHz, C₆D₆): δ 5.25 \leftrightarrow δ 5.08; δ 5.25 \leftrightarrow δ 2.18; δ 5.25 \leftrightarrow δ 1.58; δ 5.08 \leftrightarrow δ 2.18; δ 5.08 \leftrightarrow δ 1.58; δ 2.56 \leftrightarrow δ 2.18; δ 2.56 \leftrightarrow δ 1.20; δ 2.18 \leftrightarrow δ 1.20; δ 1.58 \leftrightarrow δ 1.20.

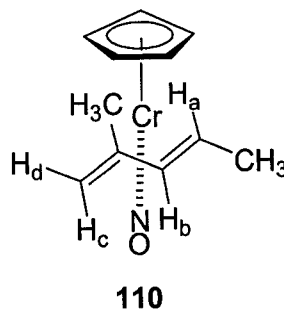
Minor isomer: ¹H NMR (300 MHz, C₆D₆): δ 5.18 (d, J = 1.4 Hz, 1H, H_b); 4.73 (dq, J = 2.3, 1.6 Hz, 1H, H_a); 4.42 (s, 5H, C₅H₅); 2.55 (br s, 1H, CH₂); 1.83 (br s, 3H, CH₃); 1.07 (br d, J = 1.3 Hz, 3H, CH₃); the remaining CH₂ proton could not be located. COSY (300 MHz, C₆D₆): δ 5.18 \leftrightarrow δ 4.73; δ 5.18 \leftrightarrow δ 1.07; δ 4.73 \leftrightarrow δ 2.55; δ 4.73 \leftrightarrow δ 1.07; δ 2.55 \leftrightarrow δ 1.83; δ 1.83 \leftrightarrow δ 1.07.



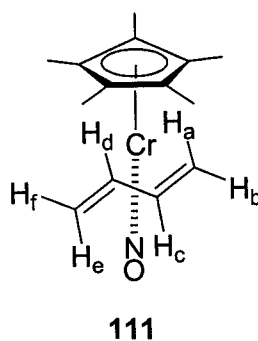
109

s-Trans η^4 -(2,3-dimethylbutadiene) complex 109: ¹H NMR (300 MHz, C₆D₆): δ 4.54 (s, 5H, C₅H₅); 3.40 (br d, J = 2.2 Hz, 1H, CH); 3.14 (br dd, J = 1.3, 0.8 Hz, 1H, CH₂); 2.98 (br d, J = 1.6 Hz, 1H, CH₂); 2.48 (br d, J = 2.2 Hz, 1H, CH₂); 1.51 (br s, 3H, CH₃); 0.93 (br s, 3H, CH₃). COSY (300 MHz, C₆D₆): δ 3.40 \leftrightarrow δ 3.14; δ 3.40 \leftrightarrow δ 2.48; δ 3.40 \leftrightarrow δ 1.51; δ 3.14 \leftrightarrow δ 2.98; δ 3.14 \leftrightarrow δ 0.93; δ 1.51 \leftrightarrow δ 0.93.

η^2 -(2-Methyl-1,3-pentadiene) complex **105** and **105'**: Cp resonances tentatively located at 4.42 and 4.39 ppm. The ^1H NMR chemical shifts of the diene protons could not be clearly identified.



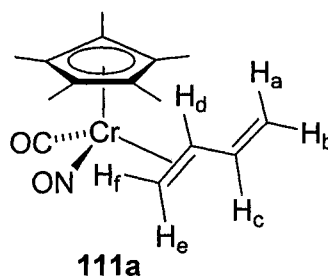
***s-Trans* η^4 -(2-methyl-1,3-pentadiene) complex 110:** ^1H NMR (300 MHz, C_6D_6): δ 4.51 (s, 5H, C_5H_5); 3.75 (dq, $J = 13.5, 6.3$ Hz, 1H, H_a); 3.26 (br d, $J = 1.1$ Hz, 1H, H_d); 2.09 (br d, $J = 13.5$ Hz, 1H, CH_b); 1.89 (br s, 1H, H_c); 1.47 (d, $J = 6.3$ Hz, 3H, CH_3); 1.49 (br s, 3H, CH_3). COSY (300 MHz, C_6D_6): δ 3.75 \leftrightarrow δ 2.09; δ 3.75 \leftrightarrow δ 1.47; δ 3.26 \leftrightarrow δ 1.89; δ 3.26 \leftrightarrow δ 1.49; δ 2.09 \leftrightarrow δ 1.89; δ 2.09 \leftrightarrow δ 1.48.



(η^5 -Permethylcyclopentadienyl)(η^4 -*s-trans*-butadiene)nitrosylchromium 111:

In a Schlenk tube, $\text{Cp}^*\text{CrNO}(\text{CO})_2$ **94** (820 mg, 3.0 mmol) was dissolved in 50 mL of benzene and ~2 mL (~25.6 mmol) of 1,3-butadiene added via bubbling. The

solution was then cooled to 5 °C and irradiated for 36 h, with venting approximately every 12 h. The resulting red-brown solution was then passed through a 1 x 7 cm silica-gel column and eluted with benzene. The dark orange eluent was then evaporated *in vacuo* and the residue dissolved in 10 mL of pentane. Several crystallizations at -35 °C then provided butadiene complex **111** as orange-brown crystals (570 mg, 70%). IR (cm⁻¹, THF): $\nu_{\text{NO}} = 1641$. ¹H NMR (400 MHz, C₆D₆): δ 3.45 (m, 1H, H_c or H_d); 3.37 (d, $J = 6.8$ Hz, 1H, H_b or H_f); 2.93 (dd, $J = 13.6, 0.8$ Hz, 1H, H_a or H_e); 2.54 (dd, $J = 6.8, 0.8$ Hz, 1H, H_b or H_f); 1.65 (m, 1H, H_c or H_d); 1.55 (dt, $J = 13.2, 1.0$ Hz, 1H, H_a or H_e); 1.48 (s, 15H, C₅Me₅). COSY (400 MHz, C₆D₆): δ 3.45 \leftrightarrow δ 3.37; δ 3.45 \leftrightarrow δ 1.65; δ 3.45 \leftrightarrow δ 1.55; δ 3.37 \leftrightarrow δ 1.55; δ 2.93 \leftrightarrow δ 2.54; δ 2.93 \leftrightarrow δ 1.65; δ 2.54 \leftrightarrow δ 1.65. ¹³C APT NMR (100 MHz, C₆D₆): δ 103.6 (-, CH); 102.1 (+, C₅Me₅); 94.7 (-, CH); 70.2 (+, CH₂); 68.2 (+, CH₂); 10.1 (-, C₅Me₅). HMQC (400 MHz, C₆D₆): δ 3.45 \leftrightarrow δ 103.6; δ 3.37 \leftrightarrow δ 70.2; δ 2.93 \leftrightarrow δ 68.2; δ 2.54 \leftrightarrow δ 68.2; δ 1.65 \leftrightarrow δ 94.7; δ 1.55 \leftrightarrow δ 70.2; δ 1.48 \leftrightarrow δ 10.1. HRMS calcd for C₁₄H₂₁CrNO: m/z 271.10281; found: 271.10259. Anal. calcd for C₁₄H₂₁CrNO: C, 61.98; H, 7.8; N, 5.16; found: C, 62.06; H, 7.98; N, 5.16.

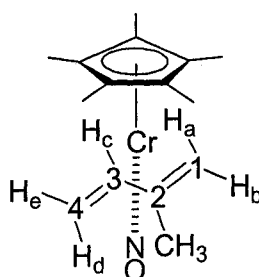


NMR analysis of an aliquot taken from the above reaction after 3 h of photolysis.

Spectroscopic evidence for the unassigned intermediate η^2 -butadiene stereoisomer **111a**:

¹H NMR (400 MHz, C₆D₆): δ 5.59 (br dt, $J = 16.8, 10.0$ Hz, 1H, H_c); 5.27 (br d, $J = 16.8$

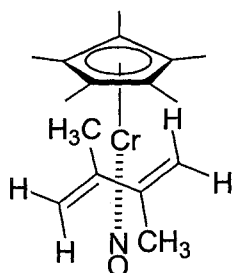
Hz, 1H, CH_a); 4.92 (br d, $J = 10.0$ Hz, 1H, H_b); 2.8 (br dd, $J = 12.8, 9.4$ Hz, 1H, H_d); 2.48 (br d, $J = 12.8$ Hz, 1H, H_e); 1.42 (br s, 15H, C₅Me₅); 1.39 (br m, 1H, H_f). COSY (400 MHz, C₆D₆): $\delta 5.59 \leftrightarrow \delta 5.27$; $\delta 5.59 \leftrightarrow \delta 4.92$; $\delta 5.59 \leftrightarrow \delta 2.8$; $\delta 5.27 \leftrightarrow \delta 4.92$; $\delta 2.8 \leftrightarrow \delta 2.48$; $\delta 2.8 \leftrightarrow \delta 1.39$. Additional broad ¹H NMR signals between 6.0 and 4.5, and 3.0 and 1.0 ppm suggest the presence of the second η^2 -butadiene intermediate complex **111b**.

**112**

(η^5 -Permethylcyclopentadienyl)(η^4 -s-trans-isoprene)nitrosylchromium **112:**

In a Schlenk tube, Cp*CrNO(CO)₂ **94** (287 mg, 1.05 mmol) was dissolved in 50 mL of benzene and 1.0 mL isoprene (10.0 mmol) added via syringe. The solution was then cooled to 5 °C and irradiated for 18 h. The resulting red-brown solution was then passed through a 1 x 5 cm silica-gel column and eluted with benzene. The dark orange eluent was then evaporated *in vacuo* and the residue dissolved in 10 mL of pentane. Several crystallizations at –35 °C then provided isoprene complex **112** as orange-brown crystals (200 mg, 67%). IR (cm^{–1}, THF): $\nu_{\text{NO}} = 1639$. ¹H NMR (400 MHz, C₆D₆): $\delta 3.25$ (br s, 1H, H_a or H_b); 3.19 (dd, $J = 14.4, 1.6$ Hz, 1H, H_d); 2.61 (ddd, $J = 7.2, 2.0, 0.8$ Hz, 1H, H_e); 1.54 (br s, 3H, CH₃); 1.50 (ov m, 1H, H_c); 1.49 (s, 15H, C₅Me₅); 1.35 (dd, $J = 1.2, 0.8$ Hz, 1H, H_a or H_b). COSY (400 MHz, C₆D₆): $\delta 3.25 \leftrightarrow \delta 2.61$; $\delta 3.25$

$\leftrightarrow \delta 1.54$; $\delta 3.25 \leftrightarrow \delta 1.35$; $\delta 3.19 \leftrightarrow \delta 2.61$; $\delta 3.19 \leftrightarrow \delta 1.50$; $\delta 2.61 \leftrightarrow \delta 1.54$; $\delta 2.61 \leftrightarrow \delta 1.50$. ^{13}C APT NMR (100 MHz, C_6D_6): δ 120.5 (+, C_2); 102.0 (+, C_5Me_5); 92.8 (–, C_3); 69.4 (+, C_1); 67.5 (+, C_4); 19.3 (–, CH_3); 10.3 (–, C_5Me_5). HMQC (400 MHz, C_6D_6): $\delta 3.25 \leftrightarrow \delta 69.4$; $\delta 3.19 \leftrightarrow \delta 67.5$; $\delta 2.61 \leftrightarrow \delta 67.5$; $\delta 1.54 \leftrightarrow \delta 19.3$; $\delta 1.49 \leftrightarrow \delta 10.3$; $\delta 1.35 \leftrightarrow \delta 69.4$. Crystals suitable for X-ray crystallography were grown from a solution of complex **112** in pentane at $-35\text{ }^\circ\text{C}$ over 12 h. Details are provided in Appendix A, part 10. HRMS calcd for $\text{C}_{15}\text{H}_{23}\text{CrNO}$: m/z 285.11847; found: 285.11827. Anal. calcd for $\text{C}_{15}\text{H}_{23}\text{CrNO}$: C, 63.14; H, 8.12; N, 4.91; found: C, 63.56; H, 8.23; N, 5.08.

**113**

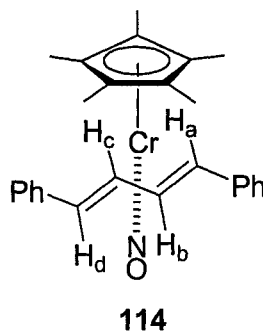
(η^5 -Permethylcyclopentadienyl)(η^4 -s-trans-2,3-dimethylbutadiene)nitrosylchromium **113:**

In a Schlenk tube, $\text{Cp}^*\text{CrNO}(\text{CO})_2$ **94** (240 mg, 0.878 mmol) was dissolved in 50 mL of benzene and 200 μL 2,3-dimethylbutadiene (1.77 mmol) added via syringe. The solution was then cooled to $5\text{ }^\circ\text{C}$ and irradiated for 22 h. The resulting red-brown solution was then passed through a 1 x 5 cm silica-gel column and eluted with benzene. The dark orange eluent was evaporated *in vacuo* and the residue dissolved in 10 mL of pentane. Several crystallizations at $-35\text{ }^\circ\text{C}$ then afforded 2,3-dimethylbutadiene complex **113** with trace amounts of the tentatively identified s-cis isomer **113'** as orange-brown

crystals (168 mg, 64%). IR (cm^{-1} , THF): $\nu_{\text{NO}} = 1636$. HRMS calcd for $\text{C}_{16}\text{H}_{25}\text{CrNO}$: m/z 299.13412; found: 299.13369. Anal. calcd for $\text{C}_{16}\text{H}_{25}\text{CrNO}$: C, 64.19; H, 8.42; N, 4.68; found: C, 64.17; H, 8.49; N, 4.64. Crystals of the major isomer suitable for X-ray crystallography were grown from a solution of complex **113** in pentane at $-35\text{ }^{\circ}\text{C}$ over 12 h. Details are provided in Appendix A, part 11.

NMR data of the *s-trans* isomer of complex **113**. ^1H NMR (400 MHz, C_6D_6): δ 3.17 (br d, $J = 1.2$ Hz, 1H, CH_2); 3.15 (br s, 1H, CH_2); 2.53 (br s, 1H, CH_2); 1.87 (br d, $J = 1.6$ Hz, 1H, CH_2); 1.63 (br s, 3H, CH_3); 1.57 (s, 15H, C_5Me_5); 1.12 (br s, 3H, CH_3). COSY (400 MHz, C_6D_6): δ 3.17 \leftrightarrow δ 2.53; δ 3.15 \leftrightarrow δ 1.87; δ 3.15 \leftrightarrow δ 1.63. ^{13}C APT NMR (100 MHz, C_6D_6): δ 102.2 (+, C_5Me_5); 67.8 (+, C_2); 67.7 (+, CH_2); 65.9 (+, C_3); 65.7 (+, CH_2); 21.9 (–, CH_3); 20.6 (–, CH_3); 10.5 (–, C_5Me_5). HMQC (400 MHz, C_6D_6): δ 3.17 \leftrightarrow δ 65.7; δ 3.15 \leftrightarrow δ 67.7; δ 2.53 \leftrightarrow δ 65.7; δ 1.87 \leftrightarrow δ 67.7; δ 1.63 \leftrightarrow δ 21.9; δ 1.57 \leftrightarrow δ 10.5; δ 1.12 \leftrightarrow δ 20.6.

NMR data of the tentatively assigned *s-cis* isomer of complex **113**: ^1H NMR (400 MHz, C_6D_6): δ 3.05 (d, $J = 3.6$ Hz, 2H, CH_2); 2.14 (s, 6H, $2\times\text{CH}_3$); 1.55 (s, 15H, C_5Me_5); -0.68 (d, $J = 3.6$ Hz, 2H, CH_2). COSY (400 MHz, C_6D_6): δ 3.05 \leftrightarrow δ -0.68 .

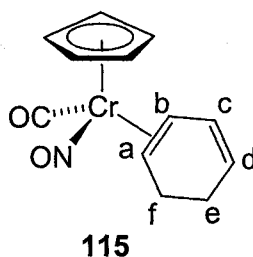


***In situ* characterization of (η⁵-permethylcyclopentadienyl)(η⁴-s-*trans*-1,4-diphenylbutadiene)nitrosylchromium 114:**

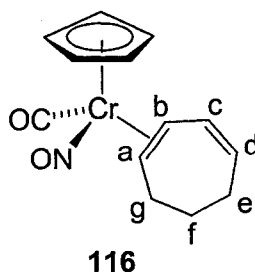
In a Schlenk tube, Cp*CrNO(CO)₂ **94** (120 mg, 0.366 mmol) was dissolved in 50 mL of benzene and 1,4-diphenylbutadiene (49.1 mg, 0.366 mmol) added. The solution was then cooled to 5 °C and irradiated for 24 h. The resulting red solution was passed through a 1 x 5 cm silica-gel column and eluted with benzene. The dark red eluent was evaporated *in vacuo* and the residue dissolved in 10 mL of pentane. Several crystallizations at −35 °C then afforded the η⁴-diphenylbutadiene complex as a red powder contaminated with unreacted 1,4-diphenylbutadiene (93.0 mg, 60% estimated from the ¹H NMR spectrum). IR and HRMS data could not be obtained. ¹H NMR (400 MHz, C₆D₆) only of the Cp* and η⁴-diene ligands: δ 4.70 (d, *J* = 13.6 Hz, 1H, H_a/H_d); 4.35 (dd, *J* = 12.8, 10.0 Hz, 1H, H_b/H_c); 3.03 (d, *J* = 12.8 Hz, 1H, H_a/H_d); 2.73 (ddd, *J* = 13.6, 10.0, 0.8 Hz, 1H, H_b/H_c); 1.25 (s, 15H, C₅Me₅). COSY (400 MHz, C₆D₆): δ 4.70 ↔ δ 2.73; δ 4.35 ↔ δ 3.03; δ 4.35 ↔ δ 2.73. ¹³C APT NMR (100 MHz, C₆D₆): δ 102.7 (+, C₅Me₅); 96.7 (−, CH); 91.3 (−, CH); 86.8 (−, CH); 85.9 (−, CH); 9.39 (−, C₅Me₅).

General procedure for the *in situ* formation and characterization of cyclic η^2 -(1,3-diene) complexes **115 and **116**:**

In an NMR tube, $\text{CpCrNO}(\text{CO})_2$ **90** (15.0 mg, 0.074 mmol) was dissolved in 0.7 mL of benzene- d_6 and 2.5 molar equivalent of the 1,3-diene added via syringe. The solution was cooled to 5 °C, jacketed with a 370 nm cutoff filter and irradiated for 12 h with a 450 W UV lamp. Conversions ranged from 60 to 90% and were based on relative integration of the Cp signals of residual complex **90** and the products.



NMR analysis of the major η^2 -(1,3-cyclohexadiene) isomer of complex **115**. ^1H NMR (300 MHz, C_6D_6): δ 6.04 (m, 1H, H_c); 5.56 (m, 1H, H_d); 4.33 (s, 5H, C_5H_5); 3.54 (dd, $J = 8.7, 5.4$ Hz, 1H, H_b); 2.63 (br dt, $J = 8.7, 2.7$ Hz, 1H, H_f); 2.41 (br dt, $J = 8.7, 2.9$ Hz, 1H, H_a); 1.75 to 1.58 (ov m, 3H, $2\times\text{H}_e$ and H_f). COSY (300 MHz, C_6D_6): δ 6.04 \leftrightarrow δ 5.56; δ 6.04 \leftrightarrow δ 3.54; δ 6.04 \leftrightarrow δ 1.67; δ 5.56 \leftrightarrow δ 1.74; δ 3.54 \leftrightarrow δ 2.41; δ 2.63 \leftrightarrow δ 1.74; δ 2.63 \leftrightarrow δ 1.58.



NMR analysis of the major η^2 -(1,3-cycloheptadiene) isomer of complex **116**. ^1H NMR (300 MHz, C_6D_6): δ 6.01 (ddt, $J = 11.7, 5.4, 2.0$ Hz, 1H, H_c); 5.51 (br dt, $J = 11.7, 4.8$ Hz, 1H, H_d); 4.34 (s, 5H, C_5H_5); 3.37 (br dd, $J = 9.9, 5.4$ Hz, 1H, H_b); 2.75 (dt, $J = 9.9, 5.4$ Hz, 1H, H_a); 2.33 (m, 1H, H_g); 2.18 to 1.47 (ov m, 5H, $2x\text{H}_e, 2x\text{H}_f$, and H_g). COSY (300 MHz, C_6D_6): δ 6.01 \leftrightarrow δ 5.51; δ 6.01 \leftrightarrow δ 3.37; δ 6.01 \leftrightarrow δ 2.18; δ 5.51 \leftrightarrow δ 2.18 δ 3.37 \leftrightarrow δ 2.18 δ 2.75 \leftrightarrow δ 2.33; δ 2.33 \leftrightarrow δ 1.61.

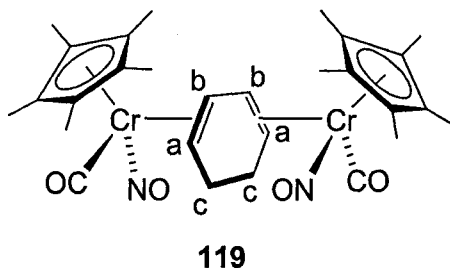
(η^5 -Permethylcyclopentadienyl)carbonylnitrosylchromium(η^2 -1,3-cyclohexadiene) **117 and [$(\eta^5$ -permethylcyclopentadienyl)carbonylnitrosylchromium] $_2$ (μ - η^2 : η^2 -1,3-cyclohexadiene) **119**:**

In a Schlenk tube, $\text{Cp}^*\text{CrNO}(\text{CO})_2$ **94** (350 mg, 0.128 mmol) was dissolved in 60 mL of benzene and 122 μL (0.128 mmol) of 1,3-cyclohexadiene added via syringe. The solution was then cooled to 5 $^\circ\text{C}$ and irradiated for 24 h. The resulting red-brown solution was then passed through a 1 x 5 cm silica-gel column and eluted with benzene. The orange-red eluent was evaporated *in vacuo* and the residue dissolved in 20 mL of pentane. Crystallization for 12 h at -35 $^\circ\text{C}$ deposited a light orange powder; the supernatant was decanted and the solid dried to provide μ -(η^2 : η^2 -1,3-cyclohexadiene) complex **119** (12.4 mg, 17%). Concentration of the supernatant by one-fourth volume followed by cooling at -35 $^\circ\text{C}$ for an additional 12 h provided a stereoisomeric mixture of

μ -(η^2 : η^2 -1,3-cyclohexadiene) complex **119'** also as a light orange powder (9.5 mg, 13%).

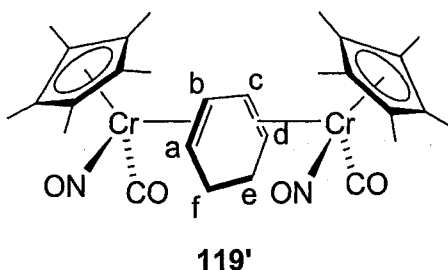
Further concentration of this supernatant by one-half volume followed by crystallization for 24 h at -35 °C then provided η^2 -(1,3-cyclohexadiene) complex **117** as a pale orange powder (13.7 mg, 33%), present in solution as a 5 : 1 mixture of unassigned isomers.

Note: the *anti* structural assignment of the major isomer complex **119** was solved by X-ray crystallography. The *anti* structures shown for the μ -(η^2 : η^2 -1,3-cyclic-diene) products **119'**, **121**, and **121'** are merely provided for illustrative purposes, and may actually exist as the *syn* congeners.



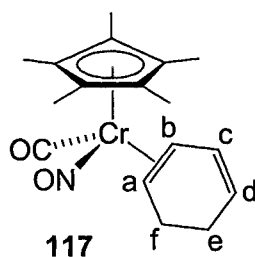
Spectral data for the μ -(η^2 : η^2 -1,3-cyclohexadiene) complex **119**. IR (cm^{-1} , THF): ν_{CO} = 1943, ν_{NO} = 1654. ^1H NMR (500 MHz, C_6D_6): δ 3.21 (2nd order m, FWHM = 10.8 Hz, 2H, H_b); 2.54 (ov m, 2H, H_c); 2.37 (ov m, 2H, H_c); 1.93 (br dt, J = 8.7, 2.6 Hz, 2H, H_a); 1.56 (s, 30H, $2\text{C}_5\text{Me}_5$). COSY (500 MHz, C_6D_6): δ 3.27 \leftrightarrow δ 1.93; δ 2.54 \leftrightarrow δ 1.93; δ 2.37 \leftrightarrow δ 1.93. ^{13}C APT NMR (125 MHz, C_6D_6): δ 248.4 (CO); 101.9 (+, C_5Me_5); 67.9 (−, CH_a); 65.8 (−, CH_b); 24.3 (+, CH_2); 9.8 (−, C_5Me_5). HMQC (500 MHz, C_6D_6): δ 3.27 \leftrightarrow δ 67.0; δ 2.54 \leftrightarrow δ 24.3; δ 2.37 \leftrightarrow δ 24.3; δ 1.93 \leftrightarrow δ 65.8; δ 1.56 \leftrightarrow δ 9.8. HMBC

(500 MHz, C_6D_6): $\delta 3.27 \leftrightarrow \delta 65.8$; $\delta 3.27 \leftrightarrow \delta 24.3$; $\delta 2.54 \leftrightarrow \delta 65.8$; $\delta 1.93 \leftrightarrow \delta 67.0$; $\delta 1.56 \leftrightarrow \delta 101.9$. Due to limited thermal instability, HRMS and consistent combustion analysis could not be obtained on this compound. Crystals suitable for X-ray crystallography, however, were grown from a solution of complex **119** in pentane at $-35\text{ }^\circ\text{C}$. Details are provided in Appendix A, part 12.



Spectral data for the unassigned $\mu-(\eta^2:\eta^2\text{-}1,3\text{-cyclohexadiene})$ complex **119'**. IR (cm^{-1} , THF): $\nu_{\text{CO}} = 1943$, $\nu_{\text{NO}} = 1654$. ^1H NMR (500 MHz, C_6D_6): $\delta 3.59$ (dd, $J = 9.0, 3.1$ Hz, 1H, H_a); $\delta 3.18$ (dddd, $J = 16.0, 7.5, 3.1$ Hz, 1H, CH_{2-e}); $\delta 3.01$ (dd, $J = 9.0, 3.1$ Hz, 1H, H_b); $\delta 2.62$ (br dd, $J = 16.0, 6.5$ Hz, 1H, CH_{2-d}); $\delta 2.45$ (dt, $J = 9.0, 2.8$ Hz, 1H, H_f); $\delta 2.39$ (br d, $J = 9.5$ Hz, 1H, CH_{2-e}); $\delta 2.33$ (br m, 1H, CH_{2-d}); $\delta 1.93$ (br m, 1H, H_c); $\delta 1.55$ (s, 15H, C_5Me_5); $\delta 1.51$ (s, 15H, C_5Me_5). COSY (500 MHz, C_6D_6): $\delta 3.59 \leftrightarrow \delta 3.01$; $\delta 3.59 \leftrightarrow \delta 1.93$; $\delta 3.18 \leftrightarrow \delta 2.62$; $\delta 3.18 \leftrightarrow \delta 2.39$; $\delta 3.18 \leftrightarrow \delta 2.33$; $\delta 3.18 \leftrightarrow \delta 1.93$; $\delta 3.01 \leftrightarrow \delta 2.45$; $\delta 3.01 \leftrightarrow \delta 1.93$; $\delta 2.62 \leftrightarrow \delta 1.93$; $\delta 2.45 \leftrightarrow \delta 2.33$; $\delta 2.36 \leftrightarrow \delta 1.93$. ^{13}C APT NMR (125 MHz, C_6D_6): $\delta 251.5$ (+, CO); $\delta 249.2$ (+, CO); $\delta 102.3$ (+, C_5Me_5); $\delta 102.0$ (+, C_5Me_5); $\delta 72.6$ (–, CH_b); $\delta 67.9$ (–, CH_c); $\delta 65.4$ (–, CH_a); $\delta 61.5$ (–, CH_f); $\delta 24.5$ (+, CH_{2-d}); $\delta 23.2$ (+, CH_{2-e}); $\delta 9.7$ (–, C_5Me_5); $\delta 9.6$ (–, C_5Me_5). HMQC (500 MHz, C_6D_6), partial data only: $\delta 3.59 \leftrightarrow \delta 65.4$; $\delta 3.01 \leftrightarrow \delta 72.6$; $\delta 2.62 \leftrightarrow \delta 23.2$; $\delta 2.45 \leftrightarrow \delta 61.5$; $\delta 2.33 \leftrightarrow \delta 24.6$; $\delta 1.93 \leftrightarrow \delta 67.9$; $\delta 1.55 \leftrightarrow \delta 9.7$; $\delta 1.51 \leftrightarrow \delta 9.6$. HMBC (500 MHz, C_6D_6): $\delta 3.59 \leftrightarrow \delta 61.5$; δ

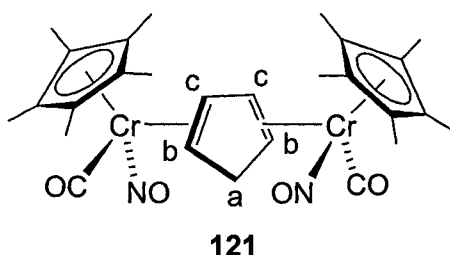
3.59 \leftrightarrow δ 23.2; δ 3.01 \leftrightarrow δ 67.9; δ 3.01 \leftrightarrow δ 24.6; δ 2.62 \leftrightarrow δ 67.9; δ 2.45 \leftrightarrow δ 23.2; δ 2.33 \leftrightarrow δ 72.6; δ 1.93 \leftrightarrow δ 72.6; δ 1.93 \leftrightarrow δ 24.6; δ 1.55 \leftrightarrow δ 102.3; δ 1.51 \leftrightarrow δ 102.0.



Spectral data for the unassigned major isomer of η^2 -1,3-cyclohexadiene complex **117**. IR (cm^{-1} , THF): $\nu_{\text{CO}} = 1945$, $\nu_{\text{NO}} = 1663$. ^1H NMR (400 MHz, C_6D_6): δ 6.15 (m, 1H, H_c); 5.57 (m, 1H, H_d); 2.73 (2nd order m, 2H, CH_{2-e}); 2.57 (2nd order m, 1H, H_b); 1.91 (br dt, $J = 8.8, 3.1$ Hz, 1H, H_a); 1.78 (ov m, 1H, CH_{2-f}); 1.73 (ov m, 1H, CH_{2-f}); 1.45 (s, 15H, C_5Me_5). COSY (400 MHz, C_6D_6): δ 6.15 \leftrightarrow δ 5.75; δ 6.15 \leftrightarrow δ 2.57; δ 6.15 \leftrightarrow δ 1.73; δ 5.57 \leftrightarrow δ 1.78; δ 2.73 \leftrightarrow δ 1.78; δ 2.73 \leftrightarrow δ 1.73; δ 2.57 \leftrightarrow δ 1.91. ^{13}C APT NMR (100 MHz, C_6D_6): δ 248.8 (+, CO); 128.1 (–, CH_c); 122.1 (–, CH_d); 102.1 (+, C_5Me_5); 66.8 (–, CH_a); 56.7 (–, CH_b); 26.8 (+, CH_{2-e}); 21.9 (+, CH_{2-f}); 9.3 (–, C_5Me_5). HMQC (400 MHz, C_6D_6), partial data only: δ 6.15 \leftrightarrow δ 128.1; δ 5.57 \leftrightarrow δ 122.1; δ 2.73 \leftrightarrow δ 26.8; δ 2.57 \leftrightarrow δ 66.8; δ 1.91 \leftrightarrow δ 56.7; δ 1.45 \leftrightarrow δ 9.3. HRMS calcd for $\text{C}_{17}\text{H}_{23}\text{CrNO}_2$: m/z 325.11340; found: 325.11356. Anal. calcd for $\text{C}_{17}\text{H}_{23}\text{CrNO}_2$: C, 62.16; H, 7.12; N, 4.3; found: C, 61.13; H, 7.04; N, 4.52.

(η^5 -Permethylcyclopentadienyl)carbonylnitrosylchromium(η^2 -cyclopentadiene) **120 and [$(\eta^5$ -permethylcyclopentadienyl)carbonylnitrosylchromium] $_2(\mu$ - η^2 : η^2 -cyclopentadiene) **121**:**

In a Schlenk tube, $\text{Cp}^*\text{CrNO}(\text{CO})_2$ **94** (255 mg, 0.933 mmol) was dissolved in 50 mL of benzene and 100 μL of cyclopentadiene added via syringe. The solution was then cooled to 5 $^\circ\text{C}$ and irradiated for 24 h. The resulting red-brown solution was then passed through a 1 x 5 cm silica-gel column and eluted with benzene. The orange-red eluent was evaporated *in vacuo* and the residue dissolved in 20 mL of pentane. Crystallization for 12 h at -35 $^\circ\text{C}$ then provided the dimeric μ -(η^2 : η^2 -cyclopentadiene) complex **121** as a light orange powder (52 mg, 10%). Concentration of the subsequent supernatant to ~ 10 mL followed by crystallization for 24 h at -35 $^\circ\text{C}$ then provided the monomeric η^2 -cyclopentadiene complex **120** as a light orange powder (29 mg, 10%).



Spectral data for the unassigned μ -(η^2 : η^2 -cyclopentadiene) complex **121**. IR (cm^{-1} , THF):

$\nu_{\text{CO}} = 1948$, $\nu_{\text{NO}} = 1654$. ^1H NMR (500 MHz, C_6D_6): δ 3.91 (d, $J = 5.5$ Hz, 2H, H_c);

3.73 (t, $J = 2.5$ Hz, 2H, H_a); 2.72 (ddd, $J = 5.5, 2.5, 2.5$ Hz, 2H, H_b); 1.48 (s, 30H,

$2\text{C}_5\text{Me}_5$). COSY (500 MHz, C_6D_6): δ 3.91 \leftrightarrow δ 3.73; δ 3.91 \leftrightarrow δ 2.72; δ 3.73 \leftrightarrow δ 2.72.

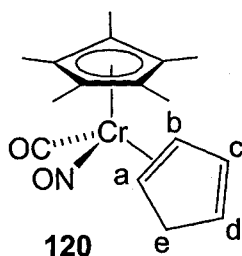
^{13}C APT NMR (125 MHz, C_6D_6): δ 247.9 (CO); 102.2 (+, C_5Me_5); 83.1 (−, CH); 66.2 (−,

CH); 43.2 (+, CH_2); 9.7 (−, C_5Me_5). HMQC (400 MHz, C_6D_6): δ 3.91 \leftrightarrow δ 83.1; δ 3.73

$\leftrightarrow \delta 43.2$; $\delta 2.72 \leftrightarrow \delta 66.2$; $\delta 1.48 \leftrightarrow \delta 9.7$. Anal. calcd for $C_{27}H_{36}Cr_2N_2O_4$: C, 5.03; H, 58.27; N, 6.52; found: C, 5.48; H, 57.79; N, 6.5.

Spectral data for the $\mu-(\eta^2:\eta^2\text{-cyclopentadiene})$ complex **121'**, isolated in trace amount.

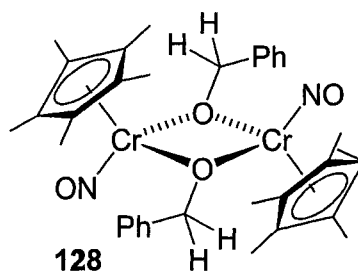
^1H NMR (400 MHz, C_6D_6): $\delta 3.70$ (d, $J = 5.6$ Hz, 2H, H_c); 3.54 (t, $J = 2.6$ Hz, 2H, H_a); 2.37 (ddd, $J = 5.6, 2.6, 2.6$ Hz, 2H, H_b); 1.58 (s, 30H, $2C_5Me_5$).



Spectral data for the unassigned major isomer of the $\eta^2\text{-cyclopentadiene}$ complex **120**.

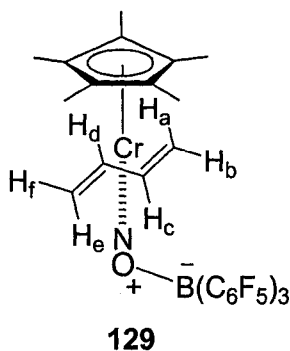
IR (cm^{-1} , THF): $\nu_{\text{CO}} = 1944$, $\nu_{\text{NO}} = 1660$. ^1H NMR (500 MHz, C_6D_6): $\delta 6.60$ (m, 1H, H_c); 5.66 (m, 1H, H_d); 3.34 (br dd, $J = 5.5, 2.2$ Hz, 2H, H_e); 3.26 (dt, $J = 3.6, 2.2$ Hz, 1H, H_a); 3.12 (ddt, $J = 5.2, 3.6, 1.0$ Hz, 1H, H_b); 1.48 (br s, 15H, C_5Me_5). COSY (500 MHz, C_6D_6): $\delta 6.60 \leftrightarrow \delta 5.66$; $\delta 6.60 \leftrightarrow \delta 3.34$; $\delta 5.66 \leftrightarrow \delta 3.34$; $\delta 3.34 \leftrightarrow \delta 3.12$; $\delta 3.26 \leftrightarrow \delta 3.12$.

Experimental details for Chapter 5:



Addition of benzaldehyde to $\text{Cp}^*\text{CrNO}(\text{C}_4\text{H}_6)$ **111**. Formation of $[(\eta^5\text{-permethylcyclopentadienyl})(\mu\text{-benzyloxy})\text{nitrosylchromium}]_2$ **128**:

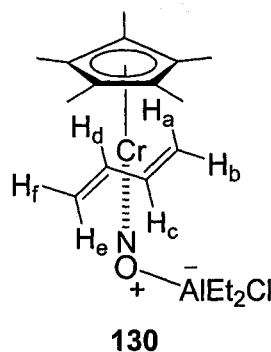
In an NMR tube, benzaldehyde (61 μL , 0.06 mmol) was added to a solution of $\text{Cp}^*\text{CrNO}(\text{C}_4\text{H}_6)$ **111** (15.0 mg, 0.055 mmol) in 0.7 mL of benzene- d_6 . Progress of the reaction was monitored by ^1H NMR spectroscopy. After 5 days at room temperature the original benzaldehyde signals were completely consumed and replaced with broad aromatic peaks. The NMR tube was then opened to a nitrogen atmosphere and the solvent allowed to evaporate over 12 days, providing the dimeric chromium(I) complex **128** as black crystals (~5 mg, 28%). The identity of these crystals was confirmed by X-ray crystallography. Details are provided in the Appendix A, part 12.



(η^5 -Permethylcyclopentadienyl)(η^4 -*s-trans*-butadiene)chromium[nitrosyl-tris(perfluorophenyl)boron] **129:**

To a solution of $\text{Cp}^*\text{CrNO}(\text{C}_4\text{H}_6)$ **111** (100 mg, 0.0369 mmol) in 5 mL of hexane was added a suspension of tris(perfluorophenyl)boron (189 mg, 0.0369) in 5 mL of hexane. After 5 min at room temperature, the brick-red suspension was filtered through Celite and the filtrate stored at -35°C for 24 h to provide zwitterionic complex **129** as a brick-red powder (93 mg, 55%). IR (cm^{-1} , Nujol): $\nu_{\text{C}_6\text{F}_5} = 1644$ (w), 1517(w).¹³ IR (cm^{-1} , microscope): 3031-2861 (var), 1793 (w), 1700 (w), 1644 (s), 1566-1284 (s), 1100 (s). ¹H NMR (500 MHz, C_6D_6): δ 3.61 (ddd, $J = 15.0, 12.0, 7.5$ Hz, 1H, H_c or H_d); 3.26 (dd, $J = 7.5, 1.5$ Hz, 1H, H_b or H_f); 3.11 (d, $J = 15.5$ Hz, 1H, H_a or H_e); 2.50 (dd, $J = 7.5, 0.7$ Hz, 1H, H_b or H_f); 1.21 (ddd, $J = 15.0, 12.0, 7.5$ Hz estimated from the coupling partner, 1H, H_c or H_d); 1.09 (s, 15H, C_5Me_5); 1.07 (br d, $J = 15.0$ Hz, H_a or H_e). COSY (500 MHz, C_6D_6): δ 3.61 \leftrightarrow δ 3.26; δ 3.61 \leftrightarrow δ 3.12; δ 3.61 \leftrightarrow δ 1.21; δ 3.61 \leftrightarrow δ 1.07; δ 3.11 \leftrightarrow δ 1.21; δ 2.50 \leftrightarrow δ 1.21; δ 1.21 \leftrightarrow δ 1.07. ¹³C APT NMR (100 MHz, C_6D_6): δ 148.5 (br d, $J_{\text{C-F}} = 249$ Hz, +, Ar); 142.5 (br d, $J_{\text{C-F}} = 256$ Hz, +, Ar); 137.6 (br d, $J_{\text{C-F}} = 253$ Hz, +, Ar); 108.5 (+, C_5Me_5); 106.0 (−, CH); 103.2 (−, CH); 77.7 (+, CH_2); 76.8 (+, CH_2); 9.8 (−, C_5Me_5). HMQC (500 MHz, C_6D_6): δ 3.61 \leftrightarrow δ 106.0; δ 3.26 \leftrightarrow δ 77.7; δ 3.11 \leftrightarrow δ 76.8; δ 2.50 \leftrightarrow δ 76.8; δ 1.21 \leftrightarrow δ 103.2; δ 1.09 \leftrightarrow δ 9.8; δ 1.07 \leftrightarrow δ 77.7. ¹⁹F

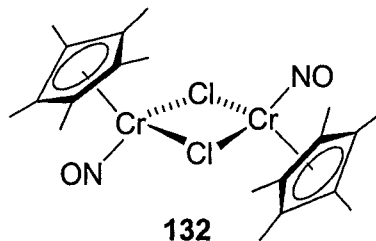
NMR (376 MHz, C_6D_6): -132.8 (br s); -156.5 (br s); -164.3 (br t, $J = 17.9$ Hz). ^{11}B (159.8 MHz, C_6D_6): 3.74 (br s). Due to thermal sensitivity, HRMS of this complex could not be obtained. Anal. calcd for $C_{32}H_{21}CrNOBF_{15}$: C, 49.07; H, 2.7; N, 1.79; found: C, 49.73; H, 3.06; N, 1.86. Due to the large percentage of fluorine atoms in the microanalysis samples, precise fluorine analysis could not be obtained. Crystals suitable for X-ray crystallography were grown from several successive recrystallizations of a solution complex **129** in diethyl ether at -35 °C. Details are provided in Appendix A, part 14.



(η^5 -Permethylcyclopentadienyl)(η^4 -*s-trans*-butadiene)chromium[nitrosyl-diethylaluminumchloride] **130:**

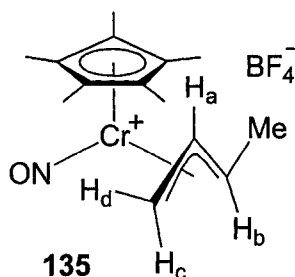
In an NMR tube, diethylaluminumchloride (5.3 mg, 0.044 mmol) in 0.7 mL of benzene- d_6 was added to $Cp^*CrNO(C_4H_6)$ **111** (12.0 mg, 0.044 mmol). NMR analysis of the resulting brick-red solution revealed signals for the thermally sensitive tentatively assigned zwitterionic complex **130**: 1H NMR (300 MHz, C_6D_6): δ 4.14 (br m, 1H, H_c or H_d); 3.57 (br d, $J = 5.7$ Hz, 1H, H_b or H_f); 3.43 (br d, $J = 14.1$ Hz, 1H, H_a or H_e); 2.59 (d, $J = 6.9$ Hz, 1H, H_b or H_f); 1.51 (br m, 1H, H_c or H_d); 1.46 (br t, $J = 8.1$ Hz, 6H, CH_2CH_3); 1.38 (br d, $J = 14.4$ Hz, 1H, H_a or H_e); 1.28 (s, 15H, C_5Me_5); 0.34 (br q, 4H, $J = 8.1$ Hz,

CH_2CH_3). COSY (300 MHz, C_6D_6), only partial data available: $\delta 4.14 \leftrightarrow \delta 1.38$; $\delta 3.43 \leftrightarrow \delta 1.41$; $\delta 2.59 \leftrightarrow \delta 1.51$; $\delta 1.46 \leftrightarrow \delta 0.34$.



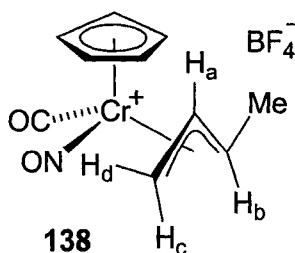
Addition of HCl to $\text{Cp}^*\text{CrNO}(\text{C}_4\text{H}_6)$ **111. Formation of $[\text{Cp}^*\text{Cr}(\text{NO})\text{Cl}]_2$ **132**:**

To a solution of $\text{Cp}^*\text{CrNO}(\text{C}_4\text{H}_6)$ **111** (37 mg, 0.136 mmol) in diethyl ether at -78°C was added HCl (4M in dioxane, $33.4\ \mu\text{L}$, 0.134 mmol) via syringe. The solution was stirred at -78°C for 30 min, during which time a colour change from orange to yellow was observed. Upon warming to room temperature, the colour of the solution turned green and a light green precipitate formed. The solid was collected on a frit, washed with $2 \times 5\ \text{mL}$ pentane, and dried to give $[\text{Cp}^*\text{Cr}(\text{NO})\text{Cl}]_2$ **132**¹⁴ (52 mg, 80%). IR (cm^{-1} , Nujol): $\nu_{\text{NO}} = 1648$. Crystals suitable for X-ray crystallography were grown from a solution of complex **132** in acetone at -35°C . Details are provided in Appendix A, part 15.



Addition of HBF₄ to Cp*CrNO(C₄H₆) 111. Formation of [(η^5 -permethylcyclopentadienyl)(η^3 -crotyl)nitrosylchromium]BF₄ 135:

In an NMR tube, Cp*CrNO(C₄H₆) 111 (30 mg, 0.111 mmol) was dissolved in 0.7 mL of CD₂Cl₂ and cooled to -78 °C. HBF₄ (54% in Et₂O, 14.2 μ L, 0.111 mmol) was added via syringe and a colour change from orange to deep red was observed, providing the cationic η^3 -crotyl complex 135 *in situ*. NMR analysis at -80 °C: ¹H NMR (400 MHz, CD₂Cl₂): δ 6.05 (br m, 1H, H_a); 4.88 (br m, 1H, H_b); 3.32 (br m, 1H, H_c or H_d); 1.72 (br s, 15H, C₅Me₅); 1.66 (ov m, 1H, H_c or H_d); 1.64 (ov m, 3H, CH₃). COSY (400 MHz, CD₂Cl₂): δ 6.05 \leftrightarrow δ 4.88; δ 6.05 \leftrightarrow δ 3.32; δ 6.05 \leftrightarrow δ 1.66; δ 6.05 \leftrightarrow δ 1.64; δ 4.88 \leftrightarrow δ 1.66; δ 4.88 \leftrightarrow δ 1.64; δ 3.32 \leftrightarrow δ 1.66. ¹³C APT NMR (100 MHz, CD₂Cl₂): δ 129.8 (1, CH); 112.8 (–, CH); 112.6 (+, C₅Me₅); 67.8 (+, CH₂); 18.7 (–, CH₃); 9.9 (–, C₅Me₅). HMQC (400 MHz, CD₂Cl₂): δ 6.05 \leftrightarrow δ 112.8; δ 4.88 \leftrightarrow δ 129.8; δ 3.32 \leftrightarrow δ 67.8; δ 1.72 \leftrightarrow δ 9.9; δ 1.66 \leftrightarrow δ 67.8; δ 1.64 \leftrightarrow δ 19.37.



[(η^5 -cyclopentadienyl)(η^3 -crotyl)carbonylnitrosylchromium]BF₄ **138:**

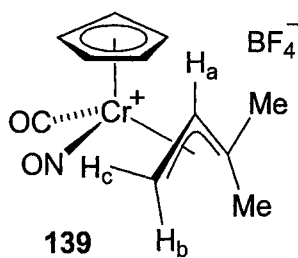
As described previously, a mixture of the η^2 -butadiene and η -4-butadiene complexes **101** and **106** was freshly prepared by the photolysis of CpCrNO(CO)₂ **90** (218 mg, 1.07 mmol) in the presence of excess butadiene. The solvent was removed *in vacuo* and the residue dissolved in 30 mL of diethyl ether, cooled to -78°C , and HBF₄ (54% in Et₂O, 134 μL , 0.975 mmol) was added via syringe. The resulting dark green suspension was stirred at -78°C for 30 min and then warmed to room temperature. After stirring for another 30 min the solvent was removed *in vacuo*, the residue dissolved in 10 mL of acetone, layered with 5 mL of diethyl ether and cooled to -35°C . After 12 h, a green powder was collected via filtration, washed with 2 x 10 mL diethyl ether and dried to give impure η^3 -crotyl complex **138** as a 1 : 1.5 : 5.0 : 22.0 mixture of isomers (118 mg, 40% estimated from the ¹H NMR spectrum). IR (cm⁻¹, Nujol): $\nu_{\text{CO}} = 2066$, $\nu_{\text{NO}} = 1744$. Anal. calcd for C₁₀H₁₂CrNO₂BF₄: C, 37.89; H, 3.82; N, 4.42; found: C, 35.75; H, 3.38; N, 4.81.

NMR analysis of the major isomer of complex **138**. ¹H NMR (500 MHz, acetone-d₆): δ 5.96 (s, 5H, C₅H₅); 5.35 (ddd, $J = 13.6, 12.8, 7.2$ Hz, 1H, H_b); 4.80 (dq, $J = 13.6, 6.8$ Hz, 1H, H_a); 4.37 (br d, $J = 7.2$ Hz, 1H, H_c); 2.81 (br d, $J = 12.8$ Hz, 1H, H_d); 2.58 (d, $J = 6.8$ Hz, 3H, CH₃). COSY (500 MHz, acetone-d₆): δ 5.35 \leftrightarrow δ 4.80; δ 5.35 \leftrightarrow δ 4.37; δ

5.35 \leftrightarrow δ 2.81; δ 4.80 \leftrightarrow δ 2.58; δ 4.37 \leftrightarrow δ 2.81; δ 2.81 \leftrightarrow δ 2.58. HMQC (500 MHz, C_6D_6): δ 5.96 \leftrightarrow δ 100.9; δ 5.35 \leftrightarrow δ 93.7; δ 4.80 \leftrightarrow δ 116.2; δ 4.37 \leftrightarrow δ 63.2; δ 2.81 \leftrightarrow δ 63.2; δ 2.58 \leftrightarrow δ 21.3.

NMR analysis of the 2nd most abundant isomer (**138'**). 1H NMR (500 MHz, acetone- d_6): δ 6.04 (s, 5H, C_5H_5); 5.41 (d, J = 7.2 Hz, 1H, H_c); 5.11 (ddd, J = 13.6, 13.2, 7.2 Hz, 1H, H_b); 4.12 (dq, J = 13.2, 6.4 Hz, 1H, H_a); 3.46 (br d, J = 13.6 Hz, 1H, H_d); 2.32 (d, J = 6.4 Hz, 3H, CH_3). COSY (500 MHz, acetone- d_6): δ 5.41 \leftrightarrow δ 5.11; δ 5.11 \leftrightarrow δ 4.12; δ 5.11 \leftrightarrow δ 3.46; δ 4.12 \leftrightarrow δ 2.32. HMQC (500 MHz, C_6D_6): δ 6.04 \leftrightarrow δ 100.6; δ 5.41 \leftrightarrow δ 73.5; δ 5.11 \leftrightarrow δ 94.0; δ 4.12 \leftrightarrow δ 100.0; δ 3.46 \leftrightarrow δ 73.5; δ 2.32 \leftrightarrow δ 19.5.

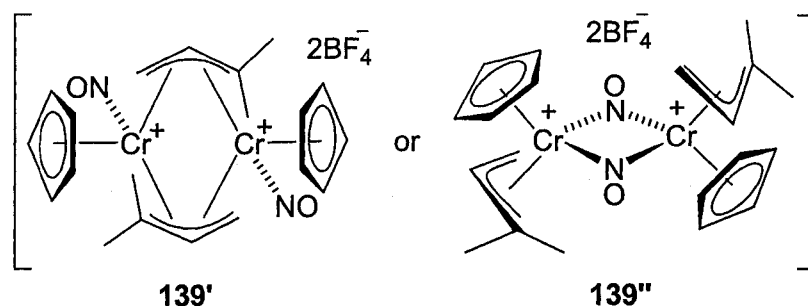
CH_3 signals of the remaining minor isomers (**138''** and **138'''**): 2.49 (d, J = 6.4 Hz) and 2.40 (d, J = 6.4 Hz).



[(η^5 -cyclopentadienyl)(η^3 -1,1-dimethylallyl)carbonylnitrosylchromium]BF₄ **139:**

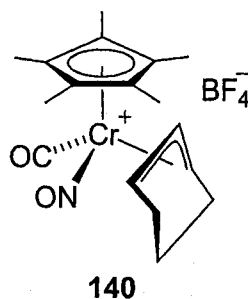
As described previously, a mixture of the η^2 -isoprene and η^4 -isoprene complexes **102** and **107** was freshly prepared by the photolysis of $CpCrNO(CO)_2$ **90** (725 mg, 3.57 mmol) with isoprene. The solvent was removed *in vacuo* and the residue dissolved in 30 mL of diethyl ether, cooled to $-78^\circ C$, and HBF_4 (54% in Et_2O , 406 μL , 2.95 mmol)

added via syringe. The dark yellow suspension was stirred at $-78\text{ }^{\circ}\text{C}$ for 30 min and then warmed to room temperature, during which time a colour change to red-brown was observed. After stirring for an additional 30 min, the solvent was removed *in vacuo* and the residue dissolved in 10 mL of acetone and cooled to $-35\text{ }^{\circ}\text{C}$. After 12 h, an orange powder was collected via filtration, washed with 2 x 10 mL diethyl ether and dried to give η^3 -(1,1-dimethylallyl) complex **139** (142 mg, 12%). IR (cm^{-1} , Nujol): $\nu_{\text{CO}} = 2066$, $\nu_{\text{NO}} = 1738$. ^1H NMR (300 MHz, CD_3CN): δ 5.69 (s, 5H, C_5H_5); 4.85 (ddt, $J = 13.2, 7.8, 0.6$ Hz, 1H, H_a); 3.9 (dd, $J = 7.8, 3.0$ Hz, 1H, H_c); 2.67 (dd, $J = 13.2, 3.0$ Hz, 1H, H_a); 2.55 (d, $J = 0.6$ Hz, 3H, CH_3); 1.58 (d, $J = 0.6$ Hz, 3H, CH_3). COSY (400 MHz, CD_3CN): δ 4.85 \leftrightarrow δ 3.9; δ 4.85 \leftrightarrow δ 2.67; δ 4.85 \leftrightarrow δ 2.55; δ 3.9 \leftrightarrow δ 2.67. ^{13}C NMR (100 MHz, acetone- d_6): δ 224.7; 111.8; 101.3; 84.1; 56.4; 22.5; 22.3. Anal. calcd for $\text{C}_{11}\text{H}_{14}\text{CrNO}_2\text{BF}_4$: C, 39.91; H, 4.26; N, 4.23; found: C, 39.96; H, 4.32; N, 4.16.



After cooling the filtrate from the isolation of complex **139** for a further two days at $-35\text{ }^{\circ}\text{C}$, a green powder was collected (23 mg), the major component of which is assigned to be the either dimeric η^3 -(μ -1,1-dimethylallyl) complex **139'** or the η^3 -(1,1-dimethylallyl)- μ -nitrosyl complex **139''** (see the discussion in Chapter 5, p. 163). IR (cm^{-1} , Nujol): $\nu_{\text{NO}} = 1685, 1657$. ^1H NMR (300 MHz, acetone- d_6): δ 6.01 (s, 5H, C_5H_5); 5.46 (br d, $J = 7.2$

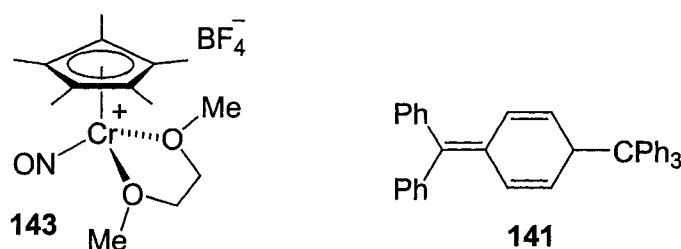
Hz, 1H, H_{syn}); 4.68 (br dd, $J = 13.5, 7.2$ Hz, 1H, $H_{central}$); 3.91 (br d, $J = 13.5$ Hz, 1H, H_{anti}); 2.54 (br s, 3H, CH_3); 1.72 (br s, 3H, CH_3). COSY (300 MHz, acetone- d_6): $\delta 5.46 \leftrightarrow \delta 4.68$; $\delta 5.46 \leftrightarrow \delta 3.91$; $\delta 4.68 \leftrightarrow \delta 3.91$.



(η^5 -Permethylcyclopentadienyl)(η^3 -cyclohexenyl)carbonylnitrosylchromium] BF_4 **140:**

To an solution of η^2 -(1,3-cyclohexadiene) complex **117** (20.0 mg, 0.0615 mmol) in 5 mL of diethyl ether cooled to -78 °C was added HBf_4 (54% in Et_2O , 8.5 μ L, 0.0615 mmol) via syringe. The orange solution was stirred at -78 °C for 30 min then warmed to room temperature, during which time a yellow precipitate formed. After stirring for a further 30 min, the solvent was removed *in vacuo* and the residue dissolved in 3 mL of acetone and cooled to -35 °C. After 12 h, yellow crystals were collected and dried to give cationic η^3 -cyclohexenyl complex **140** (10.0 mg, 39%). IR (cm^{-1} , Nujol): $\nu_{CO} = 2020$, $\nu_{NO} = 1727$. Due to the low resolution of the NMR data, definitive assignment of the proton resonances of this product was not possible. Individual signals are evident, however, for all nine of the η^3 -cyclohexenyl ligand protons. 1H NMR (400 MHz, acetone- d_6): $\delta 5.96$ (m, 1H); 5.04 (m, 1H); 4.20 (br t, $J = 7.2$ Hz, 1H); 2.69 (m, 1H); 2.59 (br m, 1H); 2.32 (m, 1H); 2.16 (m, 1H); 2.05 (s, 15 H, C_5Me_5); 1.40 (br m, 1H); 0.61 (m, 1H). COSY (400 MHz, acetone- d_6): $\delta 5.96 \leftrightarrow \delta 4.20$; $\delta 5.96 \leftrightarrow \delta 2.32$; $\delta 5.04 \leftrightarrow \delta$

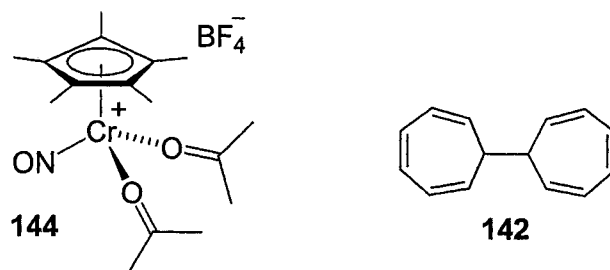
4.20; δ 5.04 \leftrightarrow δ 2.16; δ 2.69 \leftrightarrow δ 2.16; δ 2.69 \leftrightarrow δ 1.40; δ 2.69 \leftrightarrow δ 0.61; δ 2.59 \leftrightarrow δ 2.32; δ 2.59 \leftrightarrow δ 1.40; δ 1.40 \leftrightarrow δ 0.61. X-ray crystallography of these crystals established the crystals of complex **140**. Details are provided in Appendix A, part 16.



Addition of triphenylcarbenium tetrafluoroborate to Cp*CrNO(CO)(η^2 -propene) **95 in DME. Formation of [(η^5 -permethylcyclopentadienyl)(κ^2 -1,2-dimethoxyethane)-nitrosylchromium]BF₄ **143**:**

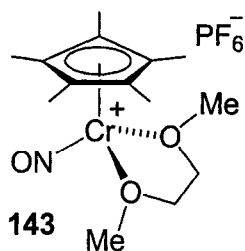
To a solution of Cp*CrNO(CO)(η^2 -propene) **95** (38.0 mg, 0.13 mmol) in 10 mL of DME was added a suspension of Ph₃CBF₄ (43.6 mg, 0.13 mmol) in 10 mL of DME. A colour change from orange-brown to green was immediately observed. After stirring for 15 h, the solvent was removed *in vacuo* and the resulting residue triturated with 3 x 10 mL of diethyl ether. The extracts were combined and the solvent removed *in vacuo* to provide trityl dimer **141**¹⁵ as an off-white solid (30.2 mg, 47%). ¹H NMR (300 MHz, C₆D₆): δ 7.28 (br d, J = 7.5 Hz, 7H, Ph); 7.06 (ov m, 18H, Ph); 6.43 (dd, J = 10.5, 1.8 Hz, 2H, CH); 5.91 (dd, J = 10.5, 3.9 Hz, 2H, CH); 4.91 (m, 1H, Ph₃CCH). HRMS calcd for C₃₈H₃₀: m/z 486.23515; found: 486.23474. The remaining ether insoluble residue was dissolved in 2 mL of acetone, layered with 2 mL of diethyl ether and stored at -35 °C to give [Cp*CrNO(DME)]BF₄ **143** as deep green crystals (20 mg, 39%). IR (cm⁻¹, NUJOL): ν_{NO} = 1663. The identity of these crystals was established by X-ray

crystallography. Details are provided in Appendix A, part 17. Consistent combustion analysis could not be obtained for this product.



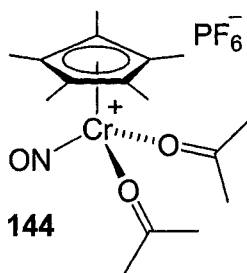
Addition of tropylium tetrafluoroborate to Cp*CrNO(CO)(η²-propene) **95 in acetone. Formation of [(η⁵-permethylcyclopentadienyl)bis(acetone)nitrosyl-chromium]BF₄ **144**:**

To a solution of Cp*CrNO(CO)(η²-propene) complex **95** (20.0 mg, 0.07 mmol) in 10 mL of DME was added a solution of C₇H₇CBF₄ (12.4 mg, 0.07 mmol) in 10 mL of acetone. While stirring for two days a colour change from orange-brown to green was observed. The solvent was removed *in vacuo* and the resulting residue triturated with 3 x 10 mL of diethyl ether. The extracts were combined and the solvent removed *in vacuo* to give ditropyl **142**¹⁵ as an off-white solid (~6.3 mg, 49%). ¹H NMR (300 MHz, acetone-d₆): δ 6.68 (t, *J* = 3.15 Hz, 2H, distal-CH); 6.24 (dt, *J* = 9.3, 2.7 Hz, 2H, mid-CH); 5.25 (br dd, *J* = 9.3, 4.3 Hz, 2H, proximal-CH); 1.91 (br m 2H, bridging-CH). The remaining ether insoluble residue was dissolved in 2 mL of acetone, layered with 2 mL of diethyl ether and stored at -35 °C to give the cationic bis(acetone) complex **144** as green crystals (12.4 mg, 42%). IR (cm⁻¹, NUJOL): ν_{NO} = 1657. The identity of these crystals was established by X-ray crystallography. Details are provided in Appendix A, part 17. Consistent combustion analysis could not be obtained for this product.



(η^5 -Permethylcyclopentadienyl)(κ^2 -1,2-dimethoxyethane)nitrosyl chromium hexafluorophosphate **143:**

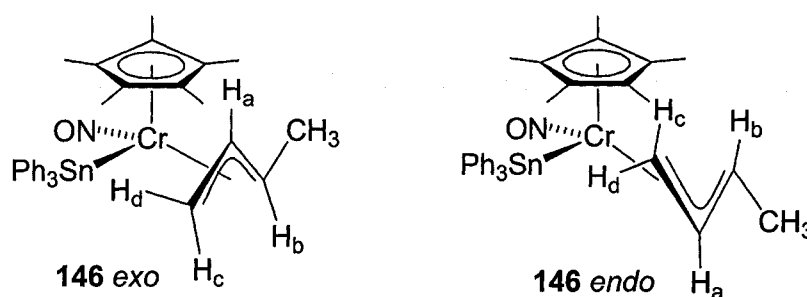
To a solution of $\text{Cp}^*\text{CrNO}(\text{CO})_2$ **94** (500 mg, 1.83 mmol) in 20 mL DME was added a suspension of ferricinium hexafluorophosphate (606 mg, 1.83 mmol) in 10 mL of DME. The blue-green mixture was stirred for one week at room temperature. The mixture was then filtered through Celite and the solvent removed *in vacuo*. Unreacted $\text{Cp}^*\text{CrNO}(\text{CO})_2$ was removed via trituration with 2 x 10 mL of pentane and the residue dried to give the PF_6^- salt of the cationic DME complex **143** as a green powder (662 mg, 80%). IR (cm^{-1} , NUJOL): ν_{NO} = 1663. Anal. calcd for $\text{C}_{14}\text{H}_{25}\text{CrNO}_3\text{PF}_6$: C, 37.18; H, 5.57; N, 3.1; found: C, 37.28; H, 5.23; N, 2.93.



(η^5 -Permethylcyclopentadienyl)bis(acetone)nitrosylchromium hexafluorophosphate **144:**

To a solution of $\text{Cp}^*\text{CrNO}(\text{CO})_2$ **94** (500 mg, 1.83 mmol) in 10 mL of acetone was added a solution of ferricinium hexafluorophosphate (606 mg, 1.83 mmol) in 10 mL of acetone; immediate effervescence was observed. After stirring for 1 h, the solvent was

removed *in vacuo* and unreacted $\text{Cp}^*\text{CrNO}(\text{CO})_2$ removed via trituration with 2 x 10 mL of pentane. The residue was then dissolved in 5 mL of acetone, layered with 5 mL of diethyl ether and stored at $-35\text{ }^\circ\text{C}$ to give the PF_6^- salt of the cationic bis(acetone) complex **144** as deep green crystals (683 mg, 78%). IR (cm^{-1} , NUJOL): $\nu_{\text{NO}} = 1657$. Anal. calcd for $\text{C}_{16}\text{H}_{27}\text{CrNO}_3\text{PF}_6$: C, 40.17; H, 5.69; N, 2.93; found: C, 38.14; H, 5.29; N, 2.8.



(η^5 -Permethylcyclopentadienyl)(η^3 -crotyl)(triphenylstannyl)nitrosylchromium **146:**

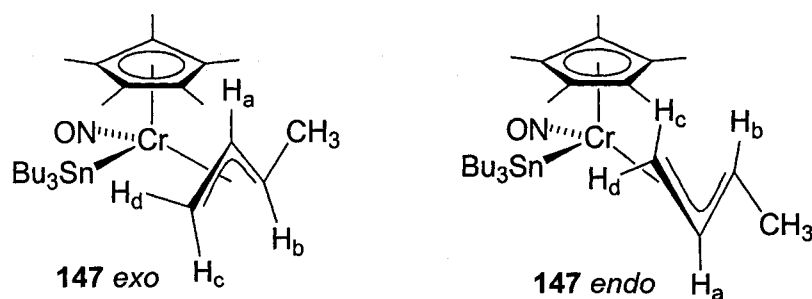
In a Schlenk tube, $\text{Cp}^*\text{CrNO}(\text{C}_4\text{H}_6)$ **111** (100 mg, 0.369 mmol) was dissolved in 50 mL of benzene and triphenyltin hydride (168 mg, 0.479 mmol) added. The solution was then heated to $45\text{ }^\circ\text{C}$ for 96 h. The resulting yellow-brown solution was passed through a 1 x 5 cm silica-gel column and eluted with benzene. The yellow eluent was evaporated *in vacuo* and the residue dissolved in 10 mL of diethyl ether. Several precipitations at $-35\text{ }^\circ\text{C}$ afforded η^3 -crotyl complex **146** as a bright yellow powder (63 mg, 63%), obtained as a 1 : 1 mixture of *endo* and *exo* isomers in solution. IR (cm^{-1} , THF): $\nu_{\text{NO}} = 1636$. HRMS calcd for $\text{C}_{32}\text{H}_{37}\text{CrNOSn}$: m/z 623.13025; found: 623.13124. Anal. calcd for $\text{C}_{32}\text{H}_{37}\text{CrNOSn}$: C, 61.76; H, 5.99; N, 2.25; found: C, 61.26; H, 5.62; N, 1.84. Crystals of the *endo* isomer suitable for X-ray crystallography were grown over 24

h from diethyl ether at $-35\text{ }^{\circ}\text{C}$. Details of the crystallography are provided in Appendix A, part 19. Also crystallized with complex **146** *endo* were a trace amount ($<5\%$) of deep green crystals. The structure of these crystals was identified as $[(\eta^5\text{-C}_5\text{Me}_5)\text{Cr}(\text{NO})-(\mu\text{-O})(\mu\text{-OH})\text{-(SnPh}_2)_2]$ **149** by X-ray crystallography. Details of the crystallography are provided in Appendix A, part 20.

NMR data for the *exo* isomer of complex **146**. ^1H NMR (500 MHz, C_6D_6): δ 8.04 (br d, $J = 6.5\text{ Hz}$, 6H, Ph); 7.27 (br ov t, $J = 6.5\text{ Hz}$, 6H, Ph); 7.19 (m, 3H, Ph); 4.08 (br dq, $J = 7.0, 1.0\text{ Hz}$, 1H, H_b); 3.33 (dd, $J = 7.0, 3.0\text{ Hz}$, 1H, H_d); 2.19 (dt, $J = 14.5, 8.5\text{ Hz}$, 1H, H_a); 1.56 (br dd, $J = 14.5, 3.0\text{ Hz}$, 1H, H_c); 1.36 (s, 15H, C_5Me_5); 0.96 (d, $J = 7.0\text{ Hz}$, 3H, CH_3), (br d, $J_{\text{Sn-H}} = 15.5\text{ Hz}$). COSY (500 MHz, C_6D_6): δ 8.04 \leftrightarrow δ 7.27; δ 7.27 \leftrightarrow δ 7.19; δ 4.08 \leftrightarrow δ 3.33; δ 4.08 \leftrightarrow δ 2.19; δ 4.08 \leftrightarrow δ 0.96; δ 3.33 \leftrightarrow δ 2.19; δ 3.33 \leftrightarrow δ 1.56; δ 2.19 \leftrightarrow δ 1.56; δ 2.19 \leftrightarrow δ 0.96. ^{13}C APT NMR (125 MHz, C_6D_6): δ 138.2 (–, Ph); 128.4 (–, Ph); 128.3 (–, Ph); 102.2 (+, C_5Me_5); 88.5 (–, CH_a); 84.7 (–, CH_b); 48.7 (+, CH_2); 15.4 (–, CH_3); 9.96 (–, C_5Me_5). HMQC (500 MHz, C_6D_6): δ 8.04 \leftrightarrow δ 138.2; δ 7.27 \leftrightarrow δ 128.4; δ 7.19 \leftrightarrow δ 128.3; δ 4.08 \leftrightarrow δ 84.7; δ 3.33 \leftrightarrow δ 48.7; δ 2.19 \leftrightarrow δ 88.5; δ 1.56 \leftrightarrow δ 48.7; δ 1.36 \leftrightarrow δ 9.96; δ 0.96 \leftrightarrow δ 15.4.

NMR data for the *endo* isomer of complex **146**. ^1H NMR (500 MHz, C_6D_6): δ 8.0 (br d, $J = 6.5\text{ Hz}$, 6H, Ph); 7.27 (br ov t, $J = 6.5\text{ Hz}$, 6H, Ph); 7.19 (m, 3H, Ph); 4.29 (dd, $J = 7.0, 2.0\text{ Hz}$, 1H, H_d), (br d, $J_{\text{Sn-H}} = 26.0\text{ Hz}$); 3.35 (ddd, $J = 14.5, 11.0, 7.0\text{ Hz}$, 1H, H_a); 1.89 (dq, $J = 11.0, 6.0\text{ Hz}$, 1H, H_b); 1.85 (d, $J = 6.0\text{ Hz}$, 3H, CH_3); 1.42 (s, 15H, C_5Me_5); 0.14 (br d, $J = 14.5\text{ Hz}$, 1H, H_c), (br d, $J_{\text{Sn-H}} = 24.0\text{ Hz}$). COSY (500 MHz, C_6D_6): δ 8.0

$\leftrightarrow \delta 7.27$; $\delta 7.27 \leftrightarrow \delta 7.19$; $\delta 4.29 \leftrightarrow \delta 3.35$; $\delta 4.29 \leftrightarrow \delta 0.14$; $\delta 3.35 \leftrightarrow \delta 1.89$; $\delta 3.35 \leftrightarrow \delta 0.14$; $\delta 1.89 \leftrightarrow \delta 1.85$. ^{13}C APT NMR (125 MHz, C_6D_6): δ 138.2 (–, Ph); 128.4 (–, Ph); 128.3 (–, Ph); 103.4 (+, C_5Me_5); 101.6 (–, CH_a); 76.5 (–, CH_b); 56.5 (+, CH_2); 17.9 (–, CH_3); 10.5 (–, C_5Me_5). HMQC (500 MHz, C_6D_6): δ 8.0 \leftrightarrow δ 138.2; δ 7.27 \leftrightarrow δ 128.4; δ 7.19 \leftrightarrow δ 128.3; δ 4.29 \leftrightarrow δ 56.5; δ 3.35 \leftrightarrow δ 101.6; δ 1.89 \leftrightarrow δ 76.5; δ 1.86 \leftrightarrow δ 17.9; δ 1.42 \leftrightarrow δ 10.5; δ 0.14 \leftrightarrow δ 56.5.



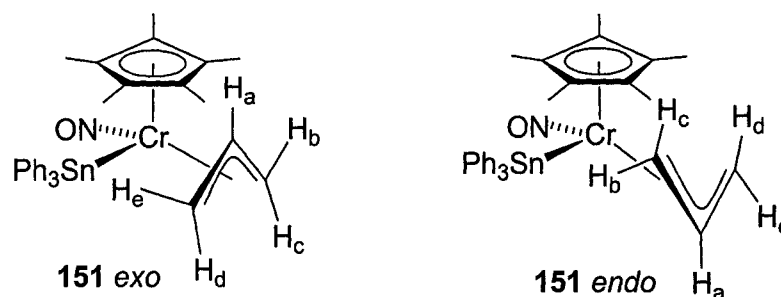
(η^5 -Permethylcyclopentadienyl)(η^3 -crotyl)(tributylstannyl)nitrosylchromium **147:**

In an NMR tube, $\text{Cp}^*\text{CrNO}(\text{C}_4\text{H}_6)$ **111** (12.3 mg, 0.0453 mmol) was dissolved in 0.7 mL of benzene- d_6 and tributyltin hydride (12.2 μl , 0.0453 mmol) added via syringe. The solution was left at room temperature for 5 days to form complex **147** as a 1 : 4 mixture of tentatively assigned *endo* and *exo* isomers, identified only *in situ*. Tentative assignment of the isomer configuration was made on the similarity of chemical shifts to that of the *endo* and *exo* isomers of η^3 -crotyl complex **146**.

NMR data for the major (*endo*) isomer of complex **147**. ^1H NMR (500 MHz, C_6D_6): 3.85 (dd, $J = 6.9, 2.7$ Hz, 1H, H_d), (br d, $J_{\text{Sn-H}} = 20$ Hz); 3.35 (m, 1H, H_a); 1.95 (br s, 3H, CH_3); 1.91 (m, 1H, H_b); 1.90 to 1.70 (ov m, Bu_3Sn); 1.50 (s, 15H, C_5Me_5); -0.27 (dd, $J =$

14.1, 2.7 Hz, 1H, H_c), (br d, $J_{Sn-H} = 22$ Hz). COSY (300 MHz, C₆D₆): $\delta 3.85 \leftrightarrow \delta 3.35$; $\delta 3.85 \leftrightarrow \delta -0.27$; $\delta 3.35 \leftrightarrow \delta 1.91$; $\delta 3.35 \leftrightarrow \delta -0.27$; $\delta 1.95 \leftrightarrow \delta 1.91$.

NMR data for the minor (*exo*) isomer of complex **147**, signals marked with an asterisk (*) were obscured by impurities and were detected indirectly via homonuclear COSY NMR: ¹H NMR (500 MHz, C₆D₆): 4.01 (dq – app quint, $J = 7.2$ Hz, 1H, H_b); 2.60 (dd, $J = 8.1$, 1.8 Hz, 1H, H_d); 2.03 (dt, $J = 13.9$, 8.1 Hz, 1H, H_a); 1.41 (H_c)*; 1.09 (CH₃)*. COSY (500 MHz, C₆D₆): $\delta 4.01 \leftrightarrow \delta 2.03$; $\delta 4.01 \leftrightarrow \delta 1.09$; $\delta 2.60 \leftrightarrow \delta 2.03$; $\delta 2.60 \leftrightarrow \delta 1.41$; $\delta 2.03 \leftrightarrow \delta 1.41$. Due to sample impurities, the Cp* and *n*-butyl proton resonances of this minor component could not be located.



(η^5 -Permethylcyclopentadienyl)(η^3 -allyl)(triphenylstannyl)nitrosylchromium **151, method A:**

In a Schlenk tube, Cp*CrNO(CO)₂ **94** (150 mg, 0.0549 mmol) was dissolved in 50 mL of benzene and allyltriphenyltin (215 mg, 0.0549 mmol) added. The solution was then cooled to 5 °C and irradiated for 24 h. The resulting yellow-brown solution was passed through a 1 x 5 cm silica-gel column and eluted with benzene. The yellow eluent was evaporated *in vacuo* and the residue dissolved in 10 mL of diethyl ether. Several precipitations at –35 °C then afforded η^3 -allyl complex **151** as a bright yellow powder

(177 mg, 53%), present as a 1 : 2 mixture of *endo* and *exo* isomers in solution. IR (cm⁻¹, THF): ν_{NO} = 1643. HRMS calcd for C₃₁H₃₅CrNOSn: m/z 609.11456; found: 609.11536. Anal. calcd for C₃₁H₃₅CrNOSn: C, 61.21; H, 5.8; N, 2.3; found: C, 61.28; H, 5.63; N, 2.06. Stereochemical assignment and spectroscopic data are provided in the following experimental.

(η^5 -Permethylcyclopentadienyl)(η^3 -allyl)(triphenylstannyl)nitrosylchromium **151, method B:**

In a Schlenk flask, Cp*CrNO(C₄H₆) **111** (50 mg, 0.184 mmol) was dissolved in 15 mL of benzene and allyltriphenyltin (72 mg, 0.184 mmol) added. The solution was then heated to 60 °C for 12 h. The resulting yellow-brown solution was then passed through a 1 x 5 cm silica-gel column and eluted with benzene. The yellow eluent was evaporated *in vacuo* and the residue dissolved in 5 mL of diethyl ether. Several precipitations at -35 °C then afforded η^3 -allyl complex **151** as a bright yellow powder (37 mg, 33%), present as a 1 : 2 mixture of *endo* and *exo* isomers in solution.

NMR data for the major (*endo*) isomer of complex **151**. ¹H NMR (400 MHz, C₆D₆): δ 8.0 (m, 6H, Ph); 7.26 (m, 6H, Ph); 7.18 (m, 3H, Ph); 3.54 (dddd, J = 13.6, 12.0, 7.2, 6.8 Hz, 1H, H_a); 3.32 (dt, J = 7.6, 2.4 Hz, 1H, H_b or H_e), (br d, $J_{\text{Sn-H}}$ = 22.4 Hz); 3.26 (br dd, J = 7.2, 2.8 Hz, 1H, H_b or H_e), (br d, $J_{\text{Sn-H}}$ = 20.8 Hz); 1.41 (s, 15H, C₅Me₅); 1.26 (br d, J = 12.0 Hz, 1H, H_c or H_d); 0.28 (br d, J = 13.6 Hz, 1H, H_c or H_d). COSY (400 MHz, C₆D₆): δ 8.0 \leftrightarrow δ 7.26; δ 8.0 \leftrightarrow δ 7.18; δ 4.41 \leftrightarrow δ 3.54; δ 4.41 \leftrightarrow δ 3.26; δ 4.41 \leftrightarrow 0.28; δ 3.54 \leftrightarrow δ 3.26; δ 3.54 \leftrightarrow δ 1.26; δ 3.54 \leftrightarrow δ 0.28; δ 1.26 \leftrightarrow δ 0.28. TROESY

(400 MHz, C₆D₆, NOE correlations): δ 8.0 \leftrightarrow δ 7.26; δ 8.0 \leftrightarrow δ 4.41; δ 4.41 \leftrightarrow δ 3.54; δ 4.41 \leftrightarrow δ 0.28; δ 3.54 \leftrightarrow δ 3.26; δ 3.26 \leftrightarrow δ 1.26; δ 1.26 \leftrightarrow δ 0.28. ¹³C APT NMR (100.58 MHz, C₆D₆): δ 138.1 (–, Ph); 128.4 (–, Ph); 128.3 (–, Ph); 103.6 (+, C₅Me₅); 100.9 (–, CH); 59.9 (+, CH₂); 59.6 (+, CH₂); 10.7 (–, C₅Me₅). HMQC (400 MHz, C₆D₆): δ 8.0 \leftrightarrow δ 138.1; δ 7.26 \leftrightarrow δ 128.3; δ 7.18 \leftrightarrow δ 128.4; δ 4.41 \leftrightarrow δ 59.9; δ 3.54 \leftrightarrow δ 100.9; δ 3.26 \leftrightarrow δ 59.6; δ 1.26 \leftrightarrow δ 59.6; δ 0.28 \leftrightarrow δ 59.9; δ 1.41 \leftrightarrow δ 10.7.

NMR data for the minor (*exo*) isomer of complex **151**. ¹H NMR (400 MHz, C₆D₆): δ 8.0 (m, 6H, Ph); 7.26 (m, 6H, Ph); 7.18 (m, 3H, Ph); 4.41 (br d, J = 6.8 Hz, 1H, H_b or H_e), (br d, J_{Sn-H} = 27.2 Hz); 3.12 (br dd, J = 7.6, 2.4 Hz, 1H, H_b or H_e), (br d, J_{Sn-H} = 25.6 Hz); 2.37 (dddd - app tt, J = 13.6, 13.6, 7.6, 7.6 Hz, 1H, H_a); 1.82 (br d, J = 13.6 Hz, 1H, H_c/H_d); 1.41 (br d, J = 13.6 Hz, 1H, H_c or H_d), 1.35 (s, 15H, C₅Me₅). COSY (400 MHz, C₆D₆): δ 8.0 \leftrightarrow δ 7.26; δ 8.0 \leftrightarrow δ 7.18; δ 3.32 \leftrightarrow δ 3.12; δ 3.32 \leftrightarrow δ 2.37; δ 3.32 \leftrightarrow δ 1.41; δ 3.12 \leftrightarrow δ 2.37; δ 3.12 \leftrightarrow δ 1.82; δ 3.12 \leftrightarrow δ 1.41; δ 2.37 \leftrightarrow δ 1.82; δ 2.37 \leftrightarrow δ 1.41. TROESY (400 MHz, C₆D₆, NOE correlations): δ 8.0 \leftrightarrow δ 7.26; δ 8.0 \leftrightarrow δ 3.32; δ 8.0 \leftrightarrow δ 1.35; δ 7.26 \leftrightarrow δ 1.35; δ 7.18 \leftrightarrow δ 1.35; δ 3.32 \leftrightarrow δ 2.37; δ 3.32 \leftrightarrow δ 1.41; δ 3.12 \leftrightarrow δ 2.37; δ 3.12 \leftrightarrow δ 1.41; δ 3.12 \leftrightarrow δ 1.35; δ 2.37 \leftrightarrow δ 1.82; δ 2.37 \leftrightarrow δ 1.35; δ 1.82 \leftrightarrow δ 1.41. ¹³C APT NMR (100.58 MHz, C₆D₆): δ 138.1 (–, Ph); 128.4 (–, Ph); 128.3 (–, Ph); 102.7 (+, C₅Me₅); 92.2 (–, CH); 65.4 (J_{Sn-C} = 25.9 Hz, +, CH₂); 51.3 (J_{Sn-C} = 101.5 Hz, +, CH₂); 9.7 (J_{Sn-C} = 9.2 Hz, –, C₅Me₅). HMQC (400 MHz, C₆D₆): δ 8.0 \leftrightarrow δ 138.1; δ 7.26 \leftrightarrow δ 128.3; δ 7.18 \leftrightarrow δ 128.4; δ 3.32 \leftrightarrow δ 51.3; δ 3.12 \leftrightarrow δ 65.4; δ 2.37 \leftrightarrow δ 92.2; δ 1.82 \leftrightarrow δ 65.4; δ 1.41 \leftrightarrow δ 51.3; δ 1.35 \leftrightarrow δ 9.9.



Tentative assignment of the isomer configuration was made on the similarity of chemical shifts to that of the *endo* and *exo* isomers of η^3 -crotyl and η^3 -allyl complexes **146** and **151**.

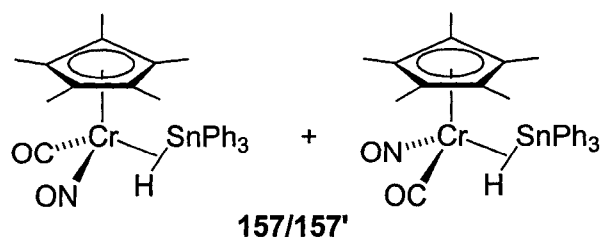
NMR data for the major (*endo*) isomer of complex **152**, signals marked with an asterisk (*) were obscured by impurities and were detected indirectly via homonuclear COSY

NMR: ^1H NMR (500 MHz, C_6D_6): δ 6.25 (m, 3H, H_h); 5.00 (m, 6H, H_i and H_j); 3.07 (br dd, $J = 7.2, 1.8$ Hz, 1H, H_b or H_e), (br d, $J_{\text{Sn-H}} = 20.0$ Hz); 2.67 (br dt, $J = 8.1, 2.1$ Hz, 1H, H_b or H_e), (br d, $J_{\text{Sn-H}} = 33.0$ Hz); 2.41 (t, $J = 9.5$ Hz, 3H, H_f or H_g), (d, $J_{\text{I19Sn-H}} = 62.3$ Hz), (d, $J_{\text{I17Sn-H}} = 43.9$ Hz); 2.30 (H_a)*; 2.29 (t, $J = 9.5$ Hz, 3H, H_f or H_g), (d, $J_{\text{I19Sn-H}} = 59.3$ Hz), (d, $J_{\text{I17Sn-H}} = 41.0$ Hz); 1.73 (br d, $J = 8.1$ Hz 1H, H_c or H_d); 1.36 (s, 15H,

C_5Me_5); 1.18 (br d, $J = 13.2$ Hz, 1H, H_c or H_d). COSY (500 MHz, C_6D_6): $\delta 6.25 \leftrightarrow \delta 5.00$; $\delta 6.25 \leftrightarrow \delta 2.41$; $\delta 6.25 \leftrightarrow \delta 2.29$; $\delta 5.00 \leftrightarrow \delta 2.41$; $\delta 5.00 \leftrightarrow \delta 2.29$; $\delta 3.07 \leftrightarrow \delta 2.67$; $\delta 3.07 \leftrightarrow \delta 1.73$; $\delta 2.67 \leftrightarrow \delta 2.30$; $\delta 2.67 \leftrightarrow \delta 1.18$; $\delta 2.30 \leftrightarrow \delta 1.73$; $\delta 2.30 \leftrightarrow \delta 1.18$; $\delta 1.73 \leftrightarrow \delta 1.18$. ^{13}C APT NMR (125 MHz, C_6D_6): $\delta 140.2$ (–, alkene CH_2); 138.0 (–, alkene CH_2); 117.7 (+, alkene CH); 102.2 (+, C_5Me_5); 91.7 (–, CH_a); 64.3 (+, η^3 -allyl CH_2); 44.4 (+, η^3 -allyl CH_2); 24.6 (+, aliphatic CH_2); 10.1 (–, C_5Me_5). HMQC (500 MHz, C_6D_6): $\delta 6.25 \leftrightarrow \delta 140.2$; $\delta 6.25 \leftrightarrow \delta 138.0$; $\delta 5.00 \leftrightarrow \delta 117.7$; $\delta 3.07 \leftrightarrow \delta 64.3$; $\delta 2.67 \leftrightarrow \delta 44.4$; $\delta 2.41 \leftrightarrow \delta 24.6$; $\delta 2.30 \leftrightarrow \delta 91.7$; $\delta 2.29 \leftrightarrow \delta 24.6$; $\delta 1.73 \leftrightarrow \delta 64.3$; $\delta 1.36 \leftrightarrow \delta 10.1$; $\delta 1.18 \leftrightarrow \delta 44.4$.

NMR data for the minor (*exo*) isomer of complex **152**, signals marked with an asterisk (*) are obscured by impurities and were detected indirectly via homonuclear COSY NMR:

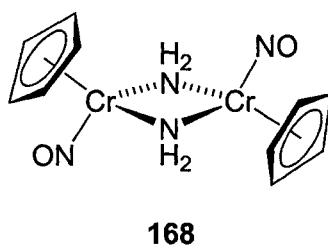
^1H NMR (500 MHz, C_6D_6): $\delta 4.14$ (br dt, $J = 6.6, 5.0$ Hz, 1H, H_b or H_e); 3.56 (H_a)*; 3.24 (br d, $J = 6.6$ Hz, 1H, H_b or H_e); 1.42 (H_c or H_d)*; 1.41 (s, 15H, C_5Me_5); 0.21 (br d, $J = 12.5$ Hz, 1H, H_c or H_d); due to overlap with starting material peaks, the alkene proton signals of the triallyltin ligand are tentatively located between 5.6 and 5.0 ppm, while those of the diastereotopic methylene group appear at 2.00 and 1.55 ppm. COSY (500 MHz, C_6D_6), only partial data available: $\delta 4.14 \leftrightarrow \delta 3.56$; $\delta 4.14 \leftrightarrow \delta 3.24$; $\delta 4.14 \leftrightarrow \delta 0.21$; $\delta 3.56 \leftrightarrow \delta 3.24$; $\delta 3.56 \leftrightarrow \delta 1.42$; $\delta 3.56 \leftrightarrow \delta 0.21$.



(η^5 -Permethylcyclopentadienyl)(η^2 -hydridotriphenylstannyl)carbonylnitrosyl-chromium 157:

In an NMR tube, Cp*CrNO(CO)₂ **94** (12.0 mg, 0.044 mmol) was dissolved in 0.7 mL of benzene-d₆ and triphenyltin hydride (15.4 mg, 0.044 mmol). The solution was then cooled to 5 °C and irradiated for 24 h to provide complex **157** with ~49% conversion, identified only *in situ* as a 10 : 1 mixture of unassigned isomers. ¹H NMR (300 MHz, C₆D₆): δ 7.86 (br d, J = 6.6 Hz, 6H, Ph); 7.23 (br t, 7.1 Hz, 6H, Ph); 7.08 (m, 3H, Ph); 1.51 (s, 15H, C₅Me₅); -3.62 (s, 1H, C-H-SnPh₃), (d, $J_{119\text{Sn-H}}$ = 360 Hz), (d, $J_{117\text{Sn-H}}$ = 344 Hz). The hydrido signal for the minor isomer appears at -3.81 ppm.

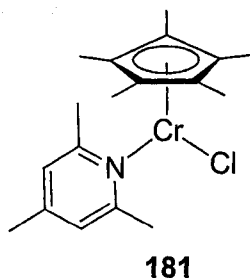
Experimental details for Chapter 6:



Reaction of bis(ammonia) complex 166¹⁶ with allyl Grignard. Formation of [CpCr(NO)(NH₂)]₂ 168:

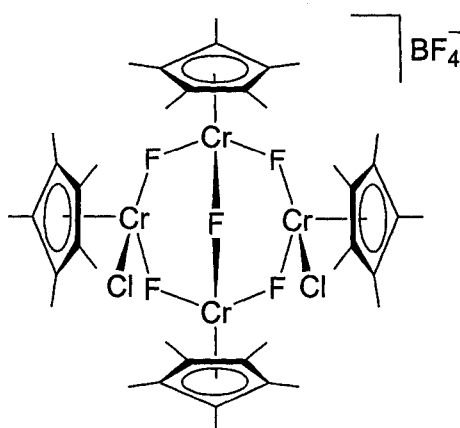
To a solution of the bis(ammonia) complex 166¹⁶ (100.0 mg, 0.325 mmol) in 10 mL of THF cooled to -78 °C was added allyl magnesium chloride (2.0 M in THF, 162.3

μL , 0.325 mmol). The mixture was stirred at $-78\text{ }^{\circ}\text{C}$ for 30 min and a colour change from green to red-brown was observed. The solution was then warmed to room temperature, the solvent removed *in vacuo* and the residue triturated with 3 x 5 mL of diethyl ether. The red extracts were combined, filtered through Celite and stored at $-35\text{ }^{\circ}\text{C}$ for one week to provide the dimeric complex **168** as red crystals (38 mg, 36%). IR (THF, cm^{-1}): $\nu_{\text{NO}} = 1625$. The structure of complex **166** was identified via X-ray crystallography, the unit cell from which is identical to that reported in the literature.¹⁷



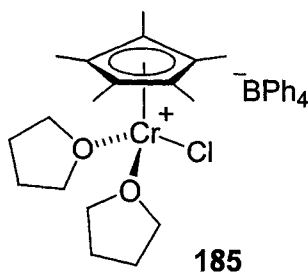
(η^5 -Permethylcyclopentadienyl)(2,4,6-trimethylpyridine)chlorochromium **181:**

To a solution of $[\text{Cp}^*\text{CrCl}]_2$ **180**¹⁸ (802 mg, 1.80 mmol) in 30 mL of pentane was added 2,4,6-trimethylpyridine (476 μL , 3.60 mmol), immediately forming a dark pink precipitate. After stirring for 1 h the precipitate was collected on a frit, washed with 2 x 10 mL of pentane, and dried to give complex **181** as a dark pink powder (896 mg, 72%). Anal. calcd for $\text{C}_{18}\text{H}_{26}\text{CrNCl}$: C, 62.87; H, 7.62; N, 4.07. Found: C, 60.65; H, 7.76; N, 3.47. Crystals suitable for X-ray diffraction were grown from toluene at $-35\text{ }^{\circ}\text{C}$. Details are provided in Appendix A, part 20.

**183**

$[(\eta^5\text{-C}_5\text{Me}_5)_4\text{Cr}_4(\mu\text{-F})_5\text{Cl}_2]\text{BF}_4$ **183:**

To a purple solution of trimethylpyridine complex **181** (26 mg, 0.076 mmol) in 5 mL of THF was added a suspension of silver tetrafluoroborate (15.0 mg, 0.076 mmol) in 5 mL of THF. A colour change to deep blue immediately occurred, along with the formation of a grey precipitate. After stirring for 2 h, the mixture was filtered through Celite, the filtrate layered with 5 mL of diethyl ether, and maintained at $-35\text{ }^\circ\text{C}$ for two days to provide the tetranuclear complex **183** as blue cubic crystals (19.7 mg, 26%). The composition of these crystals was confirmed via X-ray crystallographic comparison to the previously reported PF_6^- analogue of complex **183**.¹⁹



[(η^5 -Permethylcyclopentadienyl)bis(THF)chlorochromium]BPh₄ **185:**

To a purple solution of trimethylpyridine complex **181** (26 mg, 0.076 mmol) in 5 mL of THF was added a suspension of silver tetraphenylborate (32 mg, 0.075 mmol) in 5 mL of THF. A colour change to deep blue occurred immediately along with the formation of a grey precipitate. After stirring for 2 h the mixture was filtered through Celite, the filtrate layered with 5 mL of diethyl ether and stored at -35 °C for two days to yield the bis(THF) complex **185** as blue needle-like crystals (40 mg, 77%). Crystals suitable for X-ray crystallography were grown from a solution of complex **185** in a 1 : 1 mixture of THF and ether at -35 °C for five days. Details are provided in Appendix A, part 20.

Modified preparation of 1,3-dimesitylimidazolium chloride (IMesHCl):⁸

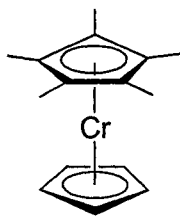
In a 500 mL round bottom flask was added 200 mL of methanol, 2,4,6-trimethylaniline (30.23 g, 224 mmol), glyoxal (40 wt% solution in water, 16.25 g, 112 mmol), and one drop of formic acid. The resulting mixture was stirred for 3 h at room temperature and the yellow precipitate filtered and dried to give glyoxal-bis-(2,4,6-trimethylphenyl)imine (29.8 g, 91%).

A 500 mL round bottom flask was charged with (8.68 g, 29.7 mmol) and 200 mL of ethyl acetate and cooled to 0 °C. A mixture of paraformaldehyde (1.16 g, 38.6 mmol),

HCl (4M in dioxane, 11.14 mL, 44.6 mmol) and 20 mL of ethyl acetate was stirred for 10 min and then added to the above solution. The reaction mixture was stirred for 5 h and the beige precipitate collected via filtration, dried and dissolved in 20 mL of dichloromethane. Sodium bicarbonate (~1.0 g) was added to the solution and the mixture stirred for 1 h or until the bubbling ceased. The solution was then filtered and the product precipitated with ~20 mL of diethyl ether, collected by filtration, washed with 2 x 20 mL of diethyl ether, and dried to give IMesHCl as a white powder (7.64 g, 75%). ¹H NMR (400 MHz, CDCl₃): δ 11.02 (t, J = 1.5 Hz, 1H, NCHN); 7.58 (d, J = 1.5 Hz, 2H, NCHCHN); 7.04 (s, 4H, Ar); 2.32 (s, 6H, *para*-CH₃); 2.20 (s, 12H, *ortho*-CH₃).

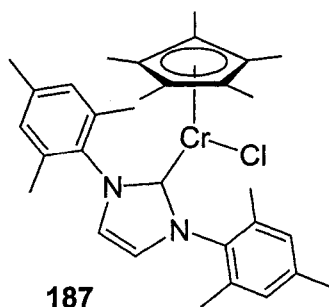
Preparation of 1,3-Dimesitylimidazolium tetraphenylborate (IMesHBPh₄):

Prepared by a modification of the procedure for the synthesis of IMesHPF₆.²⁰ A suspension of IMesHCl (1.0 g, 0.293 mmol) in 250 mL of acetone was treated with a solution of sodium tetraphenylborate (1.1 g, 0.321 mmol) in 10 mL of acetone. After stirring for 30 min, 100 mL of diethyl ether was added the reaction mixture was filtered through Celite. The filtrate was evaporated *in vacuo* and residual acetone removed under high vacuum (10⁻⁵ torr) for 12 h to provide IMesBPh₄ as an off-white powder (1.82 mg, 98%). ¹H NMR (300 MHz, CDCl₃): δ 7.32 (m, 8H, BPh₄); 7.04 (s, 4H, Ar); 6.97 (t, J = 1.8 Hz, 1H, NCHN); 6.86 (br t, J = 7.5 Hz, 8H, BPh₄); 6.73 (br t, J = 7.5 Hz, 4H, BPh₄); 6.19 (d, J = 1.8 Hz, 2H, NCHCHN); 2.40 (s, 6H, *para*-CH₃); 1.90 (s, 12H, *ortho*-CH₃). COSY (300 MHz, C₆D₆): δ 7.32 \leftrightarrow δ 6.97; δ 7.04 \leftrightarrow δ 2.40; δ 7.04 \leftrightarrow δ 1.90; δ 6.97 \leftrightarrow δ 6.19. Anal. calcd for C₄₅H₄₅BN₂: C, 86.52; H, 7.26; N, 4.48. Found: C, 86.07; H, 7.14; N, 4.23.

**186**

(η^5 -Permethylcyclopentadienyl)(η^5 -cyclopentadienyl)chromium **186:**

To a suspension of anhydrous CrCl_2 (600 mg, 4.88 mmol) in 30 mL of THF was added a suspension of Cp^*Li (680 mg, 4.78 mmol) in 20 mL of THF. After stirring for 2 h, a suspension of NaCp (422 mg, 4.78 mmol) in 10 mL of THF was added. After an additional 12 h of stirring, the solvent was removed *in vacuo* and the residue triturated with pentane (3 x 20 mL). The extracts were combined, concentrated to 15 mL and stored at $-35\text{ }^\circ\text{C}$. Several successive crystallizations then afforded pentamethylchromocene complex **186** as deep red crystals (950 mg, 79%). HRMS calcd for $\text{C}_{15}\text{H}_{20}\text{Cr}$: m/z 252.09702; found: 252.0975. Anal. calcd for $\text{C}_{15}\text{H}_{20}\text{Cr}$: C, 71.4; H, 7.99; found: C, 70.15; H, 8.11. Crystals suitable for X-ray crystallography were grown from pentane at $-35\text{ }^\circ\text{C}$ over 5 days. Details are provided in Appendix A, part 22.



(η^5 -Permethylcyclopentadienyl)(1,3-dimesitylimidazoline-2-ylidene)-chlorochromium 187:

To a solution of pentamethylchromocene **186** (18.2 mg, 0.0072 mmol) in 10 mL of THF was added a suspension of IMesHCl (23.4 mg, 0.0069 mmol) in 10 mL of THF. After stirring for 15 h, the colour of the solution had changed from red to orange-brown. The solvent was then removed *in vacuo*, the residue washed with pentane then triturated with 2 x 10 mL of diethyl ether. The ether extracts were then filtered through Celite, concentrated to ~10 mL and stored at $-35\text{ }^{\circ}\text{C}$ to yield complex **187** as purple-brown crystals (14.0 mg, 39%). HRMS calcd for $\text{C}_{31}\text{H}_{39}\text{CrN}_2\text{Cl}$: m/z 526.22070; found: 526.22026. Crystals suitable for X-ray crystallography were grown from a solution of complex **187** in hexane at $-35\text{ }^{\circ}\text{C}$ over 3 days. Details are provided in Appendix A, part 23.

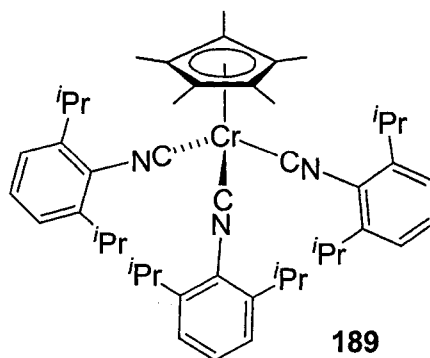
Addition of IMesHCl to $\text{Cp}^*\text{Cr}(\eta^3\text{-allyl})_2$ **191. Formation of $\text{Cp}^*\text{Cr}(\text{IMes})\text{Cl}$ **187**:**

To a suspension of IMesHCl (109 mg, 0.32 mmol) in 10 mL of THF was added a solution of $\text{Cp}^*\text{Cr}(\eta^3\text{-allyl})_2$ **191**²¹ (87.0 mg, 0.32 mmol) in 20 mL of THF cooled to $-78\text{ }^{\circ}\text{C}$. The mixture was then warmed to $-30\text{ }^{\circ}\text{C}$ over 3 h, during which time the IMesHCl suspension completely dissolved. The orange-brown solution was then warmed to room temperature over 2 h. The solvent was then removed *in vacuo* and the residue triturated

with 3 x 5 mL of diethyl ether. Crystallization of these extracts at $-35\text{ }^{\circ}\text{C}$ provided the neutral carbene complex **187** as orange-brown crystals (52 mg, 31%). HRMS calcd for $\text{C}_{31}\text{H}_{39}\text{CrN}_2\text{Cl}$: m/z 526.22070; found: 526.22273. The molecular structure of these crystals was identified via X-ray crystallography.

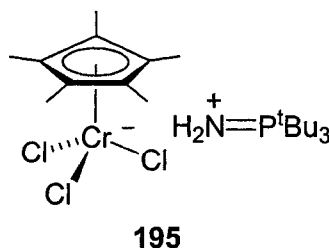
Modified preparation of 2,6-diisopropylphenylisonitrile:^{22, 23}

To a solution of 2,6-diisopropylaniline (20.03 g, 0.113 mol) in 100 mL of dichloromethane was added aqueous NaOH (50% w/v, 34.0 mL, 0.424 mol), chloroform (9.05 mL, 0.113 mol), and triethylbenzylammonium chloride (280 mg, 1.24 mmol). The mixture was heated to reflux for 72 h with vigorously stirring then cooled to room temperature. The organic layer was then separated and the aqueous layer washed with dichloromethane (3 x 30 mL). The organic fractions were washed with 100 mL of water, then 100 mL of brine, dried with potassium carbonate, filtered and the solvent removed *in vacuo*. Distillation at 0.1 mm Hg and $52\text{ }^{\circ}\text{C}$ afforded 2,6-diisopropylphenylisonitrile as a colourless liquid (10.5 g, 50%). IR (cm^{-1} , thin film): $\nu_{\text{NC}} = 2111$. ^1H NMR (400 MHz, CDCl_3): δ 7.34 (t, $J = 8.0\text{ Hz}$, 1H, H_{para}); 7.18 (d, $J = 8.0\text{ Hz}$, 2H, H_{meta}); 3.75 (br s, NH_2); 3.40 (sept, $J = 7.0\text{ Hz}$, 2H, $i\text{PrCH}$); 1.30 (d, $J = 7.0\text{ Hz}$, 12H, $i\text{PrCH}_3$). ^{13}C APT NMR (125 MHz, C_6D_6): δ 168.2 (+, CN); 144.9 (+, C_{ortho}); 129.3 (–, C_{para}); 124.3 (+, C_{ipso}); 123.3 (–, C_{meta}); 29.8 (–, $i\text{PrCH}$); 22.6 (–, $i\text{PrCH}_3$). Note: the product will slowly turn purple at room temperature but with very little resulting impurity observable in the NMR spectrum. Decomposition can be avoided by storing the product as a solid at $-35\text{ }^{\circ}\text{C}$.



(η^5 -Permethylcyclopentadienyl)tris(2,6-diisopropylphenylisonitrile)chromium **189:**

[Cp*CrCl]₂ **180**¹⁸ (75.0 mg, 0.168 mmol) was dissolved in 10 mL of THF and a solution of 2,6-diisopropylphenylisonitrile (63.0 mg, 0.337 mmol) in 2 mL of THF added. An immediate colour change from green-brown to deep red was observed. After stirring for 1 h the solvent was removed *in vacuo* and the residue triturated with 3 x 10 mL of pentane. The extracts were combined, filtered through Celite, concentrated to 5 mL and stored at -35 °C for 2 days to yield tris(isonitrile) complex **189** as a deep red powder (75.0 mg, 28%). IR (cm⁻¹, NUJOL): $\nu_{\text{NC}} = 2125$. Anal. calcd for C₄₉H₆₆CrN₃: C, 78.57; H, 8.88; N, 5.61; found: C, 77.70; H, 8.85; N, 5.50. HRMS calcd for C₄₉H₆₆CrN₃: m/z 748.46619; found: 748.46561. The solid-state molecular structure of complex **189** was identified by X-ray crystallography of crystals grown from diethyl ether, albeit with low resolution. The details for this crystallography are not available.



Reaction of [Cp*CrCl₂]₂ **178 with N-trimethylsilyl-tri(*tert*-butyl)phosphinimine.
Formation of [^tBu₃PNH₂][Cp*CrCl₃] **195**:**

In a SurfasilTM-protected Schlenk flask, ^tBu₃P=N-TMS²⁴ (38.5 mg, 0.133 mmol) in 5 mL of THF was added to a solution of [Cp*CrCl₂]₂ **178** (32.3 mg, 0.0665 mmol) in 10 mL of THF. After stirring for 30 min, the solvent was removed *in vacuo* and the residue triturated with 3 x 10 mL of diethyl ether. The remaining residue was triturated with 2 x 10 mL of toluene. The diethyl ether extract were combined, concentrated to 10 mL and stored at -35 °C for 24 h to give the complex salt **195** as blue crystals (33.0 mg, 48%). The toluene extract was also stored at -35 °C to give an intractable purple powder. Crystals of complex **195** suitable for X-ray crystallography were grown from a 1 : 1 diethyl ether : toluene mixture at -35 °C. Details are provided in Appendix A, part 24.

References

1. Carney, M. J.; Walsh, P. J.; Bergman, R. G. *J. Am. Chem. Soc.* **1990**, *112*, 6426.
2. SHELXS-86: Sheldrick, G. M. *Acta. Cryst. A* **1990**, *46*, 467.
3. DIRDIF-96: Beurskens, P. T.; Beurskens, G.; Bosman, W. P.; de Gelder, R.; Garcia Granda, S.; Gould, R. O.; Israel, R.; Smits, J. M. M. *The DIRDIF-96 program system*. Crystallography Laboratory, University of Nijmegen, The Netherlands, 1996.
4. Sheldrick, G. M. *SHELXL-93. Program for crystal structure determination*. University of Gottingen, Germany, 1993.
5. Tate, D. P.; Knipple, W. R.; Augl, J. M. *Inorg. Chem.* **1962**, *1*, 433.
6. Hoyano, J. K.; Legzdins, P.; Malito, J. T. *Inorg. Synth.* **1978**, *18*, 126.
7. Panda, T. K.; Gamer, M. T.; Roesky, P. W. *Organometallics* **2003**, *22*, 877.
8. Arduengo, A. J., III; Krafczyk, R.; Schmutzler, R. *Tetrahedron* **1999**, *55*, 14523.
9. Betz, P.; Döhring, A.; Emrich, R.; Goddard, R.; Jolly, P. W.; Krüger, C.; Romão, C. C.; Schönfelder, K. U.; Tsay, Y. H. *Polyhedron* **1993**, *12*, 2651.
10. Cardaci, G. *J. Chem. Soc., Dalton Trans.* **1984**, 815.
11. Herberhold, M.; Alt, H.; Kreiter, C. G. *Liebigs Ann. Chem.* **1976**, 300.
12. Malito, J. T.; Dhakir, R.; Atwood, J. L. *J. Chem. Soc., Dalton Trans.* **1980**, 1253.
13. Massey, A. G.; Park, A. J. *J. Organomet. Chem.* **1964**, *2*, 245.
14. Legzdins, P.; McNeil, W. S.; Rettig, S. J.; Smith, K. M. *J. Am. Chem. Soc.* **1997**, *119*, 3513.
15. Adams, H.; Bailey, N. A.; Willett, D. G.; Winter, M. J. *J. Organomet. Chem.* **1987**, *333*, 61.
16. Legzdins, P.; McNeil, W. S.; Batchelor, R. J.; Einstein, F. W. B. *J. Am. Chem. Soc.* **1995**, *117*, 10521.
17. Hames, B. W.; Legzdins, P.; Oxley, J. C. *Inorg. Chem.* **1980**, *19*, 1565.

18. Heintz, R. A.; Ostrander, R. L.; Rheingold, A. L.; Theopold, K. H. *J. Am. Chem. Soc.* **1994**, *116*, 11387.
19. Thomas, B. J.; Mitchell, J. F.; Theopold, K. H. *J. Organomet. Chem.* **1988**, *348*, 333.
20. Arduengo, A. J., III; Gamper, S. F.; Tamm, M.; Calabrese, J. C.; Davidson, F.; Craig, H. A. *J. Am. Chem. Soc.* **1995**, *117*, 572.
21. Betz, P.; Döhring, A.; Emrich, R.; Goddard, R.; Jolly, P. W.; Krüger, C.; Romão, C.; Schönfelder, K. U.; Tsay, Y.-H. *Polyhedron* **1993**, *12*, 2651.
22. Weber, W. P.; Gokel, G. W.; Ugi, I. K. *Angew. Chem. Int. Ed.* **1972**, *11*, 530.
23. Kamer, P. C. J.; Nolte, R. J. M.; Drenth, W. *J. Am. Chem. Soc.* **1988**, *110*, 6818.
24. Stephan, D. W.; Stewart, J. C.; Guerin, F.; Courtenay, S.; Kickham, J.; Hollink, E.; Beddie, C.; Hoskin, A.; Graham, T.; Wei, P.; Spence, R. E. v. H.; Xu, W.; Koch, L.; Gao, X.; Harrison, D. G. *Organometallics* **2003**, *22*, 1937.

Appendix A

References to complete reports from crystal structure determinations

Complete crystal structure reports can be obtained directly from Drs. R. McDonald and M. Ferguson at the University of Alberta X-ray Crystallography Laboratory, Department of Chemistry, University of Alberta, Edmonton, Alberta, T6G 2G2, Canada. E-mail: xray@beliveau.chem.ualberta.ca. Request report #'s below. Crystal structures that have been published in peer reviewed literature are available online from the Cambridge Crystallographic Data Centre (<http://www.ccdc.cam.ac.uk>).

1. Crystallographic details for complex **66**, request report # *jms0314*
2. Crystallographic details for complex **70**, request report # *jms0322*
3. Crystallographic details for complex **74**, request report # *jms0340*
4. Crystallographic details for complex **76**·0.5C₄H₈O, request report # *jms0401*
5. Crystallographic details for complex **77**·(DME)_{0.5}, request report # *jms0421*
6. Crystallographic details for complex **86**, request report # *jms0449*
7. Crystallographic details for complex **87**·1.5Me₂CO, request report # *jms0451*
8. Crystallographic details for complex **96**, request report # *jms0533*
9. Crystallographic details for complex **97**, request report # *jms0543*
10. Crystallographic details for complex **112**, request report # *jms0532*
11. Crystallographic details for complex **113**, request report # *jms0539*
12. Crystallographic details for complex **119**, request report # *jms0551*
13. Crystallographic details for complex **128**, request report # *jms0547*
14. Crystallographic details for complex **129**, request report # *jms0602*
15. Crystallographic details for complex **132**, request report # *jms0519*

16. Crystallographic details for complex **140**, request report # *jms0552*
17. Crystallographic details for complex **143**, request report # *jms0559*
18. Crystallographic details for complex **144**, request report # *jms0563*
19. Crystallographic details for complex **146**, request report # *jms0582*
20. Crystallographic details for complex **149**, request report # *jms0586*
21. Crystallographic details for complex **181**, request report # *jms0216*
22. Crystallographic details for complex **185**-C₄H₈O, request report # *jms0432*
23. Crystallographic details for complex **186**, request report # *jms0415*
24. Crystallographic details for complex **187**, request report # *jms0430*
25. Crystallographic details for complex **195**, request report # *jms0536*